SCLEROTINIA SCLEROTIORUM:
PHYTOTOXINS AND METABOLISM OF PHYTOALEXINS

A thesis submitted to the

College of Graduate Studies and Research

in partial fulfilment of the requirements

for the degree of

Doctor of Philosophy in the

Department of Chemistry

University of Saskatchewan

Saskatoon

by

Pearson William Kwaku Ahiahonu

PERMISSION TO USE

In presenting this thesis in partial fulfilment of the requirements for a postgraduate degree from the University of Saskatchewan, the author has agreed that the Libraries of this University may make it freely available for inspection. The author further agrees that permission for copying of this thesis in any manner, in whole or in part, for scholarly purposes may be granted by the professor who supervised the thesis work or, in her absence, by the Head of the Department of Chemistry, or the Dean of the College of Graduate Studies and Research. It is understood that copying or publication or use of this thesis or parts thereof for financial gain shall not be allowed without the author's written permission. It is also understood that due recognition shall be given to the author and to the University of Saskatchewan in any scholarly use which may be made of any material in my thesis.

Requests for permission to copy or to make other use of material in this thesis in whole or part should be addressed to:

The Head
Department of Chemistry
University of Saskatchewan
Saskatoon, Saskatchewan, CANADA
S7N 5C9

ABSTRACT

Sclerotinia sclerotiorum (Lib.) de Bary is a plant pathogenic fungus causing serious yield losses in a broad range of cultivated plants, excluding cereals. Most of the economically important brassicas such as canola, rapeseed, mustards, cabbages and others such as sunflower, peanut, bean, soybean, lettuce, and carrot are susceptible to this pathogen. No host specificity has been demonstrated in *S. sclerotiorum* and there is no specific resistance known in the host species. The main trust of this research project was to establish biotransformation pathways used by *S. sclerotiorum* to detoxify phytoalexins produced by host plants. As well, the potential production of phytotoxins and cytotoxic compounds by *S. sclerotiorum* was analyzed. The metabolite sclerin was isolated from cultures of *S. sclerotiorum* and its phytotoxicity to crucifers established for the first time. Fatty acids isolated from sclerotia of *S. sclerotiorum* of which oleic acid was a major component were found to be cytotoxic to the brine shrimp (*Artemia salina*).

Chemical defences, i.e. phytoalexins, were elicited and isolated from a resistant plant (*Erucastrum gallicum*, dog mustard): indole-3-acetonitrile, arvelexin, 1-methoxyspirobrassinin and erucalexin (new phytoalexin, a structural isomer of 1-methoxyspirobrassinin). As well, the biotransformations of the phytoalexins brassinin, produced by rapeseed, canola and brown mustard plants, camalexin, and 6-methoxycamalexin, produced by wild crucifers like *Arabidopsis thaliana*, *Capsella bursa-pastoris* and *Camelina sativa*, were investigated. It was established that *S. sclerotiorum* could efficiently metabolize these phytoalexins using a remarkable glucosylation reaction of their indole ring. Overall, results of these biotransformation studies followed by antifungal bioassays indicated that metabolism of brassinin, camalexin, and 6-methoxycamalexin were detoxification processes. Analogues of these phytoalexins were designed based on structures of the detoxification products to probe the specificity or

otherwise of the enzyme(s) involved in the metabolism of the phytoalexins. All the analogues tested were metabolized by the fungus though at slower rates. 6-Fluorocamalexin, one of the analogues, significantly slowed down the metabolism of brassinin both in cell cultures and in enzymatic assays with cell homogenates. Partial purification (five fold) of the brassinin detoxifying enzyme (brassinin glucosyltransferase) of *S. sclerotiorum* was achieved.

ACKNOWLEDGEMENTS

First and foremost, I am very grateful to God for caring and granting me the wisdom, knowledge and understanding to pursue and successfully complete a Ph.D. degree program in Chemistry. I will like to express my sincerest gratitude to my supervisor, Prof. M. Soledade C. Pedras for supervising this work. Her excellent guidance and constructive criticisms have led to the production of this nice piece of work.

I would like to thank the members of the advisory committee: Prof. Dale E. Ward, Prof. Stephen Reid, Prof. David Palmer, and Prof. Yen Lin for their advice, help and support during the cause of my program. I also thank my external examiner, Dr. Philip Hultin for his suggestions and advice. I am also grateful to Prof. Monica Palcic, of the University of Alberta for allowing me into her laboratory to learn some techniques in enzyme separation and to Dr. Adam Scpacenko, the research associate in her laboratory who actually taught me.

I wish to express my gratitude to all past and present members of Pedras group: Dr. F. Biabani, Dr. A. Desphande, Dr. R. Gadagi, Dr. N. Ismail, Dr. A. Q. Khan, Dr. S. Montaut, Dr. F. I. Okanga, Dr. O. Okeola, Dr. S. Sardari, Dr. M. Suchy, Dr. V. Uppala, Dr. Y. Xu, Dr. I. L. Zaharia, Dr. Y. Zhou, C. Biesenthal, V. Cekic, P. B. Chumala, M. Hossain, M. Jha, M. Kabir, J. Liu, D. Okinyo, C. Nycholat, G. Sarwar, and J. Sorenson. Special thanks to C. Biesenthal for introducing me to microbiological preparations and to P. B. Chumala for the meaningful discussions we had on some aspects of this work. Special mention is given to Dr. Keith Brown and Mr. Ken Thoms for their technical assistance. The financial support of the Department of Chemistry and the University of Saskatchewan is greatly appreciated. The moral support of the Ghanaian community and the African Christian Fellowship in Saskatoon is duly acknowledged.

Finally I express my heart felt gratitude to my wife Elizabeth and kids Fafa and Kafui for the love, care, and comfort I enjoyed during the period.

To my parents

Seth and Mercy Ahiahonu

To my wife

Elizabeth

TABLE OF CONTENTS

LIST OF FIGURES

LIST OF TABLES

LIST OF ABBREVIATIONS

Ac	acetyl
Ac_2O	acetic anhydride
AcOH	acetic acid
Ag 2-1	isolate of *Rhizoctonia solani*
BAP	6-benzylaminopurine
BGT	brassinin glucosyltransferase
br	broad
BSA	bovin serum albumin
^{13}C NMR	carbon-13 nuclear magnetic resonance
calcd.	calculated
CI	chemical ionization
clone #33	isolate of *Sclerotinia sclerotiorum*
clone #67	isolate of *Sclerotinia sclerotiorum*
cv	cultivar
DEAE	diethylaminoethyl cellulose
DMF	dimethylformamide
DMS	dimethylsulphide
DMSO	dimethylsulphoxide
EI	electron impact
Et	ethyl
EtOAc	ethyl acetate
EtOH	ethanol
FAB	fast atom bombardment
FCC	flash column chromatography

FTIR	Fourier transformed infrared
GC	gas chromatography
HMBC	heteronuclear multiple bond correlation
HMPA	hexamethylphosphoramide
HMQC	heteronuclear multiple quantum correlation
^{1}H NMR	proton nuclear magnetic resonance
HPLC	high performance liquid chromatography
HR	high resolution
HS	host selective
Hz	Hertz
m/z	mass/charge ratio
m-CBPA	*meta*-chloroperbenzoic acid
Me	methyl
MeI	methyl iodide
MeOH	methanol
MHz	megahertz
min	minute(s)
MS	mass spectrum
NOE	nuclear Overhauser enhancement
PDA	potato dextrose agar
PDB	potato dextrose broth
PMSF	phenyl methylsulphonyl fluoride
prepTLC	preparative thin layer chromatography
RP	reverse phase
rpm	revolutions per minute
R_t	retention time

SDS-PAGE	sodium dodecyl sulphate polyacrylamide gel electrophoresis
THF	tetrahydrofuran
TLC	thin layer chromatography
TMS	tetramethylsilane
UDP	uridine diphosphate
UDPG	uridine diphosphate glucose
UV	ultraviolet
v	volume

Crucifer plants and their fungal isolates

A. brassicae	*Alternaria brassicae* (blackspot fungus)
A. thaliana	*Arabidopsis thaliana*
B. juncea	*Brassica juncea* (brown mustard)
B. oleracea	*Brassica oleracea* (cabbages)
B. napus	*Brassica napus* (canola)
B. rapa	*Brassica rapa* (canola, rapeseed)
C. bursa-pastoris	*Capsella bursa-pastoris* (Shepherd's purse)
C. sativa	*Camelina sativa* (false flax)
E. gallicum	*Erucastrum gallicum* (dog mustard)
E. sativa	*Eruca sativa* (rocket)
P. lingam	*Phoma lingam* (blackleg fungus)
R. solani	*Rhizoctonia solani* (root rot fungus)
S. alba	*Sinapis alba* (white mustard)
S. sclerotiorum	*Sclerotinia sclerotiorum* (stem rot fungus)
T. arvense	*Thlaspi arvense* (stinkweed)

CHAPTER ONE

1. Introduction

1.1 General objectives

This thesis describes and discusses the chemical and biochemical interactions that exist between the stem rot fungus *Sclerotinia sclerotiorum* (Lib.) de Bary and susceptible and resistant crucifer plants. The susceptible plants are canola, brown mustard, white mustard and the resistant plant is dog mustard. The research involved:

(i) Bioassay guided isolation of phytotoxins and cytotoxins from *Sclerotinia sclerotiorum*;

(ii) Elicitation and isolation of phytoalexins from the resistant plant *Erucastrum gallicum* (Willd.) O. E. Schulz (dog mustard) using *Sclerotinia sclerotiorum* and $CuCl_2$ as elicitors;

(iii) Studies on the mechanisms by which the phytopathogenic fungus *Sclerotinia sclerotiorum* overcomes the natural plant defences.

This study is part of an on-going research program aimed at understanding the mechanisms of plant disease resistance. This, in our view will go a long way in developing better environmentally friendly crop protection agents to combat fungal infection in crucifers.

1.2 Cruciferous plants and their fungal pathogens

Cruciferous crops are cultivated worldwide and constitute an extremely valuable group of plants. Enormous quantities of vegetable crucifers, such as rocket (*Eruca sativa*), (Conn & Tewari, 1986; Conn et al., 1988), broccoli (*B. oleracea* var. botrytis), cauliflower (*B. oleracea* var. *italica*), turnip (*B. rapa*), kale (*B. oleracea* var. *acephala*), radish (*Raphanus sativus*) and a variety of cabbages (*B. oleracea*) are consumed annually (Pedras *et al.*, 2000). Oilseed crucifers (*Brassica* spp.) constitute the third largest source of edible vegetable oils and brown (*B. juncea*) and white (*Sinapis alba*) mustard seeds as well as wasabi (*Wasabiae japonica*) are well known condiments. A number of epidemiological studies suggest that cruciferous vegetables protect against cancer by modulating carcinogen metabolism (Talalay & Fahey, 2001). Wild crucifers include *Arabidopsis thaliana* whose genome was recently sequenced (The Arabidopsis Genome Initiative, 2000), *Erucastrum gallicum* (dog mustard) (Lefol *et al.*, 1997), *Thlaspi arvense* (stinkweed), *Camelina sativa* (false flax), and *Capsella bursa-pastoris* (Shepherd's purse) (Conn & Tewari, 1986; Conn *et al.*, 1988).

Similar to other plants, crucifers have a whole host of fungal pathogens that cause a variety of diseases. These fungal infections result in large losses of crop yields worldwide. The known fungal pathogens of crucifers include *Sclerotinia sclerotiorum* (Lib.) de Bary, *Phoma lingam* (Tode ex Fr.) Desm. [Perfect stage *Leptosphaeria* maculans (Desm.) Ces. *et* de Not.], *Rhizoctonia solani* Kuhn, and *Alternaria brassicae* (Berk.) Sacc. *P. lingam,* also known as the blackleg fungus, causes blackleg or stem canker on cruciferous plants (Pedras, 1998a). A virulent strain of the pathogen has caused significant rapeseed and canola losses in recent years in Canada and is also considered a serious agricultural problem worldwide. This fungus produces various phytotoxins, which cause necrosis and cell death of both host and non-host plants, and other secondary metabolites (Pedras, 1998a). A significant aim of brassica oilseed research is directed towards the development

of varieties with improved disease resistance, especially to the blackleg disease. Crucifers found to be resistant to the blackleg disease include *B. juncea* (Pedras *et al.*, 2002a), *E. sativa* (Pedras *et al.*, 2003c), and *T. arvense* (Pedras *et al.*, 2003b). *A. brassicae* causes blackspot disease, which is widespread and one of the most destructive fungal diseases of rapeseed (*B. napus, B. rapa*) and brown mustard (*B. juncea*). No sources of resistance to Alternaria blackspot are known within *Brassica* species (Pedras *et al.*, 2002b). Sources of blackspot resistance within the family Cruciferae (syn Brassicaceae) include white mustard (*Sinapis alba*) and some wild species such as false flax (*Camelina sativa*) and Shepherd's purse (*Capsella bursa-pastoris*) (Conn & Tewari, 1986; Conn *et al.*, 1988). *R. solani*, also known as the root rot fungus, causes root rot and post-emergence damping-off diseases on canola and rapeseed, as well as the other plant families (Pedras, 1998b). *S. sclerotiorum*, also known as the stem rot fungus is responsible for stem rot disease in crucifers, white mould in legumes and many others. Cultivars of canola currently grown are all susceptible to the stem rot disease (Kohli, 1995; Bardin & Huang, 2001). This will be discussed in more detail in the following section.

1.2.1 Secondary metabolites

Living organisms can synthesize or degrade chemical compounds by means of a series of chemical reactions mediated by enzymes. These processes are known as metabolism. There are two kinds of metabolism: primary metabolism and secondary metabolism. Through primary metabolism, organisms synthesize compounds that are essential for their survival. By contrast most organisms also utilize other metabolic pathways producing compounds that usually have a secondary utility. These compounds are called secondary metabolites. Secondary metabolites are organic compounds of natural origin that are unique to any organism or common to a small number of closely related

organisms and are only activated during particular stages of growth and development or during periods of stress, which include nutritional limitation and microbial attack (Mann, 1987). They are biosynthesized from primary precursors (building blocks). Secondary metabolites include i) fatty acids, polyacetylenes and polyketides derived from acetate-malonate; ii) isoprenoids and steroids derived from acetate-mevalonate; iii) aromatic amino acids and polyphenols derived from shikimic acid; iv) alkaloids derived from amino acids; v) metabolites from mixed biogenetic origin (Mann, 1987).

1.2.2 Phytotoxin production and applications

Phytotoxins are a class of secondary metabolites (natural products) produced by microbes that have deleterious effects on plants (Graniti *et al.*, 1989). There are two groups of phytotoxins, host selective (HS) and non-selective toxins. The HS toxins selectively affect plants that are susceptible to the pathogen whereas resistant plants show no damage even at relatively higher concentrations of the toxin (Graniti, 1991; Strobel, 1982). Phytotoxins together with other secondary metabolites can be used as chemotaxonomical markers (Pedras, 2001). For example, the blackleg fungus *P. lingam* was initially classified in two groups: highly virulent type (V) causing leaf spots and severe stem canker on rapeseed and cabbage and weakly virulent (W) causing only superfacial leaf and stem lesions on rapeseed and cabbage. This classification was made on the basis of virulence, host range, and cultural tests. However, recently a number of phytotoxins and related secondary metabolites were reported from different blackleg causing fungal isolates, suggesting that blackleg disease is caused by more than one *Phoma* species, *P. lingam,* and *P. wasabiae* (Pedras, 1998b). Furthermore, by utilizing metabolite markers, "Phoma blackleg" isolates were suggested to reclassify into three main groups comprised of: (i) virulent isolates, producing metabolites phomalide (**1**), sirodesmin PL (**2**),

deacetylsirodesmin PL (**3**), and phomamide (**5**) (Pedras, 1998b); (ii) Canadian weakly virulent isolates, producing sesquiterpenic HS toxin phomalairdenone (**6**) (Pedras *et al.*, 1999), and polyketides such as phomapyrone A (**7**); (iii) Polish weakly virulent isolates, producing various indolyl dioxopiperazines, such as L-valyl-L-tryptophan anhydride (**4**), phomapyrone A (**7**), phomapyrone B (**8**), and phomapyrone C (**9**) (Pedras & Biesenthal, 2001). Structures of these compounds are shown in Figure 1.1.

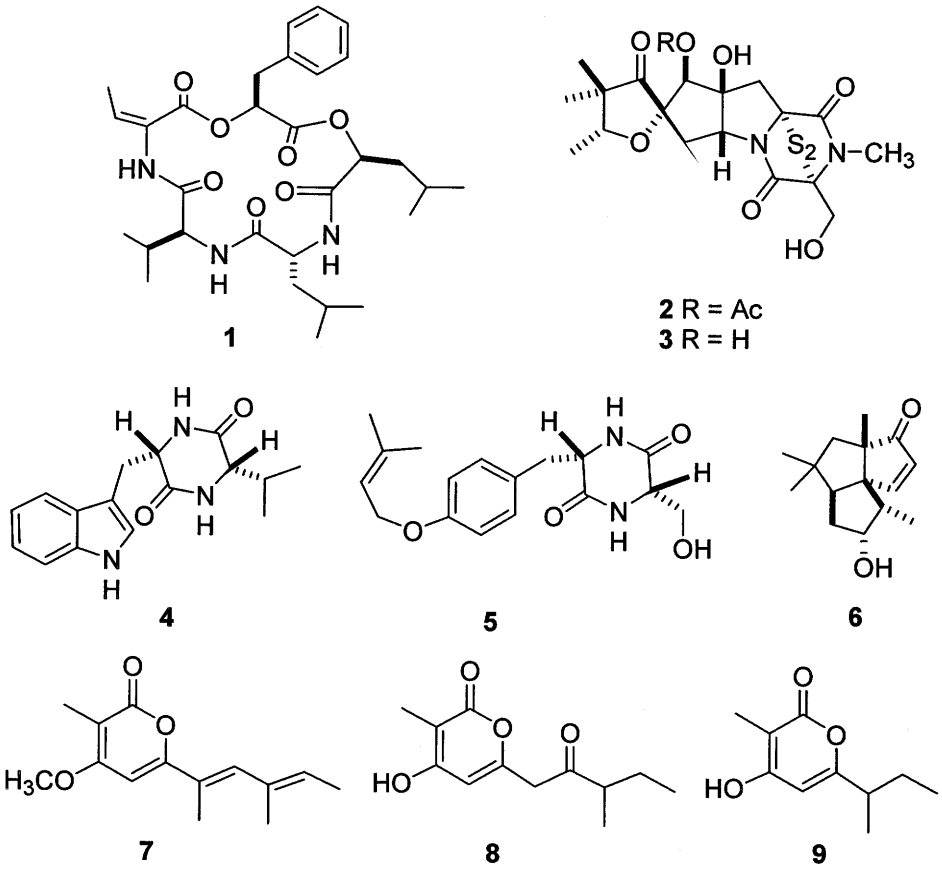

Figure 1.1 Chemical structures of secondary metabolites and phytotoxins isolated from blackleg fungus *Phoma lingam*

HS toxins are involved in diverse plant fungal diseases. Although the molecular basis for the selectivity of toxins is still not well understood, it is known that the selectivity is related with their mechanism of action in the host plant. That is the HS toxins evoke either a resistant of a susceptible plant reaction (Pedras, 1998b). A method to determine the selectivity of the plant reaction is to investigate the detoxification mechanism of plants to HS toxins. This approach could lead to the finding of the corresponding specific disease resistance gene(s) and/or gene products. The discovery of disease resistance genes will help achieving engineering plants that have specific disease resistance traits. This strategy has advantages comparing with the other disease-control methods, such as crop rotations, using certified seed, or application of fungicides. Traditional plant breeding for obtaining disease resistance is a very time-consuming process. Therefore, new methodologies for more effective transfer of disease resistance to agronomically important plants are extremely important (Pedras, 1998b).

Destruxin B (**10**), a HS toxin produced by *A. brassicae*, which causes chlorotic and necrotic foliar lesions (Pedras *et al.*, 2002b) on host plants, was metabolized by white mustard (*Sinapis alba*, blackspot resistant crucifer) to a less toxic product substantially faster than any of the susceptible *Brassica* species. This product, hydroxydestruxin B (**11**) ,(Scheme 1.1) was further transformed to the β-D-glucosyl derivative (**12**) at a slower rate (Pedras *et al.*, 2002b). Subsequent studies using leaves of *E. sativa* indicated that hydroxydestruxin B (**11**) was directly converted to (6'-*O*- malonyl)hydroxydestruxin B β-D-glucopyranoside (**13**) (Pedras *et al.*, 2003c) (Scheme 1.1). Although these hydroxylation and glucosylation reactions occurred in both resistant (*S. alba*) and susceptible (*B. napus, B. juncea, B. rapa*) species, glucosylation was the rate limiting step in the resistant species, whereas hydroxylation was the rate limiting step in the susceptible species. It was also observed that hydroxydestruxin B (**11**) induced the biosynthesis of phytoalexins in blackspot resistant species but not in susceptible species. This work indicated a unique example of phytotoxin detoxification and simultaneous phytoalexin elicitation by the

detoxification product. It was also demonstrated that the detoxification pathway present in *S. alba* is also present in three unrelated crucifers, *C. sativa*, *C. bursa-pastoris* and *E. sativa*, suggesting a conservation of this pathway across crucifers (Pedras *et al.*, 2003c).

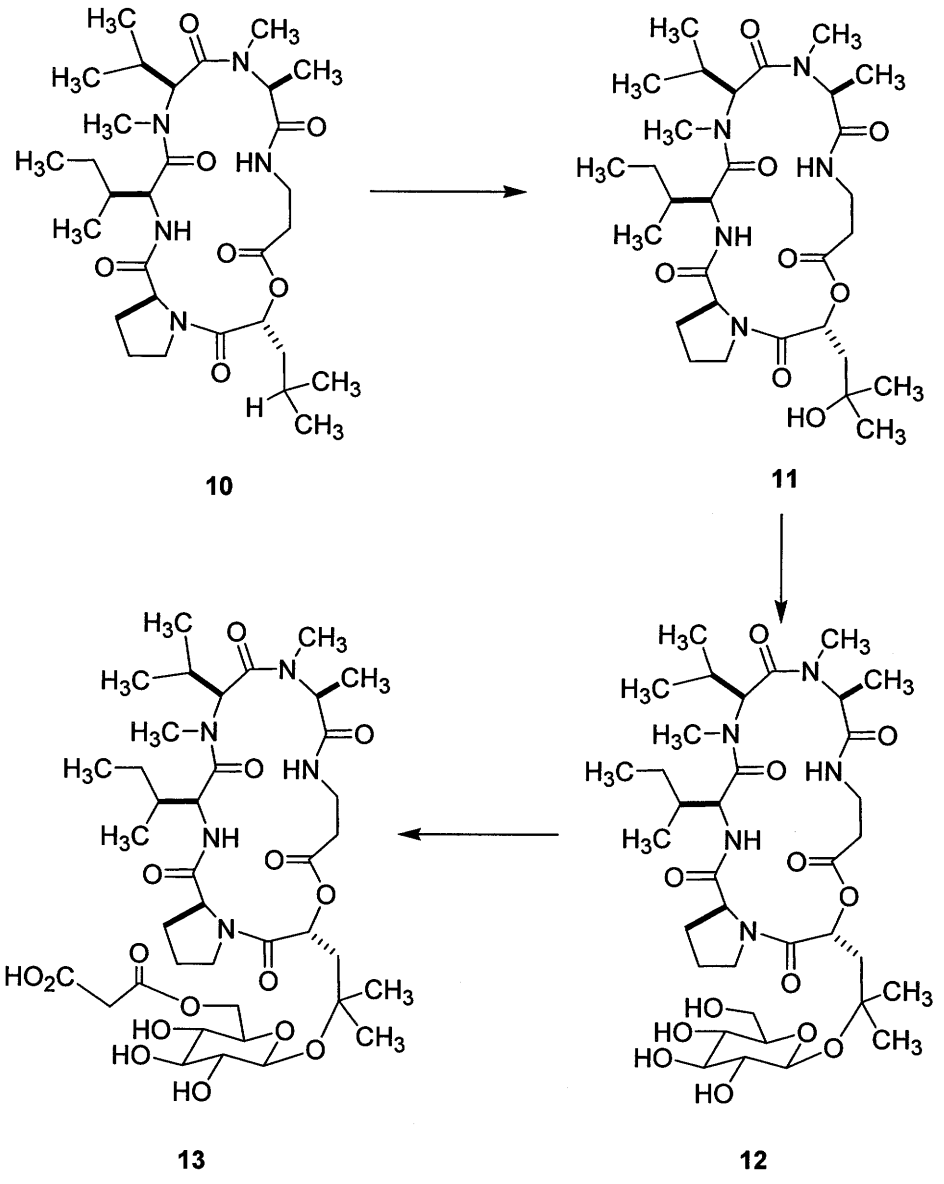

Scheme 1.1 Metabolism and detoxification of host selective toxin destruxin B (**10**) by crucifers (Pedras *et al.*, 2003c).

Therefore, knowledge of possible detoxification mechanisms operating in resistant plants may allow the determination of specific blackleg and blackspot resistant traits. This work may guide the cloning of blackleg and blackspot resistance genes (Pedras *et al.*, 2003c).

Phytotoxic metabolites isolated from culture filtrate extracts of *R. solani* (Nishimura, 1963) include phenyl acetic acid (**14**), *m*-hydroxyphenylacetic acid (**15**) and *p*-hydroxyphenylacetic acid (**16**) (Figure 1.2). Phytotoxicity bioassays using sugar beet seedlings indicated that **14** was the most toxic. The effects of these phytotoxins on potato were also examined (Frank & Francis, 1976). The disease symptoms of the root rot disease caused by *R. solani* on potato are reported to be induced by these toxins. The symptoms include root necrosis, leaf curling, stunting, and leaf margin chlorosis. The plant dies off within a week in instances of severe susceptibility. These toxins had similar effects on radish, beet, and corn seedlings and acted as growth hormones in low concentration.

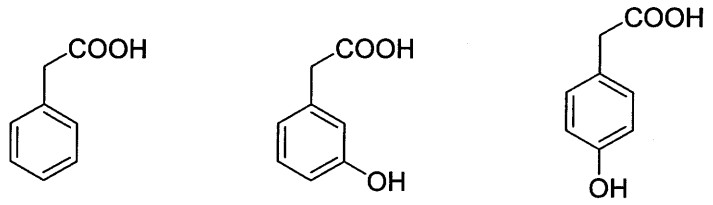

14 **15** **16**

Figure 1.2 Chemical structures of phytotoxins isolated from the root rot fungus *Rhizoctonia solani*

1.3 *Sclerotinia sclerotiorum*

Sclerotinia sclerotiorum is a phytopathogenic fungus that infects a wide range of cultivated and wild plants, excluding cereals, and is widespread, especially in temperate regions (Purdy, 1979) of the world and causes serious losses to many crops worldwide. It survives in the soil for extensive periods by producing darkly pigmented sclerotia. Sclerotia are masses of hyphae bound in a polysaccharide matrix enveloped by a layer of

cells with hard melanized walls. Sclerotia may be strictly vegetative structures or may be sites of sporulation in some classes of fungi. The pigmentation in the sclerotia has been shown to be melanin, a compound that is believed to play an important role in protecting fungi from adverse biological and environmental conditions (Starratt *et al.*, 2002). Sclerotia vary in size (from ca. 0.5 cm to 2 cm long) and shape (spherical or irregular). *S. sclerotiorum* attacks over 400 different plant species (Boland and Hall, 1994).

1.3.1 Life cycle and major plant diseases

Diseases caused by *S. sclerotiorum* are initiated either directly from soil-borne sclerotia which germinate to form hyphae that can penetrate the roots of nearby plants, as in sunflower wilt, root rot of pea and timber rot of tomato, or by airborne ascospores, as in stem rot of canola, cottony soft rot of carrot, watery soft rot of cole crops, lettuce drop of lettuce and white mould on beans (Purdy, 1979; Bardin & Huang, 2001). Disease symptoms appear as areas of light brown discolouration on stems, branches and pods. Plants infected with stem rot ripen earlier resulting in premature pods with shrivelled seeds. When the infected stems split open, hard black overwintering bodies, the sclerotia are found. Severely infected crops frequently lodge and the seedpods easily shatter resulting in yield loss. Currently, all varieties of canola, rapeseed, brown and white mustards are susceptible to *Sclerotinia* stem rot (Kohli *et al.*, 1995; Bardin & Huang, 2001). Canola petals present a surface on which the air disseminated ascospores can impact and adhere. The ascospore inoculum may originate within the field or from sources outside the field (Kohli *et al.*, 1995). Infection is initiated when infested petals dehisce, fall and adhere to the stem and leaves of the host plant. Ascospores on the petals germinate; penetrate the stem and form lesions in which sclerotia eventually develop. These lesions desiccate and shred allowing the sclerotia inside the stem to fall in the soil. Sclerotia can

survive in the soil for 4 to 5 years (Kohli *et al.*, 1995; Bardin & Huang, 2001), and may be moved by cultivation, by irrigation or by incorporation in seed lots as contaminants.

Stem rot is prevalent in Saskatchewan and all western Canada and no cultivars of *Brassica* spp. resistant to the disease are yet available to producers (Bardin & Huang, 2001). *S. sclerotiorum* attack affects plant development and may have a strong negative impact on the quality and production of crops. Common practices to prevent the spread of fungal diseases are crop rotation, use of certified seeds, removal of infected stubble, and application of fungicides, which are expensive and detrimental to the environment (Kohli *et al.*, 1995).

1.3.2 Secondary metabolites and phytotoxins

Sclerotinia sclerotiorum produces secondary metabolites some of which appear to be plant growth regulators, Secondary metabolites isolated from liquid cultures of *S. sclerotiorum* include sclerin (**17**), which plays a role in induction of sclerotial formation and melanogenesis in *Sclerotinia* species (Satomura *et al.,* 1963; Marukawa *et al.*, 1975), sclerolide (**18**), sclerotinin A (**19**), (Kubota *et al.*, 1966), and sclerotinin B (**20**) (Sassa, 1968). Compounds **19** and **20** promote the growth of rice seedlings at a concentration of 5 ppm (Tokoroyama *et al.,* 1968). Other secondary metabolites isolated from liquid cultures of *S. sclerotiorum* are sclerone (**21**), (Suzuki *et al.,* 1968) and isosclerone (**22**) (Morita & Aoki, 1974), which appear to stimulate the root elongation of rice seedlings by ca. 30% at concentrations of 1-10 ppm, and inhibits the growth of shoots and roots at concentrations above 50 ppm. However, to date no studies of the phytotoxicity of the metabolites to crucifers has been published. Biosynthetic studies with sclerin (**17**) and isosclerone (**22**) indicated that they are derived from acetate units via the polyketide pathway (Morita & Aoki, 1974). The structures of these compounds are shown in Figure 1.3.

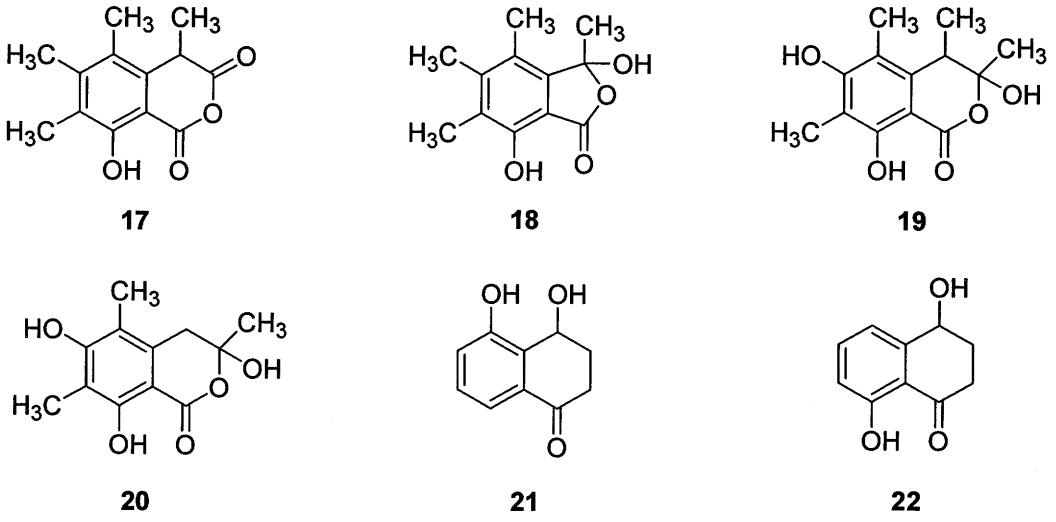

Figure 1.3 Secondary metabolites from liquid cultures of *Sclerotinia sclerotiorum*

In addition to protecting sclerotia against degradation by microorganisms, melanin may have a controlling influence on dormancy of *S. sclerotiorum* sclerotia, and in some fungi is an important determinant of pathogenicity and virulence (Starratt *et al.*, 2002). In studies towards the elucidation of the biosynthetic pathway of melanin in *S. sclerotiorum*, it was found that *S. sclerotiorum* produced significant amounts of the polyketide melanin precursor 1,8-dihydroxynaphthalene, the production of which was inhibited by tricyclazole (Starratt *et al.*, 2002). These studies resulted in the isolation of 1,8-dihydroxynaphthalene monoglucoside (**23**) from cultures of *S. sclerotiorum* (Starratt *et al.*, 2002). When cultured in the presence of tricyclazole, two other monoglucosides of 1,3,8-trihydroxynaphthalene **24** and **25** were obtained (Figure 1.4).

It was reported that oxalic acid isolated from culture filtrate extracts of *S. sclerotiorum* and from infected *B. juncea* (Rai & Dhawan, 1976) and bean (Maxwell & Lumsden, 1970) plants extracts, as well as from water extracts of hypocotyl lesions on sunflower (Noyes & Hancock, 1981) showed phytotoxic activity. However, these findings

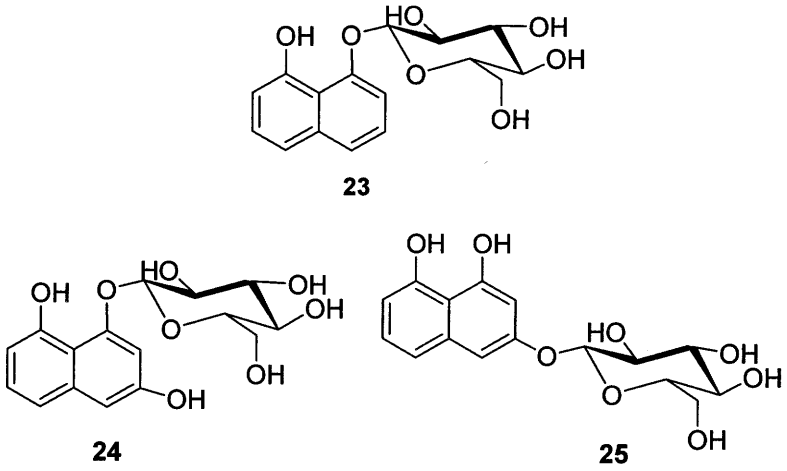

Figure 1.4 Hydroxynaphthalene monoglucosides from cultures of *Sclerotinia sclerotiorum*

dwelt mainly on culture filtrate of *S. sclerotiorum* and infected plant extracts and where oxalic acid was involved, the toxic concentrations applied were not indicated. The identity of oxalic acid present in the culture filtrate of *S. sclerotiorum* was established by comparative TLC as well as paper chromatography of standard organic acids viz. oxalic, malic, fumaric and succinic (Rai & Dhawan, 1976). Cessna and coworkers also reported that secretion of oxalic acid by *S. sclerotiorum* appears to be an essential determinant of its pathogenicity (Cessna *et al.*, 2000). Evidence for such involvement is based on the recovery of millimolar concentrations of oxalate (determined by colorimetric methods) from infected tissues and from the manual injection of oxalate, or of culture filtrate containing oxalate, into plants and observation of the development of Sclerotinia disease-like symptoms independent of the pathogen. Such correlative evidence has been strengthened by the observation that mutants of *S. sclerotiorum* that are deficient in the ability to synthesize oxalate are non pathogenic, whereas revertant strains that regain their oxalate biosynthetic capacity exhibit normal virulence (Cessna *et al.*, 2000).

A 5 KDa antifungal peptide (AP5) isolated from sunflower (*Helianthus annuus* L.) (Regente *et al.,* 1997) inhibited in vitro ascospore germination and mycelial growth of the fungal pathogen *S. sclerotiorum*. The effective concentration of AP5 giving 50% growth inhibition (IC_{50}) against *S. sclerotiorum* was 0.4 μM, far higher than all other antimicrobial proteins known (Regente *et al.*, 1997).

One objective of this work is to isolate metabolites from *S. sclerotiorum*, which have phytotoxic activity especially on some economically important cruciferous plants like *B. napus* (cv. Westar), *B. juncea* (cv. Cutlass) and *S. alba* (cv. Ochre). This thesis presents results of work done in this direction.

1.4 Phytoalexins

Plants fight pathogens with an enormous and complex arsenal of defence mechanisms (Pedras *et al.*, 2000). A significant component of these defences involve production of compounds, which may be either constitutive such as phytoanticipins (VanEtten *et al.*, 1998) or biosynthesized *de novo*, i.e. phytoalexins (Smith, 1996; Brooks & Watson, 1985).

Phytoalexins are low molecular weight antimicrobial compounds biosynthesized *de novo* by plants in response to diverse forms of stress, including microbial attack. (Dixon *et al.*, 1994). They are part of the induced chemical and biochemical defence mechanisms of plants. Phytoalexins were first described (Müller & Börger, 1940) during studies on *Phytophthora infestans* – potato interactions and since then have been found in many other plants (Bailey & Mansfield, 1982). A large body of correlative evidence supports the idea that phytoalexins have important role in the defence of plants against pathogens such as bacteria, fungi, nematodes, and insects (Enkerli *et al.*, 1998). Much of the research on phytoalexins has relied on the identification of induced antifungal compounds and

correlating their presence with resistance. Approaches that use in situ localization and quantification have provided good evidence that phytoalexins can accumulate at the right time, concentration, and location to be effective in resistance (Hammerschmidt & Dann, 1999). Studies on phytoalexin tolerance in pathogenic fungi have also shown a relationship between virulence and the ability of fungi to detoxify phytoalexins. Phytoalexins have been detected and isolated from different plant families. Many of the isolated phytoalexins from leguminous plants have an isoflavonoid skeleton; those from crucifers are indole alkaloids, those from cereals are largely cyclic hydroxamic acids, and diterpenoids, most of those from plants of the Solanaceae family include sesquiterpenoids, and polyacetylenes. Stilbenoid phytoalexins have been isolated from different plant families.

The first phytoalexin to be isolated and chemically characterized was (+)-pisatin (**26**) (Cruickshank & Perrin, 1960) from pea (*Pisum sativum*). (+)-Pisatin (**26**) was observed to be less toxic to the pea pathogen *Ascochyta pisi* than to *Monilinia fructicola*, a pathogen that does not attack pea. The toxicity of (+)-pisatin (**26**) to 50 fungal strains representing 45 species (Cruickshank, 1962) was studied. Only five of these fungi were tolerant of pisatin (less than 50% inhibited by 100 μg/mL), and all five were pathogens of pea. Only one of the 45 sensitive strains was a pea pathogen. Although subsequent surveys of the sensitivity of fungi to other phytoalexins and even to (+)-pisatin (**26**) revealed many exceptions to the correlation between tolerance and host range (Smith, 1982; VanEtten *et al.,* 1982), Cruickshank's initial observation firmly established the concept that tolerance to a phytoalexin might be important in pathogenicity. Phytoalexins accumulate in plants or cell cultures only transiently, because they are readily degraded or polymerized most of the time by extracellular peroxidases (VanEtten et al., 1982).

More direct evidence for the importance of phytoalexins as defence compounds is the increase in the resistance of tobacco (*Nicotiana tabacum*) to *Botrytis cinerea*, a fungal pathogen of tobacco (Hain *et al.*, 1993) and the increase in resistance of transgenic tomato (*Lycopersicon esculentum* Mill.) to *Phytophthora infestans* (Thomzik *et al.*, 1997). This

resistance was increased by transforming tobacco and tomato with a stilbene synthase that enabled the transformants to synthesize the grapevine (*Vitis vinifera*) phytoalexin resveratrol (**27**). The formation of stilbenes is considered to be a component of general defence mechanisms against pathogens in plants (Thomzik *et al.*, 1997). Two genes from the grapevine coding for stilbene synthase were transferred to tomato (cv. Vollendung) by means of *Agrobacterium tumefaciens*. Southern blot and Northern blot analyses demonstrated that both genes were stably integrated into the tomato genome and were expressed in transgenic regenerants and their progeny after fungal infection, wounding induction with elicitor, and UV irradiation (Thomzik *et al.*, 1997). The accumulation of the phytoalexin resveratrol (**27**), the product of stilbene synthase, was detectable shortly after fungal inoculation, resulting in a significant increase in the resistance of transgenic tomato to *Phytophthora infestans*.

1.4.1 Mechanisms by which fungi overcome plant defences

When phytopathogenic fungi can disarm the plant by detoxifying phytoalexins, the outcome of the plant-pathogen interaction can favour the pathogen and be detrimental to the plant (Pedras & Okanga, 1999). To date, several examples reported in the literature demonstrate that cruciferous fungal pathogens can efficiently detoxify phytoalexins (Pedras *et al.*, 2000). The discussion in this section will provide strong evidence that the pathogenicity of some fungi is linked to their ability to detoxify their host phytoalexins, which proves that at least in these interactions, phytoalexin production must be acting as a mechanism of disease resistance (Weltring, 1991).

1.4.1.1 Metabolism and detoxification of phytoalexins from family Leguminaceae

Most of the legume phytoalexins have the isoflavonoid skeleton, which suggests that they have similar biogenetic origin, derived from the mixed acetate-malonate and shikimate pathways. The isoflavonoids include isoflavones, isoflavanones, pterocarpans, rotenoids (Farooq & Tahara, 1999) and many others. Hydroxylation, epoxidation, hydration, reduction, conjugation, degradation, *O*-methylation and *O*-demethylation of isoflavonoids leading to the detoxification of antifungal substrates have been described in the literature through the use of various genera of plant pathogenic fungi such as *Fusarium*, *Colletotrichum*, *Ascochyta*, *Botrytis* and *Stemphylium* (VanEtten *et al.*, 1982). The plants in this family include pea (*Pisum sativum*) from which the phytoalexin (+)-pisatin (**26**) was isolated, bean (*Phaseolus vulgaris*), yam bean (*Pachyrrhizus erosus*), alfalfa (*Medicago sativa*), chickpea (*Cicer arietinum*), groundnut (*Arachis hypogaea*) and soybean. Phytoalexins from beans are kievitone (**31**) (Turbek *et al.*, 1990), phaseollidin (**32**), phaseollin (**33**), phaseollin isoflavan (**34**), 2,3-dehydrokievitone (**35**) and hydroxyphaseollin (**36**). It has been shown that phaseollidin (**32**) is the biosynthetic precursor of phaseollin (**33**), which is also the immediate precursor of phaseollin isoflavan (**34**) (Turbek *et al.*, 1992; Al-Douuri, 1997). Isoflavonoid phytoalexins from groundnut (*Arachis hypogaea*) include medicarpin (**28**), demethylmedicarpin (**29**), daidzein (**40**), formononetin (**41**), 7,4'-dimethoxy-2'-hydroxyisoflavone (**42**) and 7,2'-dihydroxy-4'-methoxyisoflavone (**43**) (Edwards & Strange, 1991). Phytoalexins from alfalfa and chickpea are medicarpin (**28**) and maackiain (**30**) (Denny & VanEtten, 1981), whereas soybean phytoalexins include glyceollin I (**37**), glyceollin II (**38**), and coumestrol (**44**) (Boue *et al.*, 1999). Cristacarpin (**39**) was isolated from *Erythrina crista-galli* together with **29** and **32** (Ingham *et al.*, 1980). Results obtained from a series of bioassays indicate that coumestrol (**44**) and the glyceollins (**37**, **38**) have antiestrogenic activity. Research has shown that antiestrogenic phytoestrogens suppress hormone-dependent cancers

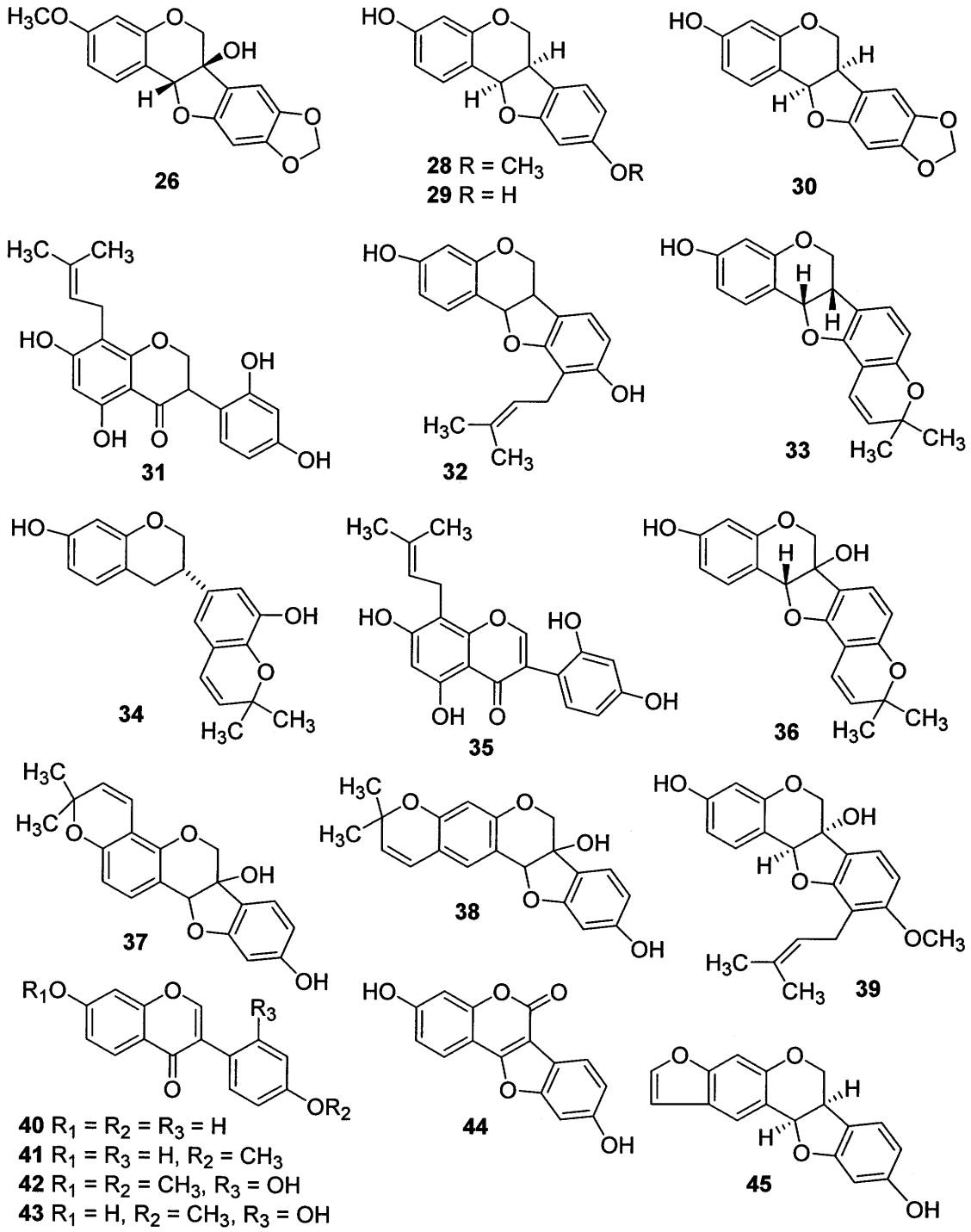

Figure 1.5 Isoflavonoid phytoalexins from legumes: (+)-pisatin (**26**); medicarpin (**28**); demethylmedicarpin (**29**); maackiain (**30**); kievitone (**31**); phaseollidin (**32**); phaseollin (**33**); phaseollin isoflavan (**34**); 2,3-dehydrokievitone (**35**); hydroxyphaseollin (**36**); glyceollin I (**37**); glyceollin II (**38**); cristacarpin (**39**); daidzein (**40**); formononetin (**41**); 7,4'-dimethoxy-2'-hydroxyisoflavone (**42**); 7,2'-dihydroxy-4'-methoxyisoflavone (**43**); coumestrol (**44**); neodunol (**45**).

(Boue *et al.*, 1999). Considering the current interest in phytoestrogens that can block the harmful effects of estradiol, soybean phytoalexins that accumulate in response to fungal elicitation may be beneficial to human health. Phytoalexins from yam bean include neodunol (**45**) and demethylmedicarpin (**29**) (Ingham, 1979). The structures of these isoflavonoid phytoalexins are shown in Figure 1.5.

The pea (*P. sativum*) phytoalexin (+)-pisatin (**26**) was metabolized by the pea fungal pathogen *Nectria haematococca* (Scheme 1.2) to (+)-6a-hydroxymaackiain (**46**) via demethylation, which is the degradation of the 3-*O*-methyl group (VanEtten *et al.*, 1975; Schäfer *et al.*, 1989). (+)-Pisatin (**26**) was also metabolized by *Ascochyta pisi* (Scheme 1.3) to (+)-6a-hydroxymaackiain (**46**) and a 1a-hydroxydienone-type metabolite (**47**) (VanEtten *et al.*, 1989).

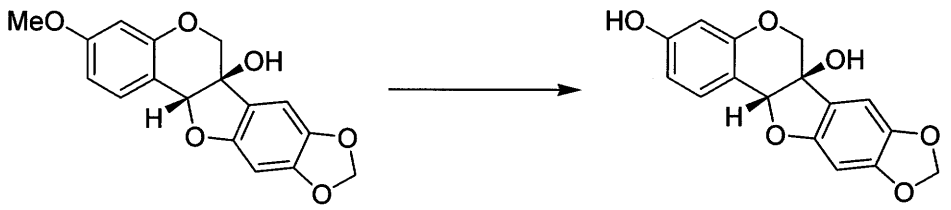

26 **46**

Scheme 1.2 Detoxification of the pea phytoalexin (+)-pisatin (**26**) by the fungal pathogen *Nectria haematococca* (VanEtten *et al.*, 1975; Schäfer *et al.*, 1989).

The antifungal activity of (+)-pisatin (**26**) and the demethylated product, (+)-6a-hydroxymaackiain (**46**) was compared to test whether this initial metabolic reaction led to detoxification (VanEtten *et al.*, 1975). It was established that several fungi (*Fusarium oxysporum*, f. sp. *pisi*, *Mycosphaerella pinodes*, *Phoma pinodella* and *Thanatephorus cucumeris* (all pea pathogens) (Desjardins & VanEtten, 1986) were substantially more sensitive to (+)-pisatin (**26**) than to (+)-6a-hydroxymaackiain (**46**) confirming that the metabolism is a detoxification process. In some isolates of *N. haematococca,* pisatin

demethylation is strongly inducible by (+)-pisatin (**26**). A number of analogues of **26** were tested for the ability to induce the demethylation activity in a highly virulent isolate (VanEtten & Barz, 1981). Some of these included (+)-6a-hydroxymaackiain, (+)-pterocarpin, 6-methoxy-1-tetralone, 7,4'-dimethoxyisoflavone and (-)-pisatin. None of these compounds was a better inducer than **26**, and all effective inducers had structural similarities to **26**. Overall, induction showed a high degree of specificity with regard to the structure of the inducer.

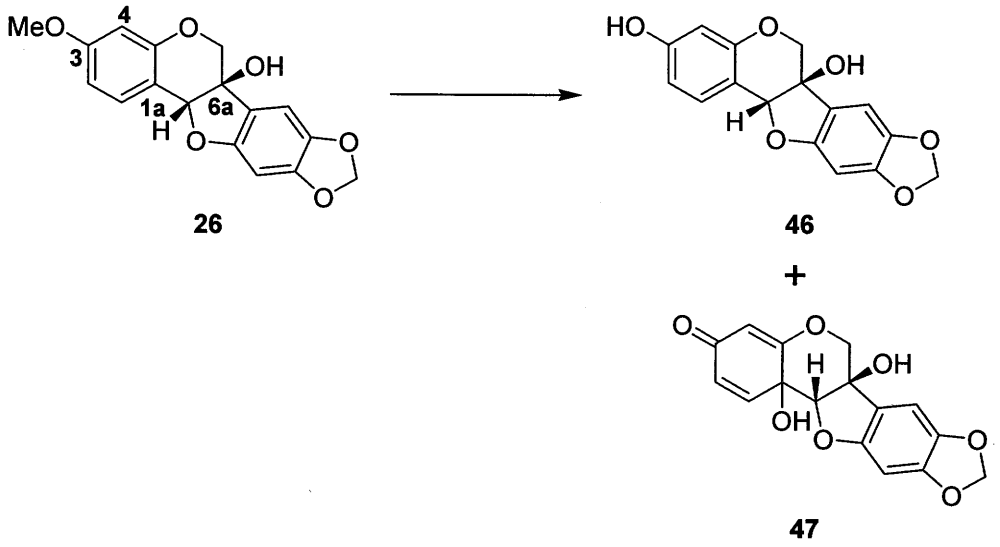

Scheme 1.3 Detoxification of the pea phytoalexin (+)-pisatin (**26**) by the fungal pathogen *Ascochyta pisi* (VanEtten *et al.*, 1989).

The detoxifying enzyme pisatin demethylase (Pda), which is inducible in *N. haematococca* Mating Population VI is a microsomal cytochrome P450 monooxygenase (Matthews & VanEtten, 1983; Maloney & VanEtten, 1994) and can be usefully compared to the cytochrome P450 system of mammalian liver, which also serves the function of detoxifying xenobiotic compounds. The Pda gene (*Pda1*) is the first member of a new family of cytochrome P450's. Through genetic analysis, six other pisatin demethylase

genes have been identified: *Pda2*, *Pda3, Pda4, Pda5, Pda6*, and *Pda7* (Mackintosh *et al.*, 1989; Funnell *et al.,* 2002). While *Pda1* and *Pda4* confer a high level of demethylase activity and hence these isolates have high virulence on pea, *Pda2*, *Pda3, Pda5, Pda6*, and *Pda7* encode low rates of demethylation. However, all highly virulent progenies always contained one of *Pda1* or *Pda4* and a combination of *Pda5* and *Pda7* (Funnell *et al.*, 2002). When *Pda1* was used to probe the DNA of other pea pathogens with *Pda* activity, only the DNA of *F. oxysporium* f. sp. *pisi* hybridized (Delserone *et al.*, 1999). A *Pda* homologue from this fungus has been cloned and sequenced and its amino acid sequence is 87% identical to the *N. haematococca* MP VI *Pda* gene and both genes have four introns in the same locations. Since *F. oxysporium* f. sp. *pisi* is taxonomically more related to *N. haematococca* MP VI than to the other fungi tested, this high degree of sequence similarity might reflect the phylogenetic similarities of the two organisms (VanEtten *et al.*, 2001).

An imposing amount of evidence suggests that the Pda of *N. haematococca* MP VI has specifically evolved to detoxify pisatin. In addition to being a P450 enzyme, Pda has a low K_m for pisatin, a high degree of substrate specificity for pisatin and a selective induction by pisatin (VanEtten et al., 2001). Furthermore, Pda induction occurs early in the infection process, pisatin appears to be the plant signal that induces Pda during pathogenesis and lack of inducibility may render the gene unable to function as a virulence trait. This line of evidence suggest that Pda evolved specifically to catalyze the detoxification of pisatin and, also, that a specific regulatory mechanism evolved to control the production of this virulence trait (VanEtten *et al.,* 2001).

The possibility that pisatin is a general defence factor, that is, that *Pda* can confer pathogenicity to fungi not normally pathogenic on pea was investigated (Schäfer *et al.*, 1989). Genes encoding Pda were transformed into and highly expressed in *Cochliobolus heterostrophus*, a fungal pathogen of maize but not of pea, and *Aspergillus nidulans*, a saprophytic fungus, neither of which produces a detectable amount of Pda. Transformants contained as much *Pda* as wild type *N. haematococca.* Recombinant *C. heterostrophus*

was normally virulent on maize, but it also caused symptoms on pea, whereas recombinant *A. nidulans* did not affect pea (Schäfer *et al.*, 1989). These studies indicated that phytoalexins can function in non-specific resistance of plants to microbes and that saprophytes lack genes for basic pathogenicity.

Earlier studies on the fungal metabolism of the phytoalexin medicarpin (**28**) revealed only alfalfa pathogenic fungi could metabolize it. The degradation of **28** was first reported using *Stemphylium botryosum* (Farooq & Tahara, 1999), which catalyzed the hydrogenolysis to yield vesitol (**48**). Hydroxylation at a tertiary carbon C-6a to yield 6a-hydroxymedicarpin (**49**) was observed by fermentation of **28** with *Botrytis cinerea* (Ingham, 1976) and *Sclerotinia trifoliorum* (Farooq & Tahara, 1999).

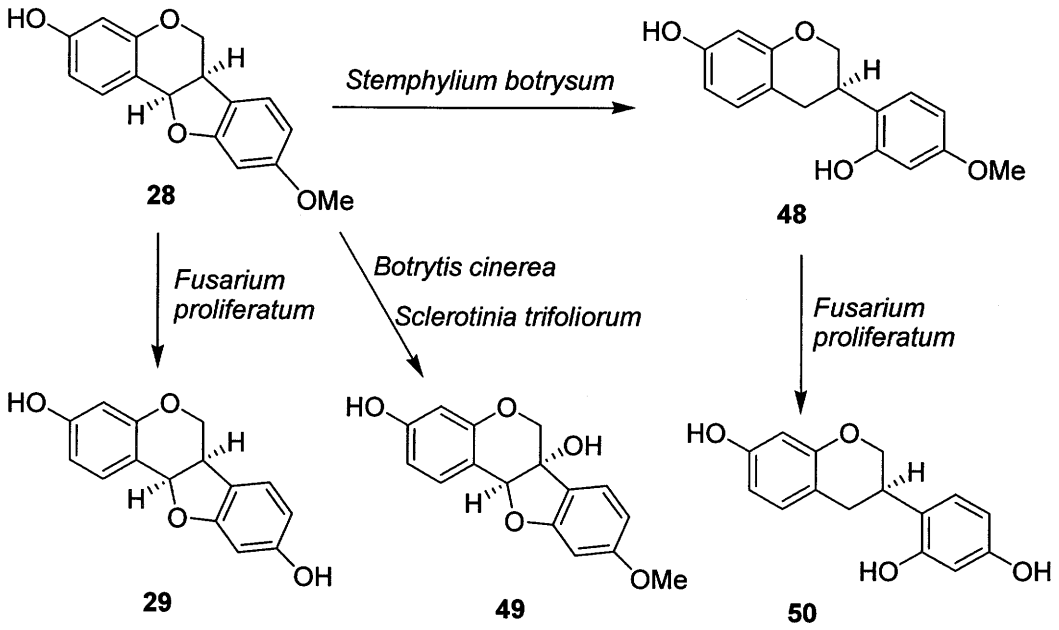

Scheme1.4 Detoxification of medicarpin (**28**) by *Fusarium proliferatum (*Weltring *et al.*, 1983), *Botrytis cinerea* (Ingham, 1976), *Sclerotinia trifoliorum* and *Stemphylum botrysum* (Farooq & Tahara, 1999), (pathogens of alfalfa and chickpea).

Demethylation products of **28** and **48** demethylmedicarpin (**29**) and demethylvesitol (**50**) were isolated when **28** and **48** were incubated with *Fusarium proliferatum*. These are outlined in Scheme 1.4. Medicarpin (**28**) was also metabolized by *Fusarium oxysporum* f. sp. *Lycopersici* (Weltring *et al.*, 1983) to isoflaven (**51**), 3-arylcoumarin (**52**), stilbene and benzoate via vesitol (**48**). Oxidative dearomatization of A ring, characteristic of the pterocarpan ring to yield a 1a-hydroxydienone-type metabolite (**53**) was catalyzed by *Nectria haematococca*, (a chickpea pathogen) which also transformed medicarpin (**28**) to less toxic 6a-hydroxypterocarpans (**49**) and to the isoflavanone vesitone (**54**) as outlined in Scheme 1.5 (Denny & VanEtten, 1982).

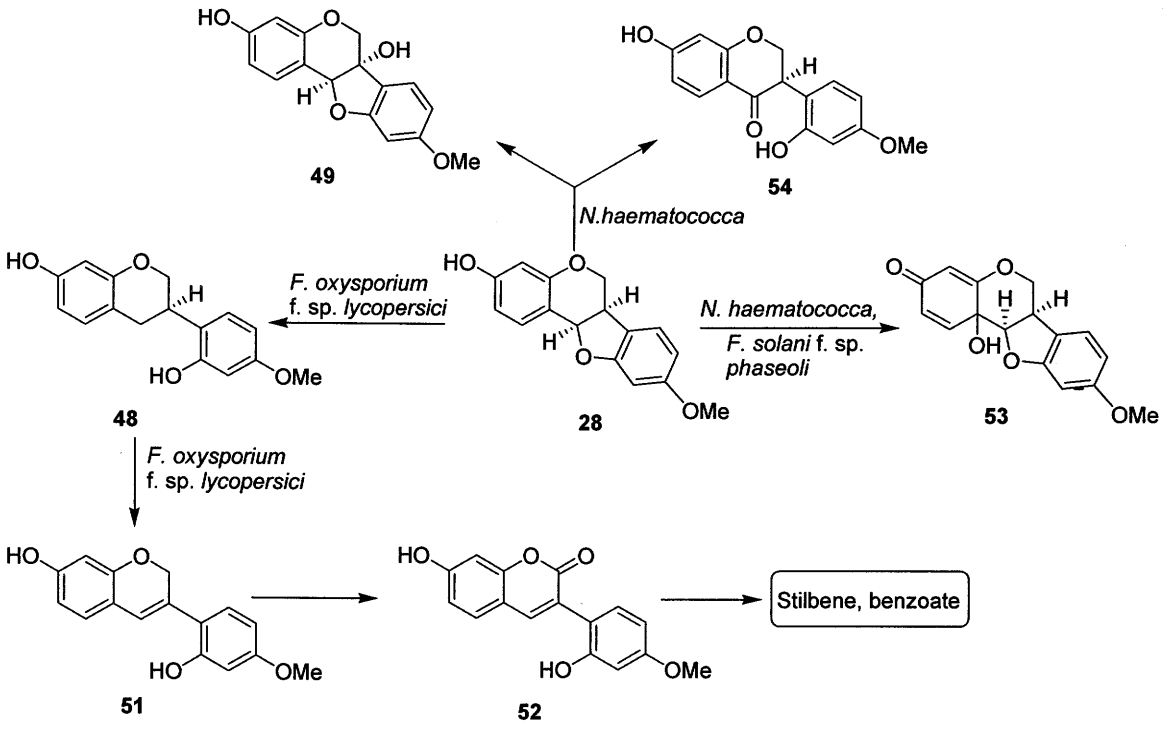

Scheme 1.5 Detoxification of medicarpin (**28**) by *Nectria haematococca*, *Fusarium oxysporium* f. sp. *lycopersici* and *Fusarium solani* f. sp. *phaseoli* (pathogens of alfalfa and chickpea) (Denny & VanEtten, 1982).

The metabolism and detoxification of medicarpin (**28**) by four strains of *Ascochyta rabiei* (Lucy *et al.*, 1988; Höhl *et al.*, 1989) another chickpea pathogen (using mycelial preparations and crude protein extract) resulted in the identification of ten metabolites (**29**, **48**, **50**, **52**, **53**, **55-59**), which seemed to be degraded to non-aromatic compounds. These metabolites were less toxic to the fungus than **28** demonstrating that the metabolism is a detoxification process (Figure 1.6).

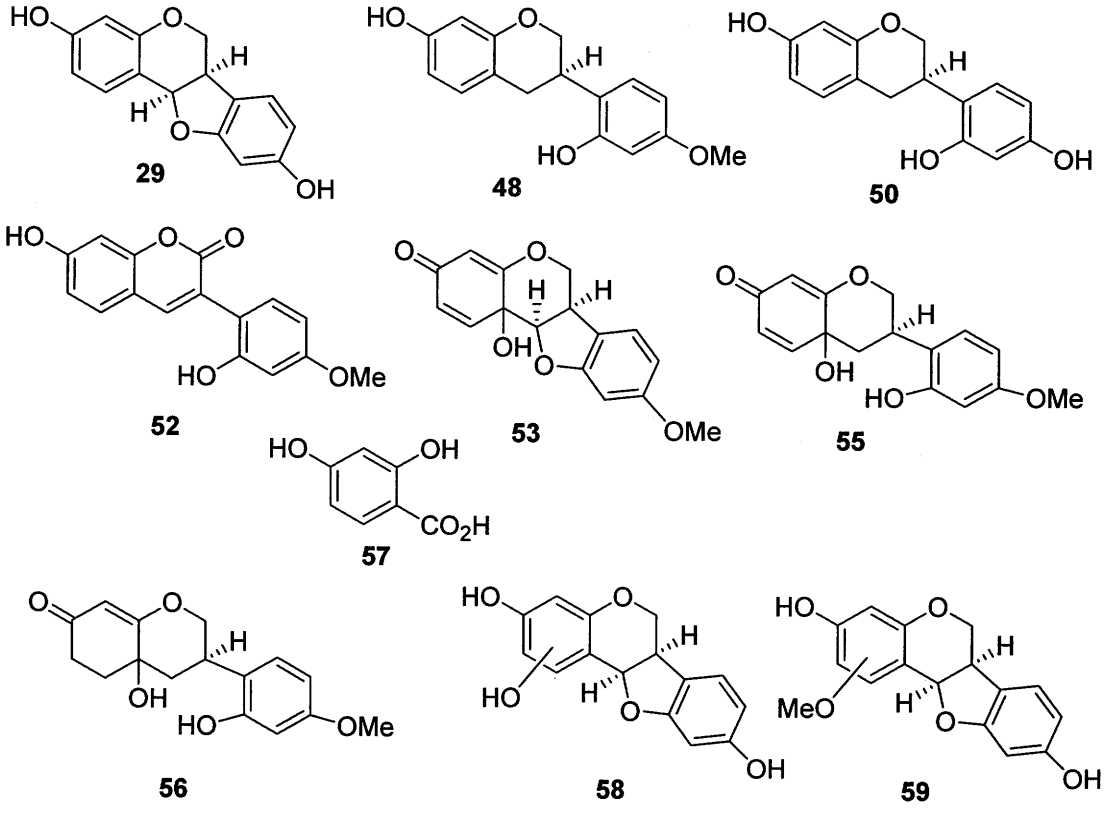

Figure 1.6 Metabolites from the detoxification of the alfalfa and chickpea phytoalexin medicarpin (**28**) by the fungal pathogen *Ascochyta rabiei* (Lucy *et al.*, 1988; Höhl *et al.*, 1989).

Microbial transformation of the phytoalexin maackiain (**30**) was first reported using *Stemphylium botryosum* (Farooq & Tahara, 1999), which metabolized **30** to maackiainisoflavan (**60**). Maackiain (**30**) has been detoxified by *N. haematococca* MP VI to afford (–)-6a-hydroxymaackiain (**46a**), a 1a-hydroxydienone-type metabolite (**61**) and sophorol (**62**) as outlined in Scheme 1.6 (Denny & VanEtten, 1982). The reductase leading to the isoflavan **60** (Höhl *et al.*, 1989) and the hydroxylase leading to the 1a-hydroxydienone **61** (Farooq & Tahara, 1999) have been purified and characterized. Field isolates of *N. haematococca* MP VI were tested for their ability to metabolize maackiain, tolerance of maackiain, and virulence on chickpea (Lucy *et al.*, 1988). The isolates differed in these traits, including which of the metabolic routes were used to metabolize maackiain as well as whether maackiain was metabolized at all. Most of the isolates were quite tolerant of maackiain, as the growth was inhibited by less than 25% at 50 μg/mL. The

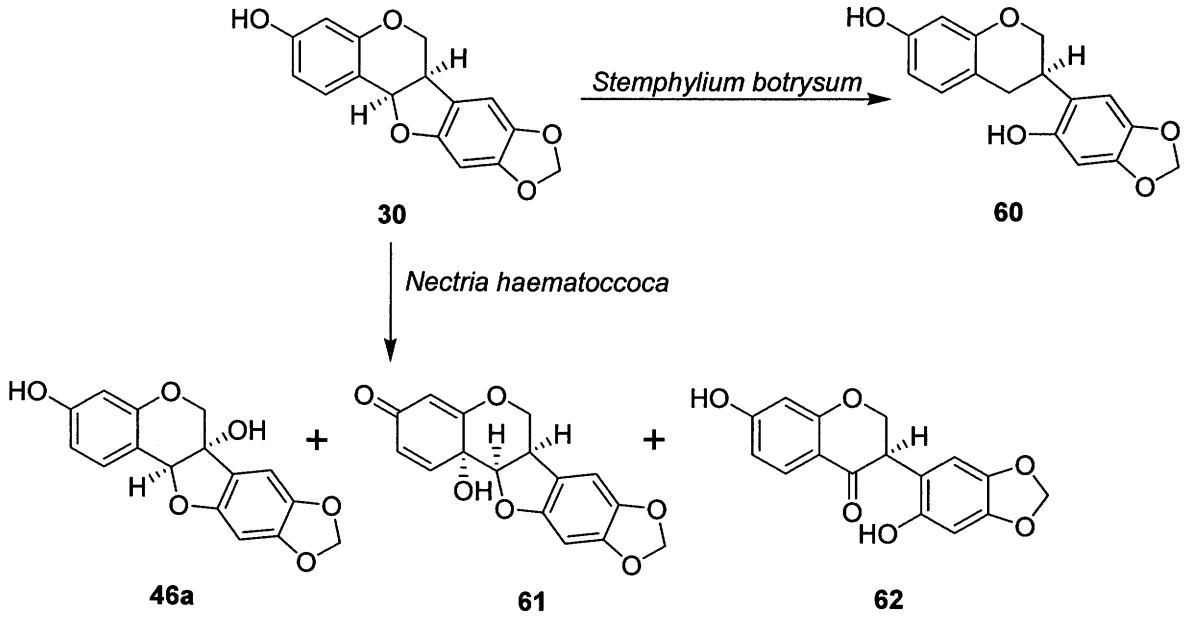

Scheme 1.6 Detoxification of the alfalfa and chickpea phytoalexin maackiain (**30**) by the fungal pathogens *Nectria haematococca* and *Stemphylium botryosum* (Denny & VanEtten. 1982).

more sensitive isolates were all low in virulence on chickpea, suggesting that some level of tolerance to maackiain is required for high virulence on this plant (Lucy *et al.,* 1988). All isolates that were able to metabolize maackiain (**30**) were tolerant of it, and most isolates lacking this ability were sensitive. However, several maackiain-tolerant isolates failed to metabolize maackiain, and one of these was virulent on chickpea, suggesting that phytoalexin tolerance mechanisms other than detoxification may also be important. Tolerance of medicarpin (**28**) was strongly correlated with maackiain (**30**) tolerance in the 53 isolates examined for both traits. By genetic analysis, three different maackiain metabolism genes have been identified in *N. haematococca* MP VI (Miao & VanEtten, 1992a). Strains carrying *Mak1* and *Mak2* detoxified maackiain (**30**) via 1a-hydroxylation to 1a-hydroxymaackiain (**61**); *Mak3* confers 6a-hydroxylation to (–)-6a-hydroxymaackiain (**46a**) (Scheme 1.6). *Mak1* and *Mak2* were unusual in that they often failed to be inherited by progeny. *Mak1* was closely linked to *Pda6*, a new member in a family of genes in *N. haematococca* that encode enzymes for detoxification of pisatin. Like *Mak1, pda6* was also transmitted irregularly to progeny (Miao & VanEtten, 1992a). Although the unusual meiotic behaviours of some *Mak1* genes complicate gene analysis, identification of these genes should afford a more thorough evaluation of the role of phytoalexin detoxification in the pathogenesis of *N. haematococca* on chickpea. Phenotypes of progeny were examined from crosses of the fungus that segregated for genes (*Mak* genes) controlling phytoalexin metabolism. *Mak1* and *Mak2* were linked to higher tolerance of the phytoalexins and high virulence on chickpea (Miao & VanEtten, 1992b). These results indicate that this metabolic reaction is a mechanism for increased phytoalexin tolerance in the fungus, which thereby allows a higher virulence on chickpea. *Mak3* also increased tolerance to maackiain (**30**) in strains which carried it; however the contribution of *Mak3* to the overall level of pathogenesis could not be evaluated because most progeny from the cross segregating for this gene were low in virulence. Thus, metabolic detoxification of phytoalexins appeared to be necessary, as demonstrated in the *Mak1* and *Mak2* crosses, but not sufficient by itself,

as in the *Mak3* cross, for high virulence of *N. haematococca* on chickpea (Miao & VanEtten, 1992b). The contribution of *Mak1* to the virulence of *N. haematococca* MP VI on chickpea was tested (Enkerli *et al.*, 1998). The *Mak1* gene was disrupted in a highly virulent Mak^+ isolate or added to a weakly virulent Mak^- isolate via transformation. The disruption of *Mak1* decreased virulence to a moderate level, while addition of multiple copies of *Mak1* increased virulence to either a moderate or high level. These data demonstrate that maackiain (**30**) detoxification is a determinant, but not the only determinant of virulence in *N. haematococca* MP VI isolates capable of causing disease on chickpea (Enkerli *et al.*, 1998). *Mak1* is located on a 1.6-Mb conditionally dispensable chromosome.

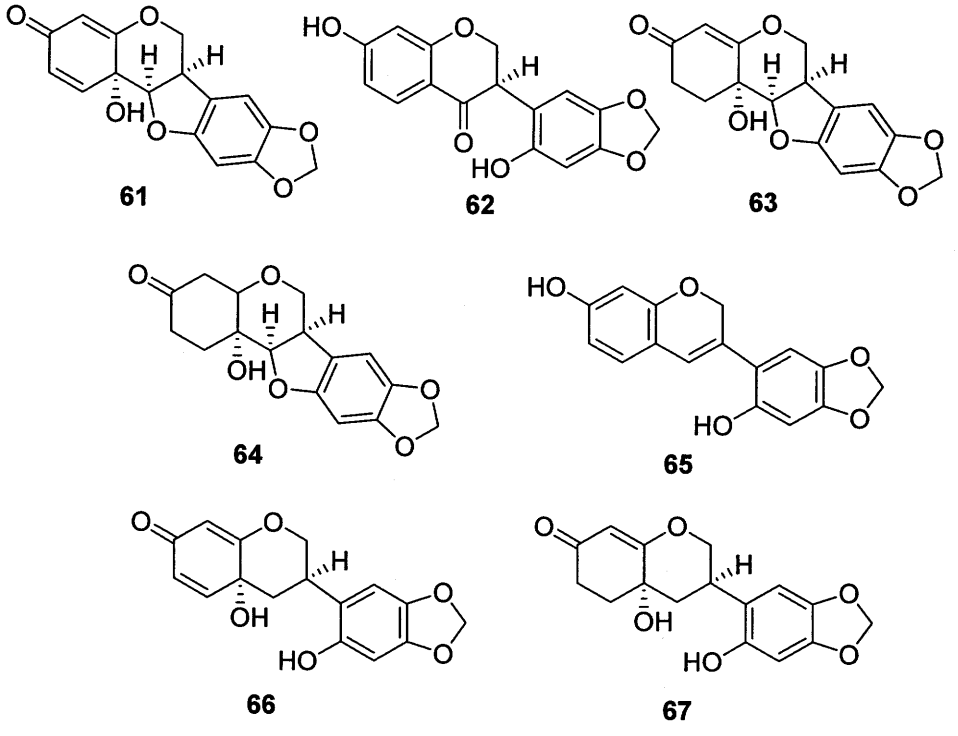

Figure 1.7 Metabolites from the detoxification of the alfalfa and chickpea phytoalexin maackiain (**30**) by the fungal pathogen *Ascochyta rabiei* (Lucy *et al.*, 1988; Höhl *et al.*, 1989).

To ascertain if there are additional genes influencing virulence towards chickpea stems on the *Mak1* chromosome, the loss of this chromosome was chemically induced in an isolate containing the disrupted *Mak1* gene. Loss of the *Mak1* chromosome did not reduce virulence towards chickpea stems further, thus indicating that no additional genes for virulence on this part of the host plant are located on the *Mak1* chromosome (Enkerli *et al.*, 1998).The metabolism and detoxification of maackiain (**30**) by ten strains of *Ascochyta rabiei* (using mycelial preparations and crude protein extract) resulted in the detection and isolation of seven metabolites **61-67**, which have lower antifungal activity than **30** (Lucy *et al.*, 1988; Höhl *et al.*, 1989). The structures of these metabolites are shown in Figure 1.7. Another fungal pathogen *Cercospora medicaginis* detoxified maackiain (**30**) to **61a** and **68** (Soby *et al.*, 1996) in which the hydroxyl groups are trans to the bridgehead protons and are the 1a epimers of the previously described cis forms **61** and **67** (Scheme 1.7). Metabolites **61a** and **68** were found to be less toxic to *N. haematococca* and *Saccharomyces cerevisiae* indicating that the metabolism is a detoxification process (Soby *et al.*, 1996).

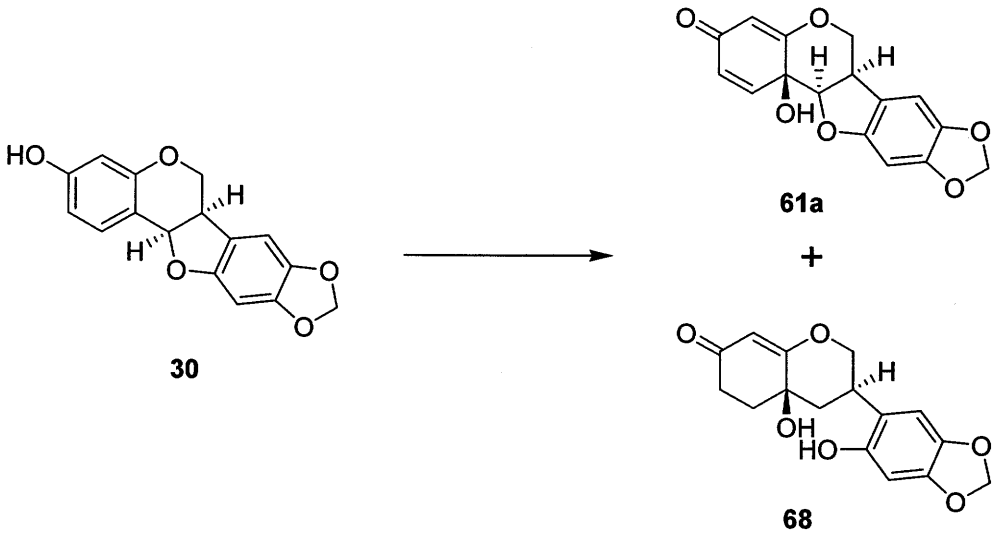

Scheme 1.7 Detoxification of the alfalfa and chickpea phytoalexin maackiain (**30**) by the fungal pathogen *Cercospora medicaginis* (Soby *et al.*, 1996).

A fungal monooxygenase, pterocarpan 1a-hydroxylase from *Ascochyta rabiei* is reported as a constitutive enzyme, which catalyzes the conversion of medicarpin (**28**) and maackiain (**30**) to their 1a-hydroxy-1,4-dien-3-one derivatives (**53** and **61**). Although the reaction centres in their substrates and the class of reaction products are apparently different, both FAD-dependent monooxygenases, Ascochyta hydroxylase and Botrytis epoxidase showed common properties: a) low amounts of FAD are necessary for maximal enzyme activity, b) NADPH is far more effective (3 – 10 times) than NADH in the reaction mixture without additional FAD, and c) in the presence of enough amounts of FAD, the efficiency of NADH as a hydride donor increases comparably to that of NADPH (Farooq & Tahara, 1999).

In recent studies, it has been shown that natural variants of pathogens, which either do not detoxify their host phytoalexin, or do so more slowly, or are more sensitive are less virulent (VanEtten *et al.,* 2001). Such observations of natural variation in phytoalexin sensitivity and virulence have been made previously with a number of other pathogenic fungi and are consistent with the hypothesis that decreasing the phytoalexin tolerance of a fungal species will decrease its virulence on a specific plant host. Results with specific mutants of *N. haematococca* have confirmed this hypothesis and shown that phytoalexin tolerance can be a virulence trait. *N. haematococca* has a broad host range that includes chickpea and pea and early studies demonstrated that all isolates pathogenic on pea had the ability to detoxify pisatin via demethylation and that most isolates virulent on chickpea had the ability to detoxify the chickpea phytoalexins medicarpin (**28**) and maackiain (**30**) (Lucy *et al.*, 1988; VanEtten *et al.*, 1980). Once the genes that encode the enzymes catalyzing these reactions were cloned, the role of these reactions in pathogenicity was determined by mutating the genes via transformation mediated gene disruptions. In both cases, the virulence of the fungus on its respective host was reduced but not eliminated, indicating that phytoalexin detoxification is a virulence trait in this fungus. In both cases, the mutants retained substantial tolerance of these phytoalexins corroborating earlier work indicating

that *N. haematococca* had non-degradative mechanisms for tolerance to all three phytoalexins (Denny *et al.*, 1987; Denny & VanEtten, 1981). Thus, in this fungus two different types of tolerance mechanisms may operate in concert and the elimination of both mechanisms may be required to make it non-pathogenic. The observation that transformation of the gene for detoxification of (+)-pisatin (**26**) into non-pathogens of pea converts the transformants into weak pathogens further supports the conclusion that pisatin detoxification is a virulence trait (VanEtten *et al.*, 2001).

The bean phytoalexin kievitone (**31**) was detoxified by *F. solani* f. sp. *phaseoli* to kievitone hydrate **69** (Scheme 1.8) (Kuhn *et al.*, 1979; Turbek *et al.*, 1990). The enzyme responsible for this transformation has also been characterized (Smith *et al.*, 1981). The enzyme called kievitone hydratase (KHase) is an acidic extracellular glycoprotein with MW 158-188 kDa, an isoelectric point of pH 5.1, optimum temperature 55 °C and optimum pH 5.5 at 27 °C. It was purified from culture broth by ion exchange and affinity chromatography, gel filtration and isoelectric focusing. The kHase cDNA and gene were cloned (Li *et al.*, 1995) and expressed in transgenic *Neurospora crassa* and *Emericella nidulans*. Total 350 amino acids of the protein are encoded whereas 19 amino acid terminal transit peptide is removed during maturation and secretion.

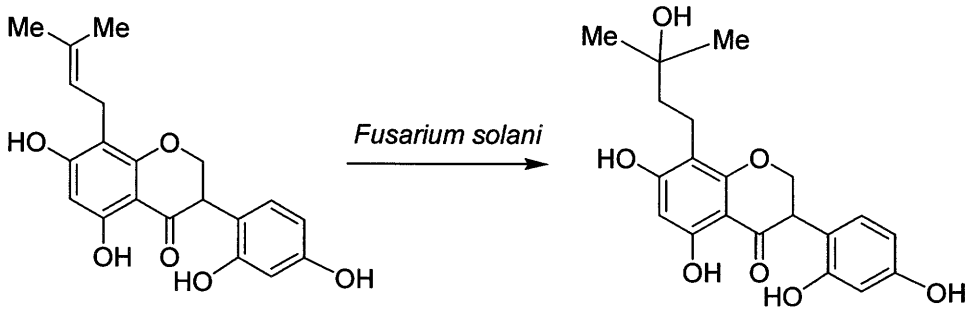

31 **69**

Scheme 1.8 Detoxification of the bean phytoalexin kievitone (**31**) by fungal pathogen *Fusarium solani* f. sp. *Phaseoli* (Smith *et al.*, 1980).

The enzyme is highly glycosylated and a polypeptide sequence possesses seven different sites for *N*-glycosylation. In a survey of different isolates and mutants of *F. solani* the level of KHase activity correlated with the degree of tolerance to kievitone and pathogenicity on bean (Weltring, 1991).

2,3-Dehydrokievitone (**35**) was metabolized by *Aspergillus flavus* and *Botrytis cinerea* (Tahara *et al.,* 1987) to three metabolites namely dihydrofurano-isoflavone (**70**), dihydropyrano-isoflavone (**71**) and 2,3-dehydrokievitone glycol (**72**) as outlined in Scheme 1.9).

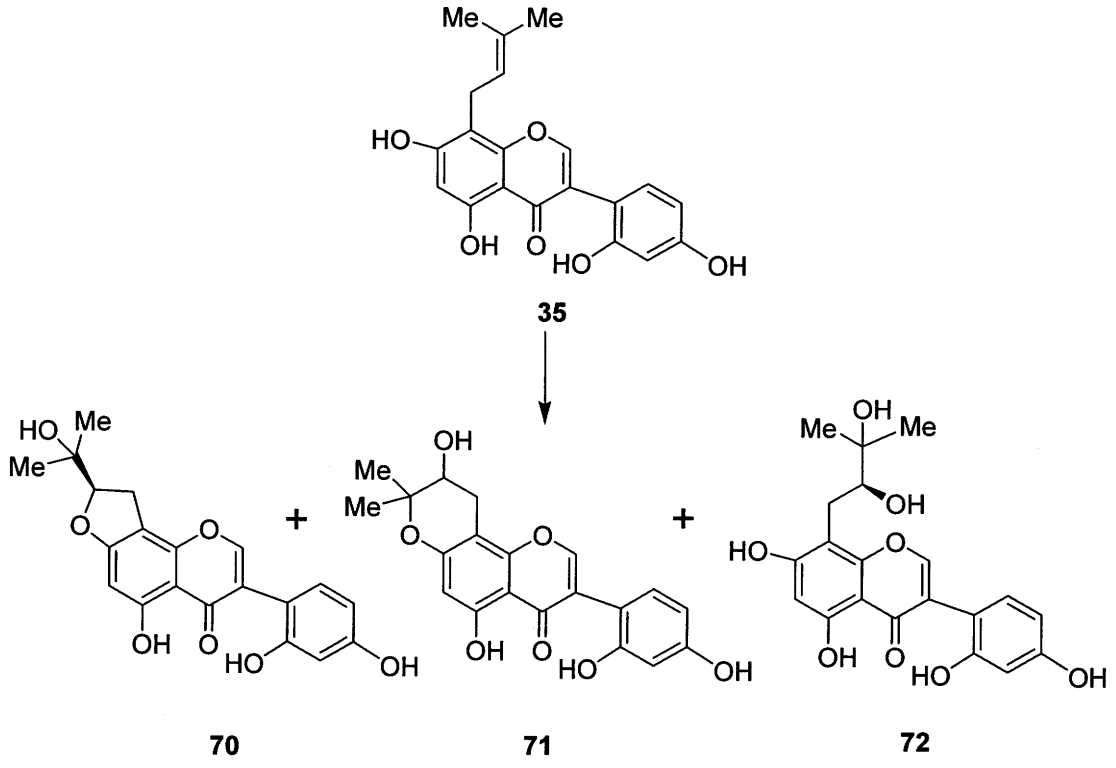

Scheme 1.9 Detoxification of the bean phytoalexin 2,3-dehydrokievitone (**35**) by fungal pathogens *Aspergillus flavus* and *Botrytis cinerea* (Tahara *et al.,* 1987).

Phaseollidin (**32**), another bean phytoalexin was detoxified by *F. solani* f. sp. *phaseoli* to phaseollidin hydrate **73** (Scheme 1.10) (Turbek *et al.*, 1992). In another set of experiments the isoflavonoid phytoalexins kievitone (**31**) and phaseollidin (**32**), added to liquid cultures of *F. solani* were simultaneously detoxified to kievitone hydrate (**69**) and phaseollidin hydrate (**73**), respectively. Both phytoalexins were transformed within 24 hours of incubation. However a purified preparation of KHase did not accomplish simultaneous detoxification; kievitone (**31**) was detoxified but phaseollidin (**32**) was not. This confirmed that the hydratases involved in the detoxification of **31** and **32** were different (Miao & VanEtten, 1992c).

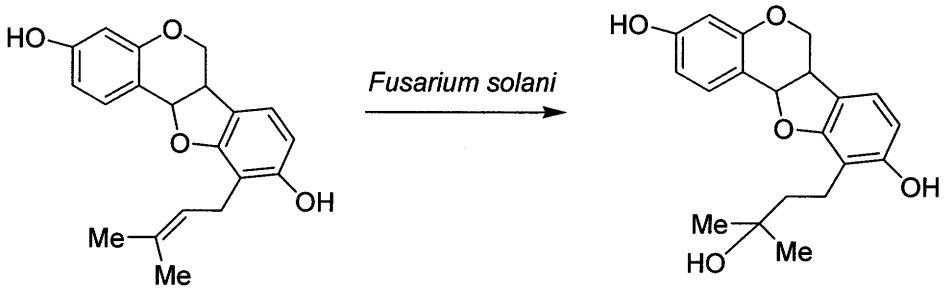

32 **73**

Scheme 1.10 Detoxification of the bean phytoalexin phaseollidin (**32**) by the fungal pathogen *Fusarium solani* f. sp. *Phaseoli* (Turbek *et al.*, 1992).

A role in pathogenesis in addition to detoxification has also been suggested for phaseollidin hydratase during the infection of bean by *Fusarium solani* f. sp. *Phaseoli* since phaseollidin (**32**) is the biosynthetic precursor of phaseollin (**33**) and phaseollin isoflavan (**34**). If phaseollidin (**32**) is made inaccessible as an intermediate in this biosynthetic scheme owing to hydration of the isopentyl side chain by the fungal enzyme (thus preventing the cyclization of this chain to produce phaseollin) then the resistance of

the host may be reduced owing to a decreased capacity to synthesize the remaining phytoalexins in the pathway (VanEtten *et al.*, 1995).

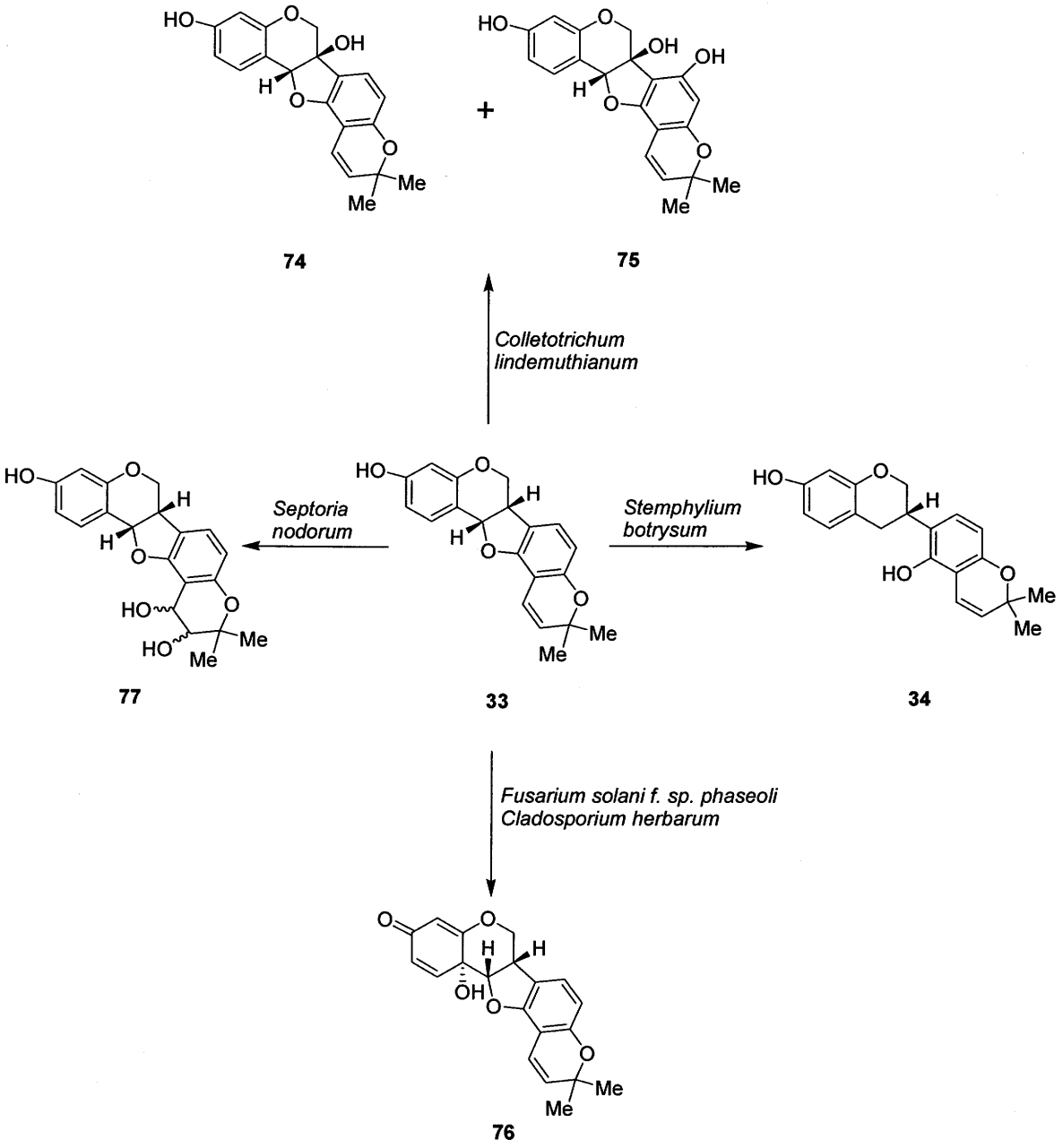

Scheme 1.11 Detoxification of the bean phytoalexin phaseollin (**33**) by fungal pathogens *Stemphylium botryosum*, *Colletotrichum lindemuthianum* (Farooq & Tahara, 1999), *Septoria nodorum* (Bailey et al., 1977), *Fusarium solani* f. sp. *phaseoli* and *Cladosporium herbarum* (Van den Heuvel *et al.*, 1974).

The metabolism of the phytoalexin phaseollin (**33**) by *Stemphylium botryosum* yielded the phytoalexin phaseollin isoflavan (**34**) and by *Collectotrichum lindemuthianum* yielded 6a-hydroxyphaseollin (**74**) and 6a,7-dihydroxyphaseollin (**75**) (Farooq & Tahara, 1999). Two pathogens, *Fusarium solani* f. sp. *phaseoli* and *Cladosporium herbarum* (Van den Heuvel *et al.*, 1974) oxidized **33** to 1a-hydroxyphaseollone (**76**). The metabolism of phaseollin (**33**) by *Septoria nodorum* (non pathogenic to *Phaseolus* species) (Scheme 1.11), afforded a mixture of isomeric 11,12-dihydrodihydroxyphaseollin (**77**) (Bailey *et al.*, 1977).

The groundnut phytoalexin daidzein (**40**) was metabolized by the fungal pathogen *Aspergillus saitoi* (Scheme 1.12) to the potent antioxidative isoflavone 8-hydroxydaidzein (**78**) (Esaki *et al.*, 1998).

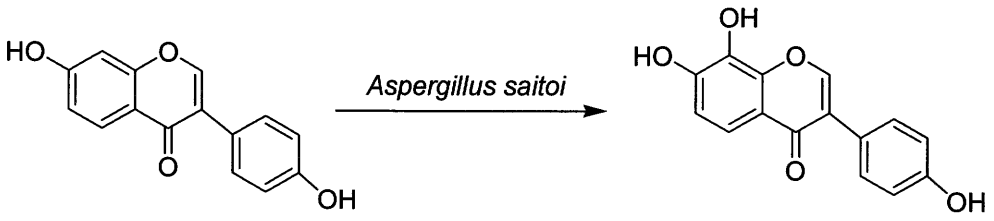

40 **78**

Scheme 1.12 Detoxification of the groundnut phytoalexin daidzein (**40**) by the fungal pathogen *Aspergillus saitoi* (Esaki *et al.*, 1998).

The groundnut phytoalexin formononetin (**41**) was also metabolized by fungal pathogen *Fusarium proliferatum* (Scheme 1.13) to the phytoalexin daidzein (**40**), and 7-*O*-methylformononetin (**79**) where **79** was the major product (Weltring, 1982). *Ascochyta rabiei,* a causative agent of blight of chickpea, like many *Fusarium* species is capable of

degrading the phytoalexins and can therefore, survive the plant defences through detoxification (VanEtten *et al.*, 1982).

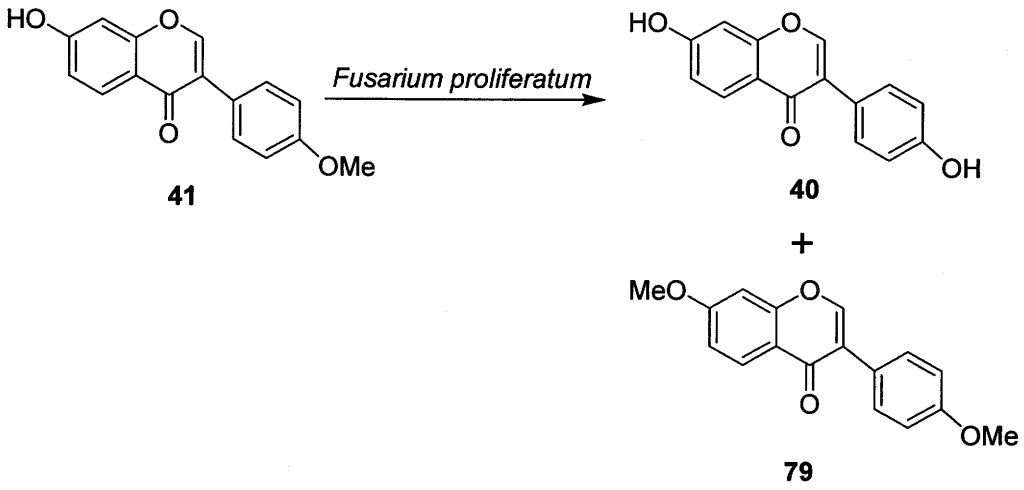

Scheme 1.13 Detoxification of the groundnut phytoalexin formononetin (**41**) by the fungal pathogen *Fusarium proliferatum* (Weltring, 1982).

1.4.1.2 Metabolism and detoxification of phytoalexins from family Solanaceae

Phytoalexins from plants of the Solanaceae family are from diverse biogenetic origins. They include the sesquiterpenoids and polyacetylenes derived from the acetate-mevalonate pathway, coumarins and stilbenoids derived from shikimate pathway, isoflavans and isoflavones derived from mixed acetate-mevalonate and shikimate pathways. Plants of the Solanaceae family include potato (*Solanum tuberosum*), tomato (*Lycopersicon esculentus*), pepper (*Capsicum annum*), tobacco (*Nicotiana tabacum*), sunflower (*Helianthus annus* L.) and carrot (*Daucus carota*).

Coumarin phytoalexins (Figure 1.8) isolated from tobacco include scopoletin (**80**), those from sunflower include scopoletin (**80**), ayapin (**81**), chlorogenic acid (**87**), and caffeic acid (**88**) (Tal & Robeson, 1986). 6-Methoxymellein (**82**) was isolated from carrot

(*Daucus carota*) (Kurosaki & Nishi, 1983), hydroquinone (**90**) and phloretin (**85**) were isolated from *Xanthium canadense* (Kuzel & Miller, 1950) and *Loiseleuria procumbens* (Cuendet *et al.*, 2000) respectively. Loureirin A, (**83**), and flavonoid phytoalexins like 7,4'-dihydroxyflavan (**89**), and 7-hydroxy-4'-methoxyflavan (**91**) were isolated from *Dracaena cochinchinensis* (Wang *et al.*, 1999).

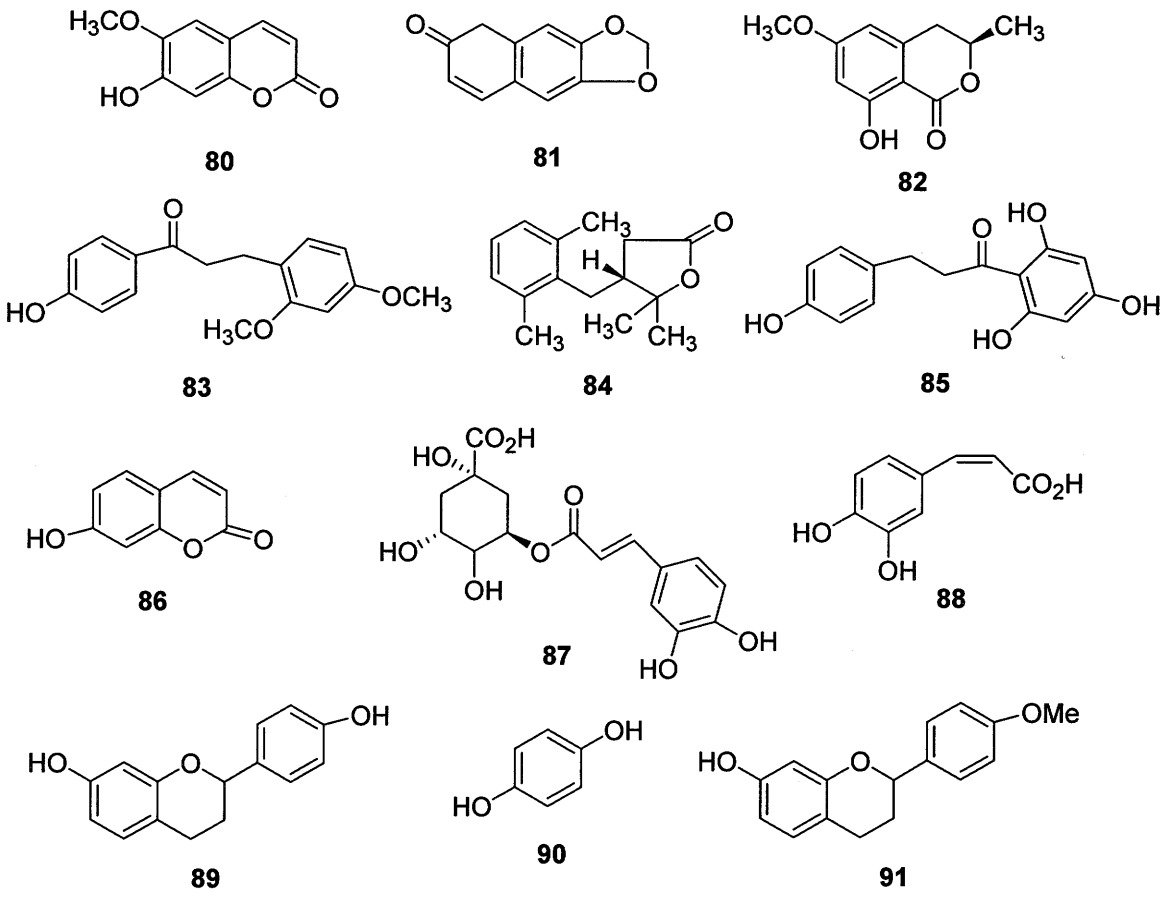

Figure 1.8 Coumarin and flavonoid phytoalexins from plants of the family Solanaceae: scopoletin (**80**); ayapin (**81**); 6-methoxymellein (**82**); loureirin (**83**); solafuranone (**84**); phloretin (**85**); umberlliferone (**86**); chlorogenic acid (**87**); caffeic acid (**88**); 7,4'-dihydroxyflavan (**89**); hydroquinone (**90**); 7-hydroxy-4'-methoxyflavan (**91**).

Solafuranone (**84**) and sesquiterpenoid phytoalexins like solavetivone (**113**) and hydroxyl solavetivone (**114**) were isolated from *Solanum indicum* (Syu *et al.*, 2001); umbelliferone (**86**) was obtained from *Chamomilla recutita* L. Rauschert (Repcak *et al.*, 2001), a medicinal plant.

Growth inhibition studies with *S. sclerotiorum* (pathogen of sunflower) revealed that both scopoletin (**80**) and ayapin (**81**) inhibited its mycelia growth in vitro, but at different rates (Urdangarin *et al.,* 1999). The concentration necessary to obtain 50% inhibition of fungal growth (IC_{50} values) determined for **80** and **81** were 0.16 mM and 1.5 mM respectively. Other sunflower phytoalexins such as chlorogenic acid (**87**) and caffeic acid (**88**) had no inhibitory effect on *S. sclerotiorum* growth at concentrations as high as 2 mM. These results, together with previously reported data, suggest that coumarin biosynthesis-accumulation in sunflower may be another target for plant breeding and genetic engineering strategies aimed at obtaining sunflower varieties with enhanced resistance to Sclerotinia rot (Urdangarin *et al.,* 1999).

Polyacetylenic phytoalexins like falcarindiol (**93**) (Kemp, 1998), falcarinol (**92**) and cis-tetradeca-6-ene-1,3-diyne-5,8-diol (**99**) (De Wit & Kodde, 1981), have been isolated from tomato (*Lysopersicon esculentus*) (Figure 1.9). Other polyacetylenic phytoalexins from tomato include wyerone (**94**), wyerone acid (**95**), wyerone epoxide (**96**), safynol (**97**) and dehydrosafynol (**98**) (Figure 1.9). **94**, **95** and **96** have also been isolated from broad bean (*Vicia fabae*), a legume (Hargreaves *et al.*, 1976), whilst **97** and **98** were isolated from safflower (Nakada *et al.*, 1977). Despite the very wide variety of structures, the metabolism of only a few types has been studied. The metabolism of the polyacetylenic phytoalexin wyerone epoxide (**96**) by *Botrytis cinerea* (Scheme 1.14) resulted in wyerol epoxide (**100**) (Hargreaves *et al.*, 1976). Similarly, *Botrytis fabae* metabolized wyerone epoxide (**96**) to wyerol epoxide (**100**) and dihydrodihydrowyerol (**101**) (Scheme 1.14). The ED_{50}'s for activity of wyerone epoxide (**100**) against germ tube growth by *B. cinerea* and *B. fabae* were 6.4 and 16.0 μg/mL respectively. The metabolites were less antifungal, but

wyerol epoxide (**100**) was more active against *B. fabae* (ED_{50} 38.5 μg/mL) than *B. cinerea* (ED_{50} 583 μg/mL). Dihydrodihydroxywyerol (**101**) did not inhibit germ tube growth at the highest concentration tested (100 μg/mL). These biotransformation results indicate that the metabolism of wyerone epoxide (**96**) by *B. cinerea* and *B. fabae* is a detoxification process (Hargreaves *et al.*, 1976).

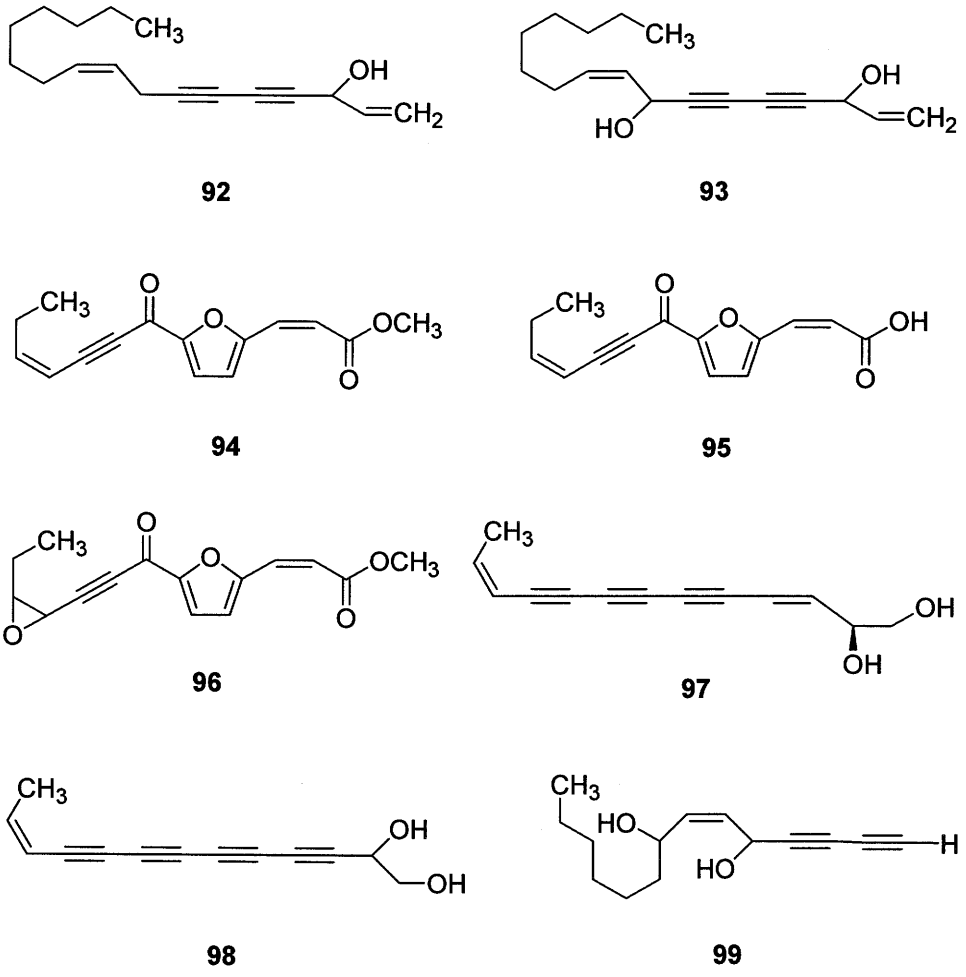

Figure 1.9 Polyacetylenic phytoalexins from tomato (Solanaceae) and broad bean (Leguminaceae): falcarinol (**92**); falcarindiol (**93**); wyerone (**94**); wyerone acid (**95**); wyerone epoxide (**96**); safynol (**97**); dehydrosafynol (**98**); *cis*-tetradeca-6-ene-1,3-diyne-5,8-diol (**99**).

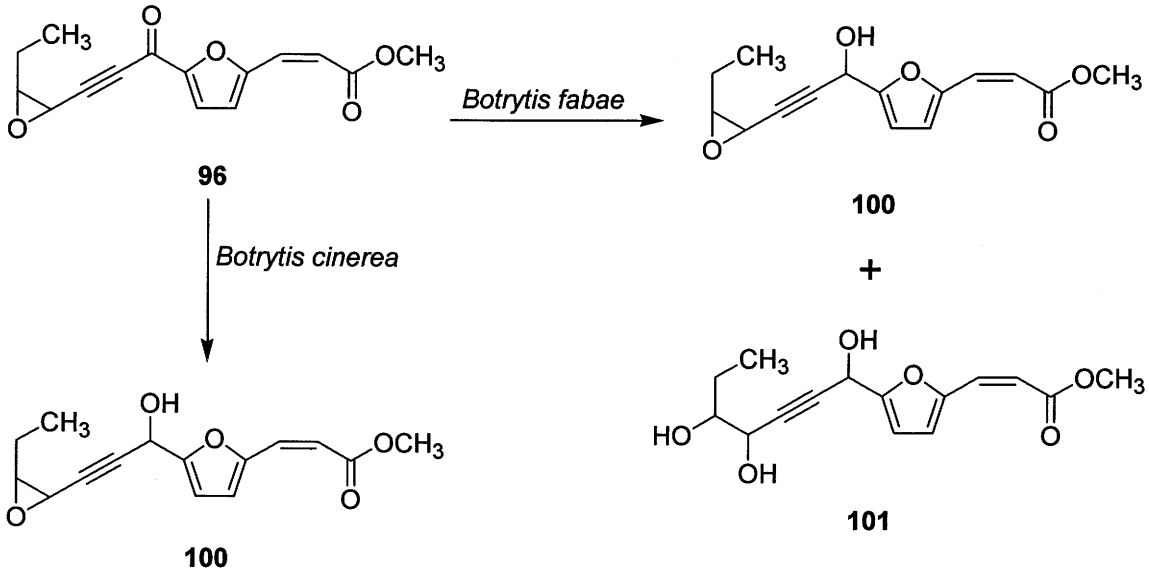

Scheme 1.14 Detoxification of the tomato phytoalexin wyerone epoxide (**96**) by fungal pathogens *Botrytis cinerea* and *Botrytis fabae* (Hargreaves *et al.*, 1976).

Sesquiterpenoid phytoalexins have been isolated from plants of the Solanaceae family (Figure 1.10). These include rishitin (**102**), phytuberin (**106**) (Walker & Wade, 1978), lubimin (**103**) oxylubimin (**104**), 3-hydroxylubimin (**105**) (Katsui *et al.*, 1974; Afzal *et al.*, 1986), from potato (*Solanum tuberosum*), 7-hydroxycostal (**110**), 7-hydroxycostol (**112**) (Schneider & Nakanishi, 1983), ipomeamaronol (**111**) (Fujita & Yoshizawa, 1987) from sweet potato (*Ipomea butatas*), lettucenin A (**108**), costunolide (**109**) (Takasugi, 1985) from lettuce (*Lactuca sativa*) and capsidiol (**115**) (Ward & Stoessl, 1972) from hot pepper fruits (*Capsicum annum* L. and C. *frutescens* L.).

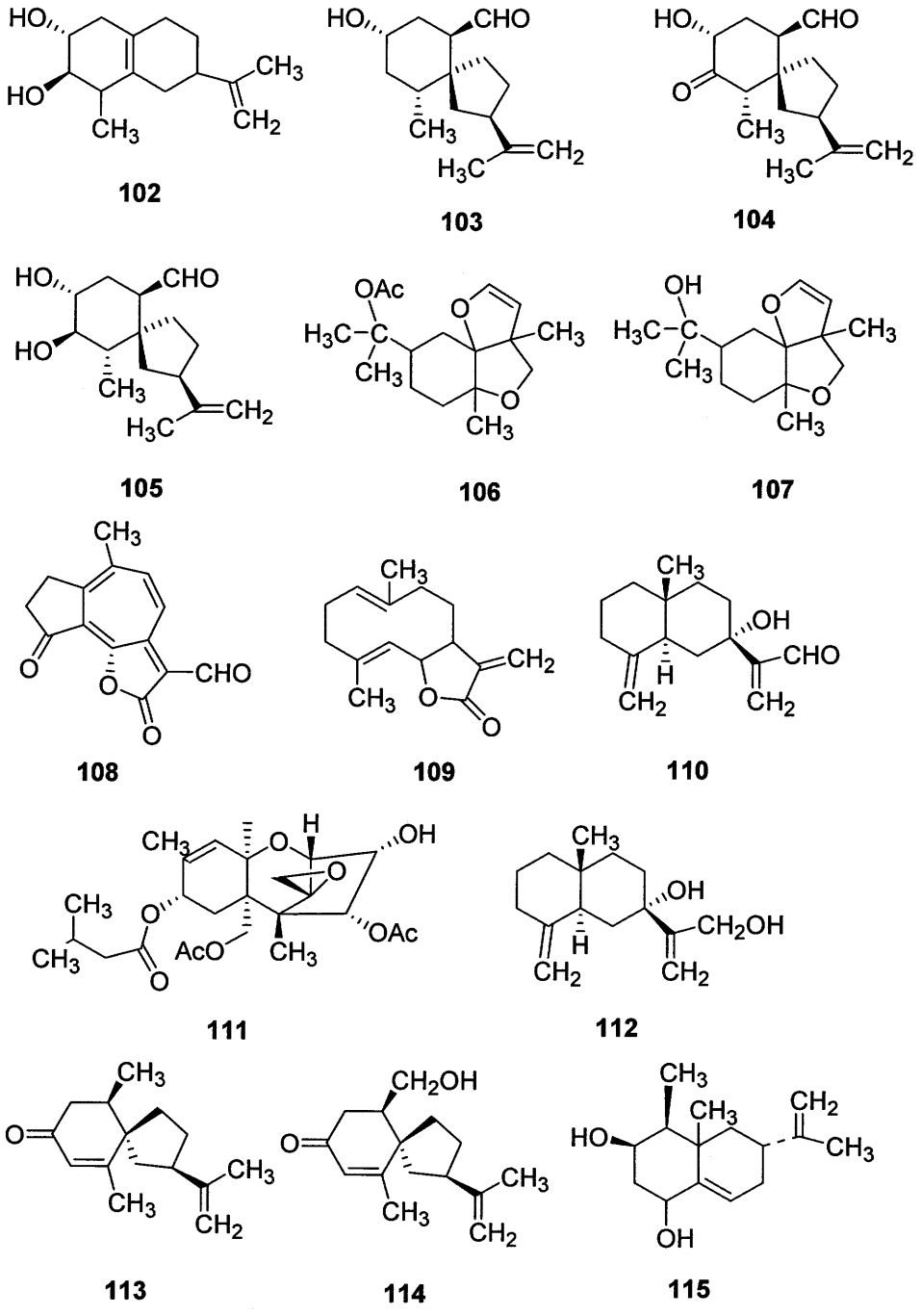

Figure 1.10 Sesquiterpenoid phytoalexins from plants of Solanaceae family: rishitin (**102**); lubimin (**103**); oxylubimin (**104**); 3-hydroxylubimin (**105**); phytuberin (**106**); phytuberol (**107**); lettucenin A (**108**); costunolide (**109**); ipomeamaronol (**110**); 7-hydroxycostal (**111**); 7-hydroxycostol (**112**); solavetivone (**113**); hydroxysolavetivone (**114**); capsidiol (**115**).

The metabolism of the pepper phytoalexin capsidiol (**115**) by *B. cinerea* and *F. oxysporum* f. *vasinfectum*, pathogens of pepper (Scheme 1.15) led to the detection and isolation of capsenone (**116**) (Ward & Stoessl, 1972). The comparative fungitoxicity of capsidiol (**115**) and capsenone (**116**) was determined by standard spore germination assays with *B. cinerea* and *F. oxysporum* f. *vasinfectum* (Ward & Stoessl, 1972). The results of these assays indicated that the biotransformation of capsidiol (**115**) by *B. cinerea* and *F. oxysporum* f. *vasinfectum* was a detoxification as capsenone (**116**) had no significant antifungal activity.

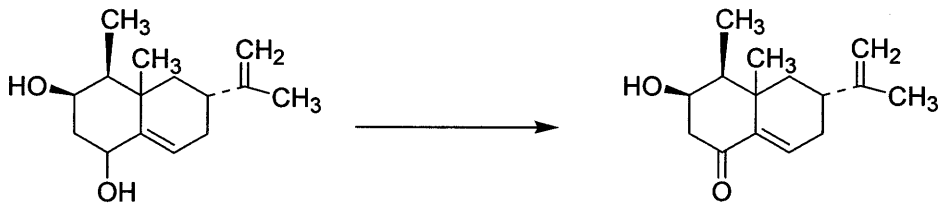

115 **116**

Scheme 1.15 Detoxification of hot pepper phytoalexin capsidiol (**115**) by fungal pathogens *Botrytis cinerea* and *Fusarium oxysporum* f. *vasinfectum* (Ward & Stoessl, 1972).

Biotransformation studies with the potato phytoalexin lubimin (**103**) on three strains (Strains R-7715 and R-583 tolerant; strain R-110 sensitive) of the potato pathogen *Gibberella pulicaris* led to very interesting results. The metabolism of lubimin sensitive strain R-110 was slow but that of the tolerant strains were rapid and complex. (Gardner *et al.*, 1988; Desjardins *et al.*, 1989). The metabolism and detoxification of lubimin (**103**) by *Gibberella pulicaris* (strain R-7715) led to the detection and isolation of seven metabolites: 2-dehydrolubimin (**117**), 15-dihydrolubimin (**118**), isolubimin (**119**), cyclodehydro isolubimin (**121**), cyclolubimin (**122**), 11,12-epoxycyclodehydrolubimin (**123**) and 11,12-epoxycyclolubimin (**124**) as shown in Scheme 1.16. These metabolites had lower

antifungal activity than lubimin (**103**). Within one hour of lubimin (**103**) addition to cultures of *G. pulicaris* strain R-7715, 2-dehydrolubimin (**117**), 15-dihydrolubimin (**118**) and isolubimin (**119**) were detected. The level of **117** rapidly reached a maximum and declined. Levels of 15-dihydrolubimin (**118**) and isolubimin (**119**) peaked at two to four hours and then declined slowly during the next two days. Cyclodehydroisolubimin (**121**) was first detected between 1.5 – 2 hours after lubimin addition, increased for 24 hours, then was slowly converted to cyclolubimin (**122**), which was not metabolized significantly afterwards. After almost five days incubation, more than 75% of the lubimin (**103**) added was transformed as tricyclic metabolites. After two days incubation the epoxide of cyclodehydroisolubimin (**123**) was detected in small amounts. The reaction producing the cyclic ethers seem to be the detoxifying step in the metabolism of **103** by *G. pulicaris* because the tricyclic products are not toxic to the fungus (Gardner *et al.,* 1988). Incubation of lubimin (**103**) with the fungus in the presence of $^{2}H_2O$ resulted in labelling at C-3 of cyclodehydroisolubimin (**121**) indicating that cyclization was directed towards the double bond of 3,4-dehydroisolubimin (**120**). 11,12-Epoxycyclolubimin (**124**) was not detected directly as a product from incubation of **103**. However, incubation of **122** with *G. pulicaris* (strain R-7715) for 4 days led to the detection of the epoxide of cyclolubimin (**124**) in small amounts. Thus the detoxification of lubimin (**103**) by *G. pulicaris* to the cyclic ethers is via **120** (Gardner *et al.,* 1988). The pattern of lubimin (**103**) metabolism in strain R-583 differed from that in strain R-7715; cyclodehydroisolubimin (**121**) was a very minor metabolite in strain R-583 ($\leq$ 13 μM), and no lubimin metabolites of any kind were detected in chloroform-methanol extracts after 48 hours incubation. Further metabolism of lubimin (**103**) by this strain may involve formation of water-soluble products by oxygenation or conjugation (Desjardins *et al.*, 1989). Although all naturally occurring strains of *G. pulicaris* possess some ability to metabolize lubimin (**103**), only lubimin tolerant strains apparently are able to rapidly convert it to completely non-toxic products. Furthermore, only strains with a high level of lubimin detoxification *in vitro* are highly

virulent on potato tubers (Desjardins *et al.*, 1989). Lubimin metabolism however is apparently not sufficient to ensure virulence on potato because some strains are not highly virulent, even though they can metabolize lubimin *in vitro*. This is not surprising since pathogenicity is a complex process depending on many genes and resistance in potato tubers to fungal pathogens can apparently involve several defence responses (Desjardins *et al.*, 1989).

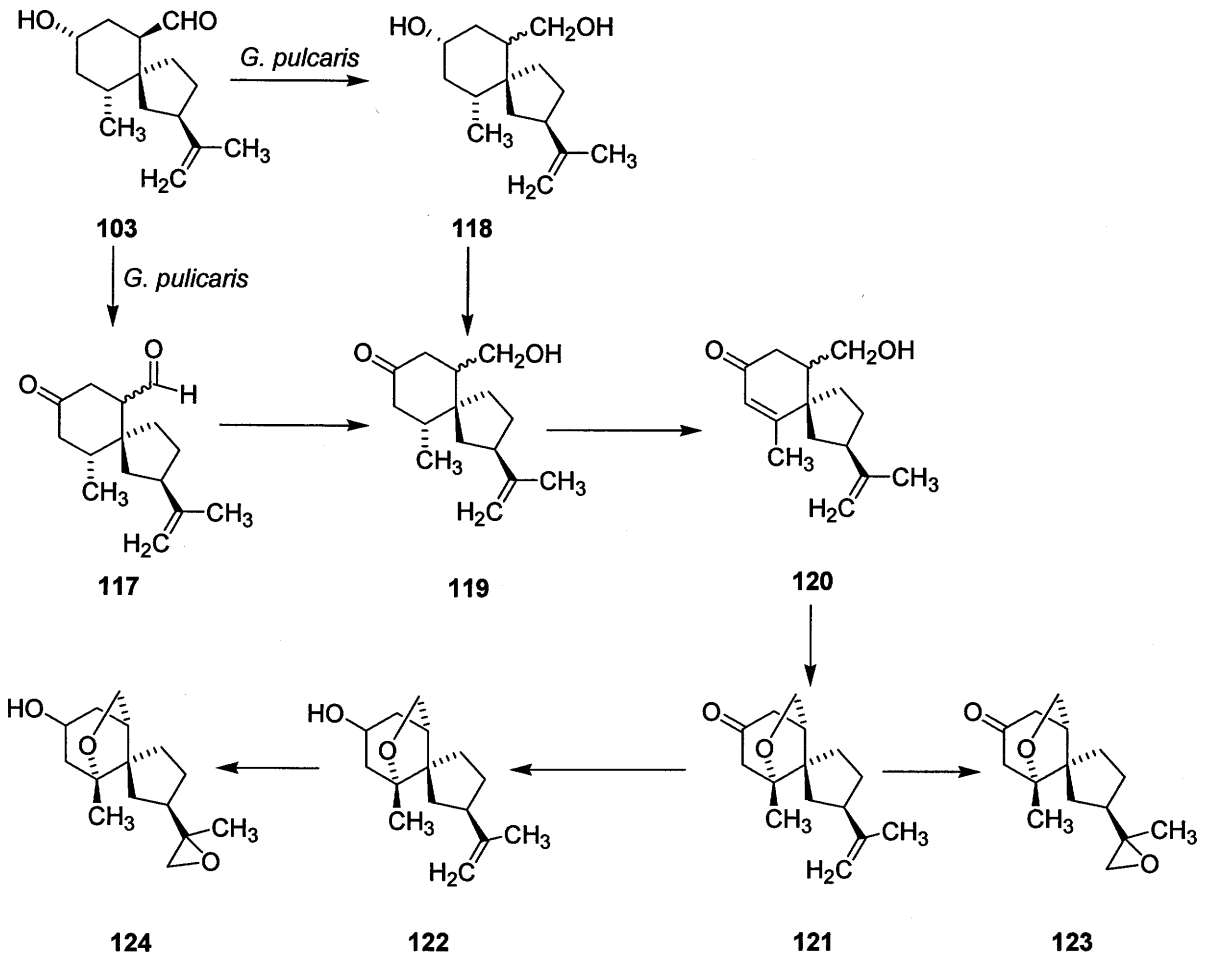

Scheme 1.16 Detoxification of the potato phytoalexin lubimin (**103**) by the fungal pathogen *Gibberella pulicaris* strain R-7715 (Gardner *et al.*, 1988; Desjardins *et al.*, 1989).

Penicillium chrysogenum, a pathogen of *Datura stramonium* L. metabolized lubimin (**103**) and 3-hydroxylubimin (**105**) to 15-dihydrolubimin (**118**) (Scheme 1.17) and 3-hydroxy-15-dihydrolubimin (**125**) (Scheme 1.18) respectively, both in fruit cavities inoculated with spores of the fungus and in pure culture (Whitehead *et al.*, 1990). The metabolism of **103** and **105** by *P. chrysogenum* occurred at remarkably different rates. Lubimin (**103**) was quantitatively converted to **118** in 3 hours whereas 3-hydroxylubimin (**105**) only slowly metabolized to **125** (only 64% in 48 hours). The 15-dihydrolubimin (**118**) formed in the fruits by the fungus was further metabolized to both isolubimin (**119**) and 3-hydroxy-15-dihydrolubimin (**125**).

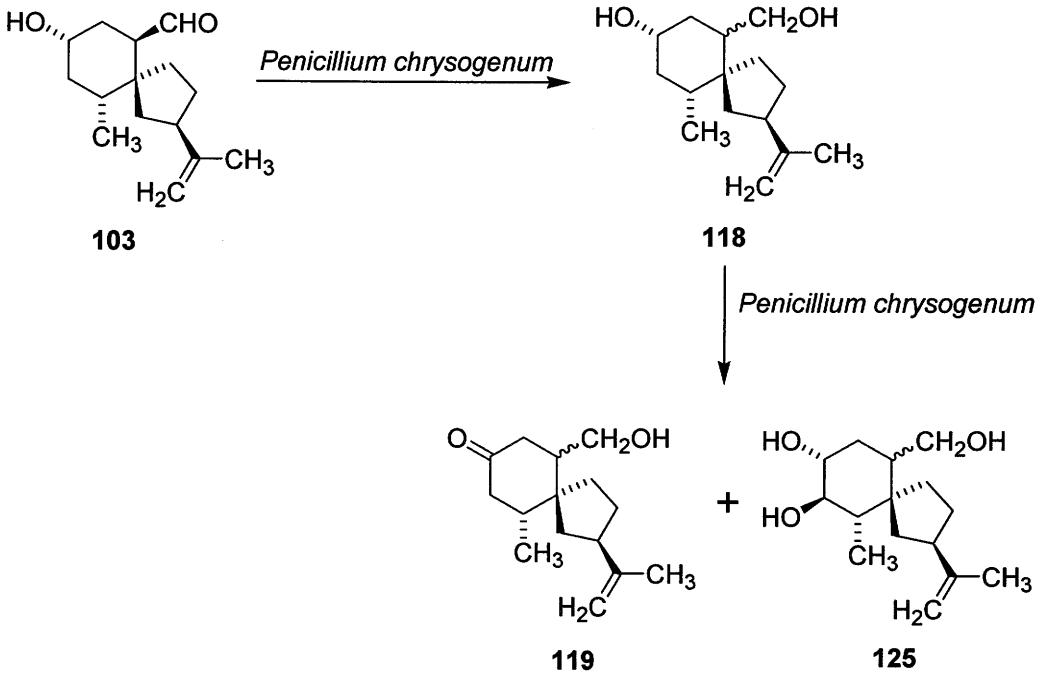

Scheme 1.17 Detoxification of the phytoalexin lubimin (**103**) by the fungal pathogen *Penicillium chrysogenum* (Whitehead *et al.*, 1990).

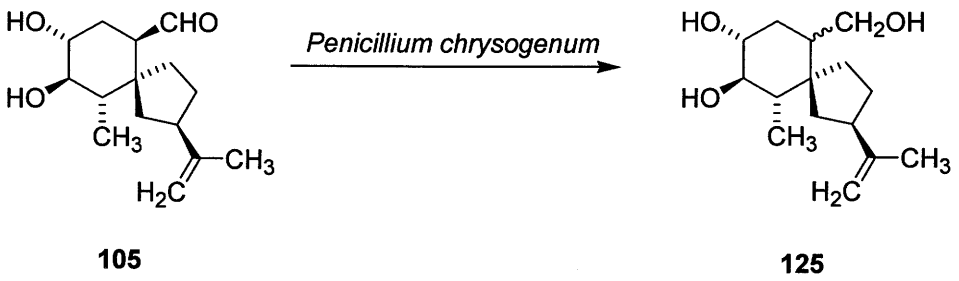

105 125

Scheme 1.18 Detoxification of the phytoalexin 3-hydroxylubimin (**105**) by *Penicillium chrysogenum* (Whitehead *et al.*, 1990).

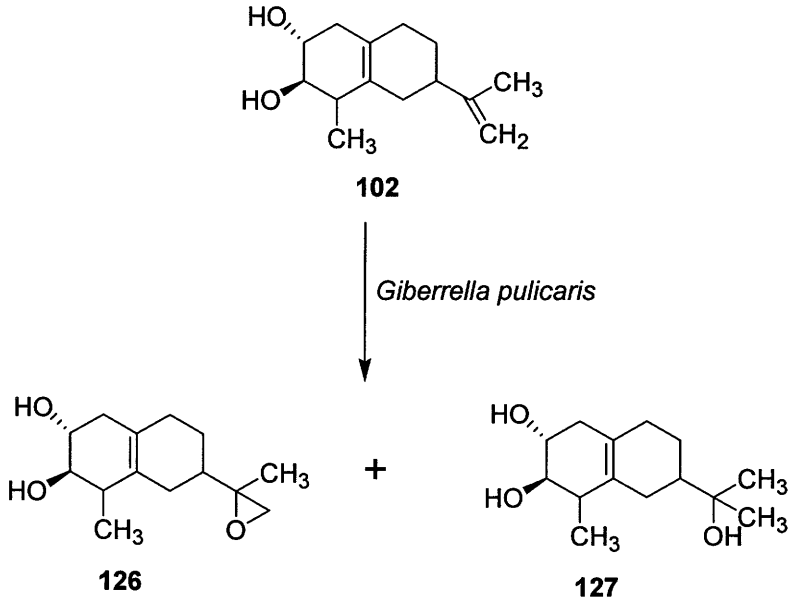

126 127

Scheme 1.19 Detoxification of the potato phytoalexin rishitin (**102**) by fungal pathogen *Gibberella pulicaris* (Gardner *et al.*, 1994).

Metabolism of the potato phytoalexin rishitin (**102**) by *Gibberella pulicaris*, a pathogen of potato, resulted in two metabolites: epoxyrishitin (**126**) and 13-hydroxyrishitin (**127**) (Scheme 1.19). Epoxyrishitin (**126**) was found to be less toxic to the fungus (Gardner *et al.*, 1994) than rishitin (**103**) suggesting that the metabolism is a detoxification process. The metabolism of rishitin (**102**) by *G. pulicaris* on solid agar medium is usually complete in 24 hours (Weltring and Altenburger, 1998). In contrast, incubations in various liquid media and buffers highly reduce metabolism of rishitin (**102**) with a maximal reduction of substrate down to 30% of the initial concentration within five days. The structurally related sesquiterpene lubimin (**103**) was metabolized completely within 12 hours in all tested liquid media. This data suggests that rishitin (**102**) metabolism is under an unusual genetic control requiring growth on a solid surface for efficient metabolism (Weltring and Altenburger, 1998).

1.4.1.3 Metabolism and detoxification of phytoalexins from family Graminaceae

Phytoalexins from the Graminaceae family (Figure 1.11) include the diterpenoids oryzalexin A (**128**), oryzalexin B (**129**), oryzalexin C (**130**), oryzalexin D (**131**), momilactone A (**132**) and momilactone B (**133**) from rice (*Oryza sativa*) (Akatsuka *et al.*, 1985) and the cyclic hydroxamic acids (Figure 1.12) like avenalumin I (**134**) avenalumin II (**135**) and avenalumin III (**136**) from oats (*Avena sativa*) (Gross, 1989; Mayama *et al.*, 1983). Cyclic hydroxamic acids with the 1,4-benzoxazin-3-one skeleton are secondary metabolites found in several grasses (Gramineae) including corn, wheat and rye (Yue *et al.*, 1998). In the intact plant, the hydroxamic acid exists as a β-glucoside, but the aglycone is rapidly cleaved by a β-glucosidase upon disruption of cellular integrity. These compounds are abundant during seedling development and are considered defence chemicals because of their wide range of biological activity against specific crop pests. The cyclic hydroxamic acids are inhibitory to several fungal plant pathogens including

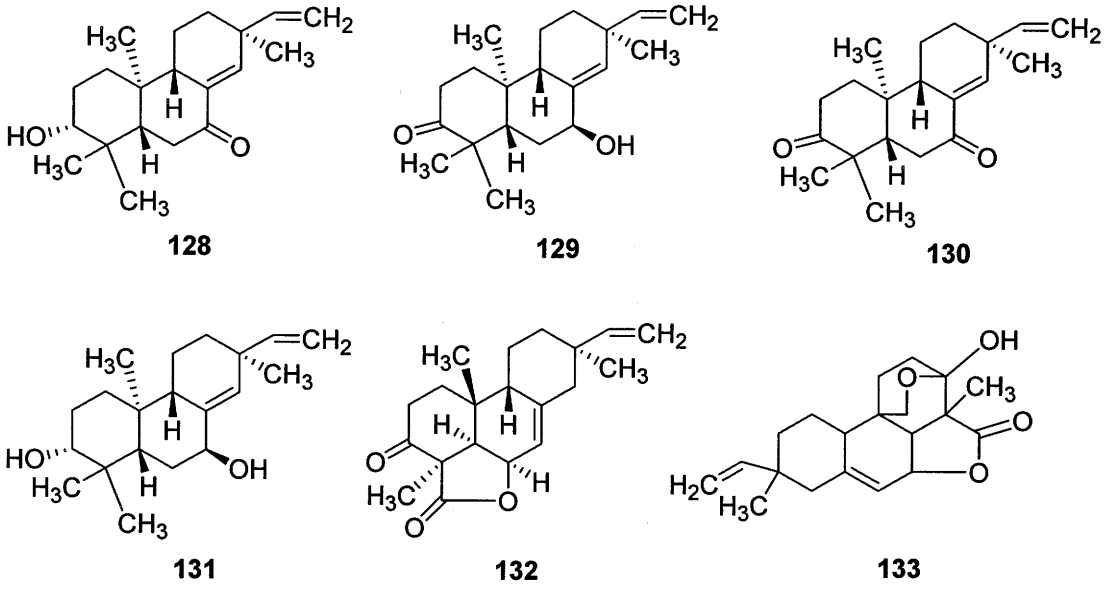

Figure 1.11 Diterpenoid phytoalexins from rice (*Oryza sativa*): oryzalexin A (**128**); oryzalexin B (**129**); oryzalexin C (**130**); oryzalexin D (**131**); momilactone A (**132**); momilactone B (**133**).

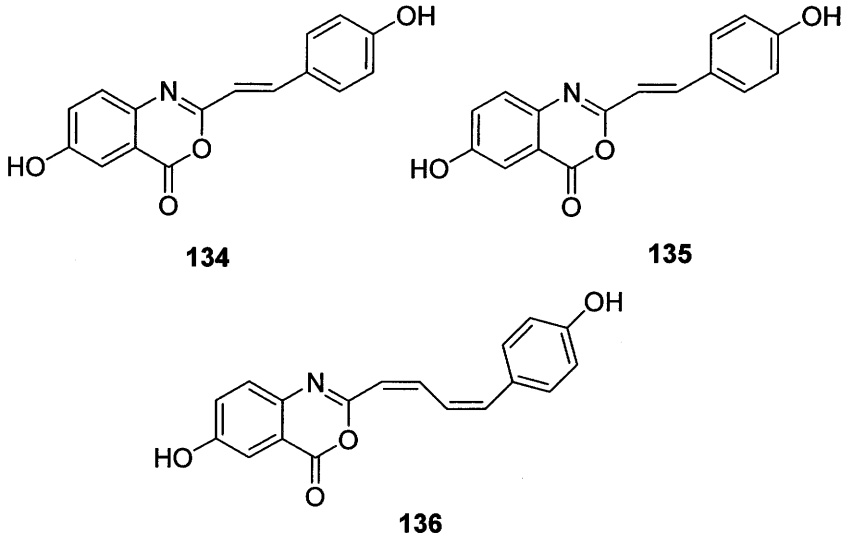

Figure 1.12 Cyclic hydroxamic acid phytoalexins from oats (*Avena sativa*): avenalumin I (**134**); avenalumin II (**135**); avenalumin III (**136**).

Helminthosporium tucicum Passerini, *Septoria nodorum* (Berk.) Berk, *Microdochium nivale* (Fries), and *Fusarium moniliforme* (Yue *et al.*, 1998).

The metabolism of the phytoalexins avenalumin I (**134**) and avenalumin II (**135**) by *Fusarium* species indicated that the phytoalexins were transformed but no biotransformation products were detected or isolated. The biotransformation products may be very polar precluding solvent extraction and isolation (Bratfaleanu & Steinhauer, 1994). This degradation occurred at a much faster rate with *F. graminearum* (highly virulent) than with other *Fusarium* species.

1.4.1.5 Metabolism and detoxification of phytoalexins from additional plant families

The phytoalexin benzoic acid (**137**) has been isolated from apples (*Malus domestica*). Biotransformation of benzoic acid (**137**) by the apple fungal pathogen *Monilia fructigena* led to the detection and isolation of 4-hydroxybenzoic acid (**138**) (Bykova *et al.*, 1977), which was less toxic to the pathogen than **137**, indicating that the metabolism is a detoxification process (Scheme 1.20).

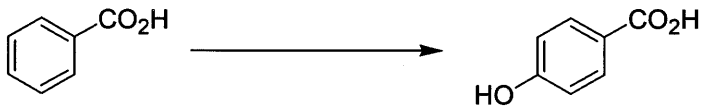

137 **138**

Scheme 1.20 Detoxification of benzoic acid (**137**) by the apple fungal pathogen *Monilia fructigena* (Bykova *et al.*, 1977).

Stilbenoid phytoalexins have been isolated from different plant families. Those from grape (*Vitis vinifera*) include resveratrol (**27**), pterostilbene (**139**), and trans ε-viniferin (**140**) (Breuil *et al.*, 1998; Pezet *et al.*, 1991). Resveratrol (**27**), pterostilbene (**139**), 4-(3-methylbut-1-enyl)-3,5,4'-trihydroxystilbene (**141**), 4-isopentenylresveratrol (**142**) and 4-(3-methylbut-1-enyl)-3,5,3',4'-tetrahydroxystilbene (**143**) (Aguamah *et al.*, 1981) have been isolated from groundnut (*Arachis hypogaea*). Dihydropinosylvin (**144**), batatasin III (**145**), batatasin IV (**146**) and demethylbatatasin (**147**) are dihydrostilbene phytoalexins isolated from white yam (Dioscorea rotundata) (Fagboun *et al.*, 1987) and water yam (Dioscorea alata) (Cline *et al.*, 1989). The structures of these stilbenoid phytoalexins are shown in Figure 1.13.

The metabolism of the stilbene phytoalexin resveratrol (**27**) (Scheme 1.21) by *Botrytis cinerea* resulted in the detection and isolation of the metabolite resveratrol *trans* - dehydrodimer (**148**) (Pezet *et al.,* 1991; Breuil *et al.,* 1998). A laccase-like stilbene oxidase produced by *B. cinerea* is responsible for the detoxification of **27** (Pezet *et al.,* 1991). Laccases are polyphenol oxidases that act on a variety of polyphenol substrates. The contribution of the *B. cinerea* laccases to stilbene detoxification and to pathogenicity remains to be determined. However, evidence that stilbenes do protect plants against attack by fungal pathogens comes from experiments in which expression of resveratrol synthase from grapevine in a number of other plant species increased disease resistance (Morrissey & Osbourn, 1999). This resveratrol (**27**) detoxification has also been observed in the conidia of *B. cinerea*. With the use of light microscopy it was observed that approximately 30% of *B. cinerea* treated with semi-lethal concentrations of **27** possessed intracellular brown colouration. This colouration was never observed in the absence of **27** or in conidia treated with **27** together with sulphur dioxide (antioxidant compound or sodium diethyldithiocarbamate (inhibitor of laccase action), suggesting that discolouration resulted from the laccase-mediated oxidation of resveratrol (**27**). Further studies using transmission

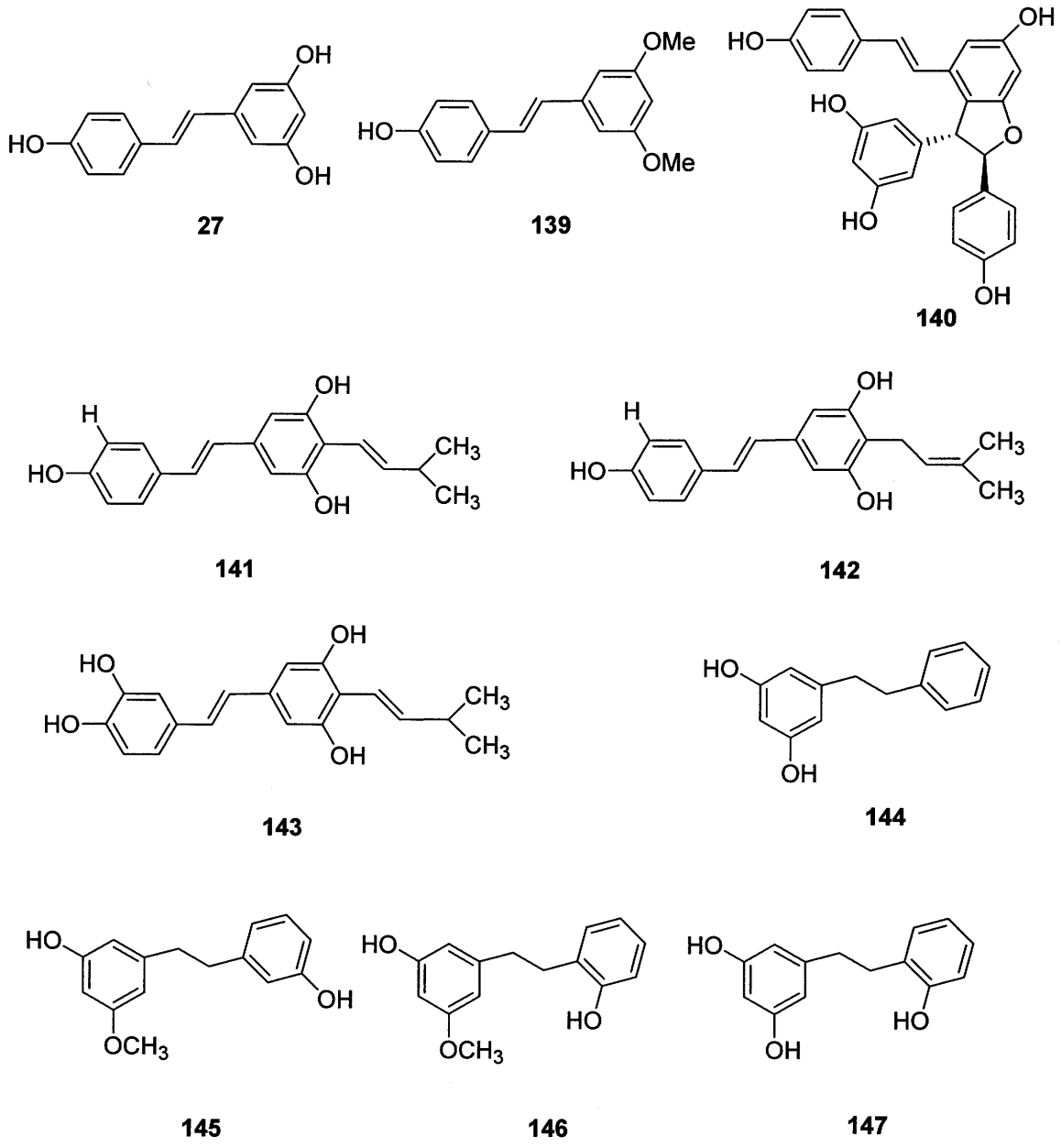

Figure 1.13 Stilbenoid phytoalexins from grapevine, groundnut, and yam: resveratrol (**27**); pterostilbene (**139**); trans-ε-viniferin (**140**); 4-(3-methylbut-1-enyl)-3,5,4'-trihydroxystilbene (**141**); 4-isopentenylresveratrol (**142**); 4-(3-methylbut-1-enyl)-3,5,3',4'-tetrahydroxystilbene (**143**); dihydropinosylvin (**144**); batatasin III (**145**); batatasin (**146**); demethylbatatasin IV (**147**).

electron microscopy enabled the observation of particular intravacuolar spherical vesicles and of granular material deposits along the tonoplast. These observations are likely to be related to the oxidation of resveratrol (**27**) by an intracellular laccase-like stilbene oxidase of *B. cinerea* (Adrian *et al.*, 1998).

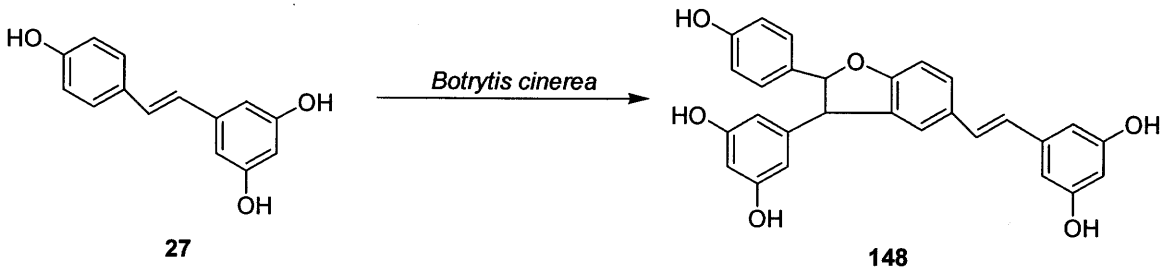

27 **148**

Scheme 1.21 Detoxification of the phytoalexin resveratrol (**27**) by fungal pathogen *Botrytis cinerea* (Pezet *et al.*, 1991; Breuil *et al.*, 1998).

1.4.1.4 Metabolism and detoxification of phytoalexins from family Cruciferae

Cruciferous phytoalexins have a characteristic indolic ring system with substitution at C-3 position. They are the first sulphur containing phytoalexins reported and collectively can be considered as indole alkaloids. Up to date, about 31 cruciferous phytoalexins have been isolated (Pedras *et al.*, 2003a); these are shown in Figure 1.14. Brassinin (**149**) and 1-methoxybrassinin (**150**), which contain a dithiocarbamate group attached to a 3-methylindolyl moiety, and cyclobrassinin (**158**) were the first brassica phytoalexins to be reported (Takasugi *et al.*, 1986). It is worthy to note that although dithiocarbamates have long been known as important pesticides and herbicides so far crucifers appear to be the only plants producing these compounds (Pedras *et al.*, 2000). Methyl 1-methoxyindolyl-3-carboxylate (**177**) (Pedras & Sorensen, 1998), indole-3-acetonitrile (**178**) (Pedras *et al.*, 2002a) and arvelexin (**179**) (Pedras *et al.*, 2003b) appear to be the first non-sulphur

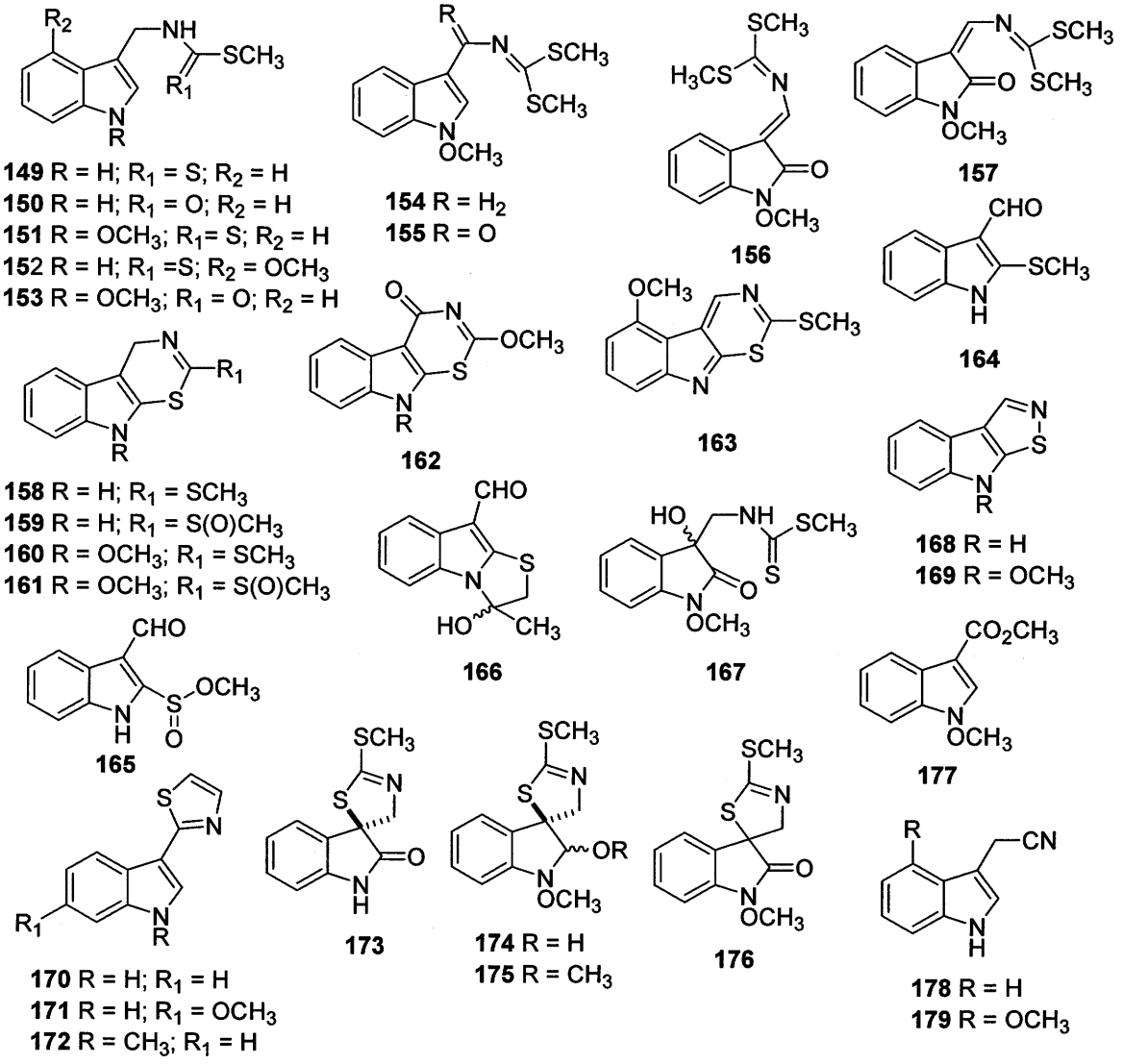

Figure 1.14 Phytoalexins from crucifers: brassinin (**149**); brassitin (**150**); 1-methoxy brassinin (**151**); 4-methoxybrassinin (**152**); 1-methoxybrassitin (**153**); 1-methoxybrassenin A (**154**); 1-methoxybrassenin B (**155**); wasalexin A (**156**); wasalexin B (**157**); cyclobrassinin (**158**); cyclobrassinin sulfoxide (**159**); sinalbin A (**160**); sinalbin B (**161**); cyclobrassinone (**162**); dehydro-4-methoxybrassinin (**163**); brassicanal A (**164**); brassicanal B (**165**); brassicanal C (**166**); dioxibrassinin (**167**), brassilexin (**168**); sinalexin (**169**); camalexin (**170**); 6-methoxycamalexin (**171**); 1-methylcamalexin (**172**); spirobrassinin (**173**); 1-methoxyspirobrassinol (**174**); 1-methoxyspirobrassinol methyl ether (**175**); 1-methoxyspirobrassinin (**176**); methyl 1-methoxyindolyl-3-carboxylate (**177**); indole-3-acetonitrile (**178**); arvelexin (**179**).

containing phytoalexins isolated from crucifers. Despite their related biogenetic origin, the cruciferous phytoalexins have rather different structures, which would suggest substantially different biological activities (Pedras *et al.*, 2000).

Biosynthetic studies carried out on cruciferous phytoalexins indicate that while (*S*)-tryptophan (**181**) is the precursor of most of the brassica phytoalexins, camalexin (**170**) isolated from wild crucifers like *Arabidopsis thaliana*, *Camelina sativa* (false flax) and *Capsella bursa-pastoris* (Shepherd's purse) appears to be derived from anthranilic acid (**180**) via indole (**182**) (Tsuji *et al.*, 1993; Zook, 1998).

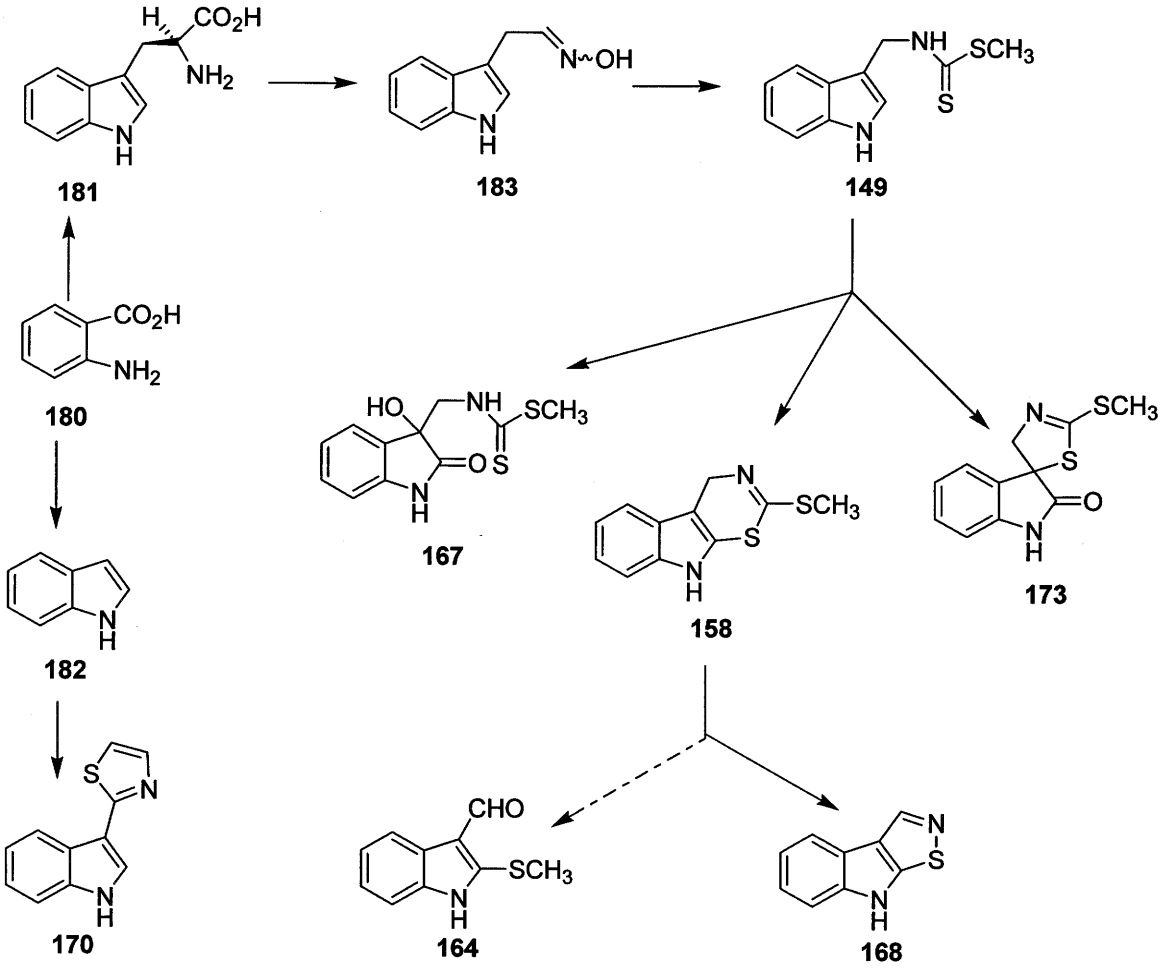

Scheme 1.22 Biosynthetic pathways of crucifer phytoalexins; dashed arrow represents potential step not yet established (Pedras *et al.*, 2003a).

Indole-3-acetaldoxime (**183**) is the intermediate between (*S*)-tryptophan (**181**) and brassinin (**149**) (Pedras *et al.*, 2002a). It is worth noting that (*S*)-tryptophan (**181**) is biosynthesized from anthranilic acid (**180**) via the shikimate pathway (Dewick, 1998).

It has also been demonstrated that brassinin (**149**), is the advanced precursor of cyclobrassinin (**158**), dioxibrassinin (**167**), spirobrassinin (**173**) (Monde *et al.*, 1991; Monde *et al.*, 1994) and brassilexin (**168**) (Pedras *et al.,* 1998b). Scheme 1.22 summarizes the presently known biosynthetic relationships among the diverse cruciferous phytoalexins.

The metabolism and detoxification of the phytoalexin brassinin (**149**) by the blackleg fungus, *Phoma lingam* led to three metabolites namely indole-3-carboxaldehyde (**184**), indole-3-carboxylic acid (**185**) and methyl 3-indolylmethyl dithiocarbamate-S-oxide (**186**) (Pedras *et al.*, 1992; Pedras & Taylor, 1991; Pedras & Taylor, 1993). It was also established that the virulence of the blackleg fungus correlated with its ability to rapidly metabolize and detoxify brassinin (**149**) (Pedras *et al.*, 1992). Further metabolism studies on the three metabolites by virulent *P. lingam* established the biotransformation pathway from brassinin as shown in Scheme 1.23.

Further investigation (Pedras & Taylor, 1993) on the metabolism and detoxification of brassinin (**149**) by avirulent *P. lingam* indicated a metabolic pathway, different from that of virulent isolates. The metabolism of brassinin (**149**) by avirulent isolates resulted in the detection and isolation of four metabolites: indole-3-carboxaldehyde (**184**), indole-3-carboxylic acid (**185**), indolyl-3-methanamine (**187**), and N_b-acetyl-3-indolyl-methanamine (**188**). While in virulent isolates the transformation of brassinin (**149**) rapidly yielded aldehyde via intermediate **186**, in avirulent isolates, brassinin (**149**) was slowly converted to the aldehyde via intermediate **186** and **188** (Pedras & Taylor, 1993). The antifungal activity of brassinin (**149**) and its metabolites was compared using spore germination and radial mycelial growth assays (Pedras & Taylor, 1993). The results of these assays indicated that the biotransformation of brassinin (**149**) by virulent and avirulent isolates of

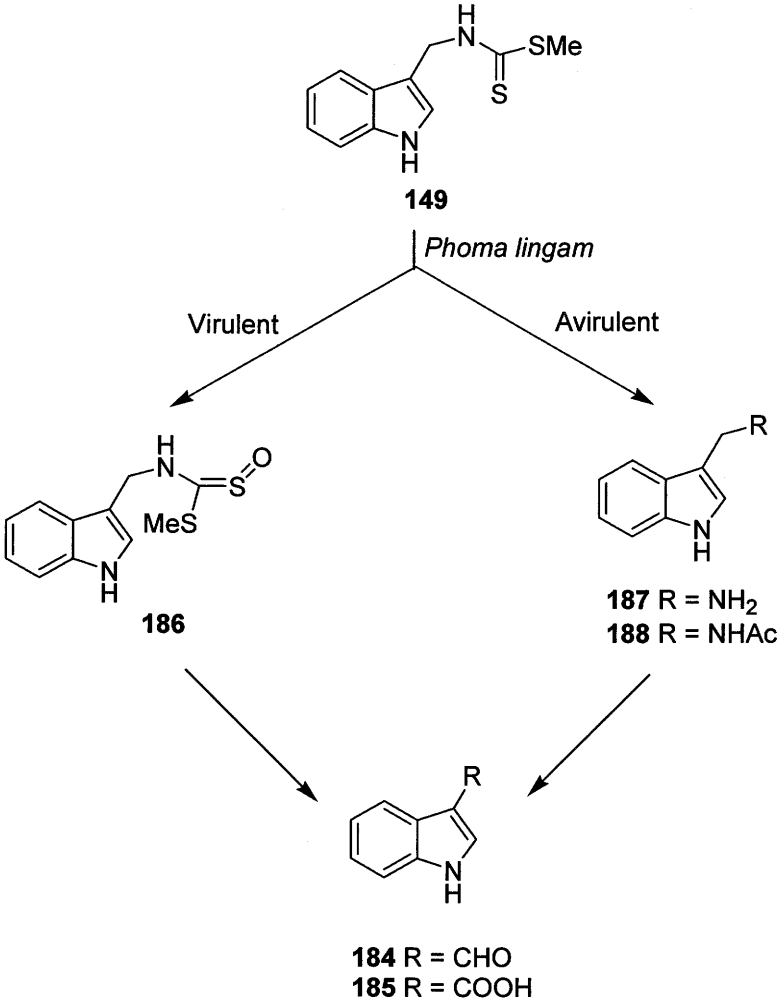

Scheme 1.23 Detoxification of brassinin (**149**) by fungal pathogen *Phoma lingam* (Pedras *et al.*, 1992; Pedras & Taylor, 1991; Pedras & Taylor, 1993).

P. lingam was a detoxification, as brassinin metabolites had no significant antifungal activity. In addition it was established for the first time that brassinin (**149**) inhibited the biosynthesis of nonselective toxins in *P. lingam*. These toxins were not detected in fungal cultures incubated with brassinin (**149**) until 6 – 8 hours after complete brassinin transformation. By contrast, incubation with any of the intermediates **184 - 188** did not noticeably affect phytotoxin production.

The metabolism of cyclobrassinin (**158**) by avirulent and virulent isolates of *P. lingam* as shown in Scheme 1.24 (Pedras & Okanga, 1998; Pedras & Okanga, 1999) was strikingly different from that of brassinin (**149**). HPLC analysis of organic extracts of cultures of avirulent isolates incubated with **158** indicated a rapid decrease in the concentration of **158** and the concurrent appearance of two additional constituents. Spectroscopic analysis established that one of the constituents was the known phytoalexin brassilexin (**168**) and the other constituent, a relatively less stable metabolite, a mixture of 3-methylenaminoindolyl-2-thione (**190**) and related tautomers (e.g. **189**). Two days after incubation of the avirulent isolates with cyclobrassinin (**158**) no brassilexin (**168**) or other putative metabolites were detected in any of the cultures, or their extracts. Similar experiments carried out with virulent isolates of *P. lingam* incubated with cyclobrassinin (**158**) afforded yet another known phytoalexin, dioxibrassinin (**167**). Two days after incubation of a virulent isolate with cyclobrassinin (**158**), no phytoalexins or derivatives were detected in any of the cultures or their extracts.

The biotransformation studies with the root rot fungus *R. solani* established that cyclobrassinin (**158**) was metabolized and detoxified via the phytoalexin brassicanal A (**164**), which was further metabolized into non-toxic products (Scheme 1.24) the intermediate **191** could explain the formation of **164** through enzymatic oxidation of **158**. These remarkable results demonstrated that cyclobrassinin (**158**) was detoxified via the phytoalexins dioxibrassinin (**167**), brassilexin (**168**), or brassicanal A (**164**), depending on the fungal species, as shown in Scheme 1.25 (Pedras & Okanga, 1999). It is worth noting that cyclobrassinin (**158**) was demonstrated to be an *in planta* biosynthetic precursor of brassilexin (**168**) (Pedras *et al.*, 1998) and also proposed to be a biosynthetic precursor of brassicanal A (**164**) (Monde *et al.*, 1996). Therefore it was suggested that some phytopathogens might have acquired a more effective mechanism for overcoming this chemical defence by adopting biosynthetic pathways operating in planta. This strategy

appeared quite plausible, especially considering that most fungal pathogens have coevolved with plants for innumerable generations (Pedras & Okanga, 1999).

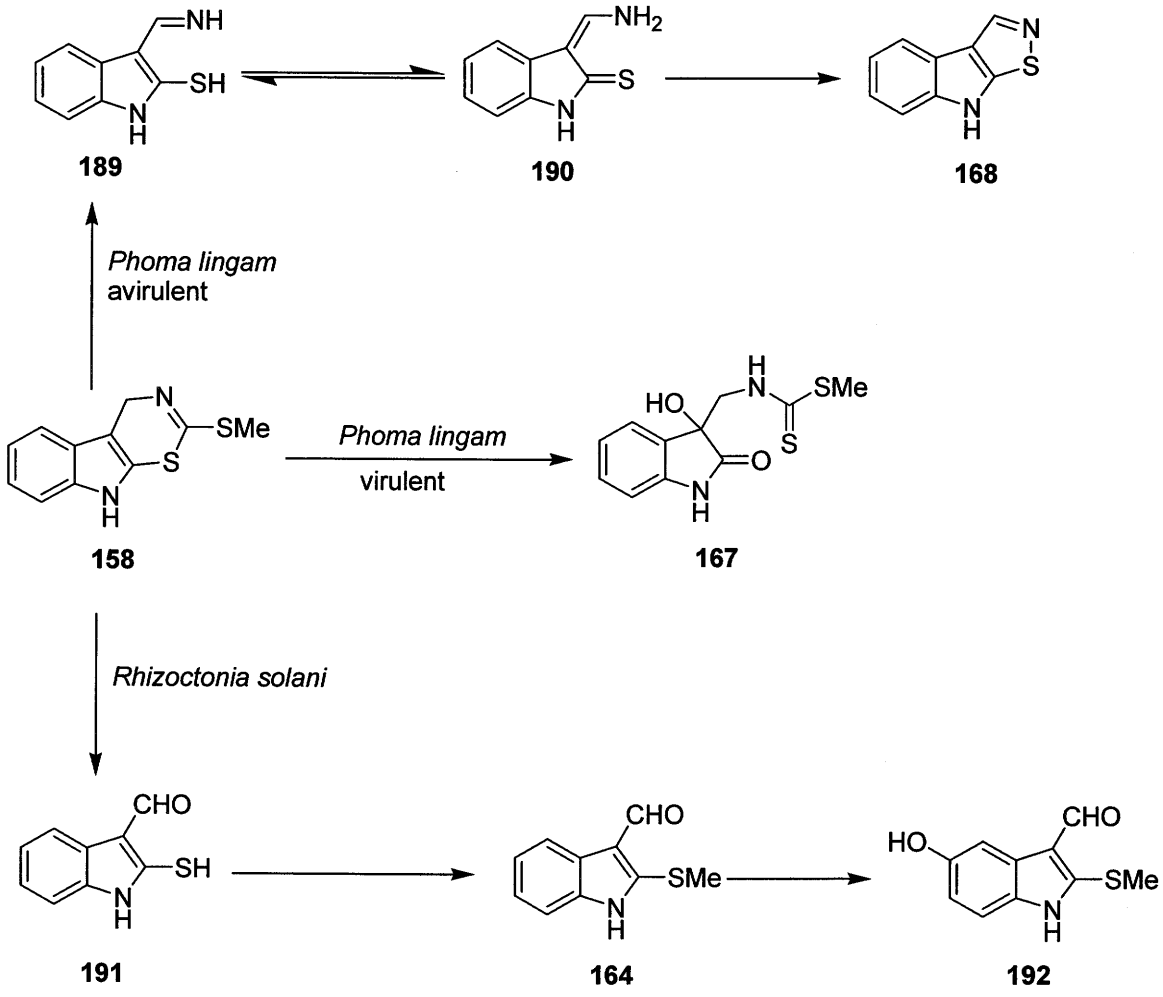

Scheme 1.24 Detoxification of cyclobrassinin (**158**) by fungal pathogens *Phoma lingam* and *Rhizoctonia solani* (Pedras & Okanga, 1998; Pedras & Okanga, 1999).

The biotransformation of the phytoalexin brassicanal A (**164**) by *P. lingam* led to the detection and isolation of three metabolites: brassicanal A sulfoxide (**193**), 3-hydroxymethylindolyl-2-methylsulfoxide (**194**) and 3-methylindolyl-2-methylsulphoxide (**195**), as shown in Scheme 1.26 (Pedras & Khan, 1996; Pedras, Khan & Taylor, 1997). In the first biotransformation step, SCH_3 group of brassicanal A was oxidized to the

corresponding sulfoxide **193**. In subsequent steps the aldehyde group of **164** was reduced to the alcohol **194** and then further to the 3-methylindole **195**. The biotransformation of brassicanal A (**164**) was shown to be a detoxification, since the antifungal activities of brassicanal A (**164**) and its metabolites indicated that brassicanal A (**164**) was significantly more inhibitory to *P. lingam* than the products **193-195**.

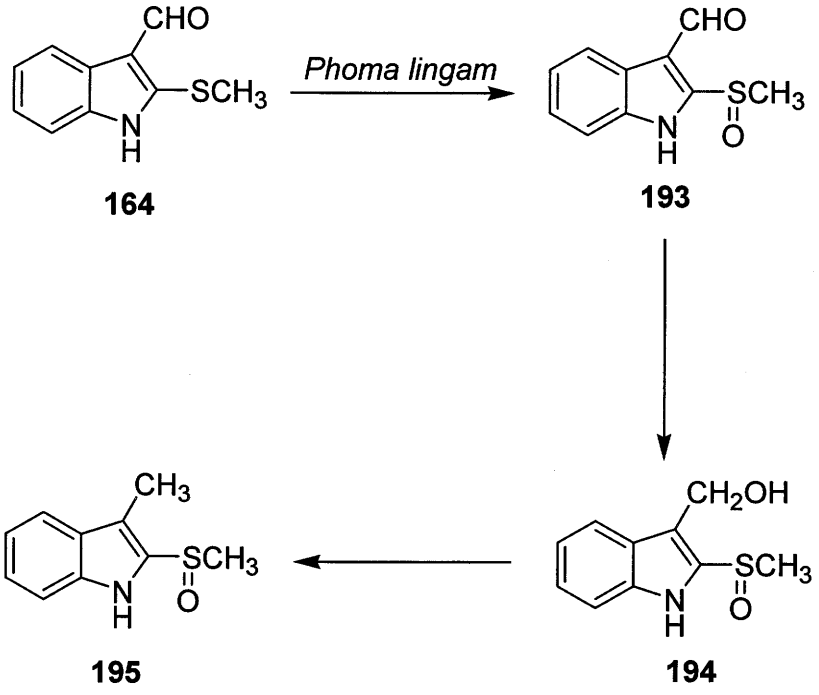

164 **193** **195** **194**

Scheme 1.25 Detoxification of brassicanal A (**164**) by fungal pathogen *Phoma lingam* (Pedras & Khan, 1996; Pedras, Khan & Taylor, 1997).

Studies on the biotransformation of the phytoalexins dioxibrassinin (**167**) and brassilexin (**168**) by *P. lingam* indicated that the phytoalexins were transformed but no biotransformation products were detected or isolated (Pedras, 1998a; Pedras *et al.*, 1997) This work confirmed the results of a previous study on fungal metabolism of brassilexin (**168**) (Rouxel, Kollman & Ballesdent, 1995). Possible metabolic products of brassilexin might be very polar and more soluble in the aqueous medium than organic solvents, thus

precluding extraction and detection. On the other hand, spirobrassinin (**173**) was stable in fungal cultures and did not appear to be metabolized or interfere with the production of fungal toxins (Pedras, 1998a).

Although blackleg fungi could metabolize and detoxify brassinin (**149**), cyclobrassinin (**158**), dioxibrassinin (**167**), brassilexin (**168**) and brassicanal A (**164**), camalexin (**170**) and spirobrassinin (**173**) were not metabolized by either virulent or avirulent type isolates of *P. lingam*. None of the blackleg fungal isolates tested metabolized camalexin (**170**) or appeared to be affected by a concentration of 5×10^{-4} M (Pedras *et al,* 1997b; Pedras *et al.*, 1998a). Camalexin (**170**) was, however, metabolized by *Rhizoctonia solani*, a pathogen of *Camelina sativa* (false flax), a plant that produces camalexin (**170**) (Pedras & Khan, 1997). Incubation of *R solani* with camalexin (**170**) resulted in the detection and isolation of metabolites **196**, **197** and **198**, whose structures were deduced from their respective spectroscopic data and confirmed by synthesis. Further biotransformation of these metabolites led to the establishment of the biotransformation sequence shown in Scheme 1.25. This was the first time that oxidation of the indole ring of a cruciferous phytoalexin was observed. Previous work with other cruciferous phytoalexins indicated that fungal oxidation occurred at the indole substituents at C-2 or C-3. The biotransformation products of camalexin (**170**) by the root rot fungus, *R. solani* (Pedras & Khan, 1997) were found to be significantly less toxic than camalexin (**170**) itself. While agar plates containing camalexin (**170**) at 5×10^{-4} M inoculated with *R. solani* showed no mycelia growth after incubation for one week, metabolites **196**, **197** and **198** at identical concentration had only a very slight inhibitory effect. This led to the conclusion that the metabolism of camalexin (**170**) by *R. solani* was a detoxification (Pedras & Khan, 1997).

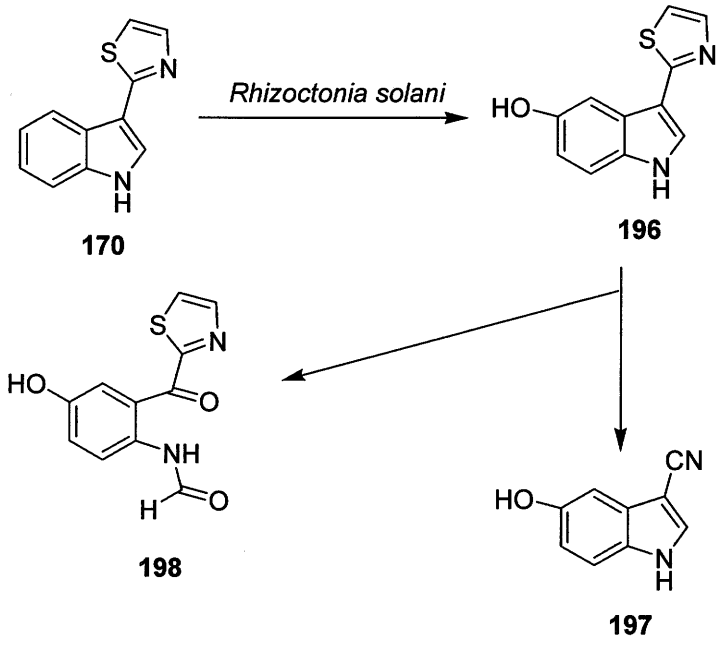

Scheme 1.26 Detoxification of camalexin (**170**) by fungal pathogen *Rhizoctonia solani* (Pedras & Khan, 1997).

To probe the selectivity of the enzymes involved in the detoxification of brassinin (**149**), the metabolism and antifungal activity of several dithiocarbamates by *P. lingam* was investigated (Pedras *et al.*, 1997). Because methyl tryptamine dithiocarbamate (**199**) was significantly more inhibitory to *P. lingam* than brassinin (**149**), its transformation by fungal cells was examined (Pedras & Okanga, 1998). Compounds **200** and **203** were the major metabolites obtained from fungal transformation of **199**, followed by acetyltryptamine (**202**) and minor components (Scheme 1.27). There appeared to be two major pathways, one leading to acid **203** via tryptamine (**201**) and acetyltryptamine (**202**) and the other leading to dithiocarbamate **200**. Interestingly, the fungal transformation of **199** occurred significantly faster in the absence of light (three to five days vs. two weeks), although a similar metabolite profile was detected. The metabolism of dithiocarbamate **199** by virulent isolates of *P. lingam* was a detoxification process, which proceeded much slower than that of the naturally occurring phytoalexin **149**. That is **149** was metabolized in 24 hours to indolyl-3-carboxylic acid while **199** could be recovered from fungal cultures even

after incubation for two weeks. The difference between the fungal metabolism of compounds **149** and **199** was attributed to either higher toxicity of **199**, or to the specificity of the enzymes involved in the transformations (Pedras & Okanga, 2000).

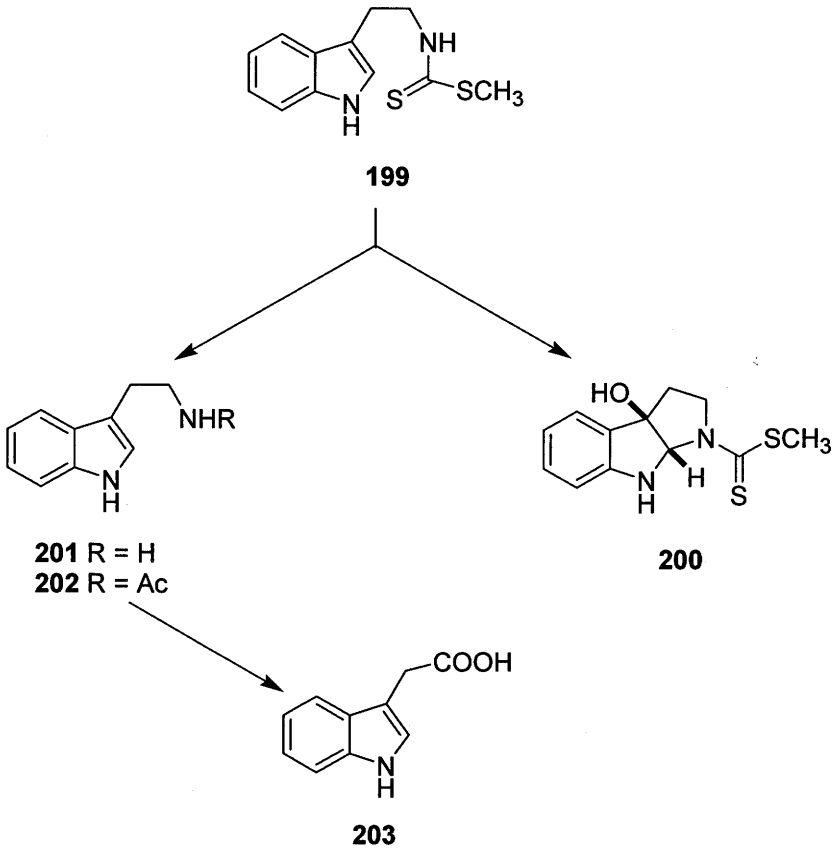

Scheme 1.27 Detoxification of methyl tryptamine dithiocarbamate (**199**) by fungal pathogen *Phoma lingam* (Pedras & Okanga, 1998; Pedras & Okanga, 2000).

Biotransformation studies were carried out with indole-3-acetaldoxime (**183**), the crucial intermediate (See Scheme 1.22) in the biosynthesis of brassica phytoalexins. It was metabolized by the three *Brassica* pathogens *P. lingam*, *R. solani* and *S. sclerotiorum* to indole-3-acetic acid (**203**) via indole-3-acetonitrile (**178**). *P. lingam*, and *R. solani* further

metabolized **178** to indole-3-carboxylic acid (**185**) as shown in Scheme 1.28 (Pedras & Montaut, 2003). To determine if the biotransformations observed were detoxification process, the antifungal activity of indole-3-acetaldoxime (**183**) and its metabolites was compared using mycelial growth inhibition assays (Pedras & Montaut, 2003). The results of these assays indicated that the biotransformation of indole-3-acetaldoxime (**183**) by these three pathogens was a detoxification process as the metabolites had no significant antifungal activity.

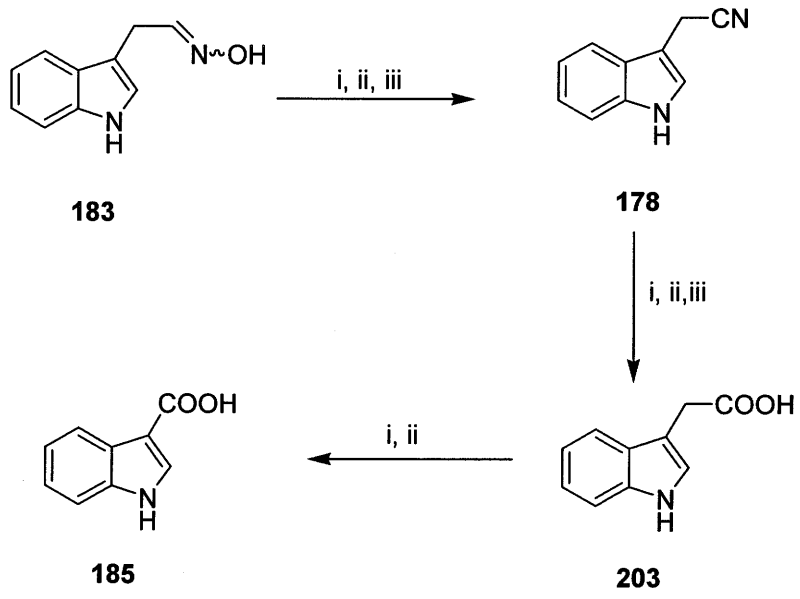

Scheme 1.28 Metabolism of indole-3-acetaldoxime (**183**) by *Brassica* pathogens i) *Phoma lingam*; ii) *Rhizoctonia solani*, and iii) *Sclerotinia sclerotiorum* (Pedras & Montaut, 2003).

Contrary to previous findings on the metabolism of crucifer phytoalexins by phytopathogens, where transformation pathways appeared characteristic of a particular phytopathogenic species, the results described above indicate that the metabolism of indole-3-acetaldoxime (**183**) is similar in all plant pathogenic species. Due to the central biogenetic role played by **183**, it would be of great interest to establish if during fungal

infection of plants, **183** is metabolized and if so, could such a process be inhibited without interfering with the normal plant development. In addition, investigation of the fungal enzymes involved in these transformations, and comparison with related and currently known plant enzymes, should provide a better understanding of their evolution. Furthermore, considering that a number of secondary metabolic steps co-occur in cruciferous pathogens and their hosts, these systems provide an ideal opportunity to investigate the co-evolution of secondary metabolism in plants and their pathogens (Pedras & Montaut, 2003).

1.5 Overview and conclusions

The interactions of plants with pathogenic fungi are very complex. As part of the defense mechanisms against pathogen attack, plants synthesize phytoalexins, while pathogens produce phytotoxins. As a response, each organism produces enzymes that degrades and detoxifies the other organism's chemical "weapons" (Pedras *et al.*, 2002b). Elucidation of such detoxification mechanisms, followed by isolation and characterization of the enzymes responsible for these processes could lead to a better understanding of the plant-pathogen interactions.

A correlation between the bioactivity of the phytoalexins and their biotransformation products will allow an understanding of the detoxification mechanisms employed by the fungus to overcome the plant's defences. Current work with plant pathogenic fungi suggests that such detoxification mechanisms are both substrate and pathogen specific (Pedras, 1998a). For example, to probe the selectivity of the fungal enzymes involved in detoxification of the phytoalexin brassinin (**149**), the metabolism of an analogue was investigated (See Scheme 1.27) (Pedras & Okanga, 2000). The much slower rate of transformation of this analogue was partly attributed to the specificity of the enzymes involved in the detoxification steps. Further work to better understand

phytoalexin detoxification mechanisms employed by plant pathogens, particularly where the outcome of the plant-pathogen interaction is highly detrimental to the plant should lead to new strategies to prevent plant diseases. It should then be possible to biorationally design antifungal agents (i.e. paldoxins) selective against the fungal pathogen (Pedras *et al.*, 2003a). By design paldoxins (**P**hyto**al**exin **d**eto**x**ification **in**hibitors**)** are non-toxic selective inhibitors, which may be used as a mixture against a variety of plant pathogens, according to crop or region. Upon optimization, such mixture might have the advantage of acting synergistically with the natural disease resistance factors of plants and be effective crop protection agents.

These findings could find practical applications; cloning of the disease resistance genes encoding phytotoxin detoxifying enzymes could lead to plants with enhanced resistance against specific fungal pathogens, while use of effective paldoxins (Pedras *et al.*, 2003a) would be an environmentally safe method for controlling phytopathogenic fungi.

CHAPTER TWO

2. Results and discussion

2.1 Metabolites produced by Sclerotinia sclerotiorum

Sclerotinia sclerotiorum (Lib.) de Bary is a plant pathogenic fungus causing serious yield losses in a broad range of cultivated plants, excluding cereals. Most of the economically important brassicas such as canola, rapeseed, and mustards are susceptible to this pathogen. This section describes and discusses the results obtained from the isolation of secondary metabolites from liquid cultures and from sclerotia of *S. sclerotiorum,* and their phytotoxic effects on the oilseed crucifers and mustards (canola, *Brassica napus*, cv. Westar; brown mustard, *B. juncea*, cv. Cutlass and white mustard, *Sinapis alba*, cv. Ochre) that are susceptible to the fungus and the wild crucifer *Erucastrum gallicum* (dog mustard) that is resistant. Cytotoxic effects of metabolites were established using brine shrimp (*Artemia salina*) larvae. This study was performed to determine a possible correlation between phytotoxin production and stem rot resistance.

2.1.1 Phytotoxins from liquid cultures of *Sclerotinia sclerotiorum*

S. sclerotiorum (clones # 33 and # 67) were cultured and extracted as reported in the experimental. Three different growth media, namely a chemically defined minimal medium, potato dextrose broth (PDB) and Czapek - Dox medium were used with sclerotia serving as the inoculum for the liquid cultures. Sclerotia were maintained on potato dextrose agar (PDA) plates at 24 ± 2 °C in the dark for 7 days. Mycelial growth was usually observed after 5 days of incubation in minimal media, after 3 days in PDB and after 10 days of incubation in Czapek - Dox media. EtOAc extracts of 14-day-old

cultures from PDB (1 L, ca. 72 mg), minimal media (1 L, ca. 44 mg) and Czapek - Dox medium (1 L, ca. 39 mg) were analyzed by HPLC (diode array detection). Inspection of the HPLC chromatograms indicated that the two clones of *S. sclerotiorum* produced similar metabolites in all three culture media.

Preliminary experiments were carried out to establish the optimum time for the production of phytotoxic metabolites. Thus, leaf puncture bioassays using EtOAc and butanol broth extracts of cultures of *S. sclerotiorum* (7, 14, and 21-day-old cultures) coupled with HPLC analyses of these extracts were performed. Two week old plants (*B. napus*, *B. juncea* and *S. alba*) susceptible to Sclerotinia stem rot disease were used for bioassays. The HPLC chromatograms of EtOAc extracts of the cultures showed a peak with R_t = 24.0 min showing the highest intensity in extracts of 14 and 21-day-old cultures; this peak was not detected in the butanol extract. Furthermore, the extracts of 14-day-old liquid cultures caused the most damage to the plants. Large brown lesions in circular patterns (ca. 4.5 mm diameter for extracts of 14-day-old culture broth vs. ca. 3.5 mm diameter for 21-day-old culture broth) were observed on the three plant species tested. The results of these experiments showed that the maximum amounts of phytotoxic metabolites peaked in 14 day-old liquid cultures of *S. sclerotiorum*.

In scale up experiments, extracts (1.02 g) of 14-day-old PDB cultures (17 L) of *S. sclerotiorum* were obtained as described in the experimental section. The extracts were phytotoxic to *B. napus*, *B. juncea* and *S. alba* (at 1 mg/mL); however, these extracts caused no damage to the leaves of *E. gallicum* (dog mustard) at similar concentration. These results could be explained in view of the fact that *E. gallicum* is resistant to the fungal pathogen *S. sclerotiorum* (Lefol, *et al.*, 1997). The extract was subjected to FCC (gradient elution: CH_2Cl_2 – MeOH) with each fraction analyzed by TLC and HPLC and also bioassayed on *B. napus*, *B. juncea* and *S. alba*. The bioactive fractions were combined and further purified by very laborious separation procedures involving multiple chromatography as described in the experimental section and summarized in

Scheme 2.1. HPLC analyses coupled with bioassays on the fractions enabled isolation of the phytotoxic metabolite **X** (50 mg, with R_t = 24 min).

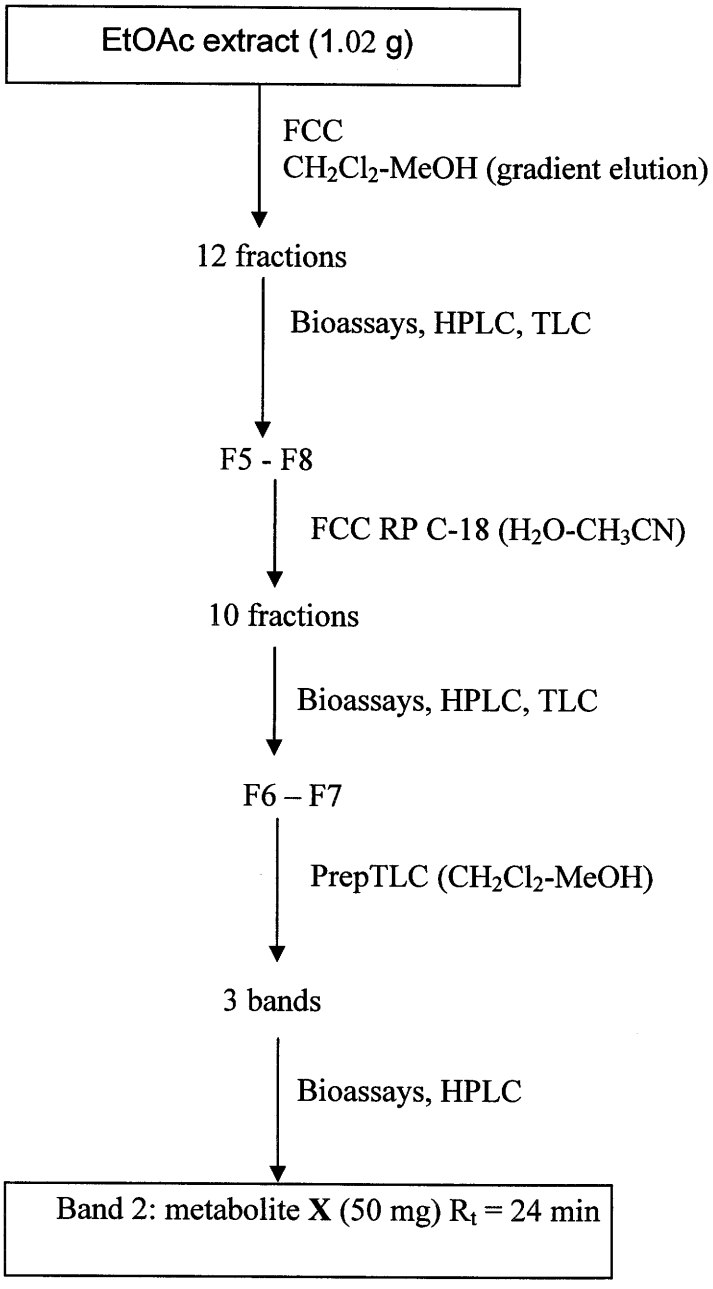

Scheme 2.1 Bioassay guided isolation of metabolite **X** with R_t = 24 min from liquid cultures of *Sclerotinia sclerotiorum*

Analysis of the HRMS-EI spectrum of compound **X** suggested a molecular formula of $C_{13}H_{14}O_4$. The absorptions at 1795 cm^{-1} and 1694 cm^{-1} in the FTIR spectrum of **X** indicated the presence of a carboxylic acid anhydride group. The ^1H NMR spectrum showed a broad singlet at δ 10.78 (D_2O exchangeable), three methyl singlets at δ 2.20 - 2.50 (likely attached to sp^2 carbons) and protons at δ 1.59 (d, J = 8 Hz) coupled to a methine proton at δ 4.18 (q, J = 8 Hz). The ^{13}C NMR data confirmed the presence of two carbonyl groups (δ 169.7, 166.7), five sp^3 carbons (δ 39.1, 22.7, 17.9, 14.9, 12.3) and six sp^2 carbons [δ 148.2 (s), 134.9 (s), 125.0 (s), 124.4 (s), 101.8 (s)], one of which was highly deshielded (δ 159.2) suggestive of a C-O linkage to aromatic ring. Analysis of the complete spectroscopic data of metabolite **X** allowed the assignment of the structure shown in Figure 2.1. The FTIR and the ^1H NMR data of this compound matched that of sclerin (**17**) previously isolated from *S. sclerotiorum* (Satomura *et al.*, 1963). Sclerin (**17**) was isolated as a racemic mixture.

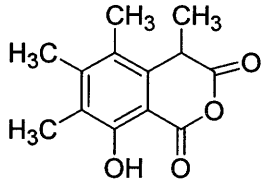

17

Figure 2.1 Sclerin (**17**), a phytotoxin from *Sclerotinia sclerotiorum*

2.1.2 Cytotoxic compounds from sclerotia of *Sclerotinia sclerotiorum*

Solid cultures (PDA plates) of *S. sclerotiorum* were grown for 7-10 days and the sclerotium collected and stored in a freezer at – 20 °C. Sclerotia from *S. sclerotiorum* were ground and sequentially extracted with EtOAc and butanol as described in the experimental. Phytotoxic assays using *B. napus*, *B. juncea*, *S. alba* and *E. gallicum* were performed on these extracts as described in the experimental. None of the extracts from the sclerotia of *S. sclerotiorum* showed phytotoxicity to *B. napus*, *B. juncea*, *S. alba* or *E. gallicum*. The cytotoxicity of these extracts was determined using the brine shrimp lethality assay (Hostettmann, 1991). Brine shrimp (*Artemia salina*) larvae were hatched in saline water (aqueous NaCl, 0.33 g /100 mL) and separate assays performed with the two extracts. The results of these assays suggested that only the EtOAc extract was cytotoxic to the brine shrimp larvae; all the shrimp larvae died in 24 hours when incubated with 1.0 mg/mL of EtOAc extract; 10 % of the larvae survived when incubated with the same extract at a lower concentration of 0.1 mg/mL. For the butanol extract, all the brine shrimp larvae survived in solutions even at concentrations of 1.0 mg/mL. These results showed that the butanol extracts of sclerotia did not appear to contain cytotoxic substances. These results suggest that most of the cytotoxic substances present in the sclerotia of *S. sclerotiorum* were extracted with EtOAc.

The EtOAc extract of sclerotia of *S. sclerotiorum* was subjected to FCC, and all the fractions were assayed against the brine shrimp larvae. Each of the cytotoxic fractions obtained caused death to the brine shrimp larvae at concentrations as low as 0.1 mg/mL. However, at a concentration of 0.01 mg/mL all the shrimp larvae survived. The cytotoxic fractions were combined and purified by preparative TLC. ^{1}H NMR analysis of the cytotoxic fraction obtained after preparative TLC indicated it to be a mixture of fatty acids. After methylation of the fatty acid mixture with diazomethane, separation and analysis was achieved by GC-MS. Analyses of the EIMS data enabled the identification of three known

fatty acids, namely hexadecanoic acid (palmitic acid, 22%), octadecanoic acid (stearic acid, 9%) and cis-9-octadecenoic acid (oleic acid, 42%). These structures were established unambiguously by comparison with authentic standards. These results are consistent with results of previous studies (Howell & Fergus, 1964), which determined that the major fatty acids of sclerotia from most fungi are the C-16 and C-18 acids. The remaining portion (27%) was thought to be composed of less common fatty acids of molecular formulae $C_{22}H_{40}O_2S$ (10%) and $C_{21}H_{38}O_2S$ (17%).

2.1.3 Phytotoxicity assays

To test the phytotoxic effects of sclerin (**17**), oxalic acid, broth and sclerotia extracts, different types of assays were developed using leaves of *B. napus*, *B. juncea*, *S. alba* and *E gallicum*. The phytotoxicity of oxalic acid was investigated because it is reported that the production of oxalic acid by *S. sclerotiorum* correlates with the pathogenicity (Cessna *et al.*, 2000). In one of the assays, to ensure that penetration of the test solution in the leaf tissue at the wound site was uniform for the four species (*B. napus* leaves are thicker, due to a protective layer of wax covering the surface), the leaf surface was scratched/punctured and the test solutions applied to these sites (Vurro *et al.*, 1998). The phytotoxic effects of extracts and sclerin (**17**) were evaluated by measuring the size of lesions on leaves. The toxicity of the extracts and metabolites was tested at different concentrations: six concentrations for sclerin (1×10^{-3}, 5×10^{-4}, 3×10^{-4}, 2×10^{-4}, 10^{-4}, and 10^{-5} M), five concentrations for oxalic acid (5×10^{-2}, 1×10^{-3}, 5×10^{-4}, 3×10^{-4} and 2×10^{-4} M), two concentrations for broth and sclerotia extracts (1 mg/mL and 2 mg/mL) and chromatographic fractions (each 1 mg/mL) dissolved in 50% aqueous methanol. Control leaves were tested using 50% aqueous methanol.

Plants were observed daily up to 7 days after droplet application to evaluate leaf damage. Results of this bioassay are presented in Table 2.1. The results showed no

significant differences between lesions observed on the scratched side of the leaf and lesions observed on the punctures side. Sclerin (**17**) showed phytotoxic effects on *B. napus, B. juncea* and *S. alba* causing necrotic and chlorotic tissue damage.

Table 2.1 Results of bioassays carried out with sclerin (**17**), oxalic acid, broth, and sclerotia extracts of *Sclerotinia sclerotiorum* applied to scratched/punctured leaves of *Brassica napus* cv. Westar (susceptible), *Brassica juncea*, cv. Cutlass (susceptible) *Sinapis alba* cv. Ochre (susceptible) and *Erucastrum gallicum*, wild (resistant) after 7 days of incubation

Phytotoxin	Concentration	*B. napus*[a] cv. Westar	*B. juncea* cv. Cutlass	*S. alba* cv. Ochre	*E. gallicum*[b] Wild plant
Sclerin (**17**)	1×10^{-3} M	+++	+++	+++	–
	5×10^{-4} M	++	++	++	–
	3×10^{-4} M	+	+	+	–
	2×10^{-4} M	–	–	–	–
Oxalic acid	1×10^{-3} M	–	–	–	–
	5×10^{-4} M	–	–	–	–
	3×10^{-4} M	–	–	–	–
	2×10^{-4} M	–	–	–	–
Broth extract	1.0 mg/mL	++	++	++	–
	2.0 mg/mL	+++	+++	+++	–
Sclerotia extract	1.0 mg/mL	–	–	–	–
	2.0 mg/mL	–	–	–	–

[a]Two-week-old plants scratched/punctured with needle and 10 μL droplet of compound (in 50% aqueous methanol) applied with micropipette; leaves scored after 1 week; ± = slight lesion < 1 mm; + = lesion diameter 1 - 2 mm; ++ = lesion diameter 2 - 3 mm; +++ = lesion diameter > 3 mm; – = no lesion.

[b]*E. gallicum* was grown for five-weeks.

Light brown lesions in circular patterns with an average diameter of about 3 mm were observed on the leaves of these crucifers when sclerin (5×10^{-4} M) and broth extract (1 mg/mL, contains 3×10^{-3} M sclerin estimated from standard curves) were applied. Oxalic acid (5×10^{-4} M) and sclerotium extract (2 mg/mL) of *S. sclerotiorum* showed no toxicity to any of the species. However, oxalic acid caused superficial damage to these crucifers only when a concentration of 5×10^{-2} M was applied. The concentration of sclerin (**17**) in broth extracts (HPLC, ca. 1 mg/mL) indicated that sclerin (**17**) is the component responsible for the phytotoxic activity of broth extracts. It is also worth noting that sclerin (**17**) did not cause damage to the leaf tissues of *E. gallicum* at the tested concentrations. Importantly, oxalic acid (1×10^{-3} M) did not cause macroscopic damage to any of the species.

In another type of assay, the leaf uptake bioassay, the test solutions were taken up through the petiole. This permitted the uniform distribution of test solution throughout the whole leaf, rather than a local effect, as in previous assay. The assay was performed with four different concentrations of sclerin (**17**) and oxalic acid ($1 \times 10^{-3}, 5 \times 10^{-4}$, 1×10^{-4} and 1×10^{-5} M) in 2% acetonitrile, and broth extract (0.6 mg/1 mL of 2% acetonitrile), as described in the experimental section. Control leaves were incubated with 2% of aqueous acetonitrile. After the test solution was taken up, the petioles of the leaves were kept in an aqueous solution of BAP (1×10^{-5} M) to prevent leaves from turning yellow, and were incubated under the same conditions up to 7 days. Sclerin (5×10^{-4} M) and broth extract of liquid cultures of *S. sclerotiorum* caused severe wilting of leaves (more intense in *S. alba*) after 4 days. Oxalic acid did not seem to have any effect on the plants tested.

In the third type of assay, the spray bioassay, 3 pots each containing *B. napus, B. juncea, S. alba* and *E. gallicum* (2 - 5 week old) plants were uniformly sprayed with 50% aqueous methanolic solution of broth extract (3 mg/25 mL, 15 mL) or 50% aqueous methanolic solution of sclerin (5×10^{-4} M, 15 mL) or 50% aqueous methanolic solution of oxalic acid (5×10^{-4} M, 15 mL), or 50% aqueous methanol (15 mL) as control. The pots

were kept in the growth chamber at 24 ± 2 °C for 7 days. Sclerin (**17**, 5×10^{-4} M), oxalic acid (5×10^{-4} M) and broth extract (3 mg/25 mL) did not seem to result in any macroscopic toxic effect on the plants.

From the results of these assays, it is evident that sclerin (**17**), one of the secondary metabolites of *S. sclerotiorum* is phytotoxic to cruciferous plants that are susceptible to Sclerotinia stem rot disease. It probably plays a significant role in damaging the plants when they are infested with the fungus.

2.1.4 Brine Shrimp lethality assays

The cytotoxicity of extracts from sclerotia of *S. sclerotiorum*, broth extracts from liquid cultures of *S. sclerotiorum*, sclerin (**17**), the fatty acid fraction from sclerotia, and the three fatty acids identified was determined using the brine shrimp lethality assay (Hostettmann, 1991). Brine shrimp (*Artemia salina*) larvae were hatched in saline water (aqueous NaCl, 0.33 g /100 mL) and separate assays performed on the samples as described in the experimental. The results of these assays are shown in Tables 2.2 and 2.3. The EtOAc extract of sclerotia (1 mg/mL), fatty acid fraction (0.4 mg/ mL) and oleic acid (5×10^{-4} M, the major component of the fatty acid fraction) caused 100% mortality to brine shrimp larvae, whilst no significant cytotoxic effect was observed for stearic acid and palmitic acid. These results indicate that oleic acid is responsible for the cytotoxic effect of sclerotia of *S. sclerotiorum*. Previous work reported in this area indicates that the fatty acids present in *S. sclerotiorum*, *S. borealis* and *Botrytis tulipae* (Sumner *et al.*, 1970; Weete *et al.*, 1970) varied if the fungi were isolated from host plants in the field or grown in the laboratory. Palmitic, oleic and linoleic acids were the major free fatty acids of the laboratory-grown sclerotia while a high proportion of linoleic acid was found in sclerotia from natural sources (Weete *et al.*, 1970).

Table 2.2 Toxicity of extracts of *Sclerotinia sclerotiorum* to brine shrimp

Compound	Concentration (mg / mL)	% Mortality[a] ± SD
Broth extract	1.0	0
Sclerotia extract	1.0	100
	0.4	85 ± 5
Fatty acid fraction	0.4	100
	0.1	90 ± 5
	0.01	0

[a] % Mortality = 100 - [(number of live shrimp after 24 h / number of live shrimp in control) × 100] ± standard deviation.

By and large, the major fatty acids isolated from sclerotia of *S. sclerotiorum* were oleic, palmitic and linoleic acids, whereas ∝-linolenic, myristic, palmitoleic and stearic acids formed minor components, lauric, pentacanoic, heptadecanoic and arachidic acids were present in trace amounts (Weete *et al.*, 1970). These results indicate that oleic acid is responsible for the cytotoxic effects of the EtOAc extracts of sclerotia of *S. sclerotiorum*. Sclerin (**17**), the phytotoxic metabolite isolated from liquid cultures of *S. sclerotiorum* and the broth extract appear to have no cytotoxic effect on *A. salina*.

Fatty acids isolated from *Aspergillis sydowi* have been reported to be cytotoxic to brine shrimp (Curtis *et al.*, 1974) and man (Lima *et al.*, 2002). Toxicity was found to increase with unsaturation in fatty acids with oleic, linoleic and linolenic acids being the most toxic. Fatty acids cause cell death via apoptosis or, when concentrations are greater, necrosis in man (Lima *et al.*, 2002).

Table 2.3 Toxicity of metabolites isolated from *Sclerotinia sclerotiorum* to brine shrimp

Compound	Concentration (M)	% Mortality[a] ± SD
Sclerin (**17**)	5×10^{-4}	0
	1×10^{-4}	0
Oleic acid	5×10^{-4}	100
	1×10^{-4}	10 ± 5
Palmitic acid	5×10^{-4}	5 ± 5
	1×10^{-4}	0
Stearic acid	5×10^{-4}	8 ± 5
	1×10^{-4}	0

[a] % Mortality = 100 - [(number of live shrimp after 24 h / number of live shrimp in control) × 100] ± standard deviation.

2.2 Phytoalexins from *Erucastrum gallicum*

Erucastrum gallicum (dog mustard) is a wild crucifer that is resistant to the stem rot disease (Lefol *et al.*, 1997) caused by *S. sclerotiorum*. One of the objectives of this work is to establish the chemical defences pertinent to the interaction between *S. sclerotiorum* and its host plants (as for example canola and rapeseed oilseeds, white mustard, brown mustard; susceptible to the pathogen). Hence, it was of great interest to investigate the phytoalexins produced by the resistant plant species *E. gallicum*. This section describes and discusses the results of elicitation, isolation and structure determination of phytoalexins from *E. gallicum*, as well as attempts at the synthesis of erucalexin (**204**), a new phytoalexin from *E. gallicum*.

2.2.1 Elicitation, isolation and chemical structure elucidation

Experiments were designed to elicit, isolate and determine the phytoalexins that *E. gallicum* produces when infected with *S. sclerotiorum* or under other stress conditions. In preliminary experiments, a time-course response to biotic elicitation with mycelia of *S. sclerotiorum* as well as abiotic elicitation with $CuCl_2$, oxalic acid and sclerin (**17**) was investigated. As stated previously, sclerin (**17**) and oxalic acid were chosen for abiotic elicitation of phytoalexins because they appear to be phytotoxins produced by the stem rot fungus. Elicitation of leaves with mycelia of *S. sclerotiorum* was carried out by placing mycelia plugs on leaf surface (4 plugs per leaf); droplet application was used in the case of sclerin (**17**) and oxalic acid whilst $CuCl_2$ and oxalic acid again were sprayed onto the leaves of whole plants. After different incubation times, leaves were excised, frozen in liquid N_2, crushed with a glass rod and extracted as described in the experimental.

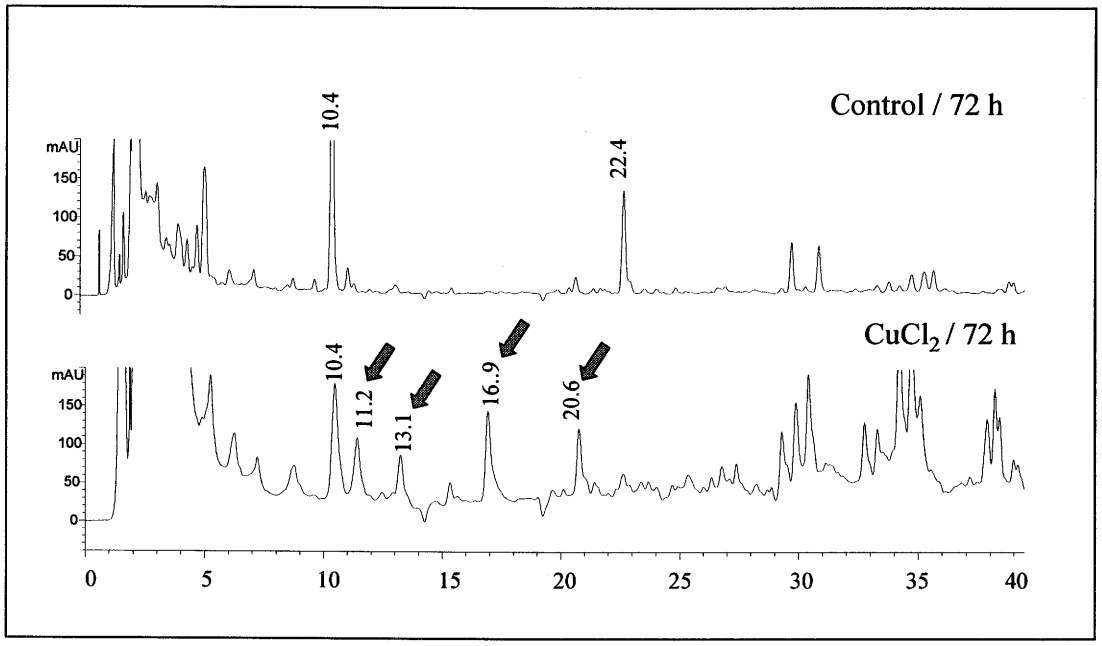

Figure 2.2 HPLC profile of extracts of elicited leaves of *Erucastrum gallicum* (elicitation performed with $CuCl_2$, arrows indicate peaks of elicited compounds).

Control (i.e. non-elicited) leaves were collected and treated in a similar manner. The HPLC chromatograms of extracts of leaves of dog mustard elicited with *S. sclerotiorum* or $CuCl_2$ indicated the presence of four compounds with R_t = 11.2 min., 13.1 min., 16.9 min., and 20.6 min, respectively, that were not present in control leaves (Figures 2.2 and 2.3). Sclerin (**17**) and oxalic acid did not seem to elicit any of these compounds even when plants were incubated up to 7 days.

Table 2.4: Elicitation of phytoalexins in leaf tissue of *Erucastrum gallicum* using mycelia of *S. sclerotiorum* as elicitor.

Phytoalexin	Incubation time	Total amount of phytoalexin (μmol/100 g of fresh leaf tissue)
Indole-3-acetonitrile (**178**)	24 h	0.54 – 0.63
	48 h	0.12 - 0.33
Arvelexin (**179**)	24 h	0.79 – 1.35
	48 h	0.23 - 0.44
1-Methoxyspirobrassinin (**176**)	24 h	2.20 - 3.68
	48 h	1. 05 - 1.51
Erucalexin (**204**)	24 h	3.63 - 6.02
	48 h	1.25 - 2.93

The compounds with R_t = 11.2 min. and 13.1 min were identified as indole-3-acetonitrile (**178**), and arvelexin (**179**), by comparison with authentic standards. Indole-3-acetonitrile (**178**) was isolated from elicited leaves of *B. juncea* (Pedras *et al.*, 2002a) whilst arvelexin (**179**) was isolated from elicited leaves of *Thlaspi arvense* (stinkweed) (Pedras *et al.*, 2003b), a wild crucifer resistant to blackleg disease. Compounds **178** and **179** were found to be strongly antifungal against the blackleg fungus *P. lingam* confirming that they are phytoalexins (Pedras *et al.*, 2002a; Pedras *et al.*, 2003b). Elicitation of

phytoalexins by *S. sclerotiorum* was significantly faster (ca. 24 h vs. 48 - 96 h) than that observed for $CuCl_2$. (Tables 2.4 and 2.5).

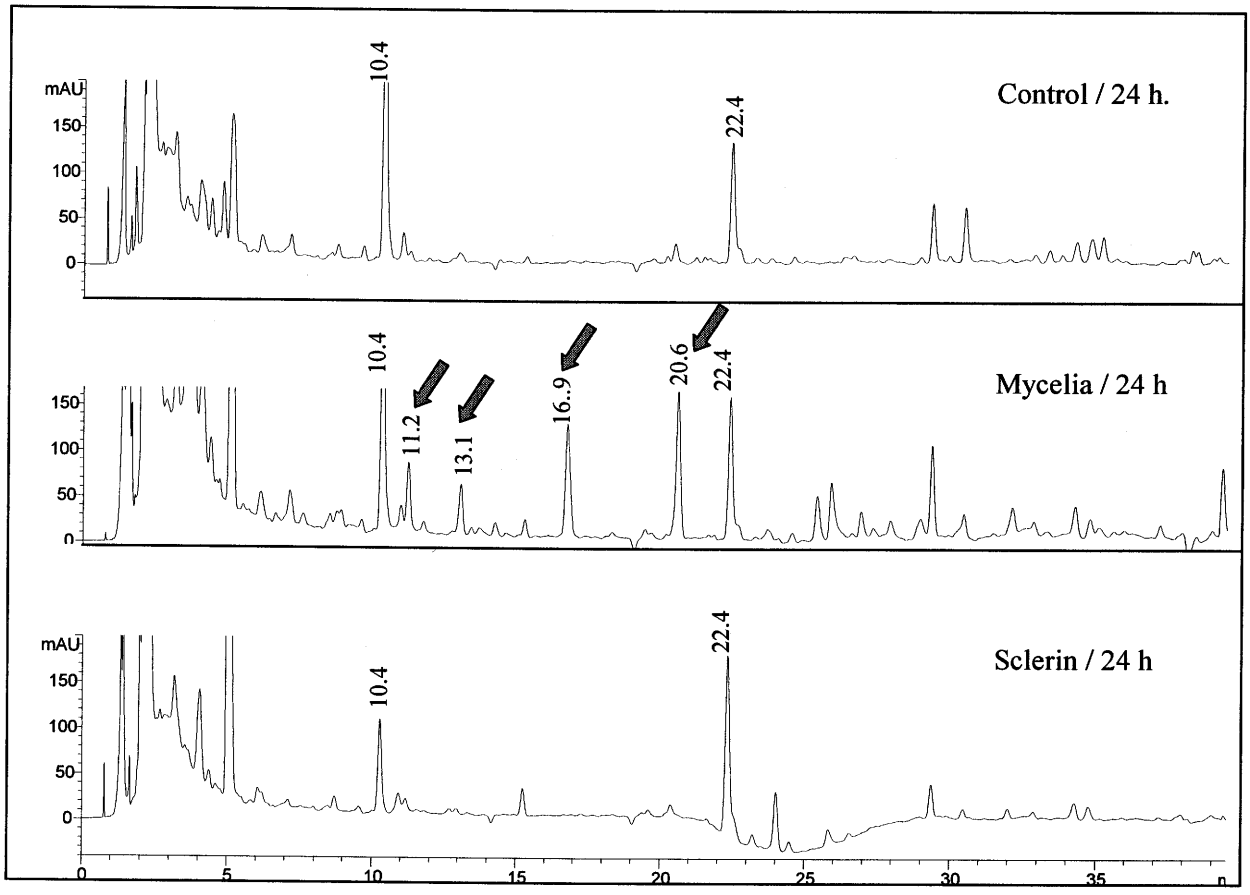

Figure 2.3 HPLC profile of extracts of elicited leaves of *Erucastrum gallicum* [elicitation performed with mycelia of *Sclerotinia sclerotiorum* and sclerin (**17**), arrows indicate peaks of elicited compounds].

In order to obtain reasonable amounts of extracts of elicited leaves necessary for isolation and structure determination of the two remaining compounds, $CuCl_2$ elicited dog mustard leaves were processed in a manner similar to that used in the time-course study but on a larger scale. This method of elicitation was chosen due to its simplicity, low cost of elicitor and short incubation time required. The EtOAc extract (1.2 g from 180 g of

leaves) was subjected to FCC using a CH_2Cl_2-MeOH gradient. The fractions containing the HPLC peaks at R_t = 16.9 min and R_t = 20.6 min were combined (284 mg) and further fractionated by multiple reverse phase chromatography to give 1.3 mg of the metabolite with R_t = 16.9 min and 2.2 mg of the metabolite with R_t = 20.6 min. This isolation procedure was repeated several times to obtain enough of **176** (5 mg) and **204** (6.8 mg) for antifungal bioassays.

Table 2.5: Elicitation of phytoalexins in leaf tissue of *Erucastrum gallicum* using $CuCl_2$ (2×10^{-3} M) as elicitor.

Phytoalexins	Incubation time	Total amount of phytoalexin (μmol/100 g of fresh leaf tissue)
Indole-3-acetonitrile (**178**)	24 h	Not detected
	48 h	0.58 – 1.08
	72 h	0.89 – 1.92
	96 h	1.89 – 2.22
Arvelexin (**179**)	24 h	Not detected
	48 h	2.54 - 4.40
	72 h	1.21 –1.96
	96 h	1.04 - 1.82
1-Methoxyspirobrassinin (**176**)	24 h	Not detected
	48 h	2.03 – 2.74
	72 h	2.66 - 3.03
	96 h	1.55 - 3.03
Erucalexin (**204**)	24 h	Not detected
	48 h	3.40 - 4.46
	72 h	5.56 - 5.95
	96 h	3.99 - 4.42

The HRMS data for the metabolite with R_t = 16.9 min (**176**) indicated a molecular formula of $C_{12}H_{12}N_2S_2O_2$ (obtained *m/z* 280.0336, calcd. 280.0340), further corroborated by analysis of the NMR spectroscopic data. The NMR spectra of this compound displayed resonances in the aromatic region indicative of a 2-oxindole moiety as in spirobrassinin (**173**) (Takasugi *et al.,* 1987), as well as signals due to methoxy (δ_H 3.99; δ_C 63.9), and thiomethyl groups (δ_H 2.62; δ_C 15.3), a carbonyl or equivalent group (δ_C 163.2) and a methylene group (δ_H 4.60, d, J = 15.5 Hz; δ_H 4.46, d, J = 15.5 Hz; δ_C 72.6). The ^{1}H NMR, FTIR and MS-EI spectral data for metabolite **176** were identical to that of 1-methoxyspirobrassinin, a phytoalexin isolated from *Brassica oleracea* (Gross *et al.*, 1994). However, the ^{13}C NMR data of 1-methoxyspirobrassinin are being reported here for the first time. To the best of our knowledge, this is the first time indole-3-acetonitrile (**178**), arvelexin (**179**) and 1-methoxyspirobrassinin (**176**) (Figure 2.4) have been isolated from the wild crucifer *E. gallicum*.

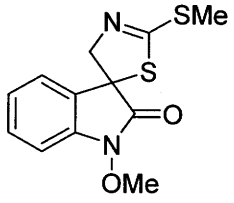

176

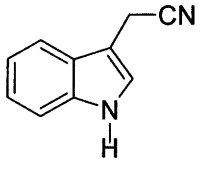

178

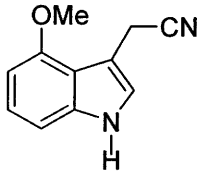

179

Figure 2.4 Phytoalexins isolated from leaves of *Erucastrum gallicum* (dog mustard)

The HRMS-EI data for the metabolite with R_t = 20.6 min (**204**) indicated a molecular formula of $C_{12}H_{12}N_2S_2O_2$ (obtained *m/z* 280.0346, calcd. 280.0340), further corroborated by analysis of the NMR spectroscopic data. The NMR spectral data of **204** (See Table 2.6) had some similarities to that of 1-methoxyspirobrassinin [(**176**), i.e. signals

Table 2.6: NMR data for erucalexin (**204**)

Position	δ_H (multiplicity, J in Hz)[a]	δ_C	HMBC correlations (C-#)	NOE correlations (% enhancement)
2	-	94.4		
3	-	192.3		
3a	-	121.2		
4	7.68 (d, J = 8)	124.3	C-7a, 6, 3	
5	7.21 (ddd, J = 8, 8, 1)	124.0	C-7, 3a, 6	
6	7.73 (ddd, J = 8, 8, 1)	138.3	C-7a, 4, 5	
7	7.32 (d, J = 8)	114.2	C-3a, 5, 6	
7a	-	160.1		
2'	-	162.6		
4a'	4.75 (d, J = 16)	71.6	C-2, 2'	H-4b' (18), -OMe (14), -SMe (15)
4b'	4.35 (br d, J = 16)	71.6	C-2', 3	H-4a' (15), -OMe (1), -SMe (1)
Other (-OMe)	3.95 (s)	65.1		H-7 (1), H-4a' (1)
Other (-SMe)	2.61 (s)	15.2	C-2', 4a', 4b'	

due to one methoxy group (δ_H 3.95; δ_C 65.1) attached to *N*-1 of indolic ring system, thiomethyl group (δ_H 2.61; δ_C 15.2), a methylene group (δ_H 4.75, J = 16 Hz; δ_H 4.35, J = 16 Hz; δ_C 71.6) and four aromatic protons on an ortho-disubstituted benzene ring]. Irradiation of the methoxy protons (δ_H 3.95) caused an NOE enhancement of the aromatic proton signal at δ 7.32 (1H, d, J = 8Hz, 7-H), and consecutive decoupling experiments assigned the remaining three aromatic protons [δ7.73 (1H, ddd, J = 8, 8, 1 Hz, 6- H), δ 7.68 (1H, d, J = 8 Hz, 4-H), δ 7.21 (1H, ddd, J = 8, 8, 1 Hz, 5-H)]. The signal at δ_C 192.3 is suggestive of a 3-indoxyl system or a 2-thioindolyl system rather than the 2-oxoindolyl system present in 1-methoxyspirobrassinin (**176**). These deductions were corroborated by analysis of the FTIR spectrum, which showed a strong absorption at 1725 cm^{-1}. This was supported by HMBC correlation between H-4 and C-3/C-2 of the indolic ring system. Other HMBC correlations were observed between the methylene protons and the carbon at δ_C 192.3, 94.4 (N-C-S), and C-2' (δ_C 162.6, S-C=N). These are shown in Figure 2.6. Based on these deductions structures **204** and **205** were proposed for the compound.

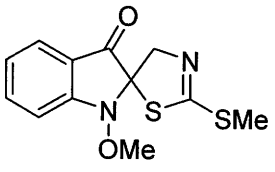

204

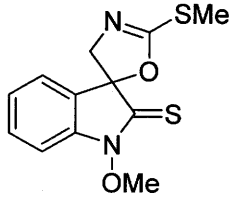

205

Figure 2.5 Proposed structures for erucalexin

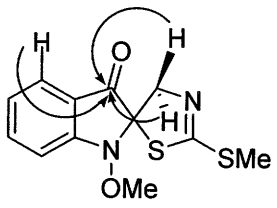

204

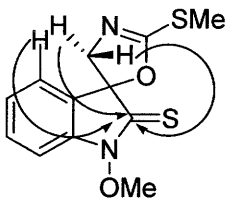

205

Figure 2.6 Selected HMBC correlations for proposed structures of erucalexin

2.2.2 Synthesis

The retrosynthetic analyses for compounds **204** and **205** are outlined in Schemes 2.2 and 2.3 respectively. Disconnection of the spiro ring in **204** results in **207**, which can be synthesized from **210** in four steps via Baeyer Villiger oxidation (**209**) and a series of steps involving addition, reduction and nucleophilic substitution reactions.

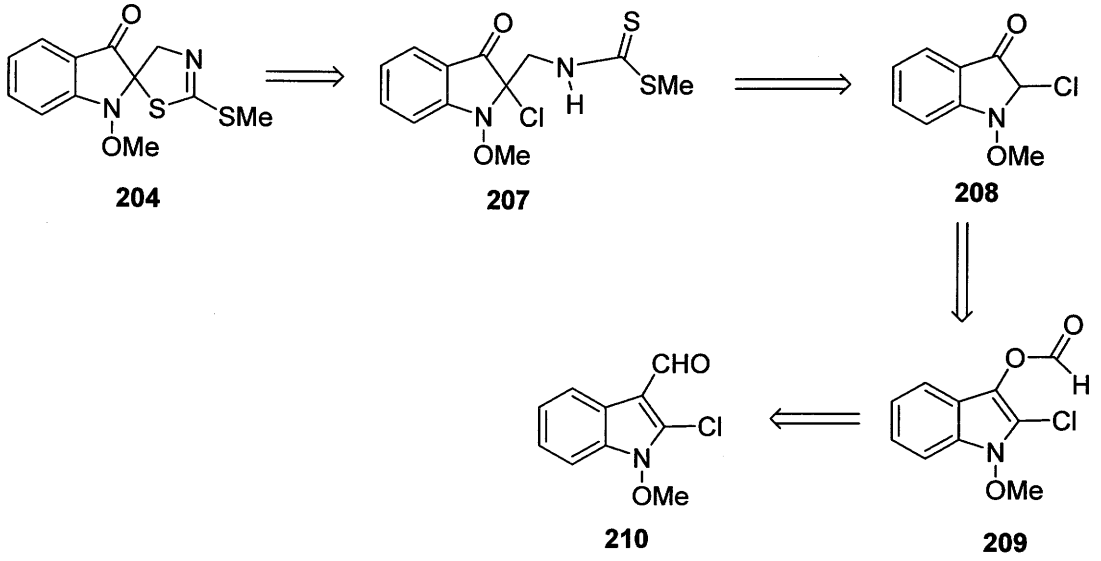

Scheme 2.2 Retrosynthetic analysis for compound **204**

For **205**, disconnection of the spiro ring results in **211** (Scheme 2.3) which can be synthesized from the isatin derivative **213** in four steps via **212** through a series of steps involving addition, reduction, and nucleophilic substitution reactions.

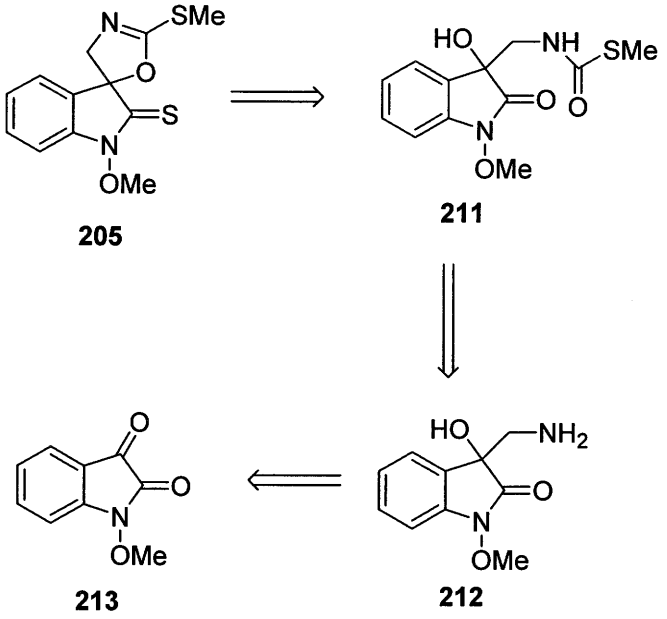

Scheme 2.3 Retrosynthetic analysis for compound **205**

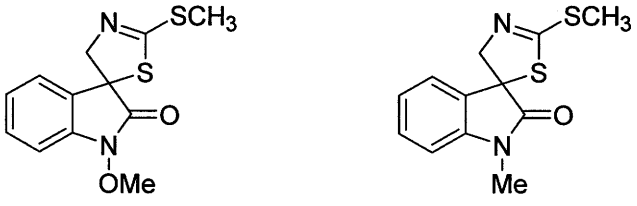

Figure 2.7 Structures of 1-methoxyspirobrassinin (**176**) and 1-methylspirobrassinin (**214**)

To establish which of the proposed structures represented erucalexin, compound **206**, the N-methyl analogue of **205**, was synthesized over five steps from 1-methylisatin (**215**) as outlined in Scheme 2.4 and described in the experimental section. Since the UV absorption spectra of 1-methoxyspirobrassinin (**176**) and 1-methylspirobrassinin (**214**) were very similar (see Table 2.7) it was thought that the absorption spectra of compounds **205** and **206** as well as all other spectroscopic data (splitting patterns in ^{1}H NMR, absorption bands in FTIR, fragmentation pattern in EIMS etc.) would also be similar, hence **206** was synthesized in lieu of **205**. This is because 1-methylisatin (**215**), the starting material is commercially available but 1-methoxyisatin is not. Addition of nitromethane to **215** under basic conditions followed by catalytic hydrogenation (Conn & Lindwall, 1936) of the hydroxynitromethane product afforded **216** in 78% yield. Subsequent cyclization of (±)-**216** with thiophosgene (as performed by Suchy *et al.*, 2001) gave (±)-**217** with the desired spiral ring system in 82% yield. The key step in the synthesis of (±)-**206** was the thiation of (±)-**217** where two different procedures were adopted. Thiation of (±)-**217** using phosphorus pentasulfide and sodium bicarbonate afforded (±)-**218** (16% yield) and (±)-**220** (34% yield). Subsequent methylation of (±)-**218** gave the desired racemic spirooxazoline (±)-2'-methylsulfanyl-spiro[1-methylindoline-3,5'-[4',5']-dihydrooxazol]-2-thione (**206**) in 92% yield. Direct methylation of (±)-**217** also afforded (±)-**219** in 96% yield.

The use of Lawesson reagent for the thiation of (±)-**217** did not seem to improve the yield of (±)-**218** (Wenkert *et al.*, 1985). It rather resulted in several products, which could not be isolated. Thiation of (±)-**219** either by Lawesson method or use of phosphorus pentasulfide did not afford (±)-**206**. Spectroscopic data of **206** revealed significant differences from that of the isolated compound indicating that compound **205** is not erucalexin.

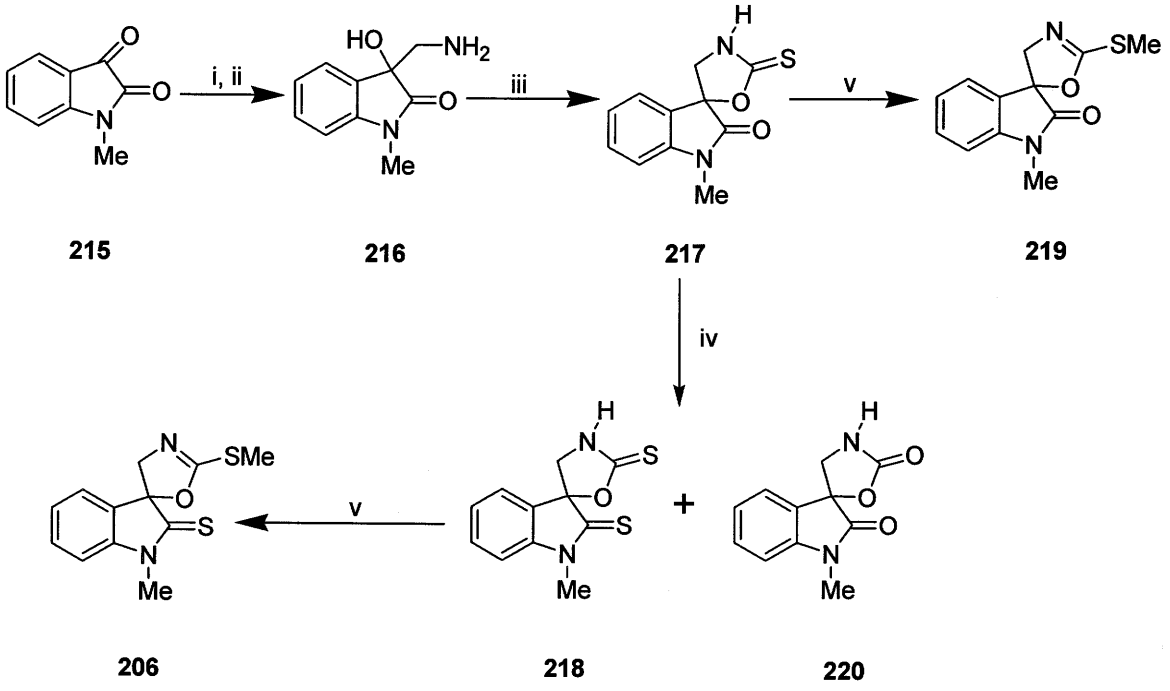

Scheme 2.4 Reagents: (i) CH_3NO_2, Et_2NH, EtOH, 0 °C; (ii) H_2, Pd-charcoal, MeOH, AcOH, 78%; (iii) $CSCl_2$, Na_2CO_3, CH_2Cl_2, 82%; (iv) P_4S_{10}, $NaHCO_3$, CH_3CN, reflux, (**218**, 16%; **220**, 34%); (v) K_2CO_3, MeI, acetone, (**206**, 92%; **219**, 96%).

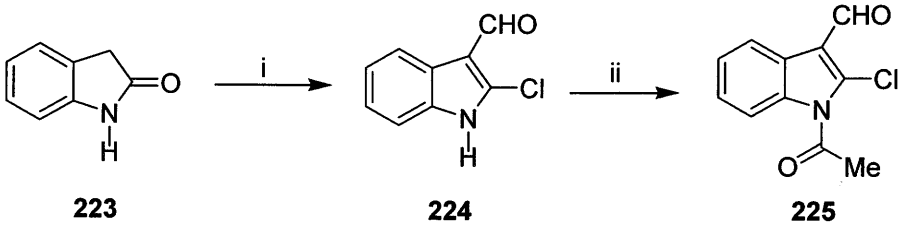

Scheme 2.5 Reagents: (i) $POCl_3$, DMF, $CHCl_3$, reflux, 42%; (ii) NaOEt, Ac_2O (quantitative conversion)

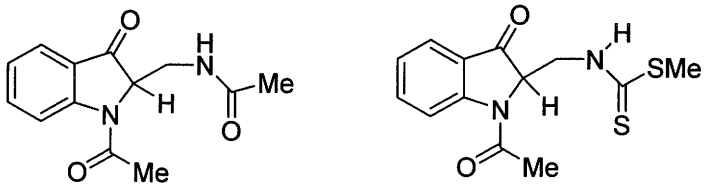

221 **222**

Figure 2.8 Analogues of proposed structure for erucalexin (**204**)

Attempts were then made to synthesize the N_b-substituted analogues **221** and **222** of proposed structure **204** for erucalexin as model compounds (Figure 2.8). Vilsmeier formylation of oxindole (**223**) as outlined in Scheme 2.5 and described in the experimental section afforded 2-chloro-1H-indolyl-3-carboxaldehyde (**224**) in 42% yield (Kutschy *et al.*, 2001). This was acetylated to **225**, and then subjected to Baeyer Villiger oxidation (Bourlot *et al.*, 1994) using *m*-CPBA yielding 1-acetyl-2-chloro-3-indolyl-3-methylformate (**226**) and (±)-1-acetyl-2-chloro-1,2-dihydro-3H-indol-3-one (**227**). Addition of nitromethane to **226** under basic conditions afforded (±)-1-acetyl-2-nitromethyl-3H-indol-3-one (**228**) in 43% yield (Scheme 2.6). Treatment of **227** with Et_2NH in nitromethane afforded **228** (11%) and (±) 1-acetyl-1,2-dihydro-2-diethylamino-3H-indol-3-one (**229**) in 30% yield (Scheme 2.6). Treatment of **227** with Et_3N in nitromethane afforded **228** in 18% yield (Scheme 2.7). Catalytic hydrogenation of **228** to **230** yielded a complex mixture (Scheme 2.8). Thus the acetylation of **230** to the desired model compound **221** and/or the reaction with CS_2 under basic conditions and then methylation was not attempted. The reduction of **228** to the desired amine **230** apparently affected the carbonyl group at C-3 position of the indole ring. There would be the need to protect this group before the reduction is carried out; however due to lack of time no further reactions were carried out.

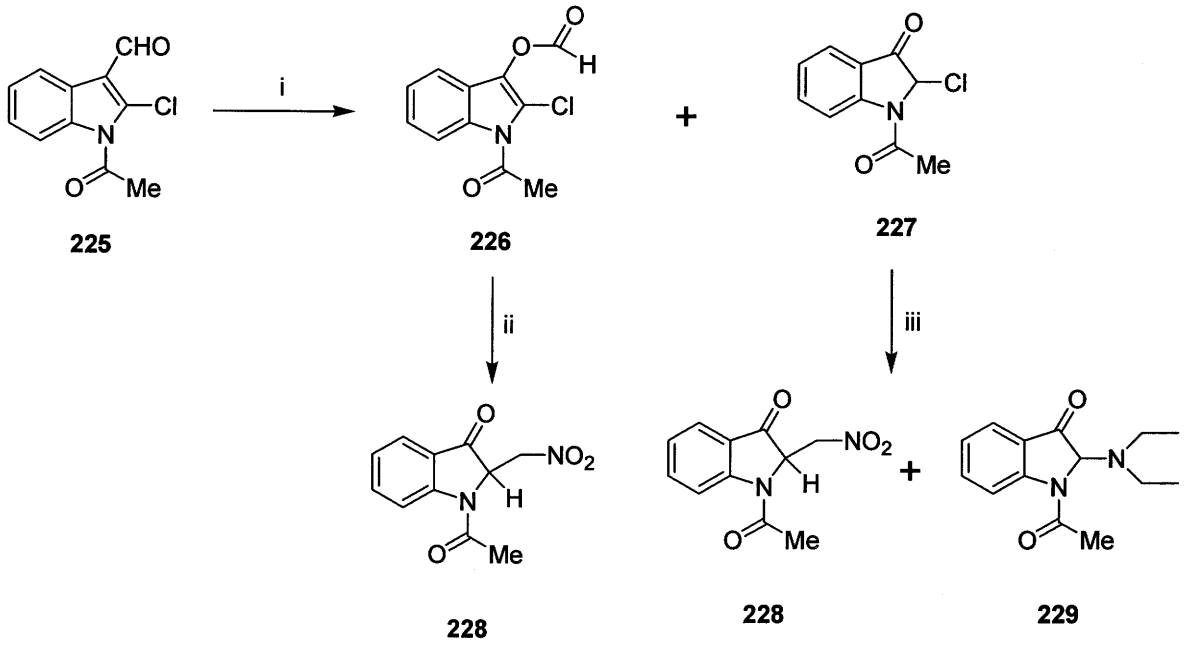

Scheme 2.6 Reagents: (i) *m*-CPBA, DMS, Na_2CO_3, 5 °C; (ii) CH_3NO_2, Et_2NH (**228**, 43%); (iii) CH_3NO_2, Et_2NH (**228**, 11%; **229**, 30%).

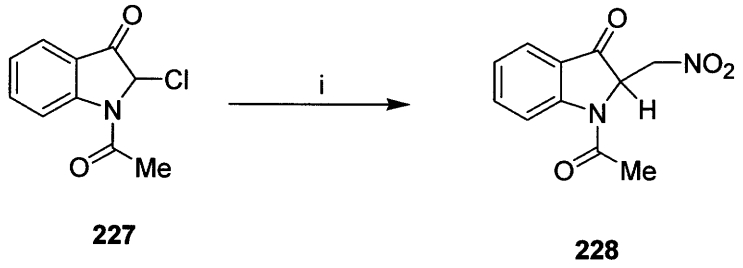

Scheme 2.7 Reagents: i) CH_3NO_2, Et_3N, 18%.

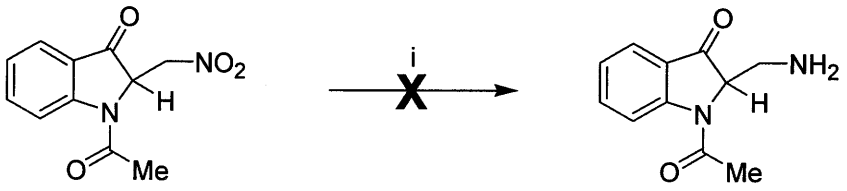

228 **230**

Scheme 2.8 Reagents: (i) H_2, Pd-charcoal, MeOH, AcOH

Table 2.7: UV spectral data of analogues of erucalexin (**204**)

Compound	λ_{max} (CH_3CN)	Log ε
Erucalexin (**204**)	234	4.6
	262	4.1
	368	3.4
1-Methoxyspirobrassinin (**176**)	218	4.4
	262	3.7
(±)-2'-Methylsulfanyl-spiro[1-methylindoline-3,5'-[4',5']-dihydrooxazol]-2-thione (**206**)	238	4.2
	287	3.8
	296	3.8
	337	4.0
1-Methylspirobrassinin (**214**)	218	4.4
	260	3.8
(±)-1-Acetyl-2-chloro-1,2-dihydro-3H-indol-3-one (**227**)	235	4.3
	262	3.7
	347	2.2
(±)-1-Acetyl-2-nitromethyl-1,2-dihydro-3H-indol-3-one (**228**)	236	4.5
	256	4.0
	344	3.6
(±)-1-Acetyl-2-diethylamino-1,2-dihydro-3H-indol-3-one (**229**)	237	4.5
	259	4.0
	343	3.5

The absorption spectra (UV) of compounds **176**, **206**, **214**, **227**, **228**, and **229** were compared with that of the isolated erucalexin (see Table 2.7). There were marked similarities between the UV absorption spectrum of the isolated metabolite erucalexin and compounds **227**, **228**, and **229**, all of which had the 3-indoxyl system. Absorption spectra of compounds **176**, **214** (they have 2-oxindolyl system), and **206** (has 2-thioindolyl system) were significantly different from that of the isolated metabolite. This rules out the presence of 2-oxindolyl and 2-thioindolyl systems and confirms unambiguously, the presence of the 3-indoxyl system in erucalexin.

From these studies the structure of erucalexin is deduced to be **204**. The synthesis of erucalexin (**204**) could not be achieved due to time constraint. This was the last project I embarked on. It has proved very challenging and thus one would need a lot of time to accomplish it.

2.2.3 Antifungal activity

The antifungal activity of 1-methoxyspirobrassinin (**176**), arvelexin (**179**) and erucalexin (**204**) was determined using the mycelia radial growth bioassay described in the experimental. Solutions of each compound in DMSO (5×10^{-2} M) were used to prepare solutions in minimal media (5×10^{-4} M, 2.5×10^{-4} M, 5×10^{-5} M); control solutions contained 1% DMSO in minimal media. These antifungal bioassays established that 1-methoxyspirobrassinin (**176**), erucalexin (**204**), and arvelexin (**179**) were active against *S. sclerotiorum* and *R. solani* (root rot fungus), two of the most important pathogens of oilseed and vegetable crucifers. Erucalexin (**204**, 5×10^{-4} M) caused complete inhibition to the growth of *R. solani* and 40% inhibition to *S. sclerotiorum* after 72 hours of incubation (Table 2.8). 1-Methoxyspirobrassinin (**176**, 5×10^{-4} M) also showed 68% inhibition to *R. solani* and 53% to *S. sclerotiorum* after 72 hours, whereas arvelexin (**179**, 5×10^{-4} M) showed 66% inhibition to *R. solani* and 46% to *S. sclerotiorum* after 72 hours.

Interestingly, erucalexin showed higher antifungal activity to *R. solani* than to *S. sclerotiorum*. Therefore erucalexin (**204**) is a new phytoalexin; arvelexin (**179**) and 1-methoxyspirobrassinin (**176**) were previously shown to be phytoalexins produced by *Thlaspi arvense* (Pedras *et al.*, 2003b) and *B. oleracea* (Gross *et al.*, 1994) respectively.

Table 2.8 Antifungal activity[a] of erucalexin (**204**), 1-methoxyspirobrassinin (**176**) and arvelexin (**179**) against *Rhizoctonia solani* and *Sclerotinia sclerotiorum* (3 days incubation, constant light).

Compound	Concentration	% Inhibition[a] *R. solani* AG 2-1	% Inhibition[a] *S. sclerotiorum* clone #33
Erucalexin (**204**)	5×10^{-4} M	100	40
	2.5×10^{-4} M	48	15
	5×10^{-5} M	0	0
1-Methoxy spirobrassinin (**176**)	5×10^{-4} M	68	53
	2.5×10^{-4} M	14	34
	5×10^{-5} M	0	10
Arvelexin (**179**)[b]	5×10^{-4} M	66	46
	2.5×10^{-4} M	36	10
	5×10^{-5} M	0	0

[a]Percent inhibition = 100 – [(growth on medium containing compound/growth on control medium) × 100]; results are the mean of three independent experiments (SD ± 0.5).

[b]Synthetic sample (Pedras *et al.*, 2003b)

To the best of our knowledge compound **204** named erucalexin is a novel phytoalexin having a 3-indoxyl system with a spiral ring at C-2. Erucalexin (**204**), produced by elicited leaves of dog mustard, not detectable in non-elicited tissues, and having antifungal activity against *S. sclerotiorum* and *R. solani*. This is also the first report of elicitation of cruciferous phytoalexins using mycelia of *S. sclerotiorum* as the elicitor. Erucalexin (**204**) is probably biosynthesized from tryptophan (**181**) just like the known brassicca phytoalexins brassinin (**149**), spirobrassinin (**173**), cyclobrassinin (**158**), dioxibrassinin (**167**), and brassilexin (**168**). However a major rearrangement would have to occur for the formation of the spiral ring system at C-2 for erucalexin.

2.3 Biotransformation of cruciferous phytoalexins

One of the objectives of this research project was to study the mechanism(s) by which the fungal pathogen *S. sclerotiorum* overcomes phytoalexins of cultivated plants like canola and rapeseed oilseeds, and wild plants like *A. thaliana, C. sativa* (false flax) and *C. bursa-pastoris* (Shepherd's purse). This section describes and discusses the results obtained from the metabolism of brassinin (**149**) and its homologue methyl tryptamine dithiocarbamate (**199**), camalexin (**170**) and 6-methoxycamalexin (**171**) (Figure 2.9) by *S. sclerotiorum*. The design and synthesis of analogues of these phytoalexins based on the structures of biotransformation products to probe the specificity of the detoxifying enzyme(s) of *S. sclerotiorum* is also described.

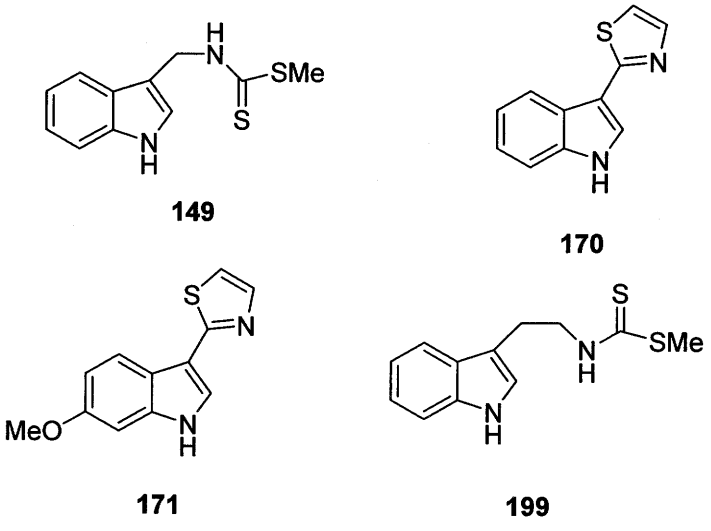

Figure 2.9 Phytoalexins **149**, **170**, **171**, and homologue **199** used for biotransformation studies

2.3.1 Syntheses of phytoalexins and analogues

The syntheses of brassinin (**149**) (Pedras *et al.*, 1992; Somei *et al.*, 1989), methyl tryptamine dithiocarbamate (**199**) (Pedras & Okanga, 1998), camalexin (**170**), and 6-methoxycamalexin (**171**) (Ayer *et al.*, 1992) were carried out as shown in Schemes 2.8 to 2.10 and reported in the experimental section. The spectroscopic data were consistent with the structures of the products and identical to reported data. Yields of synthesis of compounds **149**, **199**, **170** and **171** are listed in Table 2.9.

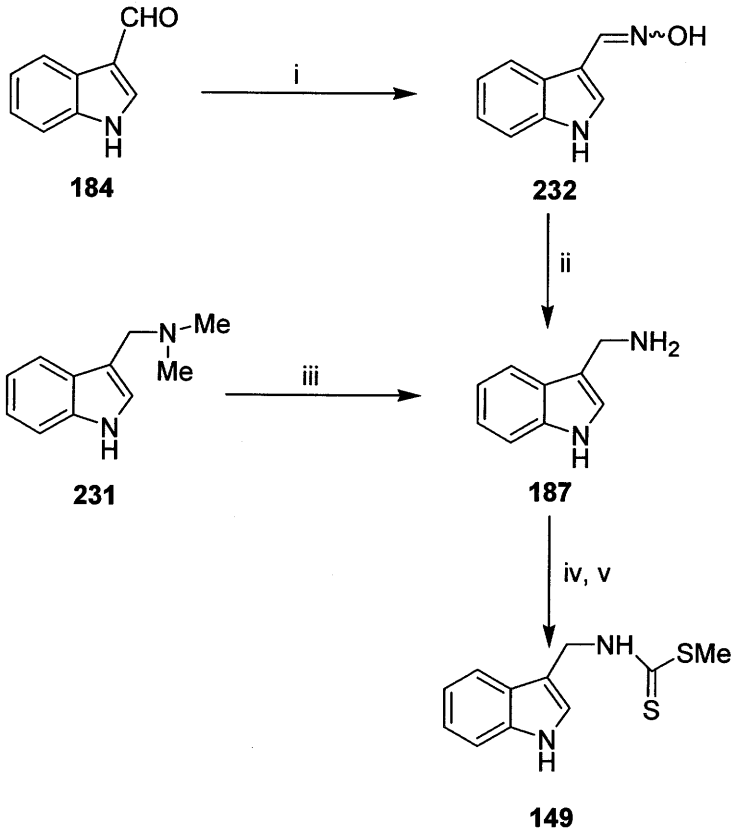

Scheme 2.8 Synthesis of brassinin (**149**). Reagents: i) $NH_2OH.HCl$, Na_2CO_3, 89%; ii) Devarda's alloy, NaOH, MeOH, 66%; iii) MeI, NH_3 (aq), THF, 46%; iv) Et_3N, pyridine, CS_2, 0 °C; v) MeI, 5 °C, 54% (Pedras *et al.*, 1992; Somei *et al.*, 1989).

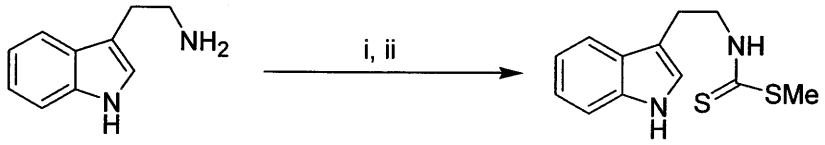

201 **199**

Scheme 2.9 Synthesis of methyl tryptamine dithiocarbamate (**199**). Reagents: i) Et_3N, pyridine, CS_2, 0 °C; ii) MeI, 5 °C, 93% (Pedras & Okanga, 1998).

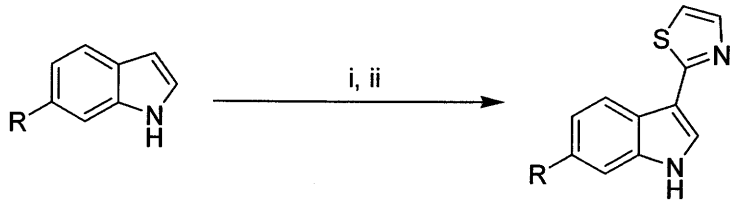

182 R = H
233 R = OMe

170 R = H
171 R = OMe

Scheme 2.10 Synthesis of camalexin (**170**) and 6-methoxycamalexin (**171**). Reagents: i) Mg, MeI, Et_2O; ii) 2-bromothiazole, benzene, reflux (Ayer *et al.*, 1992).

Table 2.9 Yields of synthesis of brassinin (**149**), methyl tryptamine dithiocarbamate (**199**), camalexin (**170**) and 6-methoxycamalexin (**171**)

Compounds	Yield (%)
Brassinin (**149**)[a]	54
Methyl tryptamine dithiocarbamate (**199**)	93
Camalexin (**170**)	72
6-Methoxycamalexin (**171**)	68

[a]Yield for conversion of amine (**187**) to brassinin (**149**).

2.3.2 Biotransformation studies

In order to determine the optimum period for isolation of metabolites, time-course experiments were conducted as detailed in the experimental section. Initial experiments established the maximum non inhibitory concentration (1×10^{-4} M) of brassinin (**149**), methyl tryptamine dithiocarbamate (**199**, brassinin homologue), camalexin (**170**) and 6-methoxy camalexin (**171**) to *S. sclerotiorum*. Subsequently, each compound was incubated separately with *S. sclerotiorum*, culture samples taken at different times and extracted first with EtOAc, then acidified to pH 2 with dilute HCl and extracted with EtOAc. The aqueous layer was made alkaline to pH 10 with aqueous NH_3, and extracted with $CHCl_3$. HPLC and TLC were used to analyze all the extracts. The chromatograms of neutral EtOAc extracts of cultures incubated with **149**, **170**, **171**, and **199** indicated the disappearance of their peaks and the emergence of new peaks not present in control samples. Thus these time-course experiments established that compounds **149**, **170**, **171**, **199** were metabolized by *S. sclerotiorum* within 48 hours.

To isolate the metabolites, scale-up experiments were carried out in 1 L batches, as described in the experimental section. After the appropriate incubation times, the cultures were filtered and extracted with EtOAc.

2.3.2.1 Metabolism of brassinin (149) and methyl tryptamine dithiocarbamate (199) by Sclerotinia sclerotiorum

The EtOAc extract from cultures (1 L) of *S. sclerotiorum* incubated with brassinin (**149**) and methyl tryptamine dithiocarbamate (**199**) were subjected separately to FCC (CH_2Cl_2-MeOH, gradient elution) and each fraction was analyzed by TLC and HPLC. The biotransformation products **234** and **235** were isolated by purification of the fractions using prepTLC and/or reverse phase prepTLC. The results of these experiments are summarized in Table 2.10.

The molecular formulas of metabolites **234** ($C_{17}H_{22}N_2O_5S_2$) and **235** ($C_{18}H_{24}N_2O_5S_2$) obtained by HRMS-FAB indicated the presence of sugar moieties. This is supported by their FTIR spectral data (3300 cm^{-1}, broad signal). The ^1H NMR spectrum of **234** showed a broad singlet at δ 8.34 (D_2O exchangeable), signals for an intact indole ring [(δ 7.64, 7.44, each one d, J = 8 Hz), 7.24 (s, 1H) and (7.24, 7.14, each one ddd, J = 8, 8, 1 Hz)], a doublet at δ 5.43 (J = 9 Hz, 1H), a singlet at δ 5.06 (side chain methylene protons), multiplets at δ 3.42 - 3.87 indicative of a sugar moiety and a methyl singlet at δ 2.59 (the thiomethyl group on the side chain). The identity of the monosaccharide unit was established through homonuclear ^1H - ^1H decoupling experiments (upon addition of D_2O). The signals of the sugar moiety were assigned using the non decoupled ^1H NMR spectrum of **234**, but based on results obtained from the decoupled spectrum. There were only large coupling constants (J = 7 - 9 Hz) indicative of axial - axial proton couplings in the pyranose ring thus allowing the assignment of a β-D-glucopyranose substituent on the indole moiety. HMBC spectral data confirmed that the β-D- glucopyranose unit was located at *N*-1 in **234** (Figure 2.10).

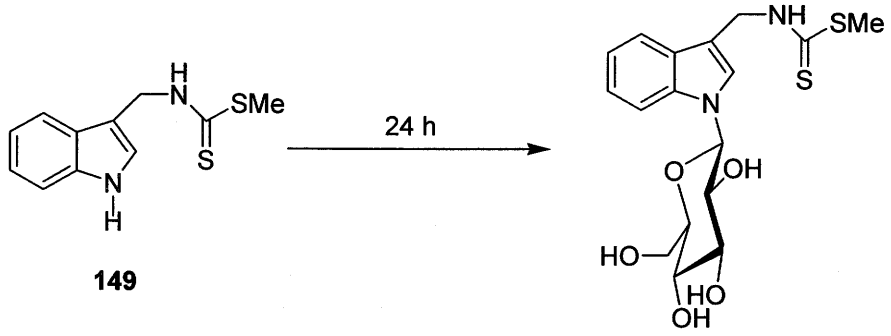

149 **234**

Scheme 2.11 Metabolism of brassinin (**149**) by *Sclerotinia sclerotiorum*

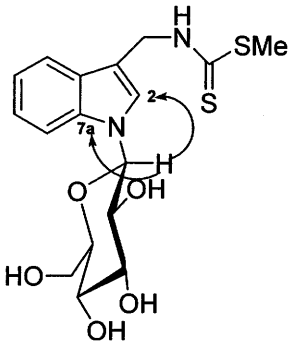

234

Figure 2.10 Selected long-range correlations in HMBC spectra of β-D-glucopyranosyl brassinin (**234**) (C-H long-range correlation of anomeric H and C-2 and C-7a).

The ^{13}C NMR spectral data confirmed the presence of the dithiocarbamate side chain [(δ 198.8 (s), 42.4 (t), and 17.6 (q)], the intact indole system [(δ 137.0 (s), 128.0 (s), 125.7 (d), 122.6 (d), 120.5 (d), 119.5 (d), 112.0 (s) and 111.0 (d)], as well as the sugar moiety (δ 85.2 (d), 79.1 (d), 77.9 (d), 72.6 (d), 70.5 (d), 61.9 (t)]. From the above spectral data, the structure of metabolite **234** was assigned as 1-β-D-glucopyranosylbrassinin.

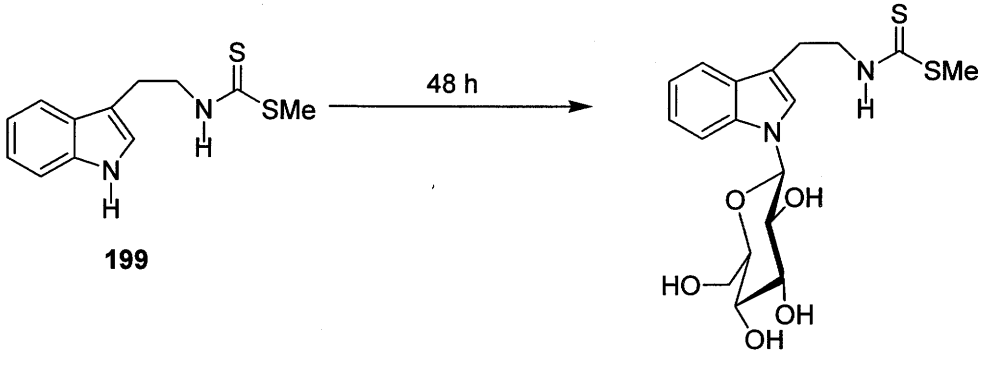

199 235

Scheme 2.12 Metabolism of methyl tryptamine dithiocarbamate (**199**) by *Sclerotinia sclerotiorum*

The ^{1}H NMR spectral data of metabolite **235** were similar to those of **234** showing the intact indole ring system, signals for the β-D-glucopyranose ring (homonuclear ^{1}H - ^{1}H decoupling experiments established the identity) and the dithiocarbamate side chain intact (similar to that of **199**, Scheme 2.12). The ^{13}C NMR spectral data confirmed these deductions and thus metabolite **235** was characterized as methyl 1-(β-D-glucopyranosyl)tryptamine dithiocarbamate.

Table 2.10 Products of metabolism of phytoalexins and homologue (1×10^{-4} M) by *Sclerotinia sclerotiorum*

Compound added to fungal cultures[a]	Products (%)[b] of metabolism
Brassinin (**149**)	Complete biotransformation in 24 h; **234** (53%)
Camalexin (**170**)	Complete biotransformation in 24 h; **236** (28%) and **237** (22%).
6-Methoxycamalexin (**171**)	Complete biotransformation in 24 h; **236** (18%), **237** (20%) and **238** (12%).
Methyl tryptamine dithiocarbamate (**199**)	Complete biotransformation in 48 h; **235** (48%)

[a] Compounds were dissolved in DMSO, added to six-day-old cultures and incubated at 24 ± 2 °C.
[b] Percentage yields of products represent isolated amounts; due to losses during extraction and separation, yields of glucosyl derivatives determined by HPLC analysis are 25-30% higher than isolated yields.

1-β-D-glucopyranosylbrassinin (**234**) accounted for 53% of **149** whilst methyl 1-(β-D-glucopyranosyl)tryptamine dithiocarbamate (**235**) accounted for 48% of **199**. The results of these experiments are summarized in Table 2.10. Further feeding of **234** and **235** to *S. sclerotiorum* indicated that the glucosides were further transformed but no biotransformation products were detected or isolated. The possible metabolic products

might be very polar and more soluble in aqueous media than in organic solvents, thus precluding extraction and detection.

2.3.2.2 Metabolism of camalexin (170) and 6-methoxycamalexin (171) by Sclerotinia sclerotiorum

The EtOAc extract from cultures (1 L) of *S. sclerotiorum* incubated with camalexin (**170**) and 6-methoxycamalexin (**171**) were subjected separately to FCC (CH_2Cl_2-MeOH, gradient elution) and each fraction was analyzed by TLC and HPLC. The biotransformation products **236** and **237** and **238** were isolated by purification of the fractions (with new peaks not present in control samples) by multiple chromatography. The results of these experiments are summarized in Table 2.10.

Camalexin (**170**) was metabolized by *S. sclerotiorum* to metabolites **236** and **237** respectively. Relative to camalexin (**170**, $C_{11}H_8N_2S$), metabolite **236** contained an additional oxygen atom ($C_{11}H_8N_2OS$), as determined by HRMS-EI. The ^1H NMR spectrum displayed a three-proton spin system (δ 7.49, d, J = 2 Hz; 7.30, d, J = 8.5 Hz; 6.77, dd, J = 8.5, 2 Hz) in addition to H-2 and to two thiazole protons, suggesting the presence of an indolic substituent located either at C-5 or C-6. The ^{13}C NMR spectrum displayed 11 carbon signals, one of which was characteristic of a deshielded sp^2 carbon atom (δ 154.1). These spectroscopic features suggested that metabolite **236** which accounts for 28% of camalexin (**170**) and 18% of 6-methoxycamalexin (**171**) contained an OH group attached to either C-5 or C-6. That the OH group was attached to C-6 rather than C-5 was finally deduced from comparison of HMBC and HMQC spectral data with that of camalexin (**170**) and 5-hydroxycamalexin (**196**) (Pedras & Khan, 2000). In addition, methylation of **236** with diazomethane yielded **171**, thus confirming the structure of **236** unambiguously.

The molecular formulas of metabolites **237** ($C_{17}H_{19}N_2O_6S$) and **238** ($C_{18}H_{20}N_2O_6S$) obtained by HRMS-FAB indicated the presence of a hexose, which was corroborated by

NMR data. The ^{1}H NMR and ^{13}C NMR spectral data of **237** were similar to that of **236** except for the appearance of additional signals at δ 4.94 (d, 7 Hz, 1H) and δ 3.36 - 3.83 (m, 10H, 4H D_2O exchangeable) in the ^{1}H NMR spectrum and at δ 102.6 (d) and δ 61.6 - 77.9, five carbon signals, (four d, one t) in the ^{13}C NMR spectrum. Homonuclear ^{1}H - ^{1}H decoupling experiments enabled the assignment of these additional signals as arising from an (*O*)-β-D-glucopyranose moiety. HMBC spectral data confirmed that this substituent was located at C-6 in **237** (C-H long range correlation between anomeric H and C-6). From these deductions **237**, which accounts for 22% of camalexin (**170**) and 20% of 6-methoxycamalexin (**171**) was characterized as 6-(O-β-D-glucopyranosyl)camalexin.

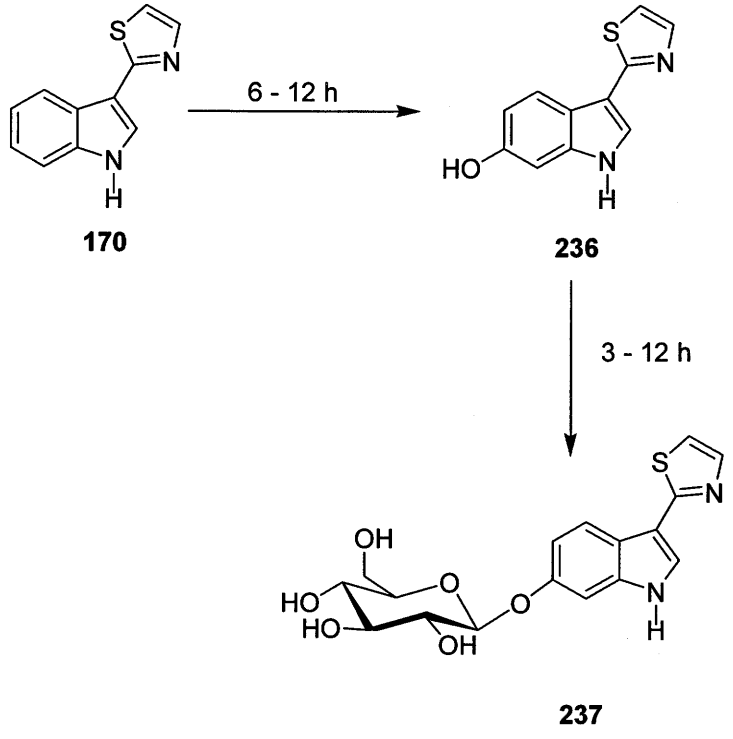

170 **236** **237**

Scheme 2.13 Metabolism of camalexin (**170**) by *Sclerotinia sclerotiorum* (Pedras & Ahiahonu, 2002)

The ^{1}H NMR and ^{13}C NMR spectral data of metabolite **238** were again similar to that of **171** except for the absence of the singlet at δ 9.57 (1H, br s, D_2O exchangeable, proton at the nitrogen of indole ring) and the presence of additional signals at δ 5.50 (d, 8.5 Hz, 1H) and δ 3.27 - 3.87 (m, 10H, 4H D_2O exchangeable) in the ^{1}H NMR spectrum and at δ 85.2 (d) and δ 61.9 - 79.4 (five carbon signals, four of them d and one t) in the ^{13}C NMR spectrum. From homonuclear ^{1}H - ^{1}H decoupling experiments as well as HMBC spectral data (C-H long range correlation between anomeric H and C-2 and C-7a), these signals were assigned as β-D-glucopyranose unit located at *N*-1 in **238**. From these deductions metabolite **238** which accounted for 12% of 6-methoxycamalexin (**171**) was assigned as 6-methoxy 1-(β-D-glucopyranosyl)camalexin.

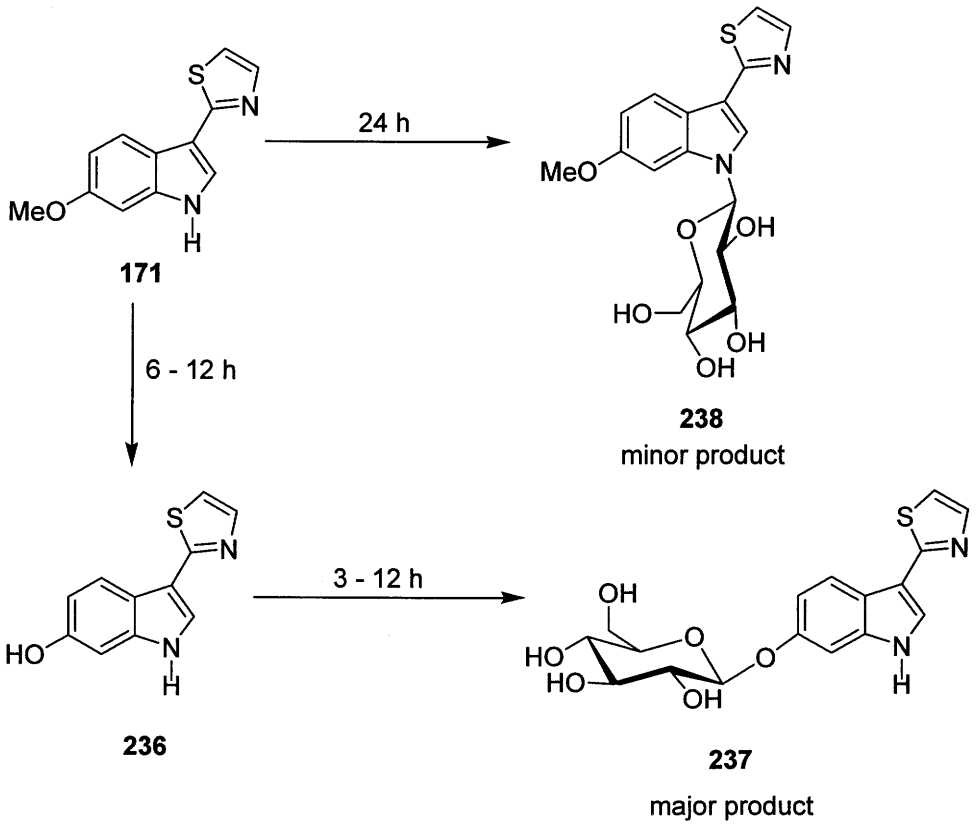

Scheme 2.14 Metabolism of 6-methoxycamalexin (**171**) by *Sclerotinia sclerotiorum* (Pedras & Ahiahonu, 2002)

To establish the sequence of biotransformation steps of camalexin (**170**) and 6-methoxycamalexin (**171**), compound **236** was administered to cultures of *S. sclerotiorum*. The cultures were incubated and samples extracted and analyzed by TLC and HPLC. As expected, **237** was detected in the cultures incubated with **236** after 3 - 6 hours; complete metabolism of **236** to **237** occurred in ca. 12 hours. These results indicated that **170** and **171** were transformed to 6-*O*-β-D-glucopyranosylcamalexin (**237**) via 6-hydroxy camalexin (**236**) (See Schemes 2.13 and 2.14). In addition, in 6-methoxycamalexin (**171**) was partly converted to **238** a minor metabolite; that is *S. sclerotiorum* converted 6-methoxycamalexin (**171**) via two pathways, with the major product **237** resulting from demethylation of the methoxy group at C-6, followed by glucosylation; the minor product **238** resulting from direct *N*-glucosylation (Scheme 2.14). The results of these experiments are summarized in Table 2.10.

2.3.2.3 Antifungal activity of brassinin (149), camalexin (170), 6-methoxycamalexin (171), methyl tryptamine dithiocarbamate (199) and their metabolites

The antifungal activity of brassinin (**149**) camalexin (**170**), 6-methoxycamalexin (**171**), methyl tryptamine dithiocarbamate (**199**, homologue of brassinin) and metabolites **234**, **235**, **237** and **238** to *S. sclerotiorum* was determined using the mycelia radial growth bioassay described in the experimental. Solutions of each compound in DMSO (5×10^{-2} M) were used to prepare solutions in minimal media (5×10^{-4} M, 5×10^{-5} M, 1×10^{-5} M); control solutions contained 1% DMSO in minimal media. After 4 days of incubation, the mycelium of control plates incubated with *S. sclerotiorum* covered 100% of the plates, while plates containing **149**, **170** and **199** (5×10^{-4} M) showed no mycelial growth, and plates containing **171** (5×10^{-4} M) showed slower growth than controls (Table 2.11). Whilst there was some mycelial growth observed for brassinin (**149**) (5×10^{-4} M) after 5 days of incubation, no growth was observed in plates containing **170** and **199** even up to 7

days. By contrast, plates containing **234**, **235**, **237** and **238** were similar to control plates. These results demonstrated for the first time that metabolism of brassinin (**149**), methyl tryptamine dithiocarbamate (**199**), camalexin (**170**) and 6-methoxycamalexin (**171**) in *S. sclerotiorum* lead to products having no detectable antifungal activity, thus the metabolism of these phytoalexins and homologue (**199**) is a detoxification process. It is worth noting that camalexin (**170**) and methyl tryptamine dithiocarbamate (**199**) have higher antifungal activity than brassinin (**149**), whose activity is in turn higher than 6-methoxycamalexin (**171**).

Table 2.11: Percentage of inhibition of *Sclerotinia sclerotiorum* incubated with phytoalexins **149**, **170**, **171** and homologue **199** (4 days incubation, constant light)

Compound	Concentration (M)	% Inhibition[a]
Brassinin (**149**)	5×10^{-4} M	100
	5×10^{-5} M	0
Methyl tryptamine dithiocarbamate (**199**)	5×10^{-4} M	100
	5×10^{-5} M	0
Camalexin (**170**)	5×10^{-4} M	100
	5×10^{-5} M	0
6-Methoxycamalexin (**171**)	5×10^{-4} M	41
	5×10^{-5} M	0

[a] % inhibition = 100 - [(growth in treated / growth in control) × 100]; results are the mean of three independent experiments (SD ± 0.5).

2.3.2.4 Metabolism and co-metabolism of analogues

For brassinin (**149**) it was anticipated that if the fungal detoxifying enzyme(s) were specific, blocking the *N*-1 site or replacing the indole ring with naphthalene would slow down if not stop the metabolism. It was also thought that replacing the dithiocarbamate side chain with carbamate, ester or amide would reduce the antifungal activity of the compounds. Subsequently, methyl 1-methyltryptamine dithiocarbamate (**239**), methyl 1-methoxytryptamine dithiocarbamate (**240**), methyl 1-naphthalenylethanoate (**241**), methyl 1-naphthalenylmethylamine dithiocarbamate (**242**), methyl 2- naphthalenylmethylamine dithiocarbamate (**243**), brassinin carbamate (**244**), tryptamine carbamate (**245**), methyl indolyl-3-propanoate (**246**), and methyl 1-methylindolyl-3-propanoate (**247**) were designed and synthesized to probe the enzyme(s) responsible for the detoxification of brassinin (**149**). The structures of these compounds are shown in Figure 2.11. In the case of camalexin (**170**) it was anticipated that blocking the C-6 of camalexin would direct glucosylation to *N*-1 site and blocking both *N*-1 and C-6 sites would slow down if not stop the metabolism. It was also thought that replacing the thiazole ring with aldehyde or amide would reduce the antifungal activity of the compounds. Based on these hypotheses, 6-fluoroindolyl-3-carboxaldehyde (**248**), 6-fluoro-1-methylindolyl-3-carboxaldehyde (**249**), 6-fluorocamalexin (**250**), 6-fluoro-1-methylcamalexin (**251**), 6-fluoro-N_b-acetylindolyl-3-ethanamine (**252**) and 6-fluoro-1- methyl-N_b-acetylindolyl-3-ethanamine (**253**) were designed and synthesized to probe the enzyme(s) responsible for the detoxification of camalexin and/or 6-methoxycamalexin. The structures of these compounds are also shown in Figure 2.11.

Analogues **239 - 240**, **246 - 253** were synthesized from their respective indoles as shown in Schemes 2.15 to 2.20 and described in the experimental section. The spectroscopic data were consistent with the structures. Compounds **241** – **245** were available in our group's library of compounds.

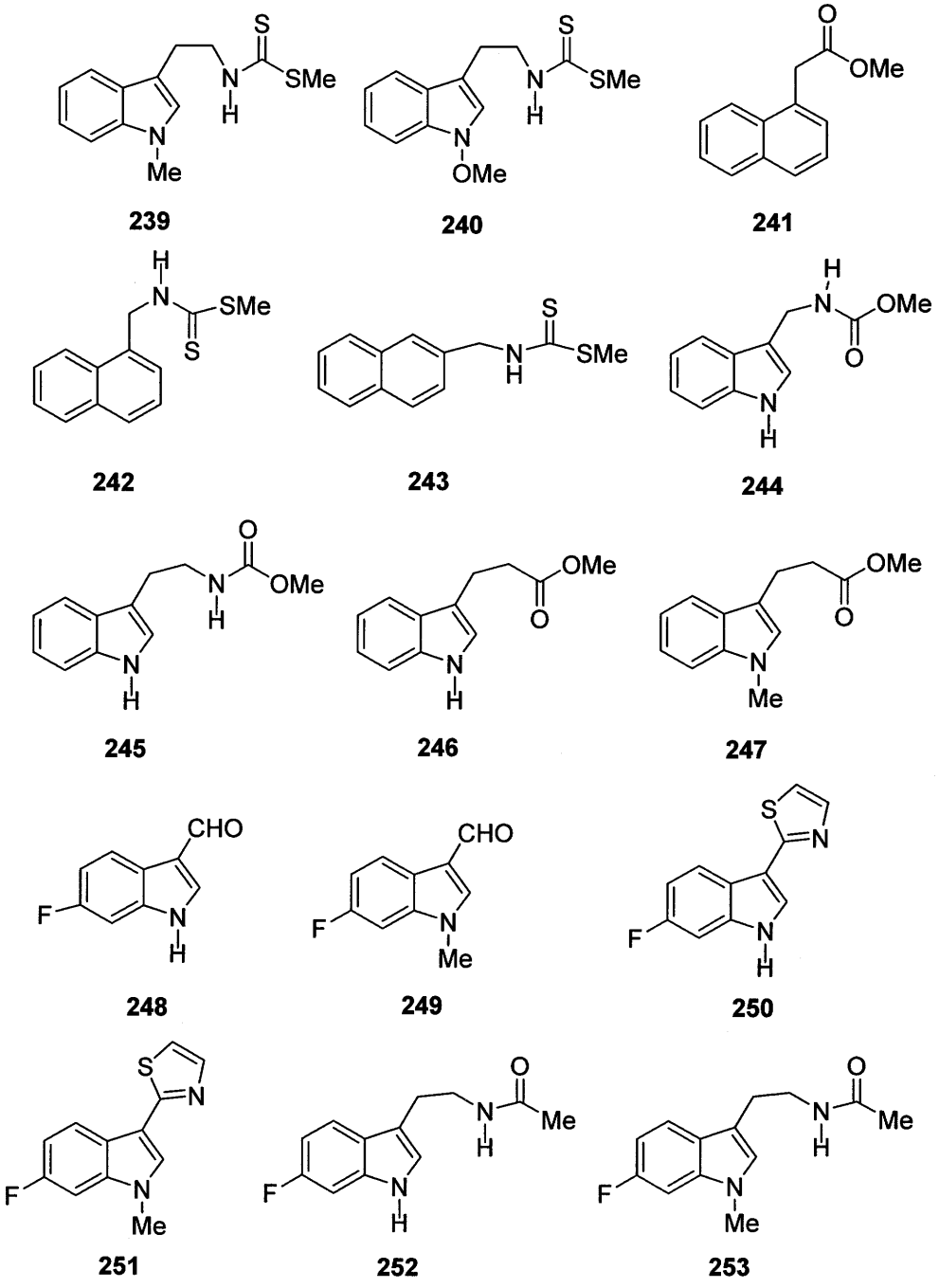

Figure 2.11 Brassinin (**149**) and camalexin (**170**) analogues synthesized to probe specificity of detoxifying enzyme

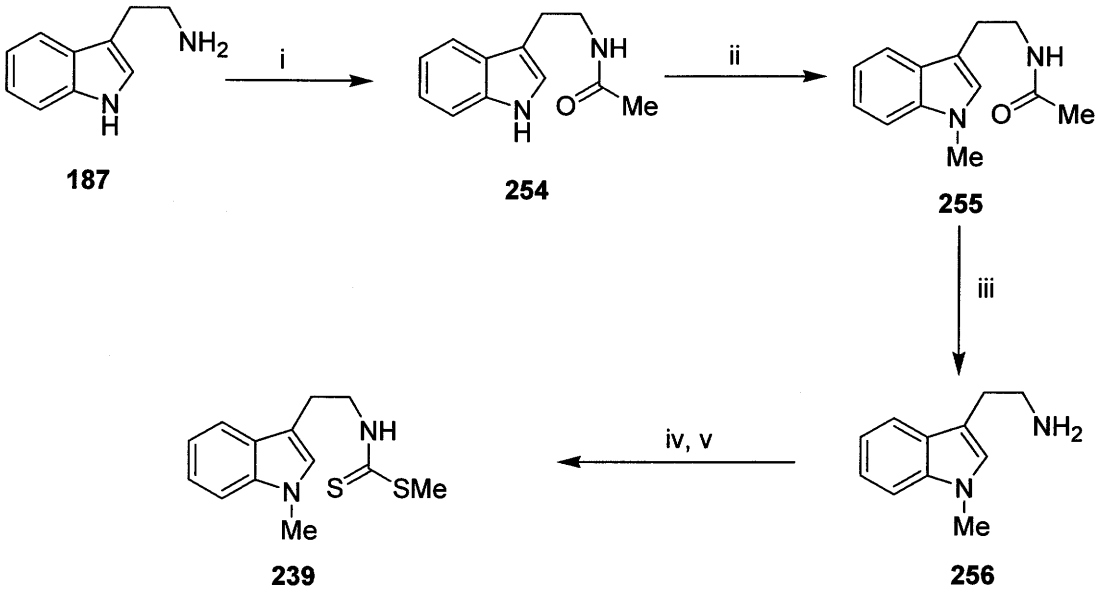

Scheme 2.15 Synthesis of methyl 1-methyltryptamine dithiocarbamate (**239**). Reagents: Pyridine, Ac_2O reflux; ii) NaH, MeI, THF, 0 °C, 95%; iii) $NaOH/H_2O$ Δ; iv) Et_3N, pyridine, CS_2, 0 °C; v) MeI, 5 °C, 82% (Pedras *et al.,* 1992)

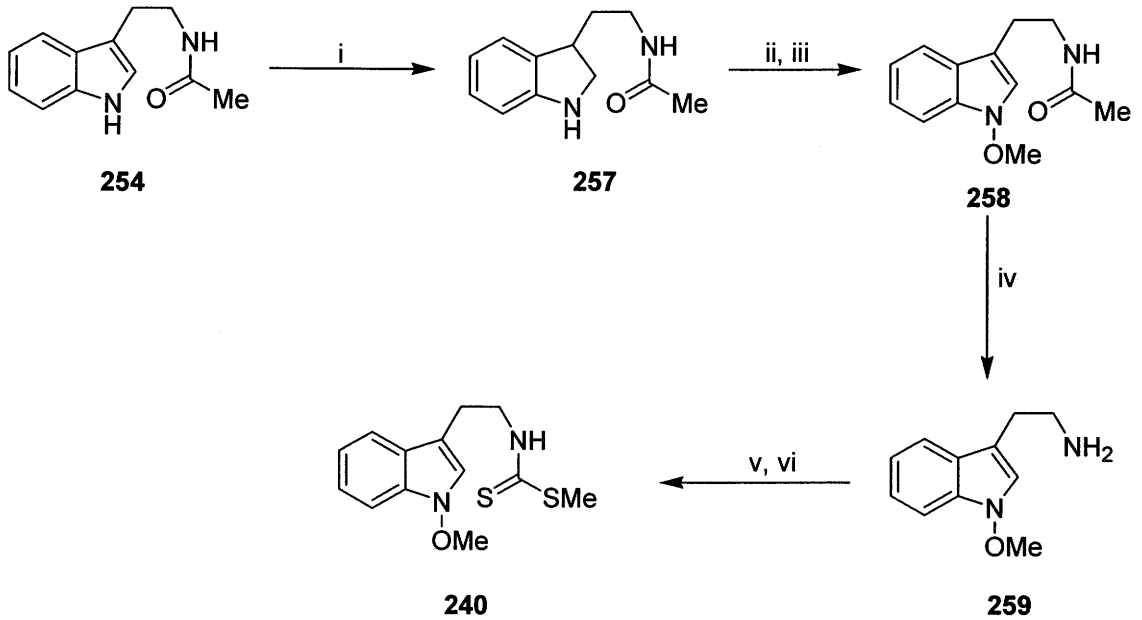

Scheme 2.16 Synthesis of methyl 1-methoxytryptamine dithiocarbamate (**240**). Reagents: i) $NaBH_3CN$, AcOH, 87%; ii) H_2O_2, $Na_2WO_4.2H_2O$, MeOH-H_2O; iii) CH_2N_2-Et_2O, 37%; iv) $NaOH/H_2O$, Δ; v) Et_3N, pyridine, CS_2, 0 °C; vi) MeI, 5 °C, 78% (Schallenberg & Meyer, 1983; Kawasaki *et al.*, 1991; Somei *et al.*, 1992).

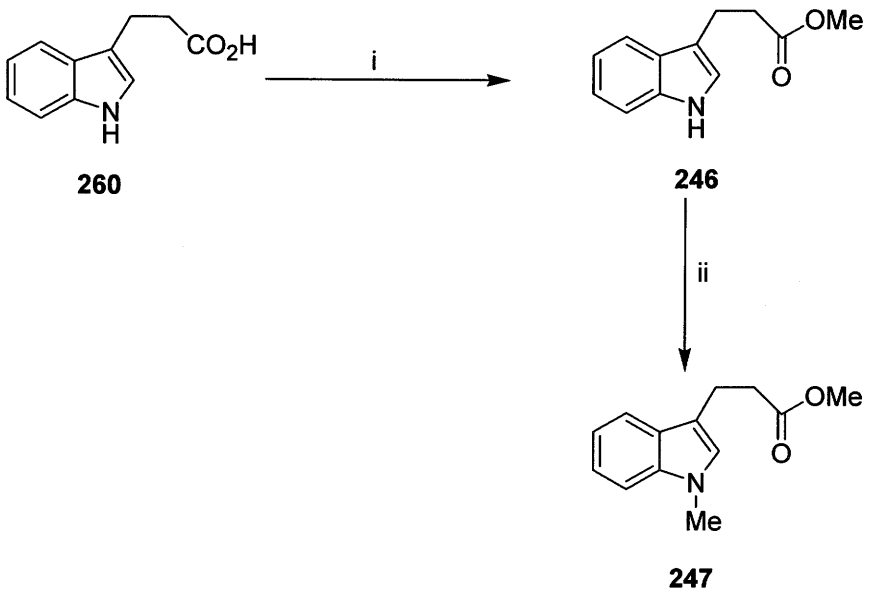

Scheme 2.17 Synthesis of methyl indolyl-3-propanoate (**247**). Reagents: i) MeOH-HCl, reflux, 98%; ii) NaH, MeI, THF, 0 °C, 82%.

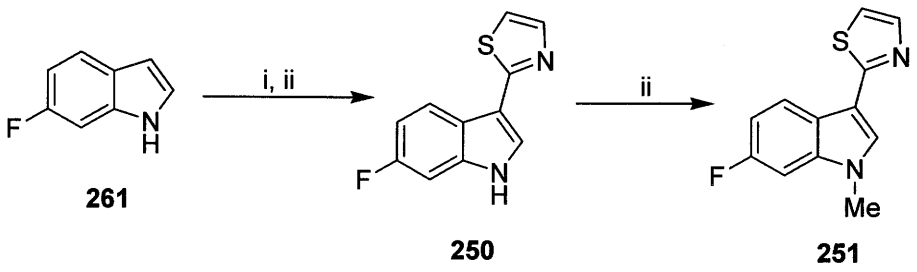

Scheme 2.18 Synthesis of 6-fluorocamalexin (**250**) and 6-fluoro-1-methylcamalexin (**251**). Reagents: Mg, MeI, Et_2O; ii) 2-bromothiazole, benzene, 59%; iii) NaH, MeI, THF, 0 °C, 96% (Pedras & Ahiahonu, 2002).

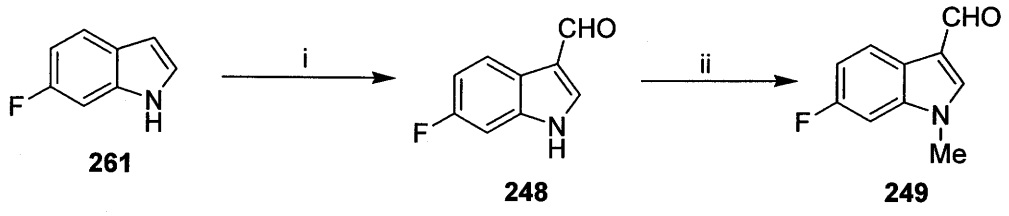

Scheme 2.19 Synthesis of 6-fluoroindolyl-3-carboxaldehyde (**248**) and 6-fluoro-1-methylindolyl-3-carboxaldehyde (**249**). Reagents: i) $POCl_3$, DMF; $NaOH/H_2O$, 86%; ii) NaH, MeI, THF, 0 °C, 96% (Pedras & Ahiahonu, 2002).

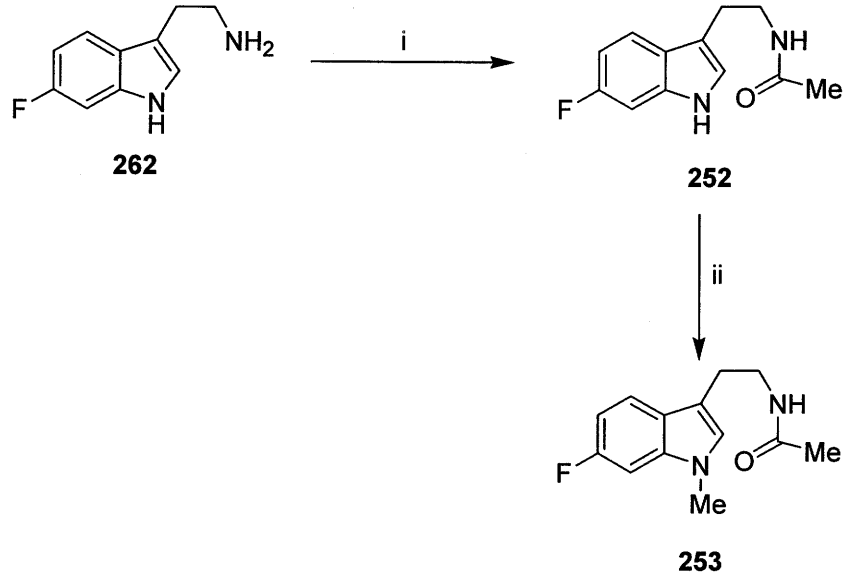

Scheme 2.20 Synthesis of N_b-acetyl-6-fluoroindolyl-3-ethanamine (**252**) and N_b-acetyl-6-fluoro-1-methylindolyl-3-ethanamine (**253**). Reagents: i) pyridine, Ac_2O, 100%; ii) NaH, MeI, THF, 0 °C, 95%.

Biotransformation experiments established the maximum non inhibitory concentration (1×10^{-4} M) of each of these analogues to *S. sclerotiorum*. Subsequently, each compound was incubated separately with *S. sclerotiorum*, culture samples taken at different times, extracted with EtOAc, and analyzed by HPLC. Scale-up experiments were carried out in 1 L batches on brassinin analogues **239**, **240** and **243**, and on camalexin analogues **250** and **251**, just as was done with brassinin (**149**) and camalexins **170** and **171** to isolate their biotransformation products. After the appropriate incubation times, the cultures were filtered, extracted with EtOAc and analyzed by HPLC.

Methyl 1-methyltryptamine dithiocarbamate (239)

The EtOAc extract from cultures (1 L) of *S. sclerotiorum* incubated with methyl 1-methyltryptamine dithiocarbamate (**239**) indicated three new peaks in its HPLC chromatogram not present in control samples. The extract was subjected to FCC (CH_2Cl_2-MeOH, gradient elution) and each fraction was analyzed by TLC and HPLC. The biotransformation products **263** and **264** were isolated by prepTLC. The results of these experiments are summarized in Table 2.12.

The molecular formula of **263** ($C_{19}H_{26}N_2O_6S_2$) obtained by HRMS-FAB revealed the presence of a sugar moiety. The FTIR spectral data were very similar to those of **235** (broad absorption band in the 3300 cm^{-1} region) indicative of the presence of hydroxyl groups. The ^1H NMR spectrum of this metabolite was also similar to that of **235** showing signals for a substituted indole system and a β-D-glucopyranose ring (homonuclear ^1H-^1H decoupling experiments) with the dithiocarbamate side chain and the methyl singlet at *N*-1 intact (similar to that of **239**, Scheme 2.21). HMBC experiments established the connectivity between the indole moiety and the β-D-glucopyranose substituent (C-H long-range correlation between anomeric H and C-7 of the indole ring). The ^{13}C NMR spectral data confirmed the presence of the dithiocarbamate side chain [δ 198.9 (s), 47.7 (t), 23.7 (t)

and 17.5 (q)], the methyl proton at *N*-1 [δ 36.2 (q)], the intact indole system with C-7 more deshielded [δ 145.7 (s, C-7, in C-O linkage), 132.0 (s), 129.2 (d), 127.0 (s), 119 (d), 113.6 (d), 111.4 (s), 107.4 (d)], as well as the β-D-glucopyranose ring [102.1 (d), 77.3 (d), 76.9 (d), 74.2 (d), 70.6 (d) and 61.9 (t)]. From these deductions metabolite **263**, which accounts for 32% of **239** was assigned as methyl 1-methyl-7- (O-β-D-glucopyranosyl) tryptamine dithiocarbamate.

Relative to **239** ($C_{13}H_{16}N_2S_2$), metabolite **264** contained an additional oxygen atom ($C_{13}H_{16}N_2OS_2$), as determined by HRMS-EI. The FTIR data showed a strong absorption band at 1690 cm^{-1} indicative of an amide group. The ^1H NMR showed a broad singlet at δ 8.76 (D_2O exchangeable), proton signals resembling 2-oxoindolyl system [δ 7.25 - 7.33 (m, 2H), 7.09 (dd, J = 7.5, 7.5 Hz), and 6.86 (d, J = 8 Hz), that is the absence of the H-2 and the presence of a methine proton at C-3 position (δ 4.12)]. The *N*-1 methyl group (δ 3.23, s) and the dithiocarbamate side chain were intact [δ 2.62 (s, SCH_3) and four protons at δ 2.05 - 3.89 (m, -CH_2 CH_2-] as in **239**. Homonuclear ^1H - ^1H decoupling experiments enabled the assignment of the methine proton at C-3 and the four methylene protons at δ 2.05 - 3.89. The ^{13}C NMR data confirmed the presence of the dithiocarbamate side chain [δ 199.3 (s), 45.3 (t), 29.0 (t), 18.4 (q)], the 2-oxindolyl system [δ 178.9 (s), 144.1 (s), 128.9 (d), 128.7 (s), 124.1 (d), 123.6 (d), 108.9 (d) and 46.6 (q)], and the sp^3 nature of the C-3 carbon at δ 26.9 (d). From these analyses metabolite **264**, which accounts for 22% of **239** was assigned as methyl 1-methyl-2-oxotryptamine dithiocarbamate.

A third metabolite **265** (R_t = 16.5 min, broad peak), which accounts for about 12 - 25% of **239**, could not be isolated. Several attempts at isolating it resulted in mixtures of **239** and **264**. It was suspected that metabolite **265** was an S-oxide of **239** which was synthesized as shown in Scheme 2.21 and described in the experimental (Pedras & Okanga, 1998). The HRMS-EI mass measurement of **265** gave a molecular formula of $C_{13}H_{16}N_2OS_2$. The ^1H NMR spectrum of **265** displayed resonances comparable to those of **239** (within 0.1 ppm) except for the – SCH_3 (δ 2.35 for **265** vs. δ 2.58 for **239**) and - CH_2N

(δ 3.78 for **265** vs. δ 4.06 for **239**) groups. Furthermore, the ^{13}C NMR spectrum of **265** was similar to that of **239** except for resonances attributable to thiocarbonyl (δc 194.2 in **265** vs. δc 199.7 in **239**) and - SCH_3 (δc 12.8 in **265** vs. δc 18.5 in **239**) groups. These results and the FTIR spectrum of **265** (905 cm^{-1}) indicated the presence of S-oxide group (Pedras & Okanga, 1998). Methyl 1-methyl tryptamine dithiocarbamate-S-oxide (**265**) was kept in chloroform at room temperature. Within 3 weeks, it had rearranged to a mixture of **239** and **264** (Pedras & Okanga, 1998). The UV spectrum of metabolite **265** matched that of the synthesized compound.

Table 2.12 Products of metabolism of phytoalexin analogues (1×10^{-4} M) by *Sclerotinia sclerotiorum*

Compound added to fungal cultures[a]	Products (%)[b] of metabolism
Methyl 1-methyltryptamine dithiocarbamate (**239**)	Complete biotransformation in 48 h; **263** (32%) and **264** (24%) via **265**
Methyl 1-methoxytryptamine dithiocarbamate (**240**)	Complete biotransformation in 72 h; **266** (5%)
Methyl 2-naphthalenylmethylamine dithiocarbamate (**243**)	Complete biotransformation in 48 h; **267** (41%)
6-Fluorocamalexin (**250**)	Complete biotransformation in 48 h; **268** (52%)
6-Fluoro-1-methylcamalexin (**251**)	Biotransformation in 48 h; **269** (17%) and **270** (17%) with 35% of **251** recovered

[a] Compounds were dissolved in DMSO, added to six-day-old cultures and incubated at 24 ± 2 °C.

[b]Percentage yields of products represents isolated amounts; due to losses during extraction and separation, yields of glucosyl derivatives determined by HPLC analysis are 25-30% higher than isolated yields.

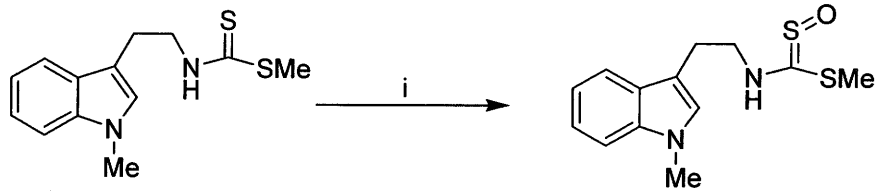

239 **265**

Scheme 2.21 Synthesis of methyl 1-methyl tryptamine dithiocarbamate-S-oxide (**265**). Reagents: i) *m*-CPBA, CH_2Cl_2, 0 °C, 42% (Pedras & Okanga, 2000).

Therefore two pathways for the metabolism of methyl 1-methyltryptamine dithiocarbamate by *S. sclerotiorum* were established; glucosylation of **239** at C-7 (probably via hydroxylation), and secondly transformation of **239** to methyl 1-methyl-2-oxotryptamine dithiocarbamate (**264**) via methyl 1-methyltryptamine dithiocarbamate-S-oxide (**265**, as shown in Scheme 2.22).

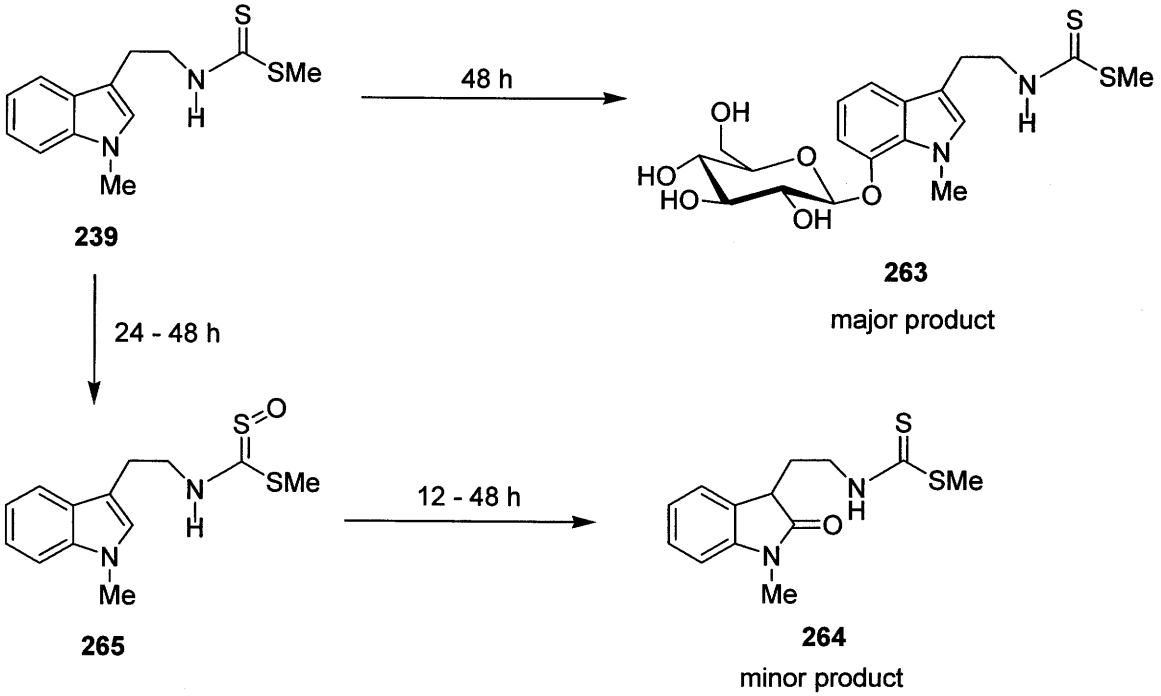

239

263
major product

265

264
minor product

Scheme 2.22 Metabolism of methyl 1-methyltyptamine dithiocarbamate (**239**) by *Sclerotinia sclerotiorum*

Methyl 1-methoxytryptamine dithiocarbamate (240)

The EtOAc extract from cultures (1 L) of *S. sclerotiorum* incubated with methyl 1-methoxytryptamine dithiocarbamate (**240**) was subjected to FCC (CH_2Cl_2-MeOH, gradient elution) and each fraction was analyzed by TLC and HPLC. The biotransformation product was isolated by multiple chromatography involving prepTLC, reverse phase prepTLC, followed by semiprep HPLC. The results of these experiments are summarized in Table 2.12.

The molecular formula of **266** ($C_{19}H_{26}N_2O_7S_2$) obtained by HRMS-FAB revealed the presence of a sugar moiety. The FTIR spectral data were very similar to those of **263** (broad absorption band in the 3300 cm^{-1} region) indicative of the presence of hydroxyl groups. The ^1H NMR spectrum of this metabolite was also similar to that of **263** showing signals for the substituted indole system, signals for the β-D-glucopyranose ring, with the dithiocarbamate side chain and the methoxy singlet at *N*-1 intact (Scheme 2.23). Based on these deductions, the structure of metabolite **266**, which accounts for only 5% of **240**, was assigned as methyl 1-methoxy-7-(*O*-β-D-glucopyranosyl)tryptamine dithiocarbamate. The purification of the extract was very laborious resulting in significant losses of the product.

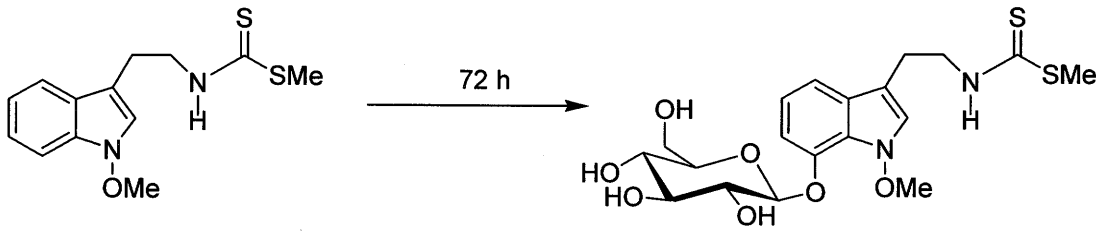

240 **266**

Scheme 2.23 Metabolism of methyl 1-methoxytryptamine dithiocarbamate (**240**) by *Sclerotinia sclerotiorum*

Methyl 2-naphthalenylmethylamine dithiocarbamate (243)

The time-course experiments established that methyl 2-naphthalenylmethylamine dithiocarbamate (**243**, R_t = 25.3 min)) was metabolized by *S. sclerotiorum* in 48 hours to three metabolites with retention times 8.9, 9.4 and 10.7 min respectively. In the scale up experiment EtOAc extract from cultures (1 L) of *S. sclerotiorum* incubated with **243** was subjected to FCC (CH_2Cl_2-MeOH, gradient elution) and each fraction was analyzed by TLC and HPLC. The major biotransformation product **267** (R_t = 9.4 min), was isolated by purification of the fractions by multiple chromatography. The results of these experiments are summarized in Table 2.12.

The HRMS-FAB mass measurement of **267** gave a molecular formula of $C_{19}H_{23}NO_6S_2$. The FTIR spectral data had a broad absorption band in the 3300 cm^{-1} region indicative of the presence of hydroxyl groups. The ^1H NMR spectrum showed a broad singlet at δ 8.54 (D_2O exchangeable), signals for the naphthalene ring system with substitution at 2 positions [δ 8.32 (d, J = 9 Hz, 1H), 7.76 (s, 1H), 7.53 (d, J = 7.5 Hz, 1H), 7.46 (dd, J = 9, 1 Hz, 1H), 7.42 (dd, J = 7.5, 7.5 Hz, 1H), 7.15 (d, J = 7.5 Hz, 1H)], signals for intact dithiocarbamate side chain [δ 5.05 (singlet methylene protons) and 2.59 (-SCH_3 group], and signals for a β-D-glucopyranose unit [δ 5.09 (d, J = 7.5 Hz, 1H) and δ 3.36 - 3.81 (m, 10H). Homonuclear ^1H - ^1H decoupling experiments established the identity of the glucosyl moiety]. The ^{13}C NMR spectral data of metabolite **267** displayed 19 carbon signals, one of which indicated a deshielded sp^2 carbon atom [(δ 154.0 (s), C-O linkage]. NOE difference experiments were used to determine the position of the deshielded carbon. The proton on C-6 of the naphthalene ring showed NOE enhancement when the anomeric proton [δ 5.09 (d, J = 7.5 Hz, 1H)] of the *O*-β-D-glucopyranose unit was irradiated indicating that the *O*-β-D-glucopyranose unit was attached to C-5 of the naphthalene ring (Scheme 2.24). From these deductions, metabolite **267**, which accounts for ca. 41% of **243**, was assigned as methyl 5-(O-β-D-glucopyranosyl)-2-naphthalenylmethylaminedithiocarba mate. Two other metabolites (with R_t = 8.9 min and 10.7 min) with UV spectral data

similar to that of **267** could not be isolated; these are likely isomers of **267** and account for ca. 15 % of **243**.

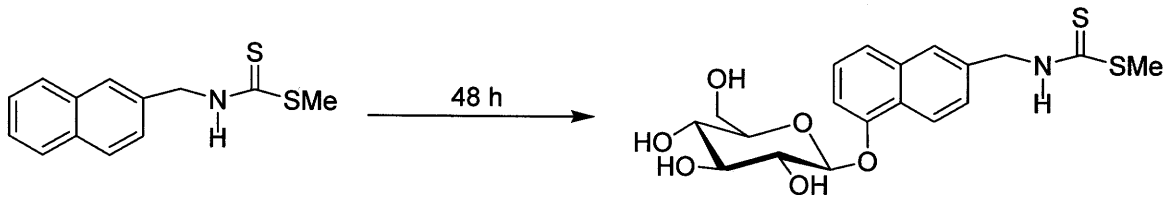

243 **267**

Scheme 2.24 Metabolism of methyl 2-naphthalenylmethylamine dithiocarbamate (**243**) by *Sclerotinia sclerotiorum*

6-Fluorocamalexin (250) and 6-fluoro-1-methylcamalexin (251)

The EtOAc extract from cultures (1 L) of *S. sclerotiorum* incubated with 6-fluorocamalexin (**250**) and 6-fluoro-1-methylcamalexin (**251**) were subjected separately to FCC (CH_2Cl_2-MeOH, gradient elution) and each fraction was analyzed by TLC and HPLC. The metabolite **268** was isolated in 52% yield from **250** whilst metabolites **269** (17% yield) and **270** (17% yield) were isolated from **251** with the recovery of 35% of **251** (Table 2.12). The chemical structures of metabolites **268** and **269** were deduced from comparison of their spectroscopic data with those of **250** and **251** as follows. The molecular formulae of metabolites **268** ($C_{17}H_{18}N_2O_5SF$) and **269** ($C_{18}H_{20}N_2O_6SF$) obtained by HRMS-FAB indicated the presence of a hexose, which was corroborated by NMR data. The ^1H NMR and ^{13}C NMR spectral data of **268** were similar to those of **250** except for the absence of the singlet at δ 9.57 (1H, br s, D_2O exchangeable, proton at the *N*-1 of indole ring) and the presence of additional signals at δ 5.43 (d, J = 9 Hz, 1H) and δ 3.27 - 3.89 (m, 10H, 4H D_2O exchangeable) in the ^1H NMR spectrum and at δ 85.7 and δ 61.9 - 79.5 (five carbon signals) in the ^{13}C NMR spectrum. These resonances were indicative of a β-D-

glucopyranosyl substituent on the indole moiety; analyses of the HMQC and HMBC spectral data confirmed that this substituent was located at *N*-1 in **268** (long-range correlation of anomeric H with C-2 and C-7a). From these deductions metabolite **268** was assigned as 6-fluoro-1-(β-D-glucopyranosyl)camalexin (Scheme 2.26).

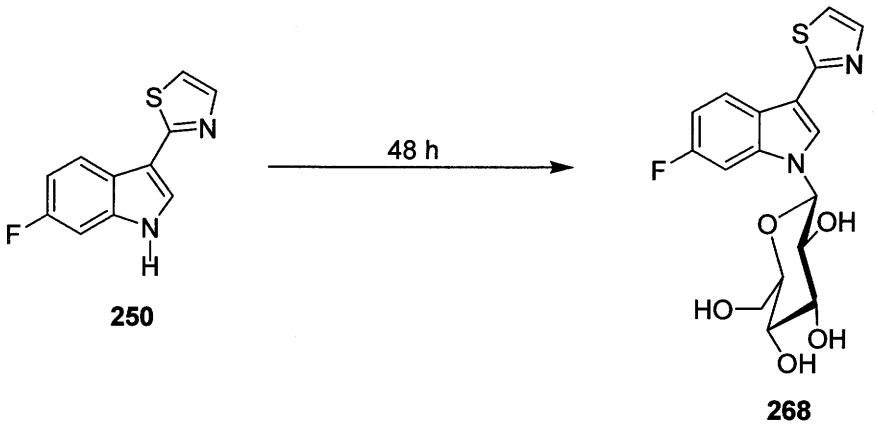

250 **268**

Scheme 2.25 Metabolism of 6-fluorocamalexin (**250**) by *Sclerotinia sclerotiorum* (Pedras & Ahiahonu, 2002)

The ^{1}H NMR and ^{13}C NMR spectral data of **269** were also similar to those of **251** except for the absence of the signal at δ 7.09 (1H, dd, J = 10, 2.5 Hz) and the presence of additional signals at δ 5.10 (d, 9 Hz, 1H) and δ 3.24 - 3.63 (m, 10H, 4H D_2O exchangeable) in the ^{1}H NMR spectrum and at δ 104.3 and δ 61.5 - 77.1 (five carbon signals) in the ^{13}C NMR spectrum. These resonances were indicative of a β-D-glucopyranosyl substituent on the indole moiety; analysis of the HMQC and HMBC spectral data confirmed that this substituent was located at C-7 in **268** (long range correlation between anomeric H and C-7) (Figure 2.12). From these deductions metabolite **268** was assigned as 6-fluoro-1-methyl-7-(*O*-β-D-glucopyranosyl)camalexin (Scheme 2.26).

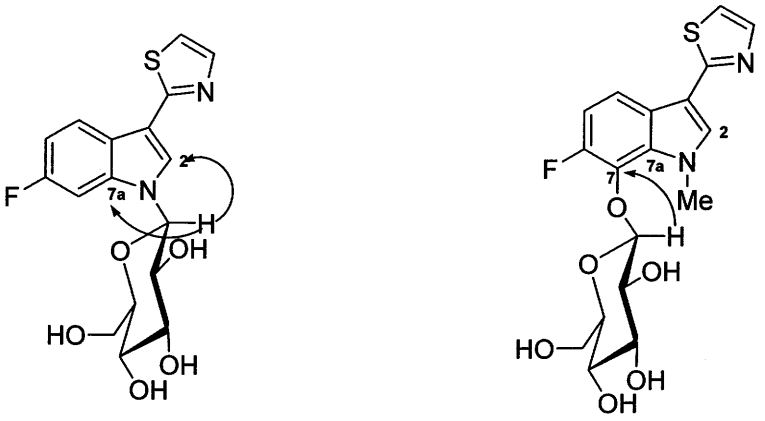

268 **269**

Figure 2.12 Selected long-range correlations in HMBC spectra of β-D-glucopyranosyl camalexins **268** and **269** (Pedras & Ahiahonu, 2002)

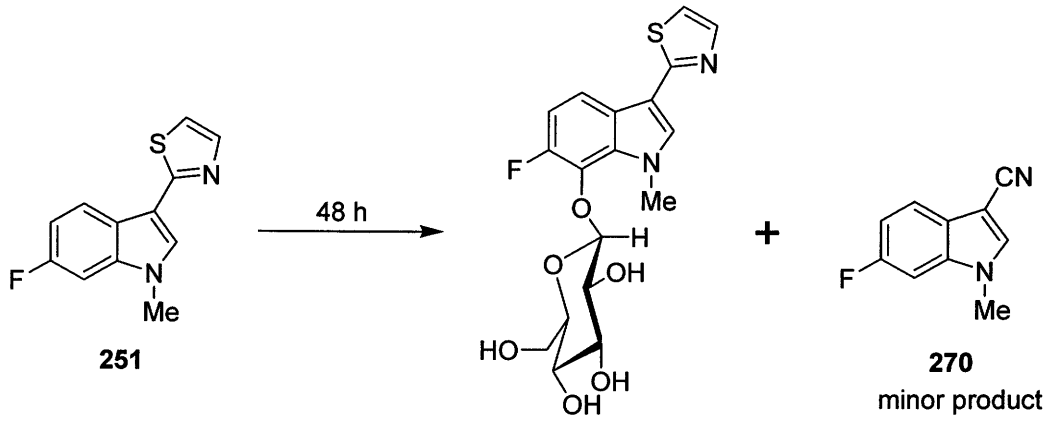

251 **269** major product **270** minor product

Scheme 2.26 Metabolism of 6-fluoro-1-methylcamalexin (**251**) by *Sclerotinia sclerotiorum*. At 48 h, 35% of **251** was recovered (Pedras & Ahiahonu, 2002)

The HRMS-EI measurement for metabolite **270** gave a molecular formula of $C_{10}H_7N_2FS$. Comparison of the ^1H NMR spectrum of this metabolite with that of **251** indicated the presence of an intact 6-fluoro-1-methylindole ring and the absence of thiazole

ring protons. The ^{13}C NMR spectrum of the metabolite confirmed this with the display of 10 carbon signals, one of which indicated a sp carbon atom (δ 115.5, revealing a C≡N group) attached to the indolic system at C-3. Thus metabolite **270** was assigned as 6-fluoro-1-methylindole-3-carbonitrile and the structure was confirmed by synthesis as shown in Scheme 2.27 and described in the experimental section (Pedras & Ahiahonu, 2002).

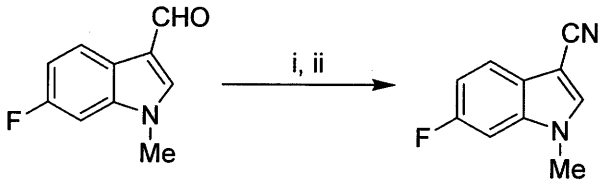

249 **270**

Scheme 2.27 Synthesis of 6-fluoro-1-methylindolyl-3-carbonitrile (**270**). Reagents: i) $NH_2OH.HCl$, pyridine, $CHCl_3$-EtOH, ii) SeO_2, $MgSO_4$, 74% (Pedras & Ahiahonu, 2002).

Co-metabolism of brassinin (149) and camalexin (170) with analogues

The results of the metabolism of brassinin (**149**) suggest that its detoxification involves direct *N*-glucosylation of its indole ring at position 1. To probe the specificity of the glucosyltransferase from *S. sclerotiorum* responsible for this detoxification step, brassinin (**149**) and each of analogues **239 - 253** (Figure 2.11, page 105) were administered to fungal cultures, and the cultures incubated and analyzed as described in the experimental section. With the exception of **250**, the metabolism of brassinin was unaffected by the presence of these analogues which were themselves metabolized by *S. sclerotiorum* (most of them within 72 hours, traces of **251** were present in cultures even after seven days). Thus there appeared to be no inhibition of the metabolism of brassinin by these compounds. However the metabolism of brassinin (**149**) co-incubated with 6-fluorocamalexin (**250**) was considerably slower. Traces of brassinin were present in

cultures up to seven days as against the usual 24 hours. These results either suggest that there is inhibition to the growth of the fungus leading to lower amounts of the brassinin detoxifying enzymes being produced or that there is some competition between substrates **149** and **250** for the active site of the brassinin detoxifying enzyme.

The results of the metabolism of camalexin (**170**) suggest that the first step for camalexin detoxification involves oxidation of C-6 followed by glucosylation of the 6-hydroxy derivative. To probe the specificity of the oxygenase(s) involved in this first step, camalexin (**170**) and each of analogues **239 - 253** were administered to fungal cultures and the cultures incubated and analyzed as previously described. With the exception of **250**, the metabolism of camalexin was unaffected by the presence of these analogues which were themselves metabolized by *S. sclerotiorum* (most of them within 72 hours). However when camalexin (**170**) was co-incubated with 6-fluorocamalexin (**250**), camalexin was metabolized to 6-hydroxycamalexin (**236**) and 6-(*O*-β-D-glucopyranosyl) camalexin (**237**) almost completely (ca. 95%) in 48 hours, whereas analogue **250** started being metabolized only after no camalexin was detected in culture. On the other hand, although analogue **251** was metabolized much slower than camalexin (ca. 24 h vs. 7 days) it did not affect the rate of camalexin transformation when co-incubated. These results indicate that there is competition between **170** and **250** but no competition between substrates **170** and **251**. Nonetheless, a better understanding of the mechanisms involved in these biotransformations will require kinetic studies with the cell homogenate and isolated detoxifying enzymes, which are of pivotal importance in the design of detoxification inhibitors of brassinin and camalexins.

2.3.2.5 Antifungal activity of analogues and their metabolites

The antifungal activity of analogues **239**, **240**, **242**, **243**, **250** and **251** and metabolites **263 - 269** to *S. sclerotiorum* was determined using the mycelia radial growth bioassay described in the experimental. Solutions of each compound in DMSO (5×10^{-2} M) were used to prepare solutions in minimal media (5×10^{-4} M, 5×10^{-5} M, 1×10^{-5} M); control solutions contained 1% DMSO in minimal media. The results are shown in Table 2.13.

Table 2.13: Mycelial growth inhibition of *Sclerotinia sclerotiorum* incubated with analogues of brassinin (**149**) and camalexin (**170**) (4 days incubation, constant light).

Compound assayed against fungal cultures	Concentration (M)	% inhibition [a]
Methyl 1-methyltryptamine dithiocarbamate (**239**)	5×10^{-4} M	100
	5×10^{-5} M	0
Methyl 1-methoxytryptamine dithiocarbamate (**240**)	5×10^{-4} M	100
	5×10^{-5} M	0
Methyl 1-naphthalenylmethyl amine dithiocarbamate (**242**)	5×10^{-4} M	80
	5×10^{-5} M	0
Methyl 2-naphthalenylmethyl amine dithiocarbamate (**243**)	5×10^{-4} M	80
	5×10^{-5} M	0
6-Fluorocamalexin (**250**)	5×10^{-4} M	70
	5×10^{-5} M	0
6-Fluoro-1-methylcamalexin (**251**)	5×10^{-4} M	100
	5×10^{-5} M	0

[a] The percentage of growth inhibition was calculated using the formula: % inhibition = 100 - [(growth in treated / growth in control)] × 100; results are the mean of at least three independent experiments (SD ± 0.7).

After four days of incubation, the mycelia of control plates incubated with *S. sclerotiorum* covered 100% of the plates while plates containing **239**, **240** or **251** (5×10^{-4} M) showed no mycelial growth, and plates containing **242**, **243** or **250** (5×10^{-4} M) showed slower growth. By contrast plates containing the metabolites **263** - **269** were similar to control plates. The biotransformation of these analogues is a detoxification, since the antifungal activities of the analogues and their metabolites indicated that the analogues were significantly more inhibitory to *S. sclerotiorum* than were the products **263** – **269**.

2.4 Partial purification of brassinin detoxifying enzyme(s)

To understand the enzymatic processes involved in the metabolism and detoxification of cruciferous phytoalexins by phytopathogenic fungi, studies involving the isolation and characterization of the detoxifying enzymes are of great importance. To this end, preliminary studies using the cell-homogenate of *S. sclerotiorum* have led to assaying the brassinin detoxifying enzyme(s). This section describes and discusses the results of these preliminary studies.

2.4 1 Preparation of cell homogenate and enzyme assays

Cultures of *S. sclerotiorum* were grown in minimal media for five days after which the mycelia were collected by filtration and stored at –20 °C for a maximum of 4 months. Frozen mycelial cells were homogenized using Tris HCl (50 mM) buffer pH 8 (containing 20% glycerol, 2-mercaptoethanol, PMSF, and Triton X-100) (Zenk *et al,* 2000) at 4 °C as described in the experimental section.

Table 2.14 Comparison of enzymatic activity of cell-homogenates of *Sclerotinia sclerotiorum* obtained from liquid cultures incubated for 2 h with different inducers.

Inducer (5×10^{-5} M)	Specific activity[a] (nmol / min / mg of protein)
No inducer (control)	-
Camalexin (**170**)	0.069 ± 0.044
Spirobrassinin (**173**)	0.017 ± 0.010
Methyl tryptamine dithiocarbamate (**199**)	0.070 ± 0.010[b]
Methyl 1-methyltryptamine dithiocarbamate (**239**)	0.068 ± 0.009

[a]Results are from three independent experiments ± SD.

[b]Results are from ten independent experiments ± SD.

The enzyme assay carried out to detect enzymatic activity involved the use of Tris HCl (50 mM) buffer pH 8, cell homogenate as enzyme source, brassinin as substrate and UDPG as glucose donor (Orlean P., 1982). After incubation of the assay mixture for 2 hours at 27 °C, solvent extraction and HPLC analysis were used for the detection and quantification of the reaction product, 1-(β-D-glucopyranosyl)brassinin (**234**).

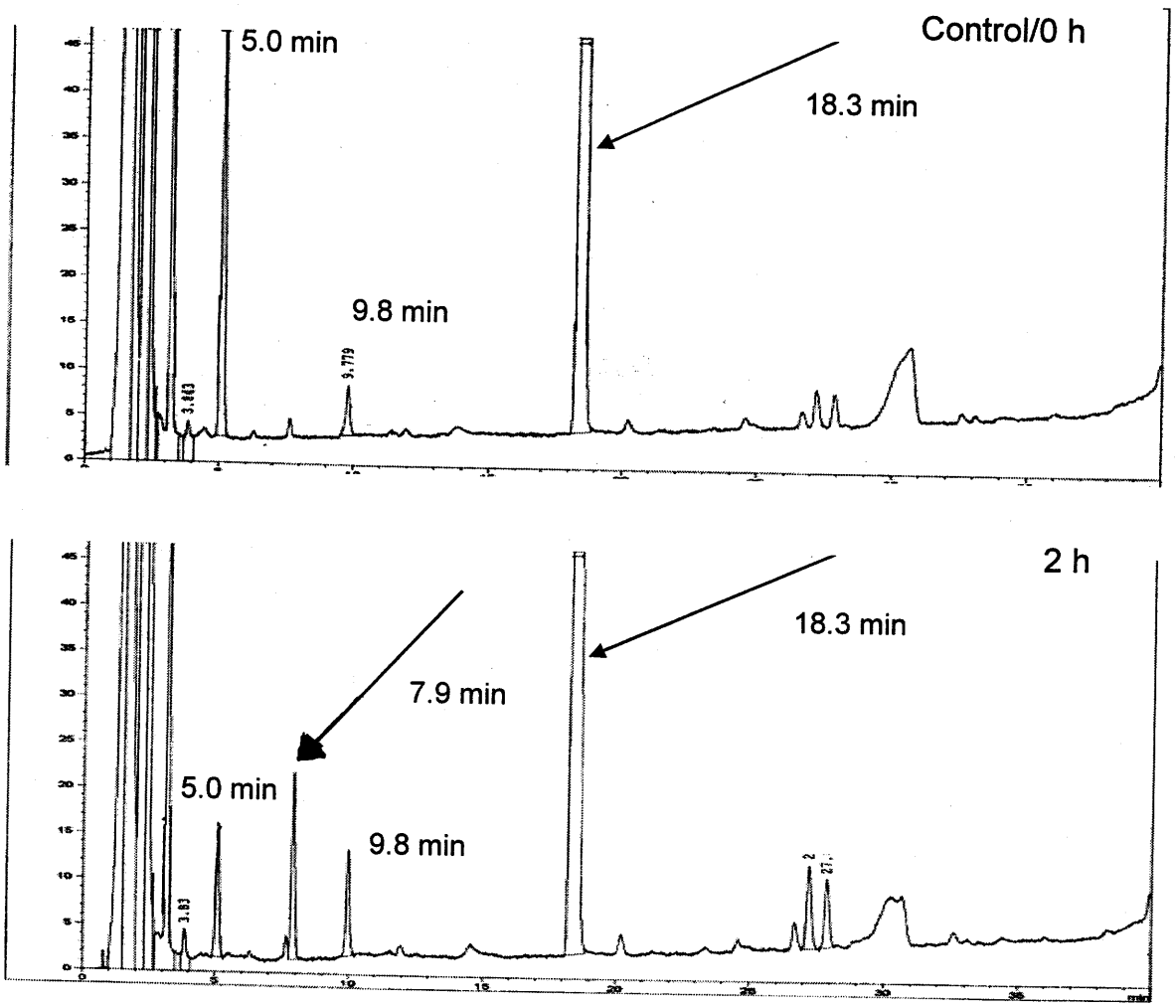

Figure 2.13 HPLC profile of enzyme assay using cell homogenate obtained from induced mycelial cells of *Sclerotinia sclerotiorum* and brassinin (**149**) as substrate. The peak at R_t = 18.3 is brassinin (**149**) and the peak at R_t = 7.9 min is 1-β-D-glucopyranosylbrassinin (**234**).

No activity was observed with these assays. Induction of the enzyme was then carried out with substrates such as camalexin (**170**), spirobrassinin (**173**), methyl tryptamine dithiocarbamate (**199**) and methyl 1-methyltryptamine dithiocarbamate (**239**) (Table 2.14). Enzymatic activity was observed with the induced mycelial cells of *S. sclerotiorum*. Camalexin (**170**), methyl tryptamine dithiocarbamate (**199**), and methyl 1-methyl tryptamine dithiocarbamate (**239**) appear to be better inducers of the brassinin glucosyltransferase (BGT) than spirobrassinin (**173**). Figure 2.13 shows the HPLC profile of enzyme assay with a specific activity of 0.07 nmol/min/mg of protein. Assays carried out with induced mycelial cells of *S. sclerotiorum* in the absence of UDPG did not show activity. This indicated that UDPG was required by the brassinin detoxifying enzyme for activity.

2.4.2 Protein measurements

The Bradford protein assay (Bradford, 1976) with bovine serum albumin (BSA) as standard was used to estimate the quantity of protein in the cell homogenate and the enzyme fractions from the ion exchange chromatography. Protein contents of cell homogenate averaged between 2.2 mg/mL to 6.00 mg/mL and that of active fractions averaged between 0.35 mg/mL to 1.5 mg/mL. This enabled the specific activity of the cell homogenate and partially purified brassinin glucosyltransferase (BGT) from *S. sclerotiorum* to be estimated (Table 2.14).

2.4.3 Partial purification by chromatography

The cell homogenate was subjected to ion exchange chromatography on a DEAE-Sephacel column using Tris HCl buffer pH 8, containing 20% glycerol, 20 mM mercaptoethanol, 0.1 M PMSF and 0.01% Triton X-100 (standard buffer A). Elution of the

enzyme was achieved with 0.1 M NaCl in standard buffer A. The profile for the DEAE chromatography is shown in Figure 2.14. The active fractions were pooled together and subjected to desalting on a Sephadex G-25 column. With this purification step, the NaCl was removed from the enzyme solution. Enzymatic activity was observed when the pooled active fractions ($A_1 - A_9$) were assayed against the substrates 6-methoxycamalexin (**171**), 6-hydroxycamalexin (**236**), cyclobrassinin (**158**), and methyl tryptamine dithiocarbamate (**199**). None of the other protein fractions showed enzymatic activity towards the substrates tested. Partial purification (5 fold) of the brassinin glucosyltransferase (BGT) from *S. sclerotiorum* was achieved (See Table 2.15).

Affinity chromatography was attempted on the pooled active fractions from the DEAE column after desalting with Sephadex G-25. Matrices tried include Reactive Green 19, Reactive Yellow 86, and Cibacron Blue 3GA. The active fractions were observed in the loading flow-through of these matrices suggesting that there was no binding of the desired enzyme to the matrices resulting in no purification.

Table 2.15: Summary of partial purification of brassinin glucosyltransferase (BGT) from mycelia of *S. sclerotiorum**.

Procedure	Total protein (mg)	Protein (mg/mL)	Total activity (nmol/min)	Specific activity (nmol/min/mg)	Yield (%)	Fold
Cell homogenate	62.5	2.50	17.0	0.219	100	1
DEAE-sephacel	7.60	0.40	9.52	0.989	12	5

*Frozen mycelia 14 g.

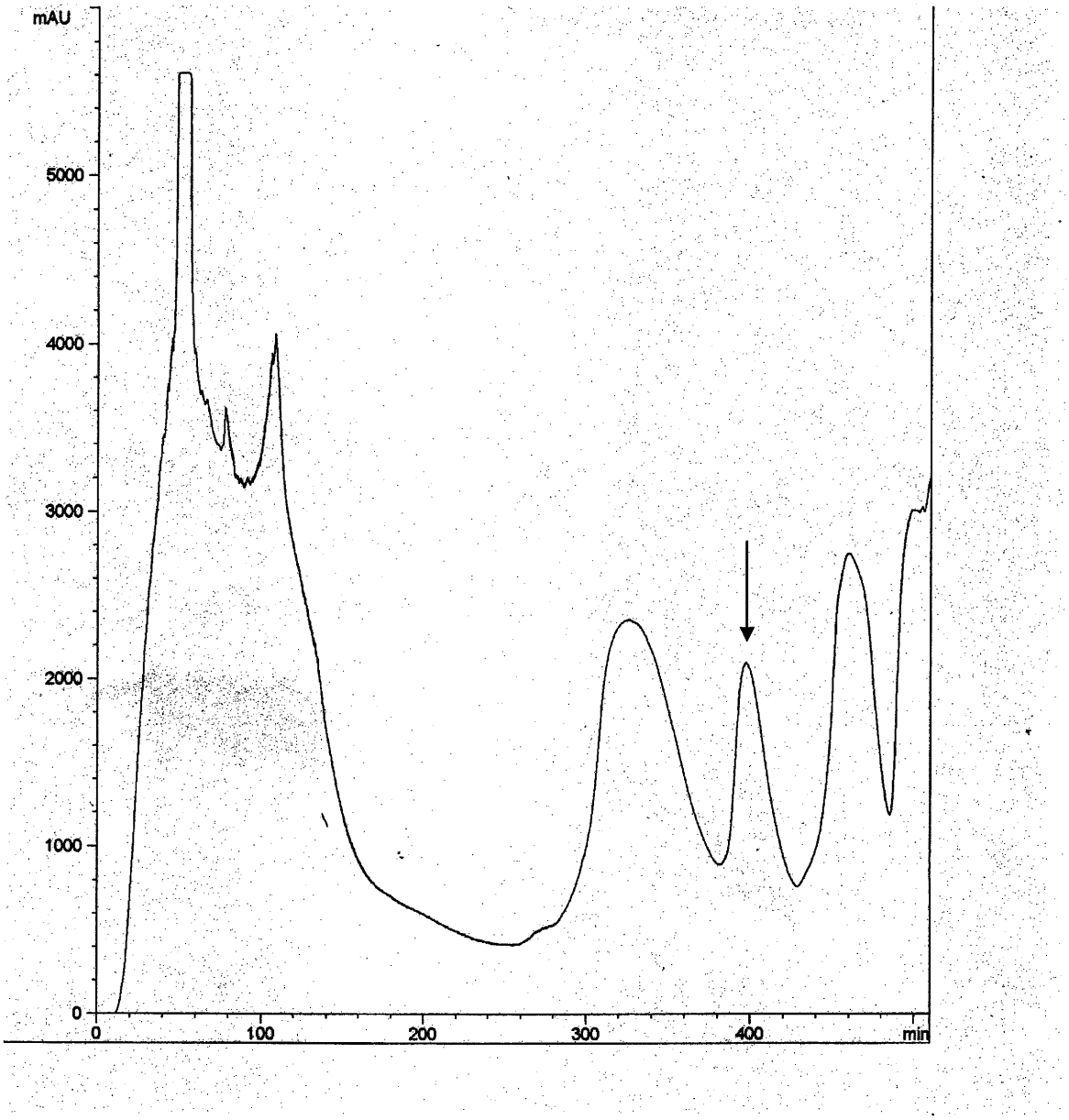

Figure 2.14 DEAE profile for partial purification of cell homogenate of *Sclerotinia sclerotiorum* (arrow indicates absorption band for active fractions); detection at 280 nm.

Gel electrophoresis (SDS-PAGE) (Laemmli, U.K., 1970) was carried out to verify partial purification from the DEAE column. Cell homogenate as well as the individual active fractions from DEAE column (Fractions A_1-A_9) were used (Figure 2.15). From the protein estimation results an equivalent amount of each sample was taken and applied onto

the gel. After development and staining with Coomassie blue dye, partial purification of the enzyme fraction from the cell-homogenate of *S. sclerotiorum* was observed (Figure 2.15).

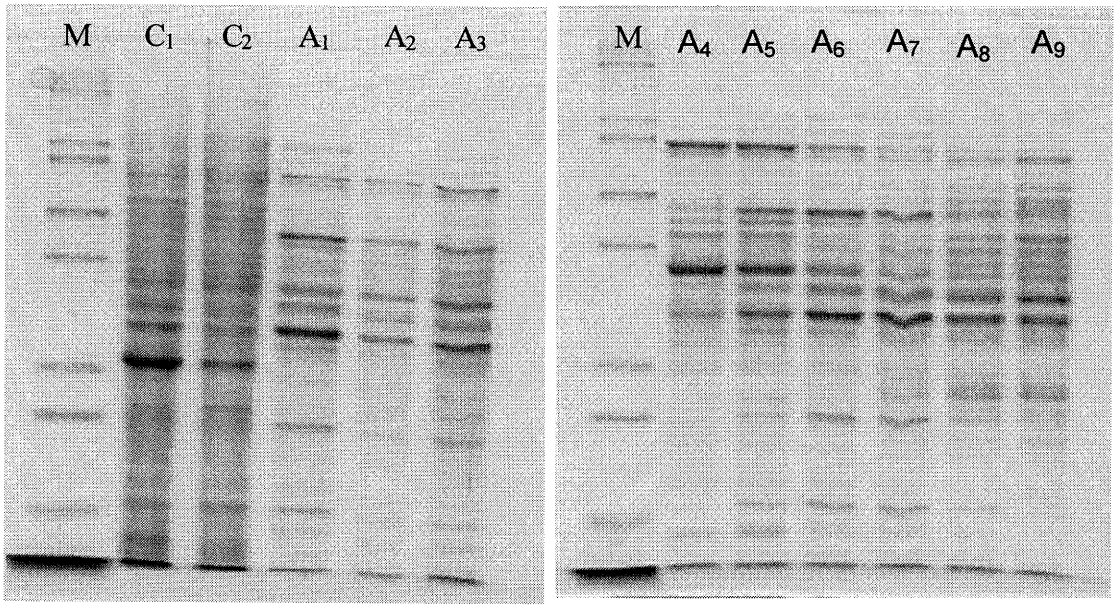

Figure 2.15 SDS-PAGE gels showing cell homogenate and active fractions from DEAE column (M = Protein standard; C_1, C_2, = Cell homogenates; A_1 – A_9 = different active fractions)

2.4.4 Substrate specificity studies

The substrate specificity of the brassinin glucosyltranferase from *S. sclerotiorum* was analyzed by incubating potential substrates (3×10^{-5} M) with cell homogenate and partially purified enzyme fractions (DEAE sephacel column) under standard assay conditions. The substrates tested include camalexin (**170**), cyclobrassinin (**158**), 6-fluorocamalexin (**250**), 6-methoxycamalexin (**171**), 6-hydroxycamalexin (**236**), 6-fluoro-1-methylcamalexin (**251**), and methyl tryptamine dithiocarbamate (**199**). While camalexin (**170**), 6-fluorocamalexin (**250**) and 6-fluoro-1-methylcamalexin (**251**) were not accepted

as substrates by the brassinin glucosyltransferase (BGT), cyclobrassinin (**158**) and methyl tryptamine dithiocarbamate (**199**) were glucosylated to levels comparable to brassinin (**149**) both in cell homogenate (Table 2.16) and active enzyme fractions from DEAE chromatography. These results correlate with results from biotransformation studies discussed previously, where, brassinin (**149**), cyclobrassinin (**158**) and methyl tryptamine dithiocarbamate (**199**) undergo direct *N*-glucosylation at position 1 of their indole moiety.

Table 2.16: Substrate specificity of brassinin glucosyltransferase (BGT) using cell homogenate as enzyme source

Substrate	Specific activity (nmol/min/mg) ± SD	Relative activity (%) [Brassinin = 100%]
Brassinin (**149**)	0.24 ± 0.03	100
Camalexin (**170**)	No conversion	0
6-Fluorocamalexin (**250**)	No conversion	0
6-Fluoro-1-methylcamalexin (**251**)	No conversion	0
Cyclobrassinin (**158**)	0.20 ± 0.03	83
6-Hydroxycamalexin (**236**)	0.10 ± 0.03	40
6-Methoxycamalexin (**171**)	0.02 ± 0.01	6
Methyl tryptamine dithiocarbamate (**199**)	0.24 ± 0.03	100

[a]Results are from three independent experiments, each one carried out in triplicate.

The slow transformation of 6-methoxycamalexin (**171**) to 6-methoxy 1-(β-D-glucopyranosyl)camalexin (**238**) (6%) via direct *N*-1 glucosylation correlates with results obtained from liquid culture metabolism by *S. sclerotiorum* where **238** was the minor metabolite obtained after incubation with 6-methoxycamalexin. These results suggest that the same glucosyltransferase from *S. sclerotiorum* is responsible for the detoxification of

cyclobrassinin (**158**), methyl tryptamine dithiocarbamate (**199**), and indeed 6-methoxycamalexin (**171**) via the minor pathway. Camalexin however is detoxified by *S. sclerotiorum* in two steps; hydroxylation followed by *O*-glucosylation and thus could not be transformed by the glucosyltransferase alone. This explains the non-conversion of camalexin observed here. However 6-hydroxycamalexin (**236**) was transformed to the glucoside by the brassinin glucosyltransferase (BGT) suggesting that the second step of camalexin detoxification probably requires the same brassinin glucosyltransferase. This hypothesis can only be confirmed when the brassinin detoxifying enzyme has been purified to homogeneity.

2.4.5 Inhibition studies using cell homogenate

Liquid cultures of *S. sclerotiorum* metabolized brassinin (**149**) considerably slower (ca. 24 h vs. 7 d) when it was co-incubated with 6-fluorocamalexin (**250**). To establish if this effect was due to growth inhibition or inhibition of the brassinin detoxifying enzyme, co-incubation of brassinin (**149**) with 6-fluorocamalexin (**250**) and the substrates 6-methoxycamalexin (**171**) and 6-fluoro-1-methylcamalexin (**251**) was carried out with cell homogenate (Table 2.17). The specific activity for the assay with brassinin (**149**) was 0.027 nmol/min/mg of protein whilst that obtained when brassinin (**149**) and 6-fluorocamalexin (**250**) were co-incubated was 0.012 nmol/min/mg of protein, a relative decrease of about 56%. The presence of 6-fluorocamalexin (**250**) in assay media with brassinin (**149**) appears to have caused a significant decrease in the production of the 1-β-D-glucopyranosyl brassinin (**237**) product compared to the effects of the other substrates tested.

Table 2.17 Co-incubation studies of brassinin (**149**) (2×10^{-5} M) with different substrates (2×10^{-5} M) for 3 hours at 27 °C

Substrates	Specific activity (nmol/min/mg) ± SD	Relative activity (%) [Brassinin = 100%]
Brassinin (**149**)	0.027 ± 0.004	100
Brassinin (**149**) + 6-methoxycamalexin (**171**)	0.018 ± 0.004	67
Brassinin (**149**) + 6-fluorocamalexin (**250**)	0.012 ± 0.002	44
Brassinin (**149**) + 6-fluoro-1-methylcamalexin (**251**)	0.022 ± 0.002	82

[a]Percent product inhibition = [(assay with brassinin and substrate/ assay with brassinin) × 100]; results are from three independent experiments, each one carried out in triplicate.

Table 2.18 Co-incubation studies of brassinin (3×10^{-5} M) with two different concentrations of 6-fluorocamalexin for 3 hours at 27 °C

Substrate (concentration)	Specific activity (nmol/min/mg)	Relative activity (%) [Brassinin = 100 %]
Brassinin (**149**)	0.242	100
Brassinin (**149**) + 6-fluorocamalexin (**250**) (3×10^{-5} M)	0.083	34
Brassinin (**149**) + 6-fluorocamalexin (**250**) (6×10^{-5} M)	0.076	31

[a]Percent product inhibition = [(assay with brassinin and substrate/ assay with brassinin) × 100]; results are from three independent experiments (SD ± 0.003).

There seems to be a higher effect as the concentration of 6-fluorocamalexin (**250**) in the assay medium increased (Table 2.18). These results indicate that 6-fluorocamalexin (**250**) is not only a fungal growth inhibitor but also seems to affect the brassinin detoxifying enzyme. Further work needs to be done to establish if 6-fluorocamalexin (**250**) is an inhibitor of the brassinin detoxifying enzyme and if so what type of inhibition occurs.

CHAPTER THREE

3. Conclusions

It was established that sclerin (**17**) one of the secondary metabolites isolated from culture filtrate extracts of *Sclerotinia sclerotiorum*, is phytotoxic to cruciferous plants that are susceptible to Sclerotinia stem rot disease. Sclerin (**17**, 5×10^{-4} M) caused severe necrosis and chlorosis to leaves of *Brassica napus* (cv. Westar), *Brassica juncea* (cv. Cutlass), and *Sinapis alba* (cv. Ochre). The claim that oxalic acid is phytotoxic to crucifers and other plants needs to be substantiated since only superficial leaf damage was observed when oxalic acid (5×10^{-2} M) was applied to these crucifers. One could argue that at such a high concentration many substances would show toxicity to plants. Also it was demonstrated that oleic acid, the major fatty acid isolated from sclerotia of *S. sclerotiorum* is responsible for its cytotoxic activity on brine shrimp (*Artemia salina*). Sclerin (**17**), the phytotoxic metabolite isolated from liquid cultures of *S. sclerotiorum*, the broth extract, and oxalic acid did not show any cytotoxic effect on the brine shrimp larvae.

Phytoalexin elicitation with mycelia of *S. sclerotiorum* in stem rot resistant leaves of *Erucastrum gallicum* (dog mustard) led to the isolation of indole-3-acetonitrile (**178**), arvelexin (**179**), 1-methoxyspirobrassinin (**176**) and erucalexin (**204**, new phytoalexin, a structural isomer of **176**). Upon isolation, the structures of indole-3-acetonitrile (**178**) and arvelexin (**179**) were deduced by comparison with authentic samples whilst those of 1-methoxyspirobrassinin (**176**) and erucalexin (**204**) were deduced from spectroscopic data (UV, FTIR, NMR, MS). 1-Methoxyspirobrassinin (**176**), arvelexin (**179**), and erucalexin (**204**) showed antifungal activity against *S. sclerotiorum* and *Rhizoctonia solani*. The isolation of these four phytoalexins from a crucifer resistant to *S. sclerotiorum* suggests that further investigation of their mechanism of action against economically important cruciferous pathogens could provide valuable information.

S. sclerotiorum metabolized brassinin (**149**), and methyl tryptamine dithiocarbamate (**199**), a homologue of **149** via *N-1* glucosylation to 1-β-D-glucopyranosylbrassinin (**234**) and methyl 1-(β-D-glucopyranosyl)tryptamine dithiocarbamate (**235**) respectively. Similarly, camalexin (**170**) and 6-methoxycamalexin (**171**) were metabolized to 6-*O*-β-D-glucopyranosylcamalexin (**237**) via 6-hydroxy camalexin (**236**). In addition, in 6-methoxycamalexin (**171**) was partly converted to 6-methoxy-1-β-D-glucopyranosylcamalexin (**238**) a minor metabolite; that is *S. sclerotiorum* converted 6-methoxycamalexin (**171**) via two pathways, with the major product **237** resulting from demethylation of the methoxy group at C-6, followed by glucosylation; the minor product **238** resulted from direct *N*-glucosylation. The structures of all the biotransformation products were deduced from spectroscopic data (UV, FTIR, NMR, MS). Further feeding of glucosides **234** and **235** to *S. sclerotiorum* indicated that they were further transformed but no biotransformation products were detected or isolated. The possible metabolic products might be very polar and more soluble in aqueous media than in organic solvents, thus precluding extraction and detection.

Antifungal radial growth bioassays indicated that the metabolism of brassinin (**149**), methyl tryptamine dithiocarbamate (**199**), camalexin (**170**) and 6-methoxycamalexin (**171**) in *S. sclerotiorum* led to products having no detectable antifungal activity, thus the metabolism of these phytoalexins and homologue **199** is a detoxification process. Comparison of the bioassay results revealed camalexin (**170**) and methyl tryptamine dithiocarbamate (**199**) to be stronger antifungal agents than brassinin (**149**), which was in turn stronger than 6-methoxycamalexin (**171**).

Analogues of brassinin (**149**) and camalexin (**170**) were designed based on structures of biotransformation products to probe the specificity of the detoxifying enzyme(s). The fungus *S. sclerotiorum* metabolized these analogues via glucosylation and through other minor pathways, though at slower rates. The structures of the biotransformation products were deduced from spectroscopic data (UV, FTIR, NMR, MS).

The glucosides of the analogues had no detectable antifungal activity indicating that the transformations were detoxification processes. It was demonstrated in co-incubation studies involving brassinin (**149**) and the analogues that 6-fluorocamalexin (**250**) significantly slowed down the metabolism of brassinin.

Finally, it was established that glucosylation of the crucifer phytoalexin brassinin (**149**) takes place via a uridine diphosphate glucose (UDPG) dependent glucosyltransferase, which appears to be inducible in *S. sclerotiorum*. Enzymatic activity was observed only in cell-homogenates obtained from liquid cultures of *S. sclerotiorum* incubated with phytoalexin / analogue in the presence of a glucose donor as coenzyme. In the glucosylation reaction, brassinin (**149**) reacted with UDP-glucose (glucose donor) to form the 1-β-D-glucopyranosylbrassinin (**234**) product. Partial purification (five fold) of the brassinin detoxifying enzyme was achieved. The brassinin glucosyltransferase (BGT) appears to be the same enzyme that detoxifies the phytoalexin cyclobrassinin (**158**) and the brassinin homologue methyl tryptamine dithiocarbamate (**199**) to their *N-1* glucosides. It was also demonstrated that 6-fluorocamalexin (**250**), an analogue of camalexin (**170**) was not just a fungal growth inhibitor and seems to affect the BGT.

Future Work

1. Synthesis of erucalexin (**204**).
2. Purification of the brassinin glucosyltransferase (BGT) to homogeneity
3. Characterization of the BGT (kinetic and substrate specificity studies, optimum pH, optimum temperature, isoelectric point, etc)
4. Co-incubation studies using 6-fluorocamalexin (**250**) and brassinin (**149**) in enzyme (purified BGT) assays to verify the role of **250** as paldoxin
5. Synthesis of analogues of brassinin (potential paldoxins) to probe the purified BGT

CHAPTER FOUR

4. Experimental

4.1 General methods

All chemicals were purchased from Sigma-Aldrich Canada (Oakville, ON). All solvents were used as received except $CHCl_3$ and CH_2Cl_2, which were redistilled. Solvents used in syntheses were dried over the following drying agents prior to use: Et_2O and THF over Na/Benzophenone, CH_2Cl_2, benzene and CH_3CN over CaH_2 and acetone over $CaSO_4$,

Analytical thin layer chromatography (TLC) was carried out on precoated silica gel TLC aluminium sheets (EM science, Kieselgel 60 F_{254}, 5×2 cm × 0.2 mm). Compounds were visualized under UV light (254/366 nm) and by dipping the plates in a 5% aqueous (w/v) phosphomolybdic acid solution containing 1% (w/v) ceric sulphate and 4% (v/v) H_2SO_4, followed by heating.

Preparative thin layer chromatography (prep TLC) was performed on silica gel plates (EM science, 60 F_{254} or reversed-phase RP-18, 20 × 20 cm, 0.25 or 0.5 mm thickness). Compounds were visualized under UV light. All solvent mixtures used were volume/volume (v/v) mixtures.

Flash column chromatography (FCC) was performed on silica gel, Merck grade 60, mesh size 230-400, 60 A° or J. T. Baker C-18 reversed-phase silica gel, 40 μm.

High performance liquid chromatography (HPLC) analysis was performed with a Hewlett Packard high-performance liquid chromatograph equipped with a quaternary pump, an automatic injector, a photodiode array detector (wavelength range 190-600 nm), degasser, and a Hypersil octadecylsilane (ODS) column (5 μM particle size silica, 200 mm × 4.6 mm internal diameter), equipped with an in-line filter. The retention times (R_t) are reported for a linear gradient elution [CH_3CN-H_2O (25:75) - CH_3CN (100)], for 35 min., and a flow rate of 1.0 mL / min was used. HPLC semi-preparative separations were

performed with the same system described above but with a bigger column (5 μM particle size silica, 200 mm × 10 mm internal diameter).

Fourier transform infrared (FTIR) spectra were recorded on a Bio-Rad FTS-40 spectrometer using the diffuse reflectance method on samples dispersed in KBr.

NMR spectra were recorded on Bruker AMX 300 or Avance 500 spectrometers. For ^{1}H NMR (300 or 500 MHz) the chemical shifts (δ) are reported in parts per million (ppm) relative to TMS. The δ values were referenced to $CDCl_3$ ($CHCl_3$ at 7.27 ppm), CD_2Cl_2 ($CHDCl_2$ at 5.32 ppm), CD_3CN (CD_2HCN at 1.94 ppm), CD_3SOCD_3 (CHD_2SOCD_3 at 2.50 ppm), or CD_3OD (CHD_2OD at 3.31 ppm). First-order behaviour was assumed in analysis of ^{1}H NMR spectra and multiplicities are as indicated by one or more of the following s = singlet, d = doublet, t = triplet, q = quartet, m = multiplet, and br = broad. Spin coupling constants (*J* values) are reported to the nearest 0.5 Hz. For ^{13}C NMR (75.5 or 125.8 MHz) the chemical shifts (δ values) were referenced to $CDCl_3$ (77.23 ppm), CD_2Cl_2 (54.00 ppm), CD_3CN (118.69 ppm), CD_3OSOCD_3 (39.51 ppm), or CD_3OD (49.15 ppm). The multiplicities of ^{13}C signals refer to the number of attached protons or fluorine atoms: s = C, d = CH or CF, t = CH_2, CF_2 or CHF, q = CH_3, CF_3, CH_2F or CHF_2 and were determined based on HMQC correlations or magnitude of *J* values. In some cases it was determined based on chemical shift and consistency within a series of similar structures as well as the relative intensity of each signal.

Mass spectra (MS) [high resolution (HR), electron impact (EI), chemical ionization (CI) or fast atom bombardment (FAB)] were obtained on a VG 70 SE mass spectrometer using a solids probe. Continuous flow FAB was performed using a Zorbax SB-C18 column (3.5 μm particle size silica, 0.3 mm ×150 mm), eluted with a linear gradient of H_2O-CH_3CN, 90:10, with glycerol (matrix) dissolved in the mobile phase.

Gas chromatography – mass spectra (GC-MS) was obtained on a Fisons GC 8000 series model 8060 connected to the VG 70 SE mass spectrometer.

Specific rotations, $[\alpha]_D$ were determined at ambient temperature on a Perkin-Elmer 141 polarimeter using a 1 mL, 10 cm path length cell; the units are 10^{-1} deg cm^2 g^{-1} and the concentrations (*c*) are reported in g/100 mL.

Protein purification was performed with a Pharmacia biotech Frac 200 connected to a Hewlett Packard series 1100 detector G1314A, Pharmacia columns AC10, AC 16 or AC 26 packed with anion exchange matrix DEAE Sephacel (wet bead size 40 – 160 μm), gel filtration matrix Sephadex G-25, and affinity chromatography matrices such as Reactive Green 19, Reactive Yellow 86, and Cibacron Blue 3GA and a Pharmacia biotech pump P-1.

Gel electrophoresis was performed with an Owl separation system model P8DS connected to a VWR ACCU model 500 power supply system. 10% SDS-PAGE gels were cast with a Joel caster model JGC-2 gel system. Unstained molecular weight markers ER 110-L were used. Staining of gels was performed with Coomassie Brilliant Blue R-250 dye.

Protein measurements were performed using the Bradford method with BSA as standard. Ultraviolet (UV) spectra of synthesized compounds and metabolites isolated and optical density (at 595 nm) for protein measurements were recorded on a Varian Cary 100 spectrophotometer using a 1 cm cell.

4.1.1 Plant material and growth

Seeds of canola (*Brassica napus*) cv. Westar, white mustard *(Sinapis alba*) cv. Ochre, brown mustard (*Brassica juncea*) cv. Cutlass and dog mustard (*Erucastrum gallicum*, a wild crucifer) were obtained from Agriculture and Agric-Food Canada Research Station, Saskatoon, SK. The seeds were sown in commercial potting soil (Redi-earth) mixture, and plants were grown in a growth chamber, under controlled environmental conditions (20/18 °C with 16/8 day/night cycle) for 2 – 5 weeks.

4.1.2 Fungal isolates, culture conditions and extractions

Fungal isolates were obtained from C. Lefol, Agriculture and Agric-Food Canada Research station, Saskatoon, SK. Sclerotia of *Sclerotinia sclerotiorum* clone # 33 and clone # 67 and *Rhizoctonia solani* AG-2 were maintained in Petri dish cultures on potato dextrose agar (PDA). Liquid cultures (1 L per batch; total amount 17 L) were inoculated with five sclerotia per 100 mL of potato dextrose broth (PDB) media in 250 mL Erlenmeyer flasks. These were incubated at 20 °C for 14 days, filtered and the broth extracted with EtOAc (3 × 300 mL). The combined EtOAc extracts were dried over anhydrous Na_2SO_4 and the solvent was then removed under reduced pressure. Liquid cultures were also prepared in minimal media (14 days incubation) and Czapek Dox media (50 days incubation) and treated the same way as described above.

Sclerotium (275 g) of *S. sclerotiorum* clone # 33 was mixed with water (500 mL) and ground (using a commercial blender). The fine pasty gel was extracted with EtOAc (600 mL, 3×). Butanol (200 mL) was added to the residue, stirred for 24 hours and extracted. The two extracts were dried over anhydrous Na_2SO_4 and the solvent removed under reduced pressure.

4.1.3 Calibration curves for phytoalexins and metabolites

From a stock solution (5×10^{-2} M in CH_3CN), solutions of six different concentrations (between 1×10^{-3} M and 1×10^{-6} M in CH_3CN) were prepared through serial dilution. Each solution was injected in triplicate and peak areas were recorded (detection at 220 nm). Calibration curves (shown in appendix, pages 217-222) were obtained by linear regression analysis of the peak area (mAu×s) versus molar concentration (M) of each phytoalexin/analogue/metabolite, using the equation $\mathbf{A = aM + b}$. The regression data for the phytoalexins 1-methoxyspirobrassinin (**176**), indole-3-acetonitrile (**178**), arvelexin

(**179**), erucalexin (**204**), and biotransformation products 1-(β-D-glucopyranosyl) brassinin (**234**), methyl 1-(β-D-glucopyranosyl) tryptamine dithiocarbamate (**235**), 6-(*O*-β-D-glucopyranosyl) camalexin (**237**), 6-methoxy 1-(β-D-glucopyranosyl)camalexin (**238**), 6-fluoro-1-(β-D-glucopyranosyl)camalexin (**268**) and 1-(β-D-glucopyranosyl)cyclobrassinin (**271**) are presented in Table 4.1.

Table 4.1 HPLC calibration data for standards determined at 220 nm.

Compounds	Slope (**a**)	Intercept (**b**)
Sclerin (**17**)	7.5×10^5	-
1-Methoxyspirobrassinin (**176**)	9.0×10^6	-
Indole-3-acetonitrile (**178**)	2.0×10^7	-
Arvelexin (**179**)	1.0×10^7	-
Erucalexin (**204**)	7.0×10^6	-
1-(β-D-glucopyranosyl) brassinin (**234**)	6.0×10^6	-
Methyl 1-(β-D-gluco pyranosyl) tryptamine dithiocarbamate (**235**)	1.0×10^7	196
6-(*O*-β-D-glucopyranosyl) camalexin (**237**)	5.0×10^6	-
6-methoxy 1-(β-D-gluco pyranosyl)camalexin (**238**)	5.0×10^6	-
6-fluoro-1-(β-D-gluco pyranosyl)camalexin (**268**)	5.0×10^6	-
1-(β-D-glucopyranosyl) cyclobrassinin (**271**)	9.0×10^6	-

$R^2 = 0.99$

4.2 Isolation of metabolites from *Sclerotinia sclerotiorum*

4.2.1 Phytotoxins from liquid cultures of *Sclerotinia sclerotiorum*

The EtOAc extract obtained from 17 L of liquid cultures of *S. sclerotiorum* (1.02 g) was dissolved in CH_2Cl_2 - MeOH (95:5, 1 mL) and fractionated by FCC on silica gel with gradient elution: CH_2Cl_2 - MeOH (95:5, 8 fractions of 100 mL), CH_2Cl_2 - MeOH (90:10, 1 fraction of 100 mL), CH_2Cl_2 - MeOH (80:20, 1 fraction of 100 mL), CH_2Cl_2 - MeOH (50:50, 1 fraction of 100 mL), and MeOH (1 fraction of 100 mL). All the 12 fractions were analyzed by HPLC and TLC and also bioassayed on *B. napus*, *B. juncea* and *S. alba*. Fractions 5 to 8 showed phytotoxicity and a prominent peak at R_t = 24 min (HPLC) were combined (138 mg) and fractionated by RP-FCC [C-18 silica gel with gradient elution: system A, acetonitrile - water (1: 1, 8 fractions of 40 mL); B, acetonitrile (100 mL) and C, methanol (100 mL)]. Fractions 6 and 7 whose HPLC chromatograms showed the peak at R_t = 24 min and showed phytotoxicity were combined. Separation by PrepTLC (silica gel, CH_2Cl_2 - MeOH, 95:5) gave sclerin (**17**, 50 mg).

Spectroscopic data for Sclerin (17)

HPLC R_t = 24 min

^{1}H NMR (500 MHz, $CDCl_3$): δ 10.78 (s, 1H, D_2O exchangeable), 4.18 (q, J = 7.5 Hz, 1H), 2.32 (s, 3H), 2.26 (s, 3H), 2.20 (s, 3H) 1.59 (d, J = 7.5 Hz, 3H).

^{13}C NMR (125 MHz, $CDCl_3$): δ 169.2 (s), 166.7 (s), 159.2 (s), 148.2 (s), 134.9 (s), 125.0 (s), 124.4 (s), 101.8 (s), 39.1 (d), 22.7 (t), 17.9 (t), 14.9 (t), 12.3 (t).

HRMS-EI *m/z*: measured 234.0890 (M^+, calcd. 234.0892 for $C_{13}H_{14}O_4$).

MS-EI *m/z* (relative intensity): 234 (M^+, 54), 206 (100), 191 (13), 163 (20), 147 (12), 91 (12).

FTIR ν_{max}: 3203, 2987, 2933, 2872, 1795, 1694, 1606, 1455, 1331, 1267, 1136, 1103, 1011, 946, 796, 730, 560 cm^{-1}.

UV (EtOH) λmax (log ε): 212 (4.3), 264 (3.8), 328 (3.5).

4.2.2 Cytotoxic compounds from sclerotia of *Sclerotinia sclerotiorum*

The EtOAc extract (390 mg) of sclerotia of *S. sclerotiorum* was subjected to FCC on silica gel with gradient elution: CH_2Cl_2 - MeOH (99:1, 10 fractions of 100 mL), CH_2Cl_2 - MeOH (95:5, 1 fraction of 100 mL), CH_2Cl_2 - MeOH (90:10, 1 fraction of 100 mL), CH_2Cl_2 - MeOH (80:20, 1 fraction of 100 mL), CH_2CI_2 - MeOH (50:50, 1 fraction of 100 mL) and MeOH wash (1 fraction of 100 mL). In all 15 fractions were collected. The fractions were bioassayed on the brine shrimp larva, *Artemia salina*. Fractions 3 and 4, showed toxicity and were combined (40 mg) and further subjected to prepTLC using CH_2Cl_2-MeOH (99:1, developed three times) to give a fraction (12.2 mg) that turned out to be a mixture of fatty acids. This fraction (2 mg) was treated with excess ethereal diazomethane at room temperature for 3 hours. The solvent was then removed under reduced pressure to give the methyl esters of fatty acids (2.6 mg). This was subjected to GC-MS analysis and the amount of each fatty acid present was estimated. Oleic, stearic and palmitic acids (2 mg each; purchased from Sigma-Aldrich Co.) were separately treated with excess ethereal diazomethane at room temperature for 3 hours and subsequently subjected to GC-MS analysis. GC-HRMSEI was used to identify the various fatty acid methyl esters.

4.2.3 Phytotoxicity assays

4.2.3.1 Leaf puncture assay

Fully expanded leaves of the plants described above were scratched and/or punctured (4 punctures per leaf, and 2 leaves per plant). Droplets (10 μL) of each test solution (composed of 50% aqueous methanol) were applied at each puncture. Six concentrations for sclerin (**17**, 1×10^{-3}, 5×10^{-4}, 3×10^{-4}, 2×10^{-4}, 1×10^{-4}, and 1×10^{-5} M) and five concentrations for oxalic acid (5×10^{-2}, 1×10^{-3}, 5×10^{-4}, 3×10^{-4}, 2×10^{-4} M) were prepared by serial dilution, broth extract of liquid culture of *S. sclerotiorum* (1 mg/mL and 2 mg/mL), chromatographic fractions (each 1 mg/mL) and sclerotia extract (1 mg/mL and 2 mg/mL) were applied. Symptom appearance was observed daily up to 7 days after droplet application. Each treatment was repeated at least three times. Solutions of 50% aqueous methanol were applied as control.

4.2.3.2 Leaf uptake assay

Four toxin concentrations of sclerin (**17**) and oxalic acid (1×10^{-3}, 5×10^{-4}, 1×10^{-4} and 1×10^{-5} M) in 2% acetonitrile were prepared by serial dilution, as well as broth extract (0.6 mg /1 mL) in 2% acetonitrile and a control solution composed of 2% aqueous acetonitrile. Leaves were cut at the base of their petiole and each leaf was immediately placed in a 1.5 mL Eppendorf tube containing assay solution (1 mL per tube per leaf). After the test solution was taken up, an aqueous solution of BAP (1×10^{-5} M) was added to each tube and leaves were incubated under the same conditions. Three independent experiments were carried out, each one in duplicate. Symptoms were observed daily up to 7 days.

4.2.3.3 Spray assay

3 pots each containing *B. napus, B. juncea, S. alba* and *E. gallicum* (2 - 5 week old) plants grown as described above were uniformly sprayed, using a hand sprayer, with 15 mL of 50% aqueous methanol solution of broth extract (3 mg/25 mL) or 15 mL of 50% aqueous methanolic solution of sclerin (**17**, 5×10^{-4} M) or oxalic acid (5×10^{-4} M), or 15 mL of 50% aqueous methanol as control. The pots were kept in the growth chamber at 24 °C for 7 days.

4.2.4 Brine Shrimp lethality assay

The eggs of brine shrimp *Artemia salina* were incubated in a Petri dish containing 0.33 g of sodium chloride in 100 mol of water (saline solution) in the presence of fluorescent light (24 ± 2 °C for 48 h). The EtOAc extract of sclerotia of *S. sclerotiorum* clone # 33 (10 mg), the fraction composed of fatty acids (10 mg) and the EtOAc extract of liquid cultures of *S. sclerotiorum* clone # 33 (10 mg) were separately dissolved in methanol (1 mL) and from this solution 500 μL, 50 μL, and 5 μL were transferred into separate 2-dram vials corresponding to 1 mg/mL, 0.1 mg/mL and 0.01 mg/mL respectively. Three toxin concentrations of sclerin (**17**), oleic acid, palmitic acid and stearic acid (5×10^{-4}, 10^{-4}, 10^{-5} M) were prepared in serial dilution and transferred into separate vials and the solvent was then removed under reduced pressure. DMSO (40 μL) was added to each vial (a separate vial containing DMSO (40 μL) served as control), saline solution (3.96 mL) was added to each vial followed by addition of brine shrimp larvae (about 10 to 15 in 1 mL saline solution). The vials were stoppered and kept at 24 °C (fluorescent light). After 24 hours, the live brine shrimp larvae in each vial were counted. Three independent experiments were performed, each one in duplicate.

4.3 Phytoalexins from *Erucastrum gallicum*

4.3.1 Elicitation, isolation and chemical characterization

4.3.1.1 Elicitation Experiments

Leaf elicitation with *Sclerotinia sclerotiorum*

Two leaves from 5-week-old *Erucastrum gallicum* (dog mustard) plants were cut and immediately placed in a Petri dish. The petiole of each leaf was wrapped with pre-moistened cotton wool. Each leaf was inoculated with five mycelium plugs (4 mm cut from 3-day-old PDA plates of *S. sclerotiorum* clone # 33) placed upside down and distributed evenly over the leaf surface. The Petri dish was sealed and incubated under constant fluorescent light for 7 days. Ten of such preparations were made. After every 24 hours, leaves from one Petri dish was placed in a 250 mL Erlenmeyer flask frozen in liquid nitrogen, crushed with a glass rod and extracted with EtOAc (ca. 50 mL, 2×) by shaking at 120 rmp for 30 min. The EtOAc was filtered, dried over anhydrous Na_2SO_4 and the solvent removed under reduced pressure. The extract was dissolved in 0.2 mL acetonitrile, filtered through a tight cotton plug and analyzed by HPLC. Two independent experiments were carried out. The HPLC analysis of the EtOAc extracts indicated the presence of 4 compounds with R_t = 11.2, 13.1, 16.9 and 20.6 min not present in control samples. Quantification of the compounds was done using HPLC built standard calibration curves.

Leaf elicitation with spraying of $CuCl_2$ and/or oxalic acid

Four (5-week-old) dog mustard plants were sprayed to the point of run-off with $CuCl_2$ and/or oxalic acid (2×10^{-3} M) solution at 24-hour intervals for three days. Two leaves were excised at 24 h intervals for 7 days. Two control leaves were harvested from separate plants at the same time and treated in a similar manner throughout. All leaves

were incubated with a 16-h photoperiod. After various incubation periods leaves were worked up as described previously and extracts were analyzed by HPLC. Three independent experiments were carried out.

Leaf elicitation with sclerin (**17**) and/or oxalic acid

Fully expanded leaves of 5-week-old dog mustard plants were punctured (4 punctures per leaf, 2 leaves per plant). Droplets (10 μL) of sclerin (**17**) and/or oxalic acid (5×10^{-4} M) solutions in 50% aqueous methanol were applied at each punctured spot. All leaves were incubated with a 16-h photoperiod. Droplets of 50% aqueous methanol were applied as control. Two leaves were excised at 24 hour intervals. After various incubation periods leaves were worked up as described previously and extracts were analyzed by HPLC. Two control leaves were harvested from separate plants at the same time and treated in a similar manner throughout. Three independent experiments were carried out.

4.3.1.2 Isolation of 1-methoxyspirobrassinin(176) and erucalexin (204)

Dog mustard plants (40, 5-week-old) were sprayed with $CuCl_2$ (2×10^{-3} M) solution to the point of run-off, three times at 24-hour intervals and allowed to stand for three days. Harvested elicited leaves (180 g, fresh weight) were frozen in liquid nitrogen, crushed with a glass rod, placed into Erlenmeyer flasks (four, 1L) and extracted with EtOAc (3 × 300 mL per flask), in a manner similar to that followed for the time course experiment. The EtOAc extract (1.2 g) was subjected to FCC [(gradient elution, CH_2Cl_2 (100%) to CH_2Cl_2-MeOH (20:80)]. The fractions containing the HPLC peaks at R_t = 16.9 min and R_t = 20.6 min were combined (284 mg) and further fractionated by reverse phase FCC [(gradient elution, CH_3CN-H_2O (20:80) to CH_3CN (100%)] to give a fraction composed of a mixture of the metabolites with R_t = 16.9 min. and R_t = 20.6 min (4.8 mg). The isolation of the metabolites from this fraction was achieved by reverse phase micro flash [2 cm plug of

reverse phase C-18 silica gel in a Pasteur pipette, CH_3CN-H_2O (60:40)]. This gave 1-methoxyspirobrassinin (**176**, 1.3 mg, R_t = 16.9 min) and erucalexin (**204**, 2.2 mg, R_t = 20.6 min). This isolation procedure was repeated four times to obtain **176** (5.0 mg) and **204** (6.8 mg).

4.3.1.3 Spectroscopic data

1- Methoxyspirobrassinin (176)

HPLC R_t = 16.9 min.; $[\alpha]_D$ = 40.8 (c 0.09, MeOH).

^{1}H NMR (500 MHz, CD_3CN): δ 7.42 (m, 2H), 7.17 (dd, *J* = 7.5, 7.5 Hz, 1H), 7.06 (d, *J* = 7.5 Hz, 1H), 4.60 (d, *J* = 15.5 Hz, 1H), 4.46 (d, *J* = 15.5 Hz, 1H), 3.99 (s, 3H), 2.62 (s, 3H).

^{13}C NMR (125.8 MHz, CD_3CN): δ 171.0 (s, C-2), 163.2 (s, C-2'), 139.9 (s, C-7a), 130.3 (d, C-6), 126.9 (s, C-3a), 124.7 (d, C-4), 124.3 (d, C-5), 108.1 (d, C-7), 74.6 (t, C-4'), 72.6 (s, C-3), 63.9 (q, -OCH_3), 15.3 (q, -SCH_3).

HRMS-EI *m/z*: measured 280.0336 (M^+, calcd. 280.0340 for $C_{12}H_{12}N_2S_2O_2$).

MS-EI *m/z* (relative intensity): 280 (100, M^+), 252 (9, M^+ - CO), 249 (13, M^+ - C_2H_3NS), 234 (15, M^+ - SCH_3), 221 (25), 176 (52, M^+ - [OCH_3 + C_2H_3NS]), 148 (50), 87 (37).

FTIR ν_{max}: 2924, 2852, 1738, 1616, 1585, 1465, 1087, 944, 749 cm^{-1}.

UV (CH_3CN) λ_{max} (log ε): 218 (4.4), 262 (3.7).

Erucalexin (204)

HPLC R_t = 20.6 min.; $[\alpha]_D$ = 72.6 (c 0.09, MeOH).

^{1}H NMR data and ^{13}C NMR data in Table 2.6

HRMS-EI *m/z*: measured 280.0346 (M^+, calcd. 280.0340 for $C_{12}H_{12}N_2S_2O_2$).

MS-EI *m/z* (relative intensity): 280 (67, M^+), 249 (74, M^+ - OCH_3), 233 (9, M^+ - SCH_3), 207 (35, M^+ - C_2H_3NS), 176 (100, M^+- [OCH_3 + C_2H_3NS]), 149 (23, M^+ - $C_4H_5NS_2$), 132 (59), 130 (49, M^+- [OCH_3 + SCH_2 + C_2H_3NS]), 87 (36).

FTIR ν_{max}: 2923, 2850, 1725, 1608, 1576, 1461, 1301, 1106, 1064, 985, 759 cm^{-1}.

UV (CH_3CN) λ_{max} (log ε): 234 (4.6), 262 (4.1), 368 (3.4).

4.3.2 Synthesis

(±) 1-Methyl-3-hydroxyindol-3-ylaminomethane [(±)-(216)]

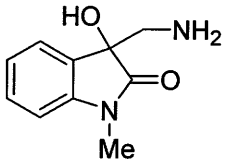

216

Et_2NH (20 μL, 0.193 mmol) was added to 1-methylisatin (**215**, 310 mg, 1.93 mmol) suspended in a solution of CH_3NO_2 (315 μL, 5.80 mmol) and ethanol (1 mL) at 0 °C. The reaction mixture was kept at –20 °C for 24 hours, and the solvent was removed under reduced pressure to give an oily product (427 mg). To a solution of this oily product in a solution of methanol (6 mL) and glacial acetic acid ((0.5 mL), 10% Pd/C (50 mg) was added and mechanically agitated at 3 atmospheres of H_2 for 15 hours. The product obtained after filtering off the Pd/C was subjected to FCC (silica gel, $CHCl_3$-MeOH-28% aqueous NH_3, 80:20:1) to give (±)-1-methyl-3-hydroxyindol-3-ylaminomethane [(±)-**216**, 290 mg, 78%)] as pale-yellow semi solid.

Spectroscopic data for (±)-**216**

^{1}H NMR (500 MHz, CD_3OD): δ 7.39 (m, 2H), 7.14 (dd, J = 7.5, 7.5 Hz, 1H), 7.02 (d, J = 7.5 Hz, 1H) 3.21 (s, 3H), 2.99 (d, J = 13.5 Hz, 1H), 2.93 (d, J = 13.5 Hz, 1H).

^{13}C NMR (125.8 MHz, CD_3OD): δ 178.4 (s), 143.9 (s), 130.2 (s), 130.0 (d), 123.7 (d), 123.4 (d), 108.9 (d), 76.1 (s), 55.9 (t), 25.4 (q).

HRMS-FAB *m/z*: measured 193.0972 ($[M + 1]^+$, calcd. 193.0977 for $C_{10}H_{13}N_2O_2$).

MS-FAB *m/z* (relative intensity): 193 (100, $[M + 1]^+$), 176 (60), 163 (15), 146 (10).

FTIR ν_{max}: 3267, 3058, 2937, 1714, 1614, 1471, 1375, 754 cm^{-1}.

(±)-Spiro[1-methylindoline-3,5'-oxazolidine]-2-one-2'-thione [(±)-(217)]

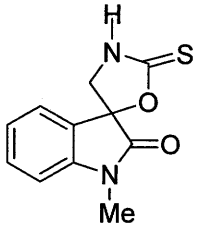

217

To a solution of (±)-1-methyl-3-hydroxyindol-3-ylaminomethane (**216**, 74.2 mg, 0.386 mmol) in CH_2Cl_2 (2 mL), $CSCl_2$ (30 μL, 0.425 mmol) was added and the mixture was stirred at room temperature for 30 min. Aqueous Na_2CO_3 (5%, 3 mL) was added to the reaction mixture, the mixture poured into ice-cold water and extracted with EtOAc (50 mL, 2×). The crude product was subjected to FCC (silica gel, EtOAc-Hexane, 2:1) to yield (±)-spiro[1-methylindoline-3,5'-oxazolidine]-2-one-2'-thione [(±)-**217**, 73.6 mg, 82%] as off white powder.

Spectroscopic data for (±)-**217**

HPLC R_t = 6.8 min.

^{1}H NMR (500 MHz, CD_3CN): δ 8.02 (s, 1H, D_2O exchangeable), 7.54 (d, J = 7.5 Hz, 1H), 7.49 (dd, J = 8.0, 7.5 Hz, 1H), 7.18 (dd, J = 7.5 Hz, 7.5 Hz, 1H) 7.01 (d, J = 8.0 Hz, 1H), 4.01 (d, J = 11.0 Hz, 1H), 3.96 (d, J = 11.0 Hz, 1H) 3.17 (s, 3H).

^{13}C NMR (125.8 MHz, CD_3CN): δ 188.8 (s), 172.3 (s), 145.1(s), 132.3 (d), 125.5 (s), 125.1 (d), 123.9 (d), 109.7 (d), 85.1 (s), 51.2 (t), 26.4 (q).

HRMS-EI *m/z*: measured 234.0463 (M^+, calcd. 234.0463 for $C_{11}H_{10}N_2SO_2$).

MS-EI *m/z* (relative intensity): 234 (M^+, 44), 178 (56), 177 (11), 162 (100), 77 (10).

FTIR ν_{max}: 3058, 2925, 2852, 1730, 1616, 1524, 1471, 1165, 755 cm^{-1}.

UV (CH_3CN) λ_{max} (log ε): 211 (4.3), 249 (3.9), 296 (3.3).

(±)-2'-Methylsulfanyl-spiro[1-methylindoline-3,5'-[4',5']-dihydrooxazol]-2-one [(±)-(219)]

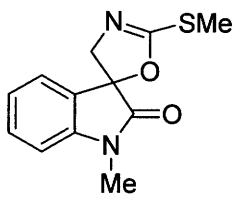

219

To a stirred suspension of powdered K_2CO_3 (40 mg, 0.29 mmol) in dry acetone (2 mL) was added (±)-spiro[1-methylindoline-3,5'-oxazolidine]-2-one-2'-thione (**217**, 60.8 mg, 0.26 mmol) and MeI (45 μL, 0.71 mmol). After stirring for 8 hours, the reaction mixture was poured into ice-cold water (50 mL) and extracted with EtOAc (50 mL, 2×). The organic layer was dried over anhydrous Na_2SO_4 and the solvent removed under

reduced pressure to give (±)-2'-methylsulfanyl-spiro[1-methylindoline-3,5'-[4',5']-dihydrooxazol]-2-one [(±)-**219**, 62.2 mg, 96%)].

Spectroscopic data for (±)-**219**

HPLC R_t = 11.2 min.

^{1}H NMR (500 MHz, CD_3CN): δ 7.43 (dd, *J* = 7.5, 7.5 Hz, 1H), 7.40 (d, *J* = 7.5, 1H), 7.14 (dd, *J* = 8.0 Hz, 7.5 Hz, 1H) 6.98 (d, *J* = 8.0 Hz, 1H), 4.20 (d, *J* = 14.0 Hz, 1H), 4.07 (d, *J* = 14.0 Hz, 1H) 3.16 (s, 3H), 2.54 (s, 3H).

^{13}C NMR (125.8 MHz, CD_3CN): δ 174.2 (s), 165.0 (s), 144.7 (s), 131.5 (d), 127.8 (s), 124.4 (d), 123.7 (d), 109.5 (d), 84.6 (s), 64.4 (t), 26.3 (q), 14.5 (q).

HRMS-EI *m/z*: measured 248.0625 (M^+, calcd. 248.0620 for $C_{12}H_{12}N_2SO_2$).

MS-EI *m/z* (relative intensity): 248 (M^+, 70), 201 (43), 173 (100), 159 (38), 130 (27), 87 (65), 71 (32).

FTIR ν_{max}: 2935, 2867, 1727, 1614, 1494, 1471, 1352, 1141, 976, 752 cm^{-1}.

UV (CH_3CN) λ_{max} (log ε): 215 (4.3), 253 (3.7), 297 (3.2).

(±)-Spiro[1-methylindoline-3,5'-oxazolidine]-2,2'-dithione [(±)-(218)] and (±)-spiro[1-methylindoline-3,5'-oxazolidine]-2,2'-dione [(±)-(220)]

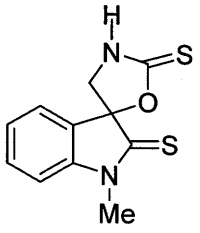

218

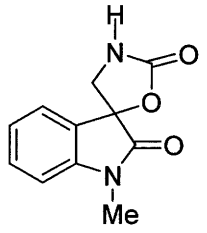

220

To a solution of P_4S_{10} (80.3 mg, 0.18 mmol) and (±)-spiro[1-methylindoline-3,5'-oxazolidine]-2-one-2'-thione (**217**, 35 mg, 0.15 mmol) in CH_3CN (4 mL) under argon atmosphere was added $NaHCO_3$ (51.6 mg, 0.60 mmol). After refluxing for 6 hours the solvent was removed under reduced pressure, ice-cold water (30 mL) was added and the reaction mixture extracted with CH_2Cl_2 (50 mL, 2×). The organic layer was dried over anhydrous Na_2SO_4 and after the removal of solvent the crude product was subjected to prepTLC (silica gel, EtOAc-Hexane, 2:1) to give (±)-spiro[1-methylindoline-3,5'-oxazolidine]-2,2'-dithione [(±)-**218**, 4.2 mg, 16% based on recovered starting material] and (±)-spiro[1-methylindoline-3,5'-oxazolidine]-2,2'-dione [(±)-**220**, 8.3 mg, 38% based on recovered starting material].

Spectroscopic data for (±)-**218**

HPLC R_t = 12.8 min (broad peak).

^1H NMR (500 MHz, CD_3CN): δ 8.02 (s, 1H, D_2O exchangeable), 7.54 (d, J = 7.5 Hz, 1H), 7.49 (dd, J = 8.0, 7.5 Hz, 1H), 7.18 (dd, J = 7.5 Hz, 7.5 Hz, 1H) 7.01 (d, J = 8.0 Hz, 1H), 4.01 (d, J = 11.0 Hz, 1H), 3.96 (d, J = 11.0 Hz, 1H) 3.17 (s, 3H).

^{13}C NMR (125.8 MHz, CD_3CN): δ 200.9 (s), 188.2 (s), 145.6 (s), 132.2 (d), 130.2 (s), 125.6 (d), 124.4 (d), 111.1 (d), 91.6 (s), 54.4 (t), 31.6 (q).

HRMS-EI *m/z*: measured 250.0231 (M^+, calcd. 250.0235 for $C_{11}H_{10}N_2SO_2$).

MS-EI *m/z* (relative intensity): 250 (M^+, 10), 217 (50), 175 (40), 97 (50), 57 (100).

FTIR ν_{max}: 3267, 2955, 2925, 2854, 1701, 1614, 1527, 1467, 1376, 1164, 1098, 752 cm^{-1}.

UV (CH_3CN) λ_{max} (log ε): 243 (4.2), 287 (3.8), 295 (3.8), 337 (3.9).

Spectroscopic data for (±)-**220**

HPLC R_t = 5.6 min.

^{1}H NMR (500 MHz, CD_3CN): δ 7.55 (d, J = 7.5 Hz, 1H), 7.46 (dd, J = 8.0, 7.5 Hz, 1H), 7.17 (dd, J = 7.5 Hz, 7.5 Hz, 1H) 6.99 (d, J = 8.0 Hz, 1H), 6.06 (s, 1H, D_2O exchangeable), 3.79 (d, J = 9.5 Hz, 1H), 3.73 (d, J = 9.5 Hz, 1H) 3.16 (s, 3H).

^{13}C NMR (125.8 MHz, CD_3CN): δ 173.5 (s), 158.2 (s), 144.9 (s), 131.8 (d), 126.8 (s), 124.9 (d), 123.7 (d), 109.9 (d), 79.3 (s), 48.0 (t), 26.3 (t).

HRMS-EI *m/z*: measured 218.0463 (M^+, calcd. 218.0463 for $C_{11}H_{10}N_2O_3$).

MS-EI *m/z* (relative intensity):

FTIR ν_{max}: 3315, 2928, 2856, 1770, 1730, 1616, 1524, 1471, 1375, 1258, 1084, 1004, 753 cm^{-1}.

UV (CH_3CN) λ_{max} (log ε): 212 (4.4), 259 (3.8), 301 (3.2).

Lawesson Reaction

To a solution of (±)-spiro[1-methylindoline-3,5'-oxazolidine]-2-one-2'-thione (**217**, 10 mg, 0.043 mmol) in dry HMPA (3 mL) under argon atmosphere, 2,4-bis(p-methoxyphenyl-1,3,2,4-dithiadiphosphetane 2,4–disulfide (Lawesson reagent) was added slowly. The mixture was heated at 110 °C under argon for 2 hours. The reaction mixture was then cooled, poured into water (30 mL) and extracted with Et_2O (50 mL, 2×). The organic layer was dried over anhydrous Na_2SO_4 and, after removal of solvent, the crude product was subjected to prepTLC (silica gel, EtOAc-Hexane, 2:1) to give (±)-**218** (1.3 mg, 12%), with the recovery of (±)-**217** (2 mg) and other mixtures, which could not be purified.

(±)-2'-Methylsulfanyl-spiro[1-methylindoline-3,5'-[4',5']-dihydrooxazol]-2-thione [(±)-(206)]

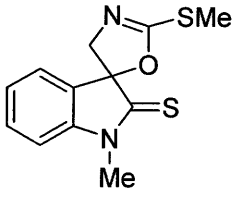

206

To a stirred suspension of powdered K_2CO_3 (2.5 mg, 0.018 mmol) in dry acetone (1 mL) was added (±)-spiro[1-methylindoline-3,5'-oxazolidine]-2,2'-dithione (**218**, 4 mg, 0.016 mmol) and MeI (5 μL, 0.08 mmol). After stirring for 8 hours, the reaction mixture was poured into ice-cold water (10 mL) and extracted with EtOAc (15 mL, 2×). The organic layer was dried over anhydrous Na_2SO_4 and the solvent removed under reduced pressure. The crude product was subjected to prepTLC (silica gel, EtOAc-Hexane, 1:1) to yield (±)-2'-methylsulfanyl-spiro[1-methylindoline-3,5'-[4',5']-dihydrooxazol]-2-thione [(±)-**206**, 3.4 mg, 81%).

Spectroscopic data for (±)-**206**

HPLC R_t = 16.8 min (broad peak).

^{1}H NMR (500 MHz, CD_3CN): δ 7.43 (dd, J = 7.5, 7.5 Hz, 1H), 7.40 (d, J = 7.5, 1H), 7.14 (dd, J = 8.0 Hz, 7.5 Hz, 1H) 6.98 (d, J = 8.0 Hz, 1H), 4.20 (d, J = 14.0 Hz, 1H), 4.07 (d, J = 14.0 Hz, 1H) 3.58 (s, 3H), 2.55 (s, 3H).

^{13}C NMR (125.8 MHz, CD_3CN): δ 203.6 (s), 164.4 (s), 145.3 (s), 132.1 (s), 131.4 (d), 125.4 (d), 124.8 (d), 110.9 (d), 91.8 (s), 68.5 (t), 31.5 (q), 14.5 (q).

HRMS-EI *m/z*: measured 264.0391 (M^+, calcd. 264.0391 for $C_{12}H_{12}N_2S_2O$).

MS-EI *m/z* (relative intensity): 264 (M^+, 58), 217 (81), 190 (35), 175 (100), 163 (34).

FTIR ν_{max}: 2926, 2854, 1741, 1620, 1466, 1375, 1146 cm^{-1}.

UV (CH_3CN) λ_{max} (log ε): 238 (4.2), 287 (3.8), 296 (3.8), 337 (4.0).

2-Chloro-1H-indole-3-carboxaldehyde (224*)*

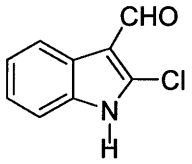

224

Phosphorus oxychloride ($POCl_3$) in $CHCl_3$ (50 mL) was added to a stirred mixture of oxindole (**223**, 3 g, 22.5 mmol), DMF (8 mL) and $CHCl_3$ (10 mL) at 0 °C, kept at room temperature for 15 hours, and then refluxed for 8 hours. The reaction mixture was poured into ice-cold water (125 mL). The $CHCl_3$ layer was washed with water (100 mL, 2×), the aqueous layers combined and allowed to stand overnight. The resulting precipitate was collected by filtration under suction, washed and dried. The crude product was crystallized from 95% ethanol to give 2-chloro-1H-indole-3-carboxaldehyde (**224**, 1.7 g, 42%).

Spectroscopic data for **224**

^1H NMR (500 MHz, CD_3OD): δ 9.93 (s, 1H), 8.05 (d, J = 7.5 Hz, 1H), 7.31 (d, J = 7.5, 1H), 7.20 (m, 2H).

^{13}C NMR (125.8 MHz, CD_3OD): δ 184.6 (d), 135.3 (s), 125.0 (s), 124.2 (d), 123.1 (d), 122.1 (s), 120.6 (d), 112.9 (s), 111.3 (d).

HRMS-EI *m/z*: measured 179.0138 (M^+, calcd. 179.0138 for C_9H_6NClO).

MS-EI *m/z* (relative intensity): 179 (M^+, 71), 178 (100), 150 (21), 123 (16).

FTIR ν_{max}: 3138, 3108, 2928, 2839, 1645, 1620, 1436, 1373, 735 cm^{-1}.

1-Acetyl-2-chloro-1H-indole-3-carboxaldehyde (225)

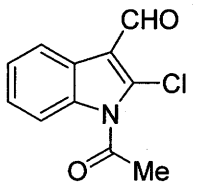

225

Sodium acetate (606 mg, 7.4 mmol) was added to a stirred solution of 2-chloro-1H-indole-3-carboxaldehyde (**224**, 500 mg, 2.79 mmol) in Ac_2O (10 mL). The reaction mixture was stirred for 45 min at room temperature and then another 45 min. at 110 °C. After cooling to room temperature, the reaction mixture was poured into ice-cold water (50 mL) and then extracted with EtOAc (50 mL, 2×). The organic layer was dried over Na_2SO_4 and after removal of solvent the crude product was subjected to FCC (silica gel, CH_2Cl_2) to give 1-acetyl-2-chloro-1H-indole-3-carboxaldehyde (**225**, 277 mg, 45%).

Spectroscopic data for **225**

HPLC R_t = 17.8 min.

^1H NMR (300 MHz, $CDCl_3$): δ 10.29 (s, 1H), 8.30 (dd, J = 7.5, 7.5 Hz, 1H), 8.24 (dd, J = 7.5, 7.5 Hz, 1H), 7.42 (m, 2H), 2.92 (s, 3H).

^{13}C NMR (125.8 MHz, $CDCl_3$): δ 185.8 (d), 169.8 (s), 136.0 (s), 133.5 (s), 127.0 (d), 126.0 (d), 124.9 (s), 121.3 (d), 118.2 (s), 116.0 (d), 28.5 (q).

HRMS-EI *m/z*: measured 221.0244 (M^+, calcd. 221.0244 for $C_{11}H_8NClO$).

MS-EI *m/z* (relative intensity): 221 (M^+, 26), 179 (100), 178 (86), 114 (10).

FTIR ν_{max}: 2924, 2853, 1732, 1668, 1527, 1441, 1368, 1268, 1134, 1012, 741 cm^{-1}.

1-Acetyl-2-chloro-1,2-dihydro-3H-indol-3-methylformate (226) and (±)-1-acetyl-2-chloro-1,2-dihydro-3H-indol-3-one [(±)-227]

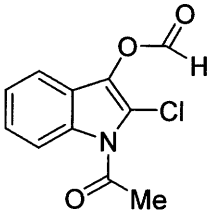

226

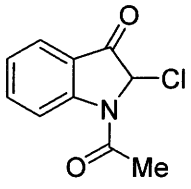

227

m-CPBA (213 mg, 1.36 mmol) was added to a solution of 1-acetyl-2-chloro-1H-indole-3-carboxaldehyde (**225**, 150 mg, 0.68 mmol) in CH_2Cl_2 (2 mL) at 5 °C and stirred for 15 hours. Dimethylsulphide (300 μL) was added followed by successive washings with saturated Na_2CO_3 (30 mL, 2×) and water (30 mL, 2×). The reaction mixture was then extracted with CH_2Cl_2 (50 mL, 2×), the organic layer was dried over anhydrous Na_2SO_4 and, after removal of solvent, the crude product was subjected to FCC (silica gel, Hexane-CH_2Cl_2, 50:50) to give 1-acetyl-2-chloro-1,2-dihydro-3H-indol-3-methyl formate (**226**, 49.4 mg, 31%) and (±)-1-acetyl-2-chloro-1,2-dihydro-3H-indol-3-one [(±)-**227**, 45.8 mg, 32%)].

Spectroscopic data for **226**

HPLC R_t = 18.9 min.

^{1}H NMR (500 MHz, $CDCl_3$): δ 8.43 (d, J = 8 Hz, 1H), 8.38 (s, 1H), 7.36 (m, 3H), 2.80 (s, 3H).

^{13}C NMR (125.8 MHz, $CDCl_3$): δ 169.6 (s), 157.7 (d), 138.6 (s), 134.0 (s), 131.5 (s), 126.8 (d), 125.7 (d), 122.2 (s), 117.2 (d), 27.8 (q).

HRMS-EI *m/z*: measured 237.0198 (M^+, calcd. 237.0198 for $C_{10}H_8NO_3Cl$).

MS-EI *m/z* (relative intensity): 237 (M^+, 23), 195 (25), 166 (100), 132 (21), 102 (20).

FTIR ν_{max}: 3056, 3016, 2961, 1749, 1717, 1603, 1445, 1336, 1288, 1067, 745 cm^{-1}.

UV (CH_3CN) λ_{max}, (log ε): 236 (4.2), 268 (4.0), 290 (3.7), 300 (3.6).

Spectroscopic data for (±)-**227**

HPLC R_t = 13.8 min.

^{1}H NMR (300 MHz, $CDCl_3$): δ 8.43 (br s, 1H), 7.79 (d, J = 7.5, 1H), 7.70 (dd, J = 7.5, 7.5 Hz, 1H), 7.26 (m, 1H) 5.79 (s, 1H), 2.52 (s, 3H).

^{13}C NMR (75.5 MHz, $CDCl_3$): δ 190.7 (s), 168.7(s), 152.1 (d), 138.5 (s), 125.5 (d), 121.6 (s), 118.9 (d), 68.3 (d), 24.2 (q).

HRMS-EI *m/z*: measured 209.0244 (M^+, calcd. 209.0244 for $C_{10}H_8NO_2Cl$).

MS-EI *m/z* (relative intensity): 209 (M^+, 23), 169 (23), 167 (72), 132 (100).

FTIR ν_{max}: 3127, 3019, 1734, 1679, 1591, 1463, 1347, 1272, 1150, 1004, 758 cm^{-1}.

UV (CH_3CN) λ_{max}, (log ε): 235 (4.3), 262 (3.7), 347 (2.2).

(±)-1-Acetyl-1,2-dihydro-2-nitromethyl-3H-indol-3-one [(±)-228]

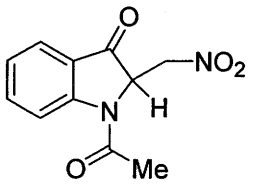

228

Et_2NH (50 μL) was added to 1-acetyl-2-chloro-1,2-dihydro-3H-indol-3-methyl formate (**226**, 14.5 mg, 0.061 mmol) dissolved in nitromethane (1 mL, 18.4 mmol) and the mixture stirred for 1 hour. The solvent was removed under reduced pressure and the crude product was subjected to prepTLC (silica gel, CH_2Cl_2-MeOH, 98:2) to give (±) 1-acetyl-1,2-dihydro-2-nitromethyl-3H-indol-3-one [(±)-**228**, 6.2 mg, 43%)].

Spectroscopic data for (±)-**228**

HPLC R_t = 9.5 min.

^{1}H NMR (500 MHz, CD_3CN): δ 7.74 – 7.78 (m, 3H), 7.30 (dd, J = 8, 8 Hz, 1H), 4.63 (m 1H), 4.54 (m, 1H) 3.73 (br s, 1H), 2.56 (m, 1H), 2.40 (s, 3H).

^{13}C NMR (125.8 MHz, CD_3CN): δ 198.5 (s), 169.4 (s), 154.0 (s), 137.8 (d), 124.5 (2×, d), 124.1 (d), 123.0 (s), 62.7 (d), 28.8 (t) 25.0 (q).

FTIR ν_{max}: 2921, 2850, 1716, 1678, 1608, 1552, 1463, 1378, 1276, 763 cm^{-1}.

UV (CH_3CN) λ_{max}, (log ε): 236 (4.5), 256 (4.0), 344 (3.6).

(±)-1-Acetyl-1,2-dihydro-2-diethylaminoindol-3-one [(±)-(229)]

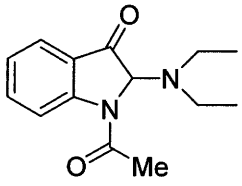

229

(±)-1-Acetyl-2-chloro-1,2-dihydro-3H-indol-3-one [(±)-**227**, 10 mg, 0.048 mmol] was dissolved in nitromethane (1 mL, 18.4 mmol) and treated with Et_2NH (50 μL. 0.48 mmol) and stirred for 1 hour. The solvent was removed under reduced pressure, and the crude product was subjected to prepTLC (silica gel, CH_2Cl_2-MeOH 98:2) to give (±)-1-acetyl-1,2-dihydro-2-nitromethylindol-3-one [(±)-**228**, 1.2 mg, 11%] and (±)-1-acetyl-1,2-dihydro-2-diethylaminoindol-3-one [(±)-**229**, 3.5 mg, 30%].

Spectroscopic data for (±)-**229**

HPLC R_t = 20.8 min.

^{1}H NMR (500 MHz, CD_3CN): δ 8.88 (d, *J* = 8.5 Hz, 1H), 7.71 (dd, *J* = 8.5, 8.5 Hz, 1H), 7.64 (dd, *J* = 7.5, 7.5 Hz, 1H), 7.23 (dd, *J* = 7.5, 7.5 Hz, 1H), 4.95 (s, 1H) 2.81 (m, 1H), 2.69 (m, 1H), 2.42 (s, 3H), 1.08 (t, *J* = 7 Hz, 6H).

^{13}C NMR (125.8 MHz, CD_3CN): δ 200.3 (s), 170.9(s), 154.0 (s), 137.8 (d), 124.2 (d), 123.7 (s), 123.0 (d), 78.9 (d), 43.2 (2×, t), 23.8 (q), 13.6 (2×, q).

HRMS-EI *m/z*: measured 246.1367 (M^+, calcd. 246.1368 for $C_{14}H_{18}N_2O_2$).

MS-EI *m/z* (relative intensity): 246 (M^+, 1), 179 (23), 163 (11), 162 (100), 137 (45), 120 (42), 119 (74).

FTIR ν_{max}: 2952, 2919, 2850, 1707, 1656, 1460, 1212, 750 cm^{-1}.

UV (CH_3CN) λ_{max}, (log ε): 237 (4.5), 259 (4.0), 343 (3.5).

Et_3N (50 μL. 0.48 mmol) was added to (±)-1-acetyl-2-chloro-1,2-dihydro-3H-indol-3-one [(±)-**227**, 10 mg, 0.048 mmol)] dissolved in nitromethane (1 mL, 18.4 mmol) and stirred for 1 hour. The solvent was removed under reduced pressure, and the crude product was subjected to prepTLC (silica gel, CH_2Cl_2-MeOH 98:2) to give (±)-1-acetyl-1,2-dihydro-2-nitromethylindol-3-one [(±)-**228**, 2 mg, 18%].

4.4.3 Antifungal Activity

The antifungal activity of 1-methoxyspirobrassinin (**176**), arvelexin (**179**) and erucalexin (**204**) was determined using the following mycelia radial growth bioassay. Solutions of each compound in DMSO (5×10^{-2} M) were used to prepare assay solutions in minimal media (5×10^{-4} M, 2.5×10^{-4} M, 5×10^{-5} M) in serial dilution; control solutions contained 1% DMSO in minimal media. Sterile tissue culture plates (12-well, 24 mm diameter) containing test solutions and control solution (1 mL per well) were inoculated with mycelia plugs placed upside down on the centre of each plate (5 mm cut from 3-day old and 7 day-old PDA plates of *S. sclerotiorum* clone # 33 and *Rhizoctonia solani* AG 2-1 respectively) and incubated under flourescent light for 7 days. Three independent experiments were carried out each one in triplicate.

4.4 Synthesis of phytoalexins and analogues

4.4.1 Synthesis of brassinin and analogues

4.4.1.1 Synthesis of brassinin

Indolyl-3-methanaloxime (232)

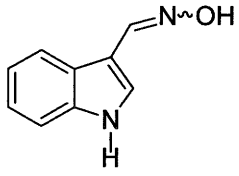

232

An aqueous solution (10 mL) of $NH_2OH.HCl$ (1.07 g, 15.8 mmol) and Na_2CO_3 (0.76 g) was added to a solution of indolyl-3-carboxyaldehyde (**184**, 100 mg, 0.689 mmol) in EtOH (15 mL). After stirring at 60 °C for 30 min, the EtOH was removed under reduced pressure. The residue was diluted with water (15 mL) and extracted with Et_2O (20 mL, 3×). The organic layer was dried over anhydrous Na_2SO_4 and the solvent removed under reduced pressure to give indolyl-3-methanaloxime (**232**, 108 mg, 89 %).

Indolyl-3-methanamine (187)

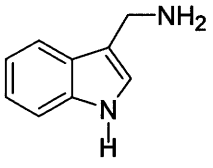

187

Indolyl-3-methanaloxime (**232**, 107 mg, 0.67 mmol) was dissolved in MeOH (10 mL); NaOH (5 mL, 5 M) and Devarda's alloy (5 g) were added and stirred for 20 min at room temperature. The reaction mixture was filtered, extracted with Et_2O (30 mL, 3×), the organic layer dried over anhydrous Na_2SO_4 and the solvent removed under reduced pressure. The crude product was subjected to FCC (silica gel, $CHCl_3$-MeOH-28% aqueous NH_3, 80:20:1) to give indole-3-methanamine (**187**, 71 mg, 66 %).

Indolyl-3-methanamine from gramine (231)

MeI (250 μL, 4.01 mmol) was added to a solution of gramine (**231**, 100 mg, 0.574 mmol) in anhydrous THF (2 mL) and the solution stirred at room temperature for 1 hour. The THF was removed under reduced pressure, NH_3 (28% aqueous solution, 12 mL) was added to the residue and the reaction mixture stirred at room temperature for 2 hours. Brine (12 mL) was added to the reaction mixture followed by extraction with CH_2Cl_2-MeOH (95:5 mixture, 20 mL, 3×). The extract was washed with brine (90 mL), dried over anhydrous Na_2SO_4 and the solvent removed under reduced pressure to obtain the crude product. Separation by FCC (silica gel, $CHCl_3$-MeOH-28% aqueous NH_3, 80:20:1) gave indole-3-methanamine (**187**, 47 mg, 46 %).

Brassinin (149)

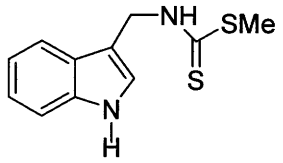

149

Et_3N (80 μL) was added to a solution of indolyl-3-methanamine (**187**, 100 mg, 0.685 mmol) in pyridine (3 mL), the solution cooled to 0 °C, and CS_2 (56 μL, 0.092 mmol)

was added. After 1 hour, MeI (70 μL, 0.112 mmol) was added and the reaction mixture kept at 5 °C for 20 hours. After addition of H_2SO_4 (1.5 M, 40 mL), the mixture was extracted with Et_2O (50 mL, 2×), the organic layer dried over anhydrous Na_2SO_4 and the solvent removed under reduced pressure to obtain the crude product. Separation by FCC (silica gel, CH_2Cl_2 - Hexane, 85:15) gave brassinin (**149**, 75.8 mg, 54 %).

Spectroscopic data for **149**

HPLC R_t = 18.3 min.

^{1}H NMR (300 MHz, $CDCl_3$) δ 8.18 (br s, 1H, D_2O exchangeable), 7.63 (d, J = 8 Hz, 1H), 7.63 (d, J = 8 Hz, 1H), 7.26 (ddd, J = 8, 8, 1 Hz, 1H), 7.23 (ddd, J = 8, 8, 1 Hz, 1H), 7.15 (br s, D_2O exchangeable, 1H), 5.05 (d, J = 3.5 Hz, 2H), 2.64 (s, 3H) and minor signals (ca. 1/4 intensity of the major peaks) due to rotamers at 4.77 (d) and 2.75 (s).

^{13}C NMR (75.5 MHz, $CDCl_3$): δ 198.2 (s), 136.3 (s), 126.5 (s), 123.9 (d), 122.9 (d), 120.4 (d), 118.7 (d), 111.5 (s), 110.9 (d), 43.2 (t), 18.15 (q) and minor signals (ca. 1/8 intensity of the major peaks) due to rotamers at 42.1 (t) and 19.1 (q).

HRMS-EI *m/z*: measured 236.0444 (M^+, calcd. 236.0442 for $C_{11}H_{12}N_2S_2$).

MS-EI *m/z* (relative intensity): 236 (43), 162 (11), 130 (100), 129 (44), 102 (18).

FTIR ν_{max}: 3398, 3308, 3055, 2993, 2914, 2858, 1617, 1554, 1487, 1455, 1338, 745 cm^{-1}.

UV (CH_3CN) λ_{max} (log ε): 219 (4.2), 271 (3.7).

4.4.1.2 Synthesis of methyl tryptamine dithiocarbamate (199)

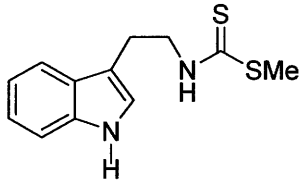

199

Et_3N (230 μL) and CS_2 (100 μL, 1.67 mmol) were added to a cooled solution of tryptamine (**201**, 200 mg, 1.25 mmol) in pyridine (1.5 mL). The mixture was kept at 0 °C with constant stirring for 1 hour. MeI (100 μL, 1.61 mmol) was then added and the reaction mixture kept at 5 °C for 15 hours. The mixture was then poured into H_2SO_4 (1.5 M, 25 mL), extracted with Et_2O (30 mL, 3×), washed with saturated Na_2CO_3 (100 mL) and water (100 mL) and dried over anhydrous Na_2SO_4. After the removal of solvent the crude product was recrystallized from $CHCl_3$-Hexane (1:1) to give methyl tryptamine dithiocarbamate (**199**, 290 mg, 93 %).

Spectroscopic data for **199**

HPLC R_t = 20.6 min.

^{1}H NMR (300 MHz, $CDCl_3$): δ 8.08 (br s, D_2O exchangeable, 1H), 7.63 (d, J = 8 Hz, 1H), 7.38 (d, J = 8 Hz, 1H), 7.23 (ddd, J = 8, 8, 1 Hz, 1H), 7.18 (ddd, J = 8, 8, 1 Hz, 1H), 7.02 (s, 1H), 7.01 (br s, 1H D_2O exchangeable), 4.08 (m, 2H), 3.09 (m, 2H), 2.58 (s, 3H), and minor signals (ca. 1/4 intensity of the major peaks) due to rotamers at 3.76 (m) and 2.67 (s).

^{13}C NMR (75.5 MHz, $CDCl_3$) δ 198.9 (s), 136.5 (s), 127.2 (s), 122.5 (d), 122.2 (d), 119.8 (d), 118.8 (d), 112.4 (s), 111.4 (d), 47.3 (t), 24.1 (t), 18.1 (q) and minor signals (ca. 1/4 intensity of the major peaks) due to rotamers at 201.0 (s), 46.2 (t), 24.6 (t) and 18.9 (q).

HRMS-EI *m/z*: measured 250.0597 (M^+, calcd. 250.0598 for $C_{12}H_{14}N_2S_2$).

MS-EI *m/z* (relative intensity): 250 (M^+, 5), 202 (65), 143 (32), 130 (100), 77 (17).

FTIR ν_{max}: 3410, 3333, 3053, 2916, 2848, 1501, 1455, 1338, 1091, 936, 745 cm^{-1}.

UV (CH_3CN) λ_{max} (log ε): 221 (4.2), 273 (3.7).

4.4.1.3 Synthesis of methyl 1-methyltryptamine dithiocarbamate (239)

N_b-Acetyl-indolyl-3-ethylamine (254)

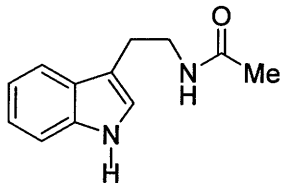

254

Tryptamine (**201**, 400 mg, 1.25 mmol) was dissolved in pyridine/acetic anhydride (0.4 mL/0.8 mL) at room temperature. After stirring for 30 min the mixture was diluted with CH_2Cl_2 and washed with a saturated solution of Na_2CO_3 (100 mL) and then water (100 mL), dried over anhydrous Na_2SO_4 and the solvent removed under reduced pressure to give N_b-acetyl-indolyl-3-ethylamine (**254**, quantitative conversion).

Spectroscopic data for **254**

^{1}H NMR (300 MHz, $CDCl_3$): δ 8.54 (br s, 1H, D_2O exchangeable), 7.59 (d, J = 7.5 Hz, 1H), 7.37 (d, J = 8 Hz, 1H), 7.23 (m, 1H), 7.12 (m, 1H), 5.72 (br s, 1H, D_2O exchangeable), 3.61 (m, 2H), 2.95 (m, 2H), 1.91 (s, 3H).

^{13}C NMR (75.5 MHz, $CDCl_3$): δ 170.6 (s), 136.7 (s), 127.6 (d), 122.4 (d), 122.3 (d), 119.6 (s), 118.6 (d), 113.0 (s), 111.6 (d), 40.1 (t), 25.5 (t), 23.6 (q).

HRMS-EI *m/z*: measured 202.1108 (M^+, calcd. 202.1108 for $C_{12}H_{14}N_2O$).

MS-EI *m/z* (relative intensity): 202 (M^+, 18), 143 (100), 130 (97), 77 (10).

N_b-Acetyl-1-methylindolyl-3-ethylamine (255)

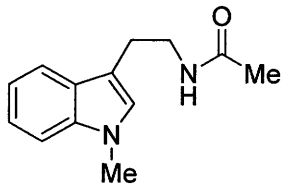

255

Sodium hydride (48.07 mg, 2.03 mmol) and MeI (287.07 mg, 2.03 mmol) were added to a cooled solution of N_b-acetyl-indolyl-3-ethylamine (**254**, 300 mg, 1.49 mmol) in anhydrous THF under argon atmosphere at 0 °C and stirred for 2 hours. The reaction mixture was poured into ice-cold water (50 mL) and then extracted with CH_2Cl_2 (50 mL, 2×), dried over anhydrous Na_2SO_4 and the solvent removed under reduced pressure to obtain the crude product. Separation by FCC (silica gel, CH_2Cl_2 - MeOH, 95:5) gave N_b-acetyl-1-methylindolyl-3-ethylamine (**255**, 304 mg, 95%).

Spectroscopic data for **255**

^{1}H NMR (300 MHz, $CDCl_3$): δ 7.61 (d, J = 8 Hz, 1H), 7.30 (d, J = 8 Hz, 1H), 7.26 (m, 2H), 6.11 (br s, 1H, D_2O exchangeable), 3.72 (s, 3H) 3.58 (m, 2H), 2.98 (m, 2H), 1.92 (s, 3H).

^{13}C NMR (75.5 MHz, $CDCl_3$): δ 170.5 (s), 137.4 (s), 128.1 (d), 127.0 (d), 121.9 (d), 119.1 (s), 111.8 (s), 109.6 (d), 40.3 (t), 39.8 (t), 32.9 (q), 25.5 (t), 23.5 (q).

HRMS-EI *m/z*: measured 216.1262 (M^+, calcd. 216.1263 for $C_{13}H_{16}N_2O$).

MS-EI *m/z* (relative intensity): 216 (M^+, 21), 157 (71), 145 (11), 144 (100).

1-Methylindolyl-3-ethylamine (256)

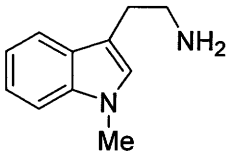

256

N_b-acetyl-1-methylindolyl-3-ethylamine (**255**, 300 mg, 1.38 mmol) was dissolved in 15% methanolic aqueous solution of NaOH (10 mL). The mixture was refluxed at 95 °C for 6 hours. The solvent was removed under reduced pressure, the residue taken in water (50 mL) and then extracted with CH_2Cl_2-MeOH (95:5, 50 mL, 2×) dried over anhydrous Na_2SO_4 and the solvent removed under reduced pressure. The crude product was used in the next step without purification.

Methyl 1-methyltryptamine dithiocarbamate (239)

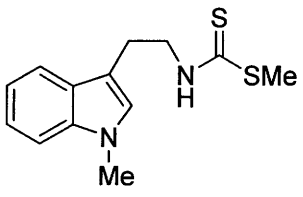

239

Triethylamine (139.5 mg, 1.38 mmol) and CS_2 (104.9 mg, 1.38 mmol) were added to a solution of 1-methylindolyl-3-ethylamine (**256**, 240 mg, 1.38 mmol) in pyridine (0.8 mL) at 0 °C. After stirring for 2 hours, MeI (219.2 mg, 1.55 mmol) was added and the mixture kept at 5 °C for 15 hours. After addition of H_2SO_4 (1.5 M, 40 mL), the mixture was extracted with EtOAc, dried over anhydrous Na_2SO_4 and the solvent removed under

reduced pressure to obtain the crude product. Separation by FCC (silica gel, CH_2Cl_2-MeOH, 95:5) yielded methyl 1-methyltryptamine dithiocarbamate (**239**, 299 mg, 82%).

Spectroscopic data for **239**

HPLC R_t = 24.5 min.

^{1}H NMR (300 MHz, $CDCl_3$) δ 7.60 (d, J = 7.96 Hz, 1H), 7.33 (d, J = 8 Hz, 1H), 7.26 (m, 1H), 7.14 (m, 1H), 7.06 (s, 1H), 6.92 (br s, 1H, D_2O exchangeable), 4.06 (m, 2H), 3.77 (s, 3H), 3.12 (m, 2H), 2.59 (s, 3H) and minor signal (ca. 1/4 intensity of the major peak) due to rotamer at 2.69 (s).

^{13}C NMR (75.5 MHz, $CDCl_3$) δ 199.7 (s), 137.4 (s), 127.9 (s), 127.5 (d), 122.2 (d), 119.4 (d), 119.1 (s), 110.9 (d), 109.6 (d), 47.7 (t), 32.9 (q), 24.2 (t), 18.3 (q) and minor signals (ca. 1/4 intensity of the major peaks) due to rotamers at 201.8 (s), 46.6 (t), 24.8 (t) and 18.4 (q).

HRMS-EI *m/z*: measured 264.0760 (M^+, calcd. 264.0755 for $C_{13}H_{14}N_2S_2$).

MS-EI *m/z* (relative intensity): 264 (M^+, 12), 216 (18), 157 (38), 144 (100).

FTIR ν_{max}: 3326, 3238, 2920, 2852, 1483, 1376, 1327, 1251, 1091, 946, 741 cm^{-1}.

UV (CH_3CN) λ_{max} (log ε): 225 (4.3), 273 (3.8).

4.4.1.4 Synthesis of methyl 1-methoxytryptamine dithiocarbamate (257)

N_b-Acetyl -2,3-dihydroindolyl -3-ethylamine

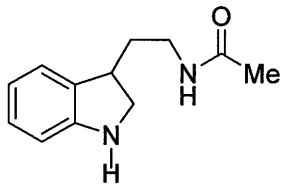

257

N_b-Acetyl-indolyl-3-ethylamine (**254**, 200 mg, 0.99 mmol) was dissolved in glacial acetic acid (4 mL) and stirred at room temperature. After 20 min $NaBH_3CN$ (93.4 mg, 1.51 mmol) was added in portions and stirring was continued under argon atmosphere for 3 hours. The reaction mixture was poured into water (50 mL), basified with 20% aqueous solution of NaOH (pH 11), extracted with Et_2O, dried over anhydrous Na_2SO_4 and the solvent removed under reduced pressure to obtain the crude product. Separation by FCC (silica gel, CH_2Cl_2-MeOH, 98:2) yielded N_b-acetyl-2,3-dihydroindolyl-3-ethylamine (**257**, 180 mg, 87 %).

Spectroscopic data for **257**

^{1}H NMR (300 MHz, $CDCl_3$): δ 6.95 - 7.01 (m, 2H), 6.72 (m, 1H), 6.66 (d, J = 8 Hz, 1H), 6.00 (br s, 1H D_2O exchangeable), 3.82 (br s, 1H D_2O exchangeable), 3.67 (t, J = 8.5 Hz, 1H), 3.15 – 3.65 (m, 4H), 1.90 – 2.02 (m, 1H), 1.94 (s, 3H), 1.73 (m, 1H).

^{13}C NMR (75.5 MHz, $CDCl_3$): δ 170.2 (s), 150.9 (s), 127.8 (d), 123.9 (d), 122.1 (d), 119.1 (d), 109.9 (d), 53.0 (t), 39.8 (t), 37.5 (d), 34.1 (t), 23.2 (q).

HRMS-EI *m/z*: measured 204.1262 (M^+, calcd. 204.1263 for $C_{12}H_{16}N_2O$).

MS-EI *m/z* (relative intensity): 204 (M^+, 56), 144 (31), 132 (38), 130 (30), 119 (25), 118 (100), 117 (38).

N_b-Acetyl-1-methoxyindolyl-3-ethylamine (258)

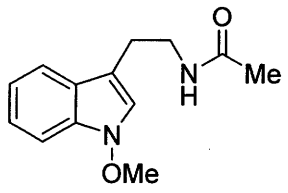

258

$Na_2WO_4.2H_2O$ (33.4 mg, 0.1 mmol) was added with stirring followed by 30% H_2O_2 (166.6 mg, 5 mmol) in portions to a solution of N_b-acetyl-2,3-dihydroindolyl-3-ethylamine (**257**, 100 mg, 0.49 mmol) in MeOH-H_2O (10:1, 4 mL). After 30 min of stirring at room temperature, the mixture was treated with a large excess of ethereal diazomethane and kept at 0 °C for 1 hour. The solvent was removed under reduced pressure, the residue dissolved in Et_2O, washed with brine, dried over anhydrous Na_2SO_4 and the solvent removed under reduced pressure to obtain the crude product. Separation by FCC (silica gel, CH_2Cl_2-MeOH, 95:5) yielded N_b-acetyl 1-methoxyindolyl-3-ethylamine (**258**, 42.2 mg, 37%).

Spectroscopic data for **258**

^{1}H NMR (300 MHz, $CDCl_3$): δ 8.22 (d, J = 8 Hz, 1H), 8.00 (d, J = 8 Hz, 1H), 7.82 (s, 1H), 7.80 (m, 1H), 7.70 (m, 1H), 5.56 (br s, 1H D_2O exchangeable), 4.06 (s, 3H), 3.54 (m, 2H), 2.95 (m, 2H), 1.97 (s, 3H).

^{13}C NMR (75.5 MHz, $CDCl_3$): δ 173.4 (s), 134.2 (s), 125.5 (d), 123.5 (d), 122.5 (d), 120.7 (d), 120.0 (s), 110.6 (s), 109.3 (d), 66.1 (q), 41.4 (t), 26.1 (t), 25.0 (q).

HRMS-EI *m/z*: measured 232.1208 (M^+, calcd. 232.1212 for $C_{13}H_{16}N_2O_2$).

MS-EI *m/z* (relative intensity): 232 (M^+, 38), 173 (100), 160 (80), 130 (30), 129 (31).

FTIR ν_{max}: 3294, 3070, 2920, 2935, 1722, 1649, 1550, 1478, 750 cm^{-1}.

UV (CH_3CN) λ_{max} (log ε): 253 (4.3), 319 (3.4)

1-Methoxytryptamine (259)

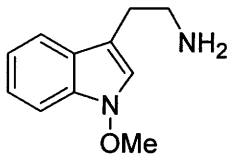

259

N_b-Acetyl 1-methoxyindolyl-3-ethylamine (**259**, 80 mg, 0.345 mmol) was dissolved in 15% methanolic aqueous solution of NaOH (10 mL). The mixture was refluxed at 95 °C for 6 hours. The solvent was removed under reduced pressure, the residue dissolved in water (50 mL) and then extracted with CH_2Cl_2-MeOH (95:5, 50 mL, 2×), dried over anhydrous Na_2SO_4 and the solvent removed under reduced pressure to give the crude product. This was used in the next step without further purification.

Methyl 1-methoxytryptamine dithiocarbamate (240)

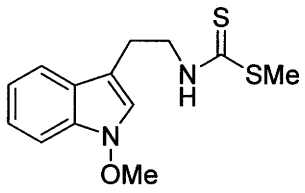

240

Triethylamine (25.07 mg, 0.248 mmol) and CS_2 (18.85 mg, 0.248 mmol) were added to a solution of 1- methoxytryptamine (**259**, 47.2 mg, 0.248 mmol) in pyridine (0.8 mL) at 0 °C. After 2 hours, MeI (39.39 mg, 0.279 mmol) was added and the mixture kept

at 5 °C for 15 hours. After addition of H_2SO_4 (1.5 M, 40 mL) the reaction mixture was extracted with EtOAc, dried over anhydrous Na_2SO_4 and the solvent removed under reduced pressure to obtain the crude product. Separation by FCC (silica gel, CH_2Cl_2-MeOH, 95:5) yielded methyl 1-methoxytryptamine dithiocarbamate (**240,** 54.2 mg, 78 %).

Spectroscopic data for **240**

HPLC R_t = 25.2 min.

^{1}H NMR (300 MHz, $CDCl_3$): δ 7.83 (br s, 1H D_2O exchangeable), 7.49 (d, J = 8 Hz, 1H), 7.42 (d, J = 8 Hz, 1H), 7.32 (m, 1H), 7.18 (m, 2H), 4.07 (s, 3H), 3.09 (m, 2H), 2.96 (m, 2H), 2.71 (s, 3H) and minor signals (ca. 1/4 intensity of the major peaks) due to rotamers at 3.74 (m) and 2.69 (s).

^{13}C NMR (75.5 MHz, $CDCl_3$): δ 199.4 (s), 136.6 (s), 126.7 (s), 123.0 (d), 122.4 (d), 121.5 (d), 119.2 (s), 111.2 (d), 108.7 (d), 66.0 (q), 47.5 (t), 24.1 (t), 18.3 (q) and minor signals (ca. 1/4 intensity of the major peaks) due to rotamers at 201.2 (s), 24.1 (t) and 18.4 (q).

HRMS-EI *m/z* measured 280.0701 (M^+, calcd. 280.0704 for $C_{13}H_{16}N_2OS_2$).

MS-EI *m/z* (relative intensity): 280 (M^+, 13), 262 (13), 249 (50), 232 (15), 173 (100), 160 (77), 142 (39), 130 (32), 115 (22), 91 (20).

FTIR ν_{max}: 3395, 3323, 3053, 2916, 2846, 1451, 1418, 1253, 1006, 944, 742 cm^{-1}.

UV (CH_3CN) λ_{max} (log ε): 223 (4.3), 276 (3.7)

4.4.1.5 Synthesis of methyl1H- indolyl-3-propanoate (246)

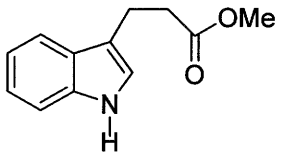

246

Indolyl-3-propanoic acid (**260**, 200 mg, 1.06 mmol) was dissolved in methanolic HCl (1 M HCl in methanol, 4 mL), and the mixture refluxed at 70 °C for 1.5 hours. The solvent was removed under reduced pressure, the residue dissolved in CH_2Cl_2 (20 mL), washed successively with saturated aqueous Na_2CO_3 (20 mL) and water (20 mL), dried over anhydrous Na_2SO_4 and the solvent removed under reduced pressure to obtain the crude product. Separation by FCC (silica gel, CH_2Cl_2-MeOH, 95:5) yielded methyl-1H indolyl-3- propanoate (**246**, 240 mg, 98 %)

Spectroscopic data for **260**

HPLC R_t = 16.2 min.

^{1}H NMR (300 MHz, $CDCl_3$): δ 8.11 (br s, 1H D_2O exchangeable), 7.66 (d, J = 8 Hz, 1H), 7.35 (d, J = 8 Hz, 1H), 7.15-7.27 (m, 2H), 6.98 (s, 1H), 3.73 (s, 3H), 3.17 (m, 2H), 2.78 (m, 2H).

^{13}C NMR (75.5 MHz, $CDCl_3$): δ 174.1 (s), 136.4 (d), 127.3 (s), 122.1 (d), 121.6 (d), 119.4 (d), 118.7 (d), 114.9 (s), 111.3 (d), 51.7 (q), 34.9 (t), 20.7 (t).

HRMS-EI *m/z*: measured 203.0946 (M^+, calcd. 203.0946 for $C_{12}H_{13}NO_2$).

MS-EI *m/z* (relative intensity): 203 (35), 130 (100).

FTIR ν_{max}: 3407, 3054, 2949, 2853, 1732, 1619, 1456, 1206, 1069, 745 cm^{-1}.

4.4.1.6 Synthesis of methyl 1-methyl-3-indolyl propanoate (247)

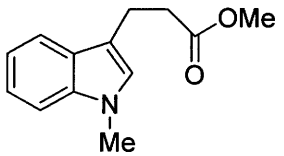

247

Sodium hydride (47.3 mg, 1.97 mmol) and MeI (184 μL, 1.97 mmol) were added to a stirred solution of methyl-3-indolyl propanoate (**246**, 200 mg, 0.985 mmol) in anhydrous THF (20 mL) under argon atmosphere at 0 °C. After stirring for 2.5 hours the reaction mixture was poured into ice - cold water (50 mL), extracted with CH_2Cl_2 (50 mL, 2×), dried over anhydrous Na_2SO_4 and the solvent removed under reduced pressure to obtain the crude product. Separation by FCC (silica gel, CH_2Cl_2) gave methyl 1-methyl-3-indolyl propanoate (**247**, 172 mg, 82 %).

Spectroscopic data for **247**

HPLC R_t = 21.1 min.

^{1}H NMR (300 MHz, $CDCl_3$): δ 7.67 (d, J = 8 Hz, 1H), 7.17 - 7.35 (m, 3H), 6.90 (s, 1H), 3.74 (s, 3H), 3.73 (s, 3H), 3.17 (m, 2H), 2.78 (m, 2H).

^{13}C NMR (75.5 MHz, $CDCl_3$): δ 173.9 (s), 137.1 (d), 127.7 (s), 126.4 (d), 121.7 (d), 118.9 (s), 113.5 (s), 109.3 (d), 51.6 (q), 35.1 (t), 32.6 (q), 20.7 (t).

HRMS-EI *m/z*: measured 217.1106 (M^+, calcd. 217.1103 for $C_{13}H_{15}NO_2$).

MS-EI *m/z* (relative intensity): 217 (33), 145 (11), 144 (100).

FTIR ν_{max}: 2948, 2825, 1735, 1614, 1482, 1326, 1163, 1012, 739 cm^{-1}.

4.4.1.7 Synthesis of 6-fluoro-Nb-acetylindolyl-3-ethylamine (252)

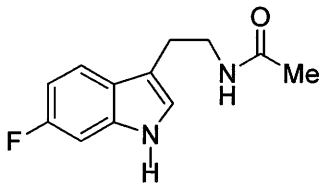

252

6-Fluorotryptamine (**262**, 400 mg, 1.25 mmol) was dissolved in pyridine/acetic anhydride (0.4 mL / 0.8 mL) at room temperature. After 30 min of stirring the mixture was diluted with CH_2Cl_2, washed successively with a saturated aqueous solution of Na_2CO_3 (100 mL) and water (100 mL), dried over anhydrous Na_2SO_4 and the solvent removed under reduced pressure to yield 6-fluoro-N_b-acetyl-indolyl-3-ethylamine (**252**, quantitative conversion).

Spectroscopic data for **252**

HPLC R_t = 8.5 min.

^{1}H NMR (300 MHz, $CDCl_3$): δ 8.43 (br s, 1H D_2O exchangeable), 7.56 (d, J = 8 Hz, 1H), 7.36 (d, J = 8 Hz, 1H), 7.21 (m, 1H), 7.09 (m, 1H), 6.99 (br s, 1H D_2O exchangeable), 5.80 (br s, 1H D_2O exchangeable), 3.55 (m, 2H), 2.97 (m, 2H), 1.9 (s, 3H).

^{13}C NMR (75.5 MHz, $CDCl_3$): δ 170.5 (s), 160.1 (d, $J_{C\text{-}F}$ = 240 Hz), 136.7 (d), 124.2 (s), 122.5 (s), 119.5 (d, $^3J_{C\text{-}F}$ = 10 Hz), 113.2 (s), 108.4 (d, $^2J_{C\text{-}F}$ = 25 Hz), 97.8 (d, $^2J_{C\text{-}F}$ = 26 Hz), 40.1 (q), 25.5 (t), 23.6 (t).

HRMS-EI *m/z*: measured 220.1011 (M^+, calcd. 220.1012 for $C_{12}H_{13}NOF$).

MS-EI *m/z*: (relative intensity): 220 (M^+, 18), 161 (100), 148 (80).

FTIR ν_{max}: 3414, 3280, 2924, 2935, 1649, 1554, 1456, 1141, 802 cm^{-1}.

UV (CH_3CN) λ_{max} (log ε): 220 (4.4), 283 (3.7).

4.4.1.8 Synthesis of 6-fluoro-Nb-acetyl-1-methylindolyl-3-ethylamine (253)

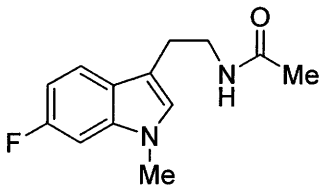

253

Sodium hydride (48.1 mg, 2.03 mmol) and MeI (287 mg, 2.03 mmol) were added to a stirred solution of 6-fluoro-N_b-acetyl-indolyl-3-ethylamine (**252**, 300 mg, 1.49 mmol) in anhydrous THF (20 mL) at 0 °C under argon atmosphere. After stirring for 2 hours, the reaction mixture was poured into ice - cold water (100 mL), extracted with CH_2Cl_2 (100 mL 2×), dried over anhydrous Na_2SO_4 and the solvent removed under reduced pressure to obtain the crude product. Separation by FCC (silica gel, CH_2Cl_2 - MeOH, 95:5) yielded 6-fluoro-N_b-acetyl-1-methylindolyl-3-ethylamine (**253**, 304 mg, 95%).

Spectroscopic data for **253**

HPLC R_t = 12.1 min.

^{1}H NMR (300 MHz, $CDCl_3$): δ 7.58 (d, J = 8 Hz, 1H), 7.28 (d, J = 8 Hz, 1H), 7.26 (m, 1H), 7.24 (m, 1H), 6.88 (br s, 1H D_2O exchangeable), 5.87 (br s, 1H D_2O exchangeable), 3.75 (s, 3H) 3.58 (m, 2H), 2.97 (m, 2H), 1.92 (s, 3H).

HRMS-EI *m/z*: measured 234.1168 (M^+, calcd. 234.1168 for $C_{13}H_{15}NOF$).

MS-EI *m/z* (relative intensity): 234 (M^+, 21), 175 (81), 176 (11), 162 (100).

FTIR ν_{max}: 3060, 2931, 1639, 1555, 1479, 1406, 1334, 1241, 1104, 917, 800 cm^{-1}.

UV (CH_3CN) λ_{max} (log ε): 224 (4.4), 287 (3.7).

4.4.2 Synthesis of camalexin (170), 6-methoxycamalexin (171) and analogues

4.4.2.1 Synthesis of camalexin (170)

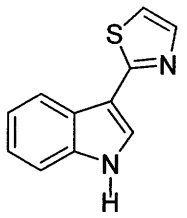

170

A solution of MeI (85 μL, 1.36 mmol) in dry Et_2O (2 mL) was added slowly by injection at room temperature under argon atmosphere to magnesium turnings (32.8 mg, 1.36 mmol) in dry Et_2O (3 mL). After all the magnesium had reacted, the Et_2O was distilled off and dry benzene (5 mL) was added. A solution of indole (**182**, 150 mg, 1.28 mmol) in benzene (3 mL) was added to the solution of methyl magnesium iodide in benzene and stirred for 10 min after which 2-bromothiazole (61 μL, 0.674 mmol) was added. The reaction mixture was refluxed under argon for 48 hours, cooled to room temperature, poured into saturated solution of NH_4Cl (50 mL) and then extracted with EtOAc (50 mL, 2×). The extract was washed with brine (50 mL), dried over anhydrous Na_2SO_4 and the solvent removed under reduced pressure to obtain the crude product (dark brown oil, 163 mg). Separation by FCC (silica gel, EtOAc-Hexane, 1:3) yielded camalexin (**170**, 148 mg, 70%).

Spectroscopic data for **170**

HPLC R_t = 16.5 min (broad peak).

^{1}H NMR (300 MHz, CD_3CN): δ 9.74 (br s, 1H, D_2O exchangeable), 8.25 (dd, J = 9, 2.5 Hz, 1H), 7.91 (d, J = 3 Hz, 1H), 7.78 (d, J = 3.5 Hz, 1H), 7.52 (dd, J = 9, 2.5 Hz, 1H), 7.34 (d, J = 3.5 Hz, 1H), 7.35 (m, 2H).

^{13}C NMR (75.5 MHz, CD_3CN): δ 166.2 (s), 145.5 (d), 139.6 (s), 128.7 (d), 127.5 (s), 125.7 (d), 123.9 (d), 123.4 (d), 118.9 (d), 114.9 (d), 114.3 (s).

HRMS-EI *m/z*: measured 200.0408 (M^+, calcd. 200.0408 for $C_{11}H_8N_2S$)

MS-EI *m/z* (relative intensity): 200 (M^+, 100), 142 (20), 56 (18).

FTIR ν_{max}: 3171, 3115, 1557, 1483, 1454, 1344, 1244, 1133, 1055, 920, 739 cm^{-1}.

UV (CH_3CN) λ_{max} (log ε): 219 (4.4), 270 (4.0), 313 (4.2).

4.4.2.2 Synthesis of 6-methoxycamalexin (171)

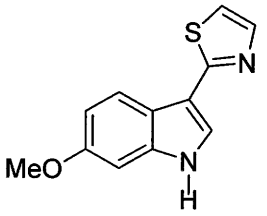

171

A solution of MeI (200 μL, 3.21 mmol) in dry Et_2O (2 mL) was added slowly by injection at room temperature under argon atmosphere to magnesium turnings (40 mg, 1.66 mmol) in dry Et_2O (2 mL). After all the magnesium had reacted, the Et_2O was distilled off and dry benzene (5 mL) was added. A solution of 6-methoxyindole (**233**, 100 mg, 0.68 mmol) in benzene (3 mL) was added to the solution of methylmagnesium iodide in benzene and stirred for 10 min after which 2-bromothiazole (100 μL, 1.11 mmol) was added. The reaction mixture was refluxed under argon for 20 hours then cooled to room temperature, poured into saturated aqueous NH_4Cl (50 mL) and extracted with EtOAc (50 mL, 2×). The extract was washed with brine (50 mL), dried over anhydrous Na_2SO_4 and the solvent removed under reduced pressure to obtain the crude product (172 mg).

Separation by FCC (silica gel, EtOAc-Hexane, 1:1) gave 6-methoxycamalexin (**171**, 106.2 mg, 68%).

Spectroscopic data for **171**

HPLC R_t = 23.4 min (broad peak).

^{1}H NMR (300 MHz, CD_3CN): δ 9.57 (br s, 1H D_2O exchangeable), 8.10 (d, J = 9 Hz, 1H), 7.78 (d, J = 3 Hz, 1H), 7.76 (d, J = 3.5 Hz, 1H), 7.32 (d, J = 3.5 Hz, 1H), 7.02 (d, J = 2.5 Hz, 1H), 6.86 (dd, J = 9, 2.5 Hz, 1H), 3.94 (s, 3H).

^{13}C NMR (75.5 MHz, CD_3CN): δ 166.3 (s), 159.9 (s), 145.6 (d), 140.5 (s), 127.4 (d), 124.0 (d), 121.8 (s), 118.8 (d), 114.4 (s), 113.9(d), 97.8 (d), 58.0 (q).

HRMS-EI *m/z*: measured 230.0513 (M^+, calcd. 230.0514 for $C_{12}H_{10}N_2SO$).

MS-EI *m/z* (relative intensity): 230 (M^+, 100), 215 (75), 187 (20), 129 (12).

FTIR ν_{max}: 3179, 2958, 2922, 2844, 1628, 1546, 1455, 1261, 1199, 1166, 1097, 800 cm^{-1}.

UV (CH_3CN) λ_{max} (log ε): 206 (4.6), 233(4.1), 262 (4.2), 287 (4.2).

4.4.2.3 Synthesis of 6-fluorocamalexin (250)

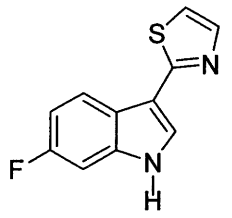

250

A solution of MeI (300 μL, 4.82 mmol) in dry Et_2O (2 mL) was added slowly via syringe at room temperature under argon atmosphere to magnesium turnings (64.8 mg, 2.70 mmol) in dry Et_2O (3 mL). After all the magnesium had reacted, the Et_2O was

distilled off and dry benzene (5 mL) was added. A solution of 6-fluoroindole (**261**, 150 mg, 1.11 mmol) in benzene (3 mL) was added to the solution of methylmagnesium iodide in benzene and stirred for 10 min after which 2-bromothiazole (164 μL, 1.82 mmol) was added. The reaction mixture was refluxed under argon for 52 hours, then cooled to room temperature, poured into saturated aqueous NH_4Cl (50 mL) and extracted with EtOAc (50 mL, 2×). The extract was washed with brine (50 mL), dried over anhydrous Na_2SO_4 and the solvent removed under reduced pressure to obtain the crude product. Separation by FCC (silica gel, EtOAc-Hexane, 1:1) yielded 6-fluorocamalexin (**250**, 130.7 mg, 59% based on recovered starting material) and unreacted 6-fluoroindole (**261**, 12.6 mg).

Spectroscopic data for **250**

HPLC R_t = 19.3 min (broad peak).

^{1}H NMR (300 MHz, CD_3CN): δ 9.74 (br s, 1H, D_2O exchangeable), 8.25 (dd, J = 9, 5.5 Hz, 1H), 7.89 (s, 1H), 7.78 (d, J = 3.5 Hz, 1H), 7.34 (d, J = 3.5 Hz, 1H), 7.23 (dd, J = 10, 2.5 Hz, 1H), 7.03 (ddd, J = 10, 9, 2.5 Hz, 1H).

^{13}C NMR (75.5 MHz, CD_3OH): δ 165.6 (s), 161.7 (d, $J_{C\text{-}F}$ = 238 Hz), 143.2 (d), 138.5 (d, $^3J_{C\text{-}F}$ = 12 Hz), 127.3 (d), 122.7 (s), 122.3 (d, $^3J_{C\text{-}F}$ = 10 Hz), 117.5 (d), 112.4 (s), 110.4 (d, $^2J_{C\text{-}F}$ = 25 Hz), 99.2 (d, $^2J_{C\text{-}F}$ = 26 Hz).

HRMS-EI *m/z*: measured 218.0315 (M^+, calcd. 218.0314 for $C_{11}H_7N_2FS$).

MS-EI *m/z* (relative intensity): 218 (100), 58 (20).

FTIR ν_{max}: 3162, 3006, 2916, 1630, 1553, 1487, 1451, 1230, 1134, 955, 840 cm^{-1}.

UV (CH_3CN) λ_{max} (log ε): 218 (4.4), 287 (4.1), 314 (4.1).

4.4.2.4 Synthesis of 6-fluoro-1-methylcamalexin (251)

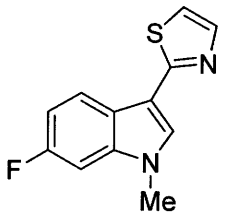

251

Sodium hydride (16.2 mg, 0.682 mmol) and MeI (64 μL, 0.682 mmol) were added to a solution of 6-fluorocamalexin (**250**, 110 mg, 0.505 mmol) in anhydrous THF under argon atmosphere at 0 °C. After stirring for 45 min, the reaction mixture was poured into ice-cold water (50 mL), extracted with EtOAc (50 mL, 2×), dried over anhydrous Na_2SO_4 and the solvent removed under reduced pressure to yield 6-fluoro-1-methylcamalexin (**251**, 112.5 mg, 96%).

Spectroscopic data for **251**

HPLC R_t = 25.4 min.

^{1}H NMR (300 MHz, CD_3CN): δ 8.17 (dd, J = 9, 5.5 Hz, 1H), 7.74 (d, J = 3.5 Hz, 1H), 7.68 (s, 1H), 7.26 (d, J = 3.5 Hz, 1H), 7.09 (dd, J = 10, 2.5 Hz, 1H), 6.98 (ddd, J = 10, 9, 2.5 Hz, 1H), 3.68 (s, 3H).

^{13}C NMR (75.5 MHz, CD_3CN): δ 165.6 (s), 162.9 (d, $J_{C\text{-}F}$ = 237 Hz), 145.5 (d), 140.4 (d, $^3J_{C\text{-}F}$ = 12 Hz), 133.1 (d), 124.8 (d, $^3J_{C\text{-}F}$ = 10 Hz), 124.6 (s), 118.8 (d), 113.4 (d), 112.1 (d, $^2J_{C\text{-}F}$ = 25 Hz), 99.4 (d, $^2J_{C\text{-}F}$ = 27 Hz), 35.6 (q).

HRMS-EI *m/z*: measured 232.0473 (M^+, calcd. 232.0471 for $C_{12}H_9N_2FS$).

MS-EI *m/z* (relative intensity): 232 (100), 174 (49), 173 (27), 58 (60).

FTIR ν_{max}: 3077, 2922, 2853, 1563, 1462, 1376, 943 cm^{-1}.

UV (CH_3CN) λ max (log ε): 224 (4.4), 290 (4.1), 322 (4.3).

4.4.2.5 Synthesis of 6-fluoroindole-3-carboxaldehyde (248)

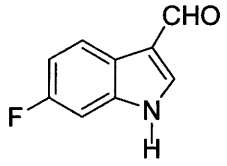

248

Phosphorus oxychloride (50 μL, 0.55 mmol, freshly distilled) was added dropwise with stirring to freshly distilled DMF (160 mg, 1.12 mL) under argon atmosphere. 6-Fluoroindole (**261**, 67.5 mg, 0.50 mmol) in DMF (40 mg, 30 μL) was then added dropwise with continuous stirring at room temperature. The reaction mixture was kept at 35 °C for 45 min and then poured into crushed ice. Aqueous NaOH solution (96 mg in 50 mL, 2.4 mmol) was added slowly to the reaction mixture until it became alkaline. The solution was boiled for 1 min, cooled to room temperature and then extracted with EtOAc (50 mL, 2×). The organic phases were combined, washed with water, dried over anhydrous Na_2SO_4 and the solvent removed under reduced pressure to yield 6-fluoroindole-3-carboxaldehyde (**248**, 70.1 mg, 86%).

Spectroscopic data for **248**

HPLC R_t = 8.5 min.

^{1}H NMR (300 MHz, CD_3CN): δ 10.03 (br s, 1H, D_2O exchangeable), 9.95 (s, 1H), 8.11 (dd, J = 9, 5.5 Hz, 1H), 7.98 (s, 1H), 7.26 (dd, J = 10, 2.5 Hz, 1H), 7.04 (ddd, J = 10, 9, 2.5 Hz, 1H).

^{13}C NMR (75.5 MHz, CD_3CN): δ 188.1 (d), 163.3 (d, $J_{C\text{-}F}$ = 238 Hz), 140.9 (d), 140.1 (d, $^3J_{C\text{-}F}$ = 13 Hz), 125.3 (d, $^3J_{C\text{-}F}$ = 10 Hz), 123.9 (s), 121.6 (s), 113.6 (d, $^2J_{C\text{-}F}$ = 24 Hz), 101.5 (d, $^2J_{C\text{-}F}$ = 27 Hz).

HRMS-EI *m/z*: measured 163.0430 (M^+, calcd. 163.0433 for C_9H_6NOF).

MS-EI *m/z* (relative intensity): 163 (88), 162 (100), 134 (31), 107 (25).

FTIR ν_{max}: 3131, 2922, 2862, 1630, 1535, 1453, 1158, 1074, 951, 823 cm^{-1}.

UV (CH_3CN) λ_{max} (log ε): 221 (4.5), 247 (4.2), 295 (4.2), 318 (4.2).

4.4.2.6 Synthesis of 6-fluoro-1-methylindole-3-carboxaldehyde (249)

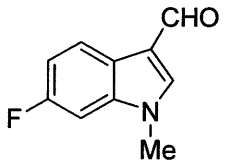

249

Sodium hydride (8.2 mg, 0.34 mmol) and MeI (32 μL, 0.34 mmol) were added to a stirred solution of 6-fluoroindole-3-carboxaldehyde (**248**, 40 mg, 0.25 mmol) in anhydrous THF (10 mL) under argon atmosphere at 0 °C. After stirring for 30 min the reaction mixture was poured cold ice-cold water (20 mL) and was extracted with EtOAc (50 mL, 2×). The extract was dried over anhydrous Na_2SO_4 and the solvent removed under reduced pressure to give 6-fluoro-1-methylindole-3-carboxaldehyde (**249**, 42.4 mg, 96%).

Spectroscopic data for **249**

HPLC R_t = 11.4 min.

^{1}H NMR (300 MHz, CD_3OD): δ 9.82 (s, 1H), 8.15 (dd, *J* = 9, 5.5 Hz, 1H), 8.06 (s, 1H), 7.27 (dd, *J* = 10, 2.5 Hz, 1H), 7.05 (ddd, *J* = 10, 9, 2.5 Hz, 1H), 3.87 (s, 3H).

^{13}C NMR (75.5 MHz, CD_3OD): δ 186.8 (d), 162.2 (d, J_{C-F} = 240 Hz), 143.7 (d), 140.1 (d, $^3J_{C-F}$ = 12 Hz), 123.8 (d, $^3J_{C-F}$ = 9 Hz), 122.9 (s), 119.2 (s), 112.2 (d, $^2J_{C-F}$ = 24 Hz), 98.3 (d, $^3J_{C-F}$ = 24 Hz), 34.1 (q).

HRMS-EI *m/z*: measured 177.0587 (M^+, calcd. 177.0590 for $C_{10}H_8NOF$).

MS-EI *m/z* (relative intensity): 177 (80), 176 (100).

FTIR ν_{max}: 3102, 2928, 2820, 1660, 1541, 1397, 1212, 1068, 919, 823, 739 cm^{-1}.

4.5 Biotransformation of phytoalexins and analogues

4.5.1 Time-course experiments

Five Erlenmeyer flasks (250 mL) each containing 100 mL of minimal media were employed. Four of the flasks were each inoculated with sclerotia of *S. sclerotiorum* clone # 33 and the flasks were incubated at 25 ± 2 °C on a shaker at 120 rmp in light. After six days brassinin (**149**, final concentration 1.0×10^{-4} M) in DMSO [final concentration 1.0 % (v/v)] was added to fungal cultures in three of the flasks and to uninoculated medium (control) in another flask. To fungal cultures (control) in the fifth flask DMSO (200 μL) was added. Samples (10 mL each) were taken from the flasks immediately after adding the compound. Subsequently 10 mL samples were taken after 1 and 2 days and final samples after 7 days. The samples were either immediately extracted or frozen for later extraction. Each sample was first extracted with EtOAc (20 mL). The resulting aqueous layer was acidified (to pH 2 with dil HCl) and extracted with EtOAc (20 mL). The resulting aqueous layer was finally made alkaline (to pH 10 with 28% aqueous NH_3) and extracted with $CHCl_3$. After evaporation of the solvent the neutral and acidic extracts were each dissolved in acetonitrile (1 mL) and filtered through a tight cotton plug into a HPLC vial for analysis. After 7 days the remaining fungal cultures (70 mL each) were extracted with an equivalent

amount of solvent to give neutral, acidic and basic extracts as described above. These were also prepared for HPLC analysis.

The above procedure was repeated using the compounds camalexin (**170**), 6-methoxycamalexin (**171**), methyl tryptamine dithiocarbamate (**199**), methyl 1-methyltryptamine dithiocarbamate (**239**), methyl 1-methoxytryptamine dithiocarbamate (**240**), methyl 2-naphthalenylmethylamine dithiocarbamate (**243**), 6-fluorocamalexin (**250**), and 6-fluoro-1-methylcamalexin (**251**).

4.5.2 Scale up experiments: Isolation and chemical characterization of metabolites

To obtain larger amounts of extract to isolate the products of metabolism of **149**, **170**, **171**, **199**, **239**, **240**, **243**, **250** and **251**, experiments were carried out in 1-L batches. Erlenmeyer flasks (250 mL, 11) each containing 100 mL of minimal media were employed. Ten of the flasks were inoculated with sclerotia of *S. sclerotiorum* clone # 33. After six days a solution of each of the compounds listed above in DMSO was added to fungal cultures (final concentration 1.0×10^{-4} M) in each of the eleven flasks and the uninoculated media and incubated for the required period. The ten flasks were combined, filtered and the broth extracted with EtOAc (300 mL, 3×). The uninoculated media was also extracted with EtOAc (30 mL, 3×). The inoculated media extract was fractionated by FCC [silica gel with gradient elution: CH_2Cl_2 (1 fraction of 100 mL), CH_2Cl_2 - MeOH (98:2, 3 fractions of 100 mL), CH_2Cl_2-MeOH (95:5, 3 fractions of 100 mL), CH_2Cl_2-MeOH (90:10, 2 fractions of 100 mL) CH_2Cl_2-MeOH (85:15, 2 fractions of 100 mL) and MeOH (100 mL)]. Each fraction was analyzed by HPLC and TLC.

The metabolites **234 - 238**, **263 – 264**, **266 – 270** (Table 4.2) were isolated from fractions (HPLC chromatograms contained peaks not present in control samples) using prepTLC (silica gel, (CH_2Cl_2-MeOH, 90:10, multiple development) and/or reverse phase

prepTLC (RP C-18 silica gel, H_2O-CH_3CN, 60:40). One metabolite with R_t = 16.5 min (HPLC), prominent in the inoculated media extract of **239** was not isolated after fractionation. Thus, in another experiment, the inoculated media extract (138 mg) of **239** was subjected to reverse phase FCC [with gradient elution, H_2O-CH_3CN (80:20, 10 fractions of 20 mL), H_2O-CH_3CN (50:50, 4 fractions of 50 mL), H_2O-CH_3CN (25:75, 100 mL)], and each fraction was analyzed by HPLC. Fraction twelve (27.2 mg, prominent peak at 16.5 min) was subjected to HPLC semi-preparative to obtain a product composed of a mixture of **239** and **264**.

Table 4.2 Summary of amounts of various metabolites obtained after separation of inoculated media extracts incubated with phytoalexins and analogues.

Phytoalexin/analogue (amount added to cultures)	Incubation time (h)	Metabolite(s) (amount, %)
Brassinin (**149**, 23.6 mg)	24	**234** (21.2 mg, 53%)
Methyl tryptamine dithiocarbamate (**199**, 25.0 mg)	48	**235** (19.6 mg, 48%)
Camalexin (**170**, 20.0 mg)	24	**236** (6.0 mg, 28%) **237** (8.2 mg, 22%)
6-Methoxycamalexin (**171**, 23.0 mg)	24	**236** (3.8 mg, 18%) **237** (7.4 mg, 20%) **238** (4.4 mg, 12%)
Methyl 1-methyltryptamine dithiocarbamate (**239**, 26.4 mg)	48	**263** (8.4 mg, 18%) **264** (6.8 mg, 24%)
Methyl 1-methoxytryptamine dithiocarbamate (**240**, 28.0 mg)	72	**266** (2.3 mg, 5%,)
Methyl 2-napthalenylmethylamine dithiocarbamate (**243**, 24.7 mg)	48	**267** (17.4 mg, 41%)
6-Fluorocamalexin (**250**, 21.8 mg)	48	**268** (19.8 mg, 52%)
6-Fluoro-1-methylcamalexin (**251**, 23.2 mg)	48	Recovered **251** (8.1 mg) **269** (4.2 mg, 17%) **270** (1.9 mg, 17%)

Metabolites **234, 235** and **236** (final solution concentration 1×10^{-4} M) in DMSO [final concentration 1.0% (v/v)] were subjected to further biotransformation by *S. sclerotiorum* clone # 33. The biotransformation was monitored by taking samples (5 mL) after 3 hours, 6 hours, 12 hours, 24 hours, 48 hours and 7 days. The samples were extracted with EtOAc (20 mL, 2×) and analyzed by HPLC.

4.5.2.1 Synthesis

Methylation of 6-hydroxycamalexin (236)

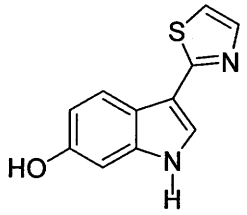

236

6-hydroxycamalexin (**236**, 2.5 mg) was treated with excess ethereal diazomethane for 4 hours. The solvent was removed under reduced pressure to yield 6-methoxy camalexin (**171**, 2.6 mg, 98%).

Methyl 1-methyltryptamine dithiocarbamate-S-oxide (265)

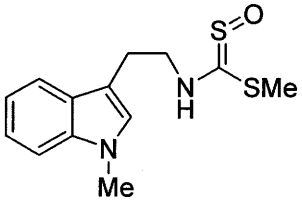

265

m-CPBA (19.6 mg, 0.08 mmol) was added to a solution of methyl 1-methyltryptamine dithiocarbamate (**239**, 20 mg, 0.08 mmol) in CH_2Cl_2 (2 mL) at 0 °C and stirred for 1.5 hours. Dimethylsulphide (500 μL) was added to the reaction mixture followed by successive washing with saturated aqueous $NaHCO_3$ (20 mL), water (20 mL) and then dried over anhydrous Na_2SO_4 and the solvent removed under reduced pressure to obtain the crude product. Separation by prepTLC (silica gel, CH_2Cl_2-MeOH, 95:5, developed twice) yielded methyl 1-methyl tryptamine dithiocarbamate-S-oxide (**265**, 9.4 mg, 42 % yield based on recovered starting material).

Spectroscopic data for **265**

HPLC R_t = 18.6 min (broad peak).

^{1}H NMR (300 MHz, CD_3CN): δ 7.62 (d, J = 8 Hz, 1H), 7.35 (d, J = 8 Hz, 1H), 7.22 (m, 1H), 7.09 (m, 1H), 7.06 (s, 1H), 3.89 (m, 2H), 3.74 (s, 3H), 3.09 (m, 2H), 2.33 (s, 3H).

^{1}H NMR (300 MHz, $CDCl_3$): δ 7.83 (br s, 1H, D_2O exchangeable), 7.62 (d, J = 8 Hz, 1H), 7.28 (d, J = 8 Hz, 1H), 7.22 (m, 1H), 7.16 (m, 1H), 3.78 (m, 2H), 3.76 (s, 3H), 3.13 (m, 2H), 2.35 (s, 3H).

^{13}C NMR (75.5 MHz, CD_3CN): δ 198.0 (s), 140.1 (s), 130.6 (d), 124.5 (d), 121.7 (d), 121.5 (s), 113.0 (d), 112.5 (d), 48.5 (q), 34.9 (t), 27.9 (t), 16.1 (q).

^{13}C NMR (75.5 MHz, $CDCl_3$): δ 194.2 (s), 137.4 (s), 127.5 (d), 122.2 (d), 119.3 (d), 118.6 (s), 109.9 (d), 109.7 (d), 45.8 (t), 32.9 (q), 25.6 (t), 12.8 (q).

HRMS-EI *m/z*: measured 280.0700 (M^+, calcd. 280.0704 for $C_{13}H_{16}N_2OS_2$).

MS-EI *m/z* (relative intensity): 280(15), 264 (100), 248 (25), 232 (24), 216 (75), 188 (20).

FTIR ν_{max}: 3133, 2922, 1675, 1614, 1530, 1328, 1249, 1157, 1011, 963, 905, 793 cm^{-1}.

6-Fluoro-1-methylindolyl-3-carbonitrile (270)

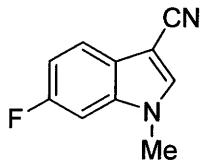

270

Pyridine (0.01 mL in 0.5 mL $CHCl_3$) was added to a refluxing mixture of $HONH_2.HCl$ (8.6 mg, 0.12 mmol) and 6-fluoro-1-methylindolyl-3-carboxaldehyde (**249**, 20 mg, 0.11 mmol) in $CHCl_3$-EtOH (7:3, v/v, 3 mL). After 3 hours, SeO_2 (13.7 mg, 0.12 mmol) was added to the reaction mixture and refluxing proceeded for 3 hours. The reaction mixture was allowed to cool to room temperature, anhydrous $MgSO_4$ (2 mg) was added and stirring continued for 10 min at room temperature. The mixture was then filtered and the solvent removed under reduced pressure. Separation by prepTLC (CH_2Cl_2, multiple development) yielded 6-fluoro-1-methylindolyl-3-carbonitrile as off-white powder (**270**, 9.1 mg, 74% based on recovered starting material) and unreacted 6-fluoro-1-methylindole-3-carboxaldehyde (**249**, 6.8 mg).

Spectroscopic data for **270**

HPLC R_t = 15.9 min.

^{1}H NMR (300 MHz, CD_3OD): δ 7.93 (s, 1H), 7.62 (dd, J = 9, 5.5 Hz, 1H), 7.33 (dd, J = 10, 2.5 Hz, 1H), 7.08 (ddd, J = 10, 9, 2.5 Hz, 1H), 3.85 (s, 3H).

^{13}C NMR (125 MHz, CD_3OD): δ 161.0 (s) (d, $J_{C\text{-}F}$ = 240 Hz), 137.8 (d), 137.0 (d, $^3J_{C\text{-}F}$ = 12 Hz), 124.4 (s), 120.2 (d, $^3J_{C\text{-}F}$ = 10 Hz), 115.5 (s), 110.8 (d, $^2J_{C\text{-}F}$ = 26 Hz), 97.4 (d, $^2J_{C\text{-}F}$ = 27 Hz), 84.7 (s), 32.8 (q).

HRMS-EI *m/z*: measured 174.0596 (M^+, calcd. 174.0593 for $C_{10}H_7N_2F$).

MS-EI *m/z* (relative intensity): 174 (100), 173 (38).

FTIR ν_{max}: 2952, 2922, 2851, 2219, 1739, 1535, 1463, 1246, 1110, 913, 829, 804 cm^{-1}.

UV (CH_3CN) λ_{max} (log ε): 215 (4.0), 283 (3.4).

4.5.2.2 Spectroscopic data

1-(β-D-glucopyranosyl)brassinin (234)

HPLC R_t = 7.9 min.; $[\alpha]_D$ = - 7.7 (*c* 0.20, MeOH).

^1H NMR (500 MHz, CD_3CN) δ 8.34 (br s, 1H D_2O exchangeable), 7.64 (d, *J* = 8 Hz, 1H), 7.52 (d, *J* = 8 Hz, 1H), 7.44 (s, 1H), 7.24 (ddd, *J* = 8, 8, 1 Hz, 1H), 7.14 (ddd, *J* = 8, 8, 1 Hz, 1H), 5.46 (d, *J* = 8 Hz, 1H), 5.08 (s, 2H), 3.42 - 3.87 (m, 10H, 4H D_2O exchangeable), 2.59 (s, 3H) and a minor signal (ca. 1/8 intensity of the major one) due to a rotamer at 2.68 (s).

^{13}C NMR (125 M Hz, CD_3CN): δ 198.8 (s), 137.0 (s), 128.0 (s), 125.7 (d), 122.6 (d), 120.5 (d), 119.5 (s), 112.0 (d), 111.0 (d), 85.2 (d), 79.2 (d), 77.9 (d), 72.5 (d), 70.5 (d), 61.9 (t), 42.4 (t), 17.6 (q).

HRMS-FAB *m/z*: measured 398.0965 (M^+, calcd. 398.0970 for $C_{17}H_{22}N_2O_5S_2$).

MS-FAB *m/z* (relative intensity): 398 (M^+, 5), 154 (100), 137 (67), 136 (85), 107 (35) 77 (40), 57 (43), 55 (69).

FT IR ν_{max}: 3317, 2952, 2922, 2852, 1740, 1581, 1462, 1377, 1115, 1076, 875, 743 cm^{-1}.

UV (CH_3CN) λ_{max} (log ε): 218 (4.0), 270 (3.6)

Methyl 1-(β-D-glucopyranosyl) tryptamine dithiocarbamate (235)

HPLC R_t = 8.9 min.; $[\alpha]_D$ = - 5.3 (*c* 0.80, MeOH).

^{1}H NMR (500 MHz, CD_3CN): δ 8.18 (br s, 1H D_2O exchangeable), 7.68 (d, J = 8 Hz, 1H), 7.52 (d, J = 8 Hz, 1H), 7.29 (s, 1H), 7.22 (ddd, J = 8, 8, 1 Hz, 1H) 7.15 (ddd, J = 8, 8, 1 Hz, 1H), 5.44 (d, J = 8 Hz, 1H), 3.93 (m, 2H), 3.86 (t, J = 8 Hz, 1H), 3.45 - 3.76 (m, 8H, 3H exchangeable with D_2O), 3.08 (m, 2H), 2.76 (s, 1H exchangeable with D_2O), 2.53 (s, 3H), and a minor signal (ca. 1/8 intensity of the major one) due to a rotamer at 2.61 (s).

^{13}C NMR (125.8 MHz, CD_3CN): δ 198.8 (s), 137.0 (s), 128.9 (s), 123.7 (d), 122.4 (d), 119.3 (d), 119.1 (d), 113.3 (s), 110.8 (d), 85.2 (d), 79.1 (d), 77.9 (d), 72.6 (d), 70.6 (d), 62.0 (t), 47.4 (t), 23.8 (t), 17.5 (q).

HRMS-FAB *m/z*: measured 413.1209 ($[M + H]^+$, calcd. 413.1205 for $C_{18}H_{25}N_2O_5S_2$).

MS-FAB *m/z* (relative intensity): 413 ($[M + H]^+$, 41), 412 (25), 329 (42), 305 (30), 261 (100), 176 (98).

FTIR ν_{max}: 3329, 2921, 2856, 1708, 1610, 1509, 1462, 1421, 1365, 1329, 1227, 1071, 1017, 930, 744, 620 cm^{-1}.

UV (CH_3CN) λ_{max} (log ε): 223 (4.2), 273 (3.7).

6-Hydroxycamalexin (236)

HPLC R_t = 11.4 min.

^{1}H NMR (300 MHz, CD_3CN): δ 9.44 (br s, 1H D_2O exchangeable), 8.04 (d, J = 8.5 Hz, 1H), 7.75 (d, J = 3.5 Hz, 1H), 7.73 (d, J = 2 Hz, 1H), 7.31 (d, J = 3.5 Hz, 1H), 6.89 (d, J = 2 Hz, 1H), 6.77 (dd, J = 8.5, 2 Hz, 1H).

^{13}C NMR (125.8 MHz, CD_3CN): δ 166.0 (s), 154.1 (s), 142.9 (d), 137.6 (s), 124.6 (d), 121.6 (s), 118.9 (d), 116.2 (s), 111.4 (d), 97.4 (d).

HRMS-EI *m/z*: measured 216.0361 (M^+, calcd. 216.0357 for $C_{11}H_8N_2OS$).

MS-EI *m/z* (relative intensity): 216 (M^+, 100), 158 (35).

FTIR ν_{max}: 3380, 2924, 2854, 1534, 1361, 1312, 1109, 1085, 799 cm^{-1}.

UV (CH_3CN) λ_{max} (log ε): 221 (4.5), 251 (4.1), 295 (4.2), 322 (4.1).

6-(*O*-β-D-Glucopyranosyl)camalexin (237)

HPLC R_t = 4.21 min.; $[\alpha]_D$ = - 12.2 (*c* 0.36, MeOH).

^1H NMR (300 MHz, CD_3CN): δ 9.67 (br s, 1H D_2O exchangeable), 8.13 (d, *J* = 9 Hz, 1H), 7.82 (d, *J* = 2.5 Hz, 1H), 7.76 (d, *J* = 3.5 Hz, 1H), 7.33 (d, *J* = 3.5 Hz, 1H), 7.22 (d, *J* = 2 Hz, 1H), 6.98 (dd, *J* = 9, 2 Hz, 1H), 4.94 (d, *J* = 7 Hz, 1H), 3.36 - 3.83 (m, 10H, 4H D_2O exchangeable).

^{13}C NMR (125.8 MHz, CD_3SOCD_3): δ 163.8 (s), 155.1 (s), 143.4 (d), 137.9 (s), 126.5 (s), 121.4 (d), 120.5 (s), 116.9 (d), 113.1 (d), 111.4 (d), 102.6 (d), 100.0 (d), 77.9 (d), 77.5 (d), 74.3 (d), 70.6 (d), 61.6 (t).

HRMS-FAB *m/z*: measured 379.0967 ($[M + H]^+$, calcd. 379.0964 for $C_{17}H_{19}N_2O_6S$).

MS-FAB *m/z* (relative intensity): 379 ($[M + H]^+$, 15), 329 (40), 176 (100).

FTIR ν_{max}: 3312, 2924, 1549, 1456, 1248, 1077 cm^{-1}.

UV (CH_3CN) λ_{max} (log ε): 222 (4.3), 251 (3.7), 286 (3.9), 321 (3.7).

6-Methoxy-1-(β-D-glucopyranosyl)camalexin (238)

HPLC R_t = 6.8 min.; $[\alpha]_D$ = - 14.4 (*c* 0.08, MeOH).

^1H NMR (300 MHz, CD_3CN): δ 8.14 (d, *J* = 9 Hz, 1H), 7.94 (s, 1H), 7.78 (d, *J* = 3.5 Hz, 1H), 7.35 (d, *J* = 3.5 Hz, 1H), 7.12 (d, *J* = 2 Hz, 1H), 6.92 (dd, *J* = 9, 2 Hz, 1H), 5.50 (d, *J* = 9 Hz, 1H), 3.87 (s, 3H), 3.27 - 3.87 (m, 10H, 4H D_2O exchangeable).

^{13}C NMR (125.8 MHz, CD_3CN): δ 163.0 (s), 154.0 (s), 143.1 (d), 137.0 (s), 125.2 (d), 121.9 (d), 118.7 (d), 116.7 (d), 111.9 (d), 109.9 (d), 94.9 (d), 85.2 (d), 79.4 (d), 77.8 (d), 72.7 (d), 70.4 (d), 61.9 (t), 55.7 (q).

HRMS-FAB *m/z*: measured 393.1117 ($[M + H]^+$, calcd. 393.1120 for $C_{18}H_{21}N_2O_6S$).

MS-FAB *m/z* (relative intensity): 393 ($[M + H]^+$, 20), 207 (40), 115 (100).

FTIR ν_{max}: 3335, 2924, 2853, 1723, 1621, 1557, 1456, 1229, 1079, 799, 741 cm^{-1}.

UV (CH_3CN) λ_{max} (log ε): 216 (4.1), 254 (3.7), 297 (3.7), 318 (3.7).

Methyl 1-methyl-7-(*O*-β-D-glucopyranosyl) tryptamine dithiocarbamate (263)

HPLC R_t = 9.5 min.; $[\alpha]_D$ = 1.5 (*c* 0.09, MeOH).

^1H NMR (300 MHz, CD_3CN): δ 8.08 (br s, 1H D_2O exchangeable), 7.27 (d, *J* = 8 Hz, 1H), 6.85 - 7.02 (m, 3H), 5.05 (d, *J* = 8 Hz, 1H), 4.00 (s, 2H), 3.92 (m, 2H), 3.36 - 3.79 (m, 10H, 4H D_2O exchangeable), 3.02 (m, 2H), 2.52 (s, 3H).

^{13}C NMR (125.8 MHz, CD_3CN): δ 198.9 (s), 145.7 (s), 132.0 (s), 129.2 (d), 127.0 (s), 119.7 (d), 113.6 (d), 111.4 (s), 107.4 (d), 102.1 (d), 77.3 (d), 76.9 (d), 74.2 (d), 70.6 (d), 61.9 (t), 47.7 (t), 36.2 (q), 23.7 (t), 17.5 (q).

HRMS-FAB *m/z*: measured 443.1321 ($[M + H]^+$, calcd. 443.1311 for $C_{19}H_{27}N_2O_6S_2$).

MS-FAB *m/z* (relative intensity): 443($[M + H]^+$, 5), 154 (35), 81 (48).

FTIR ν_{max}: 3340, 2924, 2854, 1461, 1376, 1251, 1074, 938, 740 cm^{-1}.

UV (CH_3CN) λ_{max} (log ε): 223 (4.3), 278 (3.7).

Methyl 1-methyl-2-oxotryptamine dithiocarbamate (264)

HPLC R_t = 15.7 min.

^1H NMR (300 MHz, $CDCl_3$): δ 8.76, (br s, 1H D_2O exchangeable), 7.25 - 7.33 (m, 2H), 7.09 (dd, *J* = 7.5, 7.5 Hz, 1H), 6.86 (d, *J* = 8 Hz, 1H), 4.12 (m, 1H), 3.89 (m, 1H), 3.52 (m, 1H), 3.23 (s, 3H), 2.62 (s, 3H), 2.45 (m, 1H), 2.05 (m, 1H).

^{13}C NMR (125.8 MHz, $CDCl_3$): δ 199.3 (s), 178.9 (s), 144.1 (s), 128.9 (d), 128.7 (s), 124.1 (d), 123.6 (d), 108.9 (d), 46.4 (t), 45.3 (q), 29.0 (t), 26.9 (d), 18.4 (q).

HRMS-EI *m/z*: measured 280.0708 (M^+, calcd. 280.0704 for $C_{13}H_{16}N_2OS_2$).

MS-EI *m/z* (relative intensity): 280 (M^+, 34), 232 (41), 174 (40), 173 (25), 160 (100), 147 (51).

FTIR ν_{max}: 3244, 2924, 2856, 1690, 1611, 1493, 1468, 1376, 1349, 1091, 942, 750 cm^{-1}.

UV (CH_3CN) λ_{max} (log ε): 195 (4.8), 253 (3.4).

Methyl 1-methoxy-7-(O -β -D- glucopyranosyl) tryptamine dithiocarbamate (266)

HPLC R_t = 9.5 min.; $[\alpha]_D$ = -5.1 (*c* 0.03, MeOH).

^1H NMR (300 MHz, CD_3CN): δ 8.11 (br s, 1H D_2O exchangeable), 7.38 (d, *J* = 8 Hz, 1H), 7.17 (s, 1H), 6.85 - 7.03 (m, 2H), 5.10 (d, *J* = 7.5 Hz, 1H), 4.09 (s, 3H), 3.92 (m, 2H), 3.27 - 3.77 (m, 10H, 4H D_2O exchangeable), 3.01 (m, 2H), 2.52 (s, 3H).

HRMS-FAB *m/z*: measured 459.1258 ($[M + H]^+$, calcd. 459.1260 for $C_{19}H_{27}N_2O_7S_2$).

MS-FAB *m/z* (relative intensity): 459($[M + H]^+$, 10), 428 (10), 385 (5), 369 (100).

FTIR ν_{max}: 3347, 2924, 2854, 1461, 1376, 1251, 1074, 938, 740 cm^{-1}.

UV (CH_3CN) λ_{max} (log ε): 224 (4.4), 272 (3.7).

Methyl 5-(*O*-β-D-glucopyranosyl)-2-naphthalenylmethylamine dithiocarbamate (267)

HPLC R_t = 9.4 min.; $[\alpha]_D$ = - 4.9 (*c* 0.04, MeOH).

^1H NMR (300 MHz, CH_3CN) δ 8.54 (br s, 1H, D_2O exchangeable), 8.32 (d, *J* = 9 Hz, 1H), 7.76 (s, 1H), 7.53 (d, *J* = 7.5 Hz, 1H), 7.46 (dd, *J* = 9, 1 Hz, 1H) 7.42 (dd, *J* = 7.5, 7.5 Hz, 1H), 7.15 (d, *J* = 7.5 Hz, 1H), 5.09 (d, *J* = 7.5 Hz, 1H), 5.05 (s, 1H), 3.36 - 3.81 (m, 10 H, 4H D_2O exchangeable), 2.59 (s, 3H).

^{13}C NMR (125.8 MHz, CH_3CN): δ 198.8 (s), 154.8 (s), 138.0 (s), 137.0 (s), 128.3 (d), 127.9 (d), 127.3 (d), 127.0 (s), 124.2 (d), 123.4 (d), 110.9 (d), 102.8 (d), 78.4 (d), 75.3 (d), 71.9 (d), 63.3 (t), 51.7 (t), 19.1 (q).

HRMS-FAB *m/z*: measured 426.1048 ($[M + H]^+$, calcd. 426.1045 for $C_{19}H_{24}NO_6S_2$).

FTIR ν_{max}: 3340, 3221, 2924, 2853, 1740, 1492, 1367, 1247, 1073, 929, 788 cm^{-1}.

UV (CH_3CN) λ_{max} (log ε): 220 (4.6), 274 (3.7).

6-Fluoro-1-(β-D-glucopyranosyl)camalexin (268)

HPLC R_t = 7.4 min.; $[\alpha]_D$ = - 5.0 (*c* 0.09, MeOH).

^1H NMR (300 MHz, CD_3CN): δ 8.30 (dd, *J* = 9, 5.5 Hz, 1H), 8.04 (s, 1H), 7.81 (d, *J* = 3.5 Hz, 1H), 7.39 (d, *J* = 3.5 Hz, 1H), 7.27 (d, *J* = 2.5 Hz, 1H), 7.10 (ddd, *J* = 10, 9, 2.5 Hz, 1H), 5.44 (d, *J* = 9 Hz, 1H), 3.27 - 3.89 (m, 10H, 4H D_2O exchangeable),

^{13}C NMR (125.8 MHz, CD_3CN): δ 162.8 (s), 160.5 (d, *J* = 238 Hz), 143.2 (d), 138.6 (d, *J* = 13 Hz), 127.1 (d), 122.6 (d, *J* = 10 Hz), 122.5 (s), 117.1 (d), 112.5 (s), 110.3 (d, *J* = 25 Hz), 98.2 (d, *J* = 28 Hz), 85.7 (d), 79.5 (d), 77.6 (d), 72.7 (d), 70.3 (d), 61.9 (t).

HRMS-FAB *m/z*: measured 381.0921 ($[M + H]^+$ calcd. 381.0920 for $C_{17}H_{17}N_2FSO_5$).

MS-FAB *m/z* (relative intensity): 381 (90), 329 (25), 218 (38), 176 (100), 149 (33).

FTIR ν_{max}: 3342, 2924, 2852, 1553, 1499, 1459, 1127, 1083, 1022, 960, 637 cm^{-1}.

UV (CH_3CN) λ_{max} (log ε): 221 (3.8), 315 (3.9).

6-Fluoro-1-methyl-7- (*O*-β-D-glucopyranosyl)camalexin (269)

HPLC R_t = 7.2 min.; $[\alpha]_D$ = 12.4 (*c* 0.06, MeOH).

^1H NMR (300 MHz, CD_3CN): δ 8.01 (dd, *J* = 9, 5 Hz, 1H), 7.76 (d, *J* = 3.5 Hz, 1H), 7.75 (s, 1H), 7.33 (d, *J* = 3.5 Hz, 1H), 7.06 (dd, *J* = 12, 9 Hz, 1H), 5.10 (d, *J* = 8 Hz, 1H), 4.07 (s, 3H), 3.22 - 3.63 (m, 10H, 4H D_2O exchangeable).

^{13}C NMR (125.8 MHz, CD_3CN): δ 162.9 (s), 151.7 (d, *J* = 237 Hz), 143.1 (d), 132.5 (s), 130.9 (d, *J* = 13 Hz), 130.0 (d, *J* = 28 Hz), 124.3 (d), 117.1 (d, *J* = 9 Hz), 116.5 (s), 111.0 (d, *J* = 22 Hz), 110.4 (d), 104.4 (d), 77.1 (d), 76.7 (d), 74.7 (d), 70.3 (d), 61.5 (t), 36.9 (q).

HRMS-FAB *m/z*: measured 411.1028 ($[M + H]^+$, calcd. 411.1026 for $C_{18}H_{20}N_2FSO_6$).

MS-FAB *m/z* (relative intensity): 411 ($[M + H]^+$, 10), 329 (22), 176 (100), 57 (52), 55 (58).

FTIR ν_{max}: 3331, 2950, 2924, 2853, 1629, 1466, 1381, 1074, 1024, 824, 599 cm^{-1}.

UV (CH_3CN) λ_{max} (log ε): 218 (2.9), 326 (3.3).

4.5.3 Metabolism and co-metabolism of analogues of brassinin (149) and camalexin (170)

Time course studies: co-incubation

Six Erlenmeyer flasks (250 mL) each containing 100 mL of minimal media were employed. Five of the flasks were each inoculated with sclerotia of *S. sclerotiorum* clone # 33, the flasks were incubated at 25 ± 2 °C on a shaker at 120 rpm in light. After five days potential inhibitor (final concentration 5.0×10^{-5} M) in DMSO [final concentration 1.0 % (v/v)] and brassinin (**149**) or camalexin (**170**), (final concentration 5.0×10^{-5} M) in DMSO [final concentration 1.0 % (v/v)] were added to fungal cultures in two of the flasks (flasks 1 and 2) and to uninoculated medium (flask 3, control 1). To fungal cultures in flask 4 (control 2) was added DMSO (200 µL). To flasks 5 and 6, potential inhibitor (final concentration 1.0×10^{-4} M) in DMSO [final concentration 1.0 % (v/v)] and brassinin (**149**) or camalexin (**170**) (final concentration 5.0×10^{-5} M) in DMSO [final concentration 1.0 % (v/v)] were added. Samples (10 mL each) were taken from the flasks immediately after adding the compounds. Subsequently 10 mL samples were taken every 24 hours for 7 days. Each sample was extracted with EtOAc (20 mL, 2×). After evaporation of the solvent the extracts were each dissolved in acetonitrile (1 mL), filtered through a tight cotton plug into a HPLC vial for analysis. The above procedure was followed using the compounds **239 – 253** as potential inhibitors.

4.5.4 Antifungal assays

The antifungal activity of compounds **149**, **199**, **170**, **171**, **239**, **240**, **242**, **243**, **250**, **251** and their metabolites **234**, **235**, **237**, **238**, **263**, **266**, **267**, **268**, and **269** was investigated using the following mycelial radial growth bioassay. Solutions of each compound in DMSO (5×10^{-2} M) were used to prepare assay solutions in minimal media (5×10^{-4}, 5×10^{-5} and 1×10^{-5} M); control solutions contained 1% DMSO in minimal media. Sterile tissue culture plates (6 well, 35 mm diameter) containing test solutions and control solution (2 mL per well) were inoculated with mycelium plugs placed upside down on the centre of each plate (8 mm cut from 3-day-old PDA plates of *S. sclerotiorum* clone # 33) and incubated under constant light for 7 days; measurement of the mycelium radial growth was carried out every two days. Three independent experiments were carried out and on each occasion in triplicate.

4.6 Partial purification of brassinin detoxifying enzyme(s)

4.6.1 Fungal cultures

Erlenmeyer flasks (250 mL × 10) each containing 100 mL of minimal media were employed. All the flasks were inoculated with sclerotia of *S. sclerotiorum* clone # 33. After four days solutions of potential inducer (final concentration 5.0×10^{-5} M) in DMSO [final concentration 1.0% (v/v)] were added to each of the ten flasks and incubated for 24 hours. The ten flasks were combined and filtered. The mycelial mass obtained as residue was washed with distilled water (500 mL), allowed to air-dry and then kept at - 20 °C (in the freezer) until needed. The maximum time was 4 months.

4.6.2 Preparation of cell homogenate

Frozen wet mycelia (12 – 20 g) of *S. sclerotiorum* clone # 33 was mixed with 10 - 20 mL ice cold standard buffer A (50 mM Tris-HCl, pH 8.0, containing 20% glycerol, 20 mM $HOCH_2CH_2SH$, 0.1 mM PMSF and 0.01% Triton X-100) and macerated or ground using a mortar and pestle until a homogenous mixture was obtained. This was then centrifuged at 27,216 × g for 15 min to obtain the cell homogenate (12 - 25 mL) and the pellet.

4.6.3 Chromatography

4.6.3.1 Ion exchange Chromatography

Cell homogenate (24 mL) was loaded unto the DEAE-sephacel ion exchange column (1.6 × 10 cm) pre-equilibrated with four bed volumes of standard buffer A. After washing with 100 mL of the buffer (0.6 mL min^{-1}), gradient elution was performed using varying concentrations of NaCl in standard buffer A collecting 3.5 mL per fraction. [0.01 M NaCl (15 mL), 0.05 M NaCl (50 mL), 0.1 M NaCl (30 mL), 0.2 M NaCl (50 mL) and 1 M NaCl (20 mL)]. 0.1 M NaCl eluted the fractions (fractions A_1 – A_9) with enzymatic activity.

4.6.3.2 Gel filtration Chromatography

The pooled active fractions (28 mL) from the ion exchange chromatography were loaded (5 batches) onto Sephadex G-25 column (1.6 × 10 cm) pre-equilibrated with four bed volumes of standard buffer A. Elution was performed with standard buffer A at a flow rate of 0.6 mL min^{-1}. The desalted active fractions (ca. 40 mL) were pooled together and concentrated (membrane filtration 10 kDa) to 20 mL.

4.6.3.3 Affinity Chromatography

The desalted enzyme fractions (5 mL each) were subjected to affinity chromatography on Reactive Green-19, Reactive-Yellow-86 and Cibacron Blue 3GA columns (1.0 × 6.4 cm) respectively. After pre-equilibration of the column with four bed volumes of standard buffer A, loading enzyme fractions and washing with 50 mL of same buffer (0.3 mL min^{-1}, 2.6 mL per fraction), elution was done with 0.1 M NaCl (20 mL), 0.2 M NaCl (20 mL), 0.5 M NaCl (20 mL), 0.5 M NaCl and 0.002 M UDPG (25 mL) and 0.5 M NaCl and 0.02 M UDPG (25 mL).

4.6.4 Protein measurements and gel electrophoresis

4.6.4.1 Bradford protein assay

The Bradford protein assay was used to estimate the quantities of proteins in the cell homogenate as well as the pooled active fractions from the ion exchange chromatography. With a stock solution (4 mg/mL) of bovine serum albumin (BSA), six other concentrations were prepared by serial dilution (2 mg/mL, 1 mg/mL, 0.8 mg/mL, 0.4 mg/mL, 0.2 mg/mL and 0.1 mg/mL). 100 μL each of the BSA solutions was taken into separate test tubes. 100 μL, 50 μL, 20 μL, 10 μL, and 5 μL of cell homogenate and pooled active fractions from DEAE-sephacel column were also taken into separate test tubes. Millipore water was added to each one to the 100 μL mark. A blank sample of 100 μL millipore water served as control, all samples were prepared in duplicate. Bradford reagent (5 mL) was added to each sample, incubated for about 5 min and the optical density measured at 595 nm. Protein amount was estimated using the BSA standard curve.

4.6.4.2 Gel electrophoresis

Gel electrophoresis (10% SDS-PAGE) was carried out to verify partial purification from the DEAE column. Cell homogenate and active fractions from DEAE column (fractions A_1 –A_9) were used. From the protein estimation, an equivalent amount (ca. 10 μL) of each sample was taken and applied onto the gel.

4.6.5 Enzyme assays

4.6.5.1 Time course study

The enzyme assay for the time course of reaction was carried out at 27 °C. The standard assay mixture contained 50 mM Tris HCl buffer (3 mL, pH 8.0) 15 mM UDPG (2 mL, 10 mg/mL), and 4 mL cell homogenate. The reaction was started by adding 10 mM brassinin (**149**, 20 μL) in DMSO and the mixture incubated for 8 hours with constant shaking. Aliquots (1 mL each) were immediately taken after the addition of brassinin (**149**)

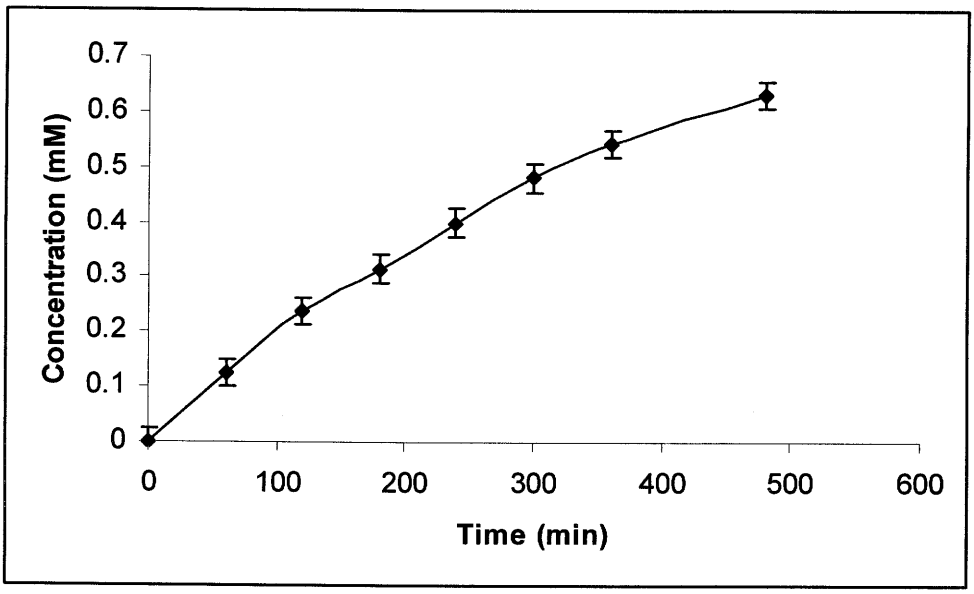

Figure 4.1 A plot for the time course enzymatic assay for 1-(β-D-glucopyranosyl)brassinin (**234**)

(0 h), and then every hour. Each aliquot was extracted separately with EtOAc (3 mL, 2×). After evaporation of the solvent the extracts were each dissolved in methanol (0.2 mL) and filtered through a tight cotton plug into a HPLC vial for analysis. Determination and quantification of the brassinin glucoside product (**234**) was determined using HPLC built standard curves. Two independent experiments were carried out. Figure 4.3 shows a concentration of **234** versus time plot for this time course assay.

4.6.5.2 Assays for substrate specificity studies

The standard assay mixture contained 50 mM Tris HCl buffer (98 μL, pH 8.0), UDPG (15 mM, 100 μL), and cell homogenate and/or enzyme fractions from DEAE column (400 μL). The reaction was started by adding brassinin (**149**) or potential substrate in DMSO (10 mM, final concentration in assay media 3×10^{-5} M) and incubated for 3 hours with constant shaking at 27 °C. After the incubation time it was extracted with EtOAc (2 mL, 2×). The solvent was removed under reduced pressure, the extract dissolved in methanol (0.2 mL, HPLC grade), filtered through a tight cotton plug into a HPLC vial for analysis. Determination and quantification of products were determined using HPLC built standard curves for the glucosyl products of the substrates (See Table 4.1). Three independent experiments were performed. Potential substrates used were methyl tryptamine dithiocarbamate (**199**), cyclobrassinin (**158**), camalexin (**170**), 6-hydroxycamalexin (**236**), and 6-methoxycamalexin (**171**)

4.6.5.3 Assays for co-incubation studies

The enzyme assay for the co-incubation studies was carried out at 27 °C. The standard assay mixture contained 50 mM Tris HCl buffer (1.6 mL, pH 8.0) 15 mM UDPG

(1.5 mL), and 13 mL of cell homogenate. After the addition of brassinin (**149**) in DMSO (10 mM, final concentration 2×10^{-5} M) and thorough shaking, the assay mixture was re-distributed into 15 vials (1 mL per vial). Three of the vials were immediately extracted (0 hour) with EtOAc (3 mL, 2×). Three other vials were incubated at 27 °C for 3 hours with constant shaking (control vials). To the remaining vials was added the potential inhibitors [each inhibitor added to 3 separate vials (in triplicate), final concentration in each vial 2×10^{-5} M] and incubated at 27 °C for 3 hours with constant shaking. After the incubation period, assay vials were worked up as described previously and extracts were analyzed by HPLC. Determination and quantification of products were determined using HPLC built standard curve for the 1-β-D-glucopyranosylbrassinin (**234**). Potential inhibitors used were 6-methoxycamalexin (**171**), 6-fluorocamalexin (**250**) and 6-fluoro-1-methylcamalexin (**251**). Three independent experiments were performed.

In another enzyme assay similar to the one described above the other substrates were added to the assay mixture before brassinin (**149**) was added.

CHAPTER FIVE

5. References

Adrian, M.; Rajaei, H.; Jeandet, P.; Veneau, J.; Bessis, R. Resveratrol oxidation in *Botrytis cinerea* conidia. *Phytopathol.* **1998**, *88*, 472-476.

Afzal, M.; Al-Oriquat, G. ^{13}C and proton-NMR spectra of sesquiterpenoid and related phytoalexins. *Heterocycles* **1986**, *24*, 2943-2961.

Aguamah, G. E.; Langcake, P.; Leworthy, D. P.; Page, J. A.; Pryce, R. J.; Strange, R. N. Two novel stilbene phytoalexins from *Arachis hypogaea*. *Phytochemistry* **1981**, *20*, 1381-1383.

Akatsuka, T.; Kodama, O.; Sekido, H.; Kono, Y.; Takeuchi, S. Novel phytoalexins (oryzalexins A, B, and C) isolation, characterization and biological activities of oryzalexins. *Agric. Biol. Chem.* **1985**, *49*, 1689-1694.

Al-Douri, N. A. Stress metabolites of *Phaseolus vulgaris* growing in Iraq. *Alexandria J. Pharm. Sci.* **1997**, *11*, 125-126.

Ayer, W. A.; Craw, P. A.; Yu-ting Ma; Miao, S. Synthesis of camalexin and related phytoalexins. *Tetrahedron* **1992**, *48*, 2919-2924.

Bailey, J. A.; Burden, R. S.; Mynett, A.; Brown, C. Metabolism of phaseollin by *Septoria nodorum* and other non-pathogens of *Phaseolus vulgaris*. *Phytochemistry* **1977**, *16*, 1541-1544.

Bailey, J. A.; Mansfield, J. W. Eds., in *Phytoalexins*. Blackie and Son, Glasgow, U.K., 1982, p. 334.

Bardin, S. D.; Huang, H. C. Research on biology and control of Sclerotinia diseases in Canada. *Can J. Plant Pathol.* **2001**, *23*, 88-98.

Bennett, M. H.; Mansfield, J. W.; Lewis, M. J.; Beale, M. H. Cloning and expression of sesquiterpene synthase genes from lettuce (*Lactuca sativa*, L.). *Phytochemistry* **2002**, *60*, 255-261.

Boland, G. J.; Hall, R. Index of plant hosts of *Sclerotinia sclerotiorum*. *Can. J. Plant Pathol.* **1994**, *16*, 93-108.

Boue, S. M.; Burow, M. E.; Carter, C. H.; Ehrlich, K. C.; Clevaland, T. E.; McLachlan, J. A. Accumulation of soybean phytoalexins with antiestrogenic activity from cotyledons inoculated with fungi. 218 th ACS National Meeting, New Orleans Aug. 22-26, 1999, (Abstr.).

Bourlot, A. S.; Desarbre, E.; Merour, J. Y. A Convenient Synthesis of 1.2-Dihydro-3*H*-indol-3-ones and 1,2-Dihydro-2*H*-indol-2-ones by Baeyer–Villiger Oxidation *Synthesis* **1994,** 411-416.

Bratfaleanu, O.; Steinhauer, B. Degradation of avenalumins by fungi in vitro and in vivo. *Mededelingen – Facultiet Landbouwkundige en Toegepaste Biologische Wetenschappen* **1994**, *59*, 877-884.

Breuil, A.; Adrian, M.; Pirio, N.; Meunier, P.; Bessis, R.; Jeandet, P. Metabolism of Stilbene Phytoalexins by *Botrytis cinerea*. *Tetrahedron Lett.* **1998**, *39*, 537-540.

Brooks, C. J. W.; Watson, D. G. Terpenoid phytoalexins. *Nat. Prod. Rep.* **1991**, *8*, 367-89.

Brooks, C. J. W.; Watson, D. G. Phytoalexins. *Nat. Prod. Rep.* **1985**, *2*, 427-459.

Browne, L. M.; Conn, K. L.; Ayer, W. A.; Tewari, J. P. The camalexins: new phytoalexins produced in the leaves of *Camelina sativa* (Cruciferae). *Tetrahedron* **1991**, 47, 3909-3914.

Bykova, T. D.; Davydova, M. A.; Ozeretskovskaya, O. L.; Moiseeva, N. A. Antifungal substances in apples. *Mikologiya i Fitopatologiya* **1977**, *11*, 116-122.

Cessna, S. G., Dickman, M. B., Sears, V. E., Low P. S. Oxalic Acid, a pathogenenicity factor for *Sclerotinia sclerotiorum*, suppresses the oxidative Burst of the host plant. *The Plant Cell* **2000**, *12*, 2191-2199.

Cline, E. I.; Adesanya, S. A.; Ogundana, S. K.; Roberts, M. F. Induction of PAL activity and dihydrostilbene phytoalexins in *Dioscorea alata* and their plant growth inhibitory properties. *Phytochemistry* **1989**, *28*, 2621-2625.

Conn, W. R.; Lindwall, H.G. Oxindole amines from isatin. *J. Amer. Chem. Soc.* **1936**, *58*, 1236-1239.

Conn, K. L.; Tewari, J. P. Hypersensitive reaction induced by *Alternaria brassicae* in *Eruca sativa*, an oil-yielding crucifer. *Can. J. Plant. Pathol.* **1986**, *8*, 348 (abstr.).

Conn, K. L.; Tewari, J. P.; Dahiya J. S. Resistance to *Alternaria brassicae* and phytoalexin elicitation in rapeseed and other crucifers. *Plant Science* **1988**, *56*, 21-25.

Cruickshank, I. A. M. Studies on phytoalexins, IV. The antimicrobial spectrum of pisatin. *Aust. J. Biol. Sci.* **1962**, *15*, 147-159.

Cruickshank, I. A. M.; Perrin, D. R. Isolation of a phytoalexin from *Pisum sativum* L. *Nature* **1960**, *187*, 799-800.

Cuendet, M.; Potterat, O.; Salvi, A.; Testa, B.; Hostettmann, K. A stilbene and dihydrochalcones with radical scavenging activities from *Loiseleuria procumbens*. *Phytochemistry* **2000**, *54*, 871-874.

Curtis, R. F.; Coxon, D. T.; Levett, G. Toxicity of fatty acids in assays for mycotoxins using the brine shrimp (*Artemia salina*). *Food Cosmet. Toxicol.* **1974**, *12*, 233-235.

De Wit, P. J. G. M.; Kodde, E.; Induction of polyacetylenic phytoalexins in *Lycopersicon esculentus* after inoculation with *Clasdosporium fulvum* (syn. *Fulvia fulva*). *Physiol. Plant Pathol.* **1981**, *18*, 143-148.

Delserone, L. M.; McCluskey, K.; Matthews, D. E.; Vanetten, H. D. Pisatin demethylation by fungal pathogens and nonpathogens of pea: association with pisatin tolerance and virulence. *Physiol. Mol. Plant Pathol.* **1999**, *55*, 317-326.

Denny, T. P.; VanEtten, H. D. Tolerance by *Nectria haematococca* MP VI of the chickpea (*Cicer arietinum*) phytoalexins medicarpin and maackiain. *Physiol. Plant. Pathol.* **1981**, *19*, 419-437.

Desjardins, A. E.; Gardner, H. W.; Plattner, R. D. Detoxification of the potato phytoalexin lubimin by *Gibberella pulicaris*. *Phytochemistry* **1989**, *28*, 431-437.

Desjardins, A. E.; Gardner, H. W.; Weltring, K. M. Detoxification of sesquiterpene phytoalexins by *Gibberella pulicaris*. *J. Ind. Microbiol.* **1992**, *9*, 201-211.

Desjardins, A. E.; VanEtten, H. D. Partial purification of pisatin demethylase, a cytochrome P-450 from the pathogenic fungus *Nectria haematococca*. *Arch. Microbiol.* **1986**, *144*, 84-90.

Dewick, P. M. The biosynthesis of shikimate metabolites. *Nat. Prod. Rep.* **1998**, *15*, 17-58.

Dixon, R. A., Harrison, M. J., Lamb, C. J. Early events in the activation of plant defense responses. *Annual Rev. Plant Phytopathol.* **1994**, 32, 479-501.

Edwards, C.; Strange, R. N. Separation and identification of phytoalexins from leaves of groundnut (*Arachis hypogaea*) and development of a method for their determination by reversed-phase high performance liquid chromatography. *J. Chrom.* **1991**, *547*, 185-193.

Enkerli, J.; Bhatt, G.; Covert, S. F. Maackiain detoxification contributes to the virulence of *Nectria haematococca* MP VI on chickpea. *Molecular Plant-Microbe Interactions* **1998**, *11*, 317-326.

Esaki H.; Kawakishi S; Morimitsu Y; Osawa T. New potent antioxidative o-dihydroxyiso flavones in fermented Japanese soybean products. *Biosci. Biotechnol. Biochem.* **1999**, *63*, 1637-1639.

Fagboun, D. E.; Ogundana, S. K.; Adesanya, S. A.; Roberts, M. F. Induction of PAL activity and dihydrostilbene phytoalexins in *Dioscorea alata* and their plant growth inhibitory properties. *Phytochemistry* **1987**, *26*, 3187-3189.

Farooq, A.; Tahara, S. Fungal metabolism of flavonoids and related phytoalexins. *Current topics in Phytochemistry* **1999**, *2*, 1-33.

Frank, J. A.; Francis, S. K. The effect of a *Rhizoctonia solani* phytotoxin on potatoes. *Can. J. Bot.* **1976**, *54*, 2536-2540.

Fujita, M.; Yoshizawa T. Induction of sweet potato phytoalexins by trichothecene mycotoxins. *Mycotoxins* **1987**, *25*, 29-30.

Funnell, D. L.; Matthews, P. S.; VanEtten, H. D. Identification of new pisatin demethylase genes (*Pda5* and *Pda7*) in *Nectria haematococca* and non-Mendelian segregation of pisatin demethylating ability and virulence on pea due to loss of chromosomal elements. *Fungal Genetics and Biology* **2002**, *37*, 121-133.

Gardner, H. W.; Desjardins, A. E.; McCormick, S. P.; Weisleder, D. Detoxification of the potato phytoalexin rishitin by *Gibberella pulicaris*. *Phytochemistry* **1994**, *37*, 1001-1005.

Gardner, H. W.; Desjardins, A. E.; Weisleder, D.; Plattner, R. D. Biotransformation of the potato phytoalexin, lubimin, by *Gibberella pulcaris*. Identification of major products. *Biochimica et Biophysica Acta*. **1988**, *966*, 347-356.

Graniti, A. Phytotoxins and their involvement in plant disease. *Experientia* **1991**, 47, 751-755.

Graniti, A., Durbin, R. D., Ballio, A. *Phytotoxins and Plant Pathogenesis* **1989**, Springer-Verlag, Berlin.

Gross, D. Antimicrobial defense compounds in Gramineae. *Zeitschrift fuer Pflanzenkrankheiten und Pflanzenschutz* **1989**, *96*, 535-553.

Gross, D.; Porzel, A.; Schmidt, J. Indole phytoalexins from the kohlrabi (*Brassica oleraceae* var. gongylodes) *Zeitschrift fur Naturforschung* **1994**, 49c, 281-285.

Hagemeier, J., Schneider, B., Oldham, N. J., Hahlbrock K. Accumulation of soluble and wall-bound indolic metabolites in *Arabidopsis thaliana* leaves infected with virulent or avirulent *Psedomonas syringae* pathovar tomato strains. *Proc. Natl. Acad. Sci.* USA, **2000**, *10*, 1073-1079.

Hain, R.; Reif, H. J.; Krause, E.; Langebartels, R.; Kindl, H.; Vornam, B.; Wiese, W.; Schmelzer, E.; Schreier. P. H.; Stocker, R. H.; Strenzel, K. Disease resistance

results from foreign phytoalexin expression in a novel plant. *Nature* **1993**, *361*, 153-156.

Hammerschmidt, R.; Dann, E. K. The role of phytoalexins in plant protection. *Novartis Foundation Symposium* **1999**, *223*, 175-190.

Hargreaves, J. A.; Mansfield, J. W.; Coxon, D. T.; Price, K. R. Wyerone epoxide as a phytoalexin in *Vicia faba* and its metabolism by *Botrytis cinerea* and *B. fabae* in vitro. *Phytochemistry* **1976**, *15*, 1119-1121.

Höhl, B.; Arnemann, M.; Schwenen, L.; Stöckl, D.; Bringmann, G.; Jansen, J.; Barz, W. Degradation of the pterocarpan phytoalexin (-)-maackiain by *Ascochyta rabiei*. *Z. Naturforsch* **1989**, *44c*, 771-776.

Hostettmann, K., 1991. Assays for Bioactivity, *Methods in Plant Biochemistry,* 6, 8-10.

Howell, D. M.; Fergus, C. L. The component fatty acids found in sclerotia of Sclerotium rolfsii. *Can. J. Microbiol.* **1964**, *10*, 616-618.

Ingham, J. L. Induced and constitutive isoflavonoids from stems of chickpeas (Cicer arietinum L.) inoculated with spores of Helminthosporium carbonum Ullstrup. Phytopathologische Zeitschrift **1976**, *87*, 353-367.

Ingham, J. L. Isoflavonoid phytoalexins from yam bean. *J. Biosci.* **1979**, *34C*, 683-688.

Ingham, J. L.; Markham, K. R.; Identification of the Erythrina phytoalexin, cristacarpin, and a note on chirality of other 6a-hydroxypterocarpans. *Phytochemistry*, **1980**, *19*, 1203-1207.

Katsui, N; Matsunaga, A.; Masamune, T.; Studies on the phytoalexins. XI. Structure of lubimin and oxylubimin, antifungal metabolites from diseased potato tubers. *Tetrahedron Lett.*, **1974**, *51/52*, 4483-4486.

Kawasaki, T.; Kodama, A.; Nishida, T.; Shimizu, K.; Somei, M. Preparation of 1-hydroxyindole derivatives and a new route to 2-substituted indoles. *Heterocycles,* **1991**, 32, 221-227.

Kemp, M. S. Falcarindiol: An antifungal polyacetylene from *Aegopodium podagraria*. *Phytochemistry* **1978**, *17*, 1002.

Kohli, Y.; Brunner, L. J.; Yoell, H.; Milgroom, M. G.; Anderson, J. B.; Morrall, R. A. A.; Kohn, L. M. Clonal dispersal and spatial mixing in populations of the plant pathogenic fungus, *Sclerotinia sclerotiorum*. *Molecular Ecology* **1995**, *4*, 69-77.

Kubota, T.; Tokoroyama, T.; Kamikawa, T.; Satomura, Y. The structures of sclerin and sclerolide, metabolites of *Sclerotinia libertiana*. *Tetrahedron Lett.* **1966**, *42*, 5205-5210.

Kuhn, P. J.; Smith, D. A. Isolation from *Fusarium solani* f. sp. phaseoli of an enzymic system responsible for kievitone and phaseollidin detoxification. *Physiol. Plant Pathol.* **1979**, *14*, 179-190.

Kurosaki, F.; Futamura, K.; Nishi, A. Factors affecting phytoalexin production in cultured carrot cells. *Plant and Cell Physiol.* **1985**, *26*, 693-700.

Kurosaki, F.; Nishi, A. Isolation and antifungal activity of the phytoalexin 6-methoxymellein from cultures carrot cells. *Phytochemistry* **1983**, *22*, 669-672.

Kutschy, P. Suchy, M.; Andreani, A.; Dzurilla M.; Rossi, M. A new photocyclization approach to the rare 1,3-thiazino[6,5-*b*]-indol-4-one derivatives. *Tetrahedron lett.* **2001**, *42*, 9281-9283.

Kuzel, N. R.; Miller, C. E. A phytochemical study of *Xanthium canadense*. *J. Am. Pharm. Assoc.* **1950**, *39*, 202-204.

Lefol, C.; Seguin-Swartz, G.; Morrall, R. A. A. Resistance to *Sclerotinia sclerotiorum* in a weed related to canola. *Can. J. Plant Pathol.* **1997**, *19*, 113 (Abstr.).

Letcher, R. M.; Widdowson, D. A.; Deverall, B. J.; Mansfield, J. W. Identification and activity of wyerone acid as a phytoalexin in broad bean (*Vicia faba*) after infection by *Botrytis*. *Phytochemistry* **1970**, *9*, 249-252.

Li, D.; Chung, K. R.; Smith, D. A.; Schardl, C. L. The *Fusarium solani* gene encoding kievitone hydratase, a secreted enzyme that catalyzes detoxification of a bean phytoalexin. *Mol. Plant-Micro Int.* **1995**, *8*, 388-397.

Lima, T. M.; Kanunfre, C. C.; Pompeia, C.; Verlengia, R.; Curi, R. Ranking the toxicity of fatty acids on Jurkat and Raji cells by flow cytometric analysis. *Toxicology in vitro* **2002**, *16*, 741-747.

Lucy, M. C.; Matthews, H. D.; VanEtten, H. D. Metabolic detoxification of the phytoalexins maackiain and medicarpin by *Nectria haematococca* field isolates: relationship to virulence on chickpea. *Physiol. Mol. Plant. Pathol.* **1988**, 33, 187-199.

Mackintosh, S. F.; Matthews, D. E.; VanEtten, H. D. Two additional genes for pisatin demethylation and their relationship to the pathogenicity of *Nectria haematococca* on pea. *Molecular Plant-Microbe Interactions* **1989**, *2*, 354-362.

Maloney, A. P.; VanEtten, H. D. A gene from the fungal plant pathogen *Nectria haematococca* that encodes the phytoalexin-detoxifying enzyme pisatin demethylase defines a new cytochrome P450 family. *Molecular and General Genetics* **1994**, *243*, 506-514.

Mann, J. Secondary Metabolism (second edition). 1987, Clarendon Press, Oxford, pp. 6-8.

Marukawa, S.; Funakawa, S.; Satomura, Y. Role of sclerin on morphogenesis in *Sclerotinia sclerotiorum* de Bary (including *S. libertiana* Fuckel). *Agric. Biol. Chem.* **1975**, *39*, 645-650.

Matthews, D. E.; VanEtten, H. D. Detoxification of the phytoalexin pisatin by a fungal cytochrome P-450. *Arch. Biochem. Biophys.* **1983**, *224*, 494-505.

Maxwell, D. P.; Lumsden, R. D. Oxalic acid production by *Sclerotinia sclerotiorum* in infected bean and in culture. *Phytopathol.* **1970**, *60*, 1395-1398.

Mayama, S. The role of avenalumin in the resistance of oats to crown rust. *Kagawa Daigaku Nogakubu Kiyo* **1983**, *42*, 1-64

Miao, V. P. W.; VanEtten, H. D. Genetic analysis of the role of phytoalexin detoxification in virulence of the fungus *Nectria haematococca* on chickpea (*Cicer arietinum*). *Appl. Env. Microbiol.* **1992a**, *58*, 809-814.

Miao, V. P. W; VanEtten, H. D. Three genes for metabolism of the phytoalexin maackiain in the plant pathogen *Nectria haematococca*: meiotic instability and relationship to a new gene for pisatin demethylase. *Appl. Env. Microbiol.* **1992b**, *58*, 801-808.

Monde, K.; Takasugi, M. Biosynthesis of cruciferous phytoalexins: the involvement of a molecular rearrangement in the biosynthesis of brassinin. *J. Chem. Soc. Chem. Commun.* **1991**, 1582-1583.

Monde, K.; Takasugi, M.; Ohnishi, T. Biosynthesis of cruciferous phytoalexins. *J. Amer. Chem. Soc.* **1994**, *116*, 6650-6657.

Monde, K.; Tanaka, A.; Takasugi, M. Trapping experiment with aniline for a biosynthetic intermediate of sulfur containing cruciferous phytoalexins. *J. Org. Chem.* **1996**, *61*, 9053-9054.

Morita, T.; Aoki, H. Isosclerone, a new metabolite of *Sclerotinia sclerotiorum* (Lib.) de Bary. *Agric. Biol. Chem.* **1974**, *38*, 1501-1505.

Morrissey, J. P.; Osbourn A. E. Fungal resistance to plant antibiotics as a mechanism of pathogenesis. *Microbiol. Mol. Biol. Rev.* **1999**, *63*, 708-724.

Müller, K. O.; Börger, H. Experimentelle untercuchunger uber die phytophtora: resistenz der kartoffel, *Arb. Biol. Anst. Reichsanst.* **1940**, *23*, 189-231.

Nakada, H.; Kobayashi, A.; Yamashita, K. Stereochemistry and biological activity of phytoalexin "safynol" from safflower. *Agric. Biol. Chem.* **1977**, *41*, 1761-1765.

Nishimura, S.; Sabaki, M. Isolation of the phytotoxic metabolites of *Pellicularia filamentosa. Ann. Phytopathol. Soc. Jpn.* **1963**, *28*, 228-234.

Noyes, R. D.; Hancock, J. G. Role of oxalic acid in the Sclerotinia wilt of sunflower. *Physiol. Plant Pathol.* **1981**, *18*, 123-132.

Orlean, Peter A. B. (1,3)-β-D-Glucan Synthase from budding and filamentous cultures of the dimorphic fungus *Candida albicans. Eur. J. Biochem.* **1982**, *127*, 397-403.

Pedras, M. S. C. Metabolism of cruciferous phytoalexins by phytopathogenic fungi: mimicking or overcoming plant defenses? *Recent Res. Devel. in Phytochem.* **1998a**, *2*, 259-267.

Pedras, M. S. C. Towards an understanding and control of plant fungal diseases in Brassicaceae. *Recent Res. Devel. in Phytochem.* **1998b**, *2*, 513-532.

Pedras, M. S. C. Phytotoxins from fungi causing blackleg disease on crucifers: isolation, structure determination, detection, and phytotoxic activity. *Recent Res. Devel. Phytochem.* **2001**, *5*, 109-117.

Pedras, M. S. C.; Ahiahonu, P. W. K. Probing the phytopathogenic stem rot fungus with phytoalexin analogues: unprecedented glucosylation of camalexin and 6-methoxycamalexin. *Bioorg. & Med. Chem.* **2002**, *10*, 3307-3312.

Pedras, M. S. C.; Biesenthal, C. J. Isolation, structure determination, and phytotoxicity of unusual dioxopiperazines from the phytopathogenic fungus *Phoma lingam. Phytochemistry* **2001**, *58*, 905-909.

Pedras, M. S. C.; Borgmann, I.; Taylor, J. L. Biotransformation of brassinin is a detoxification mechanism in the "blackleg" fungus. *Phytochemistry* **1992**, *11*, 1-7.

Pedras, M. S. C.; Chumala, P. B.; Suchy, M. Phytoalexins from *Thlaspi arvense*; a wild crucifer resistant to *Leptosphaeria maculans*: structures, synthesis and antifungal activity. *Phytochemistry* **2003b**, in press.

Pedras, M. S. C.; Erosa-Lopez, C. C.; Quail, J. W.; Taylor, J. L. Phomalairdenone: a new host-selective phytotoxin from a virulent type of the blackleg fungus *Phoma lingam. Bioorg. & Med. Chem.* **1999**, *9*, 3291-3294.

Pedras, M. S. C.; Jha, M.; Ahiahonu, P. W. K. The synthesis and biosynthesis of phytoalexins produced by cruciferous plants. *Curr. Org. Chem.* **2003a**, in press.

Pedras, M. S. C.; Khan A. Q. Biotransformation of the phytoalexin camalexin by the phytopathogen *Rhizoctonia solani. Phytochemistry* **2000**, *53*, 59-69.

Pedras, M. S. C.; Khan A. Q. Unprecedented detoxification of the cruciferous phytoalexin camalexin by a root phytopathogen. *Bioorg. Med. Chem. Lett.* **1997**, *7*, 2255-2260.

Pedras, M. S. C.; Khan, A. Q. Biotransformation of the brassica phytoalexin brassicanal A by the blackleg fungus. *J. Agric. Food Chem.* **1996**, *44*, 3403.

Pedras, M. S. C.; Khan, A. Q.; Smith, K. C.; Stettner, S. L.; Shawndra L. Preparation, biotransformation, and antifungal activity of methyl benzyldithiocarbamates *Can. J. Chem.* **1997a**, *75*, 825-828.

Pedras, M. S. C.; Khan, A. Q.; Taylor, J. L. Phytoalexins from brassicas: overcoming plant's defenses. In *Phytochemicals for Pest Control*; Hedin, P. A., Hollingworth, R. M., Masler, E. P., Miyamoto, J., Thompson D. G. Eds.; ACS symposium Series 658, 1997b; pp. 155-166.

Pedras, M. S. C.; Khan, A. Q.; Taylor, J. L. The phytoalexin camalexin is not metabolized by *Phoma lingam, Alternaria brassicae*, or phytopathogenic bacteria. *Plant Sci. (Shannon, Irel.)* **1998a**, *139*, 1-8.

Pedras, M. S. C.; Loukaci, A.; Okanga, F. I. The cruciferous phytoalexin brassinin and cyclobrassinin are imtermediates in the biosynthesis of brassilexin. *Bioorg. & Med. Chem. Lett.* **1998b**, *8*, 3037-3038.

Pedras, M. S. C.; Montaut, S. Probing crucial metabolic pathways in fungal pathogens of crucifers: biotransformation of indole-3-acetaldoxime, 4-hydroxyphenylacetald oxime and their metabolites. *Bioorg. Med. Chem.* **2003**, *11*, 3115-3120.

Pedras M. S. C.; Montaut, S.; Zaharia, I. L.; Gai, Y.; Ward, D. E. Transformation of the host-selective toxin destruxin B by wild crucifers: *Phytochemistry* **2003c**, in press.

Pedras, M. S. C.; Nycholat, C.; Montaut S.; Xu, Y.; Khan, A.Q. Chemical defenses of crucifers: elicitation and metabolism of phytoalexins and indole-3-acetonitrile in brown mustard and turnip. *Phytochemistry* **2002a**, *59*, 611-625.

Pedras, M. S. C.; Okanga, F. I. Metabolism of analogs of the phytoalexin brassinin by plant pathogenic fungi. *Can. J. Chem.* **2000**, *78*, 338-346.

Pedras, M. S. C.; Okanga, F. I. Probing the phytopathogenic blackleg fungus with a phytoalexin homolog. *J. Org. Chem.*, **1998**, *63*, 416-417.

Pedras, M. S. C.; Okanga, F. I. Strategies of cruciferous pathogenic fungi: detoxification of the phytoalexin cyclobrassinin by mimicry. *J. Agric. Food Chem.* **1999**, *47*, 1196-1202.

Pedras, M. S. C.; Okanga, F. I.; Khan, A. Q. Zaharia, I. L. Phytoalexins from crucifers: synthesis, biosynthesis, and biotransformation. *Phytochemistry* **2000**, *53*, 161-176.

Pedras, M. S. C.; Sorensen, J. L. Phytoalexin accumulation and antifungal compounds from the crucifer wasabi. *Phytochemistry* **1998**, *49*, 1959-1965.

Pedras, M. S. C.; Taylor, J. L. Metabolic transformation of the phytoalexin brassinin by the "blackleg" fungus. *J. Org. Chem.* **1991**, *56*, 2619-2621.

Pedras, M. S. C.; Taylor, J. L. Metabolism of the phytoalexin brassinin by the blackleg fungus. *J. Nat. Prod.* **1993**, *56*, 731-738.

Pedras, M. S. C.; Zaharia, I. L.; Ward, D. E. The destruxins: synthesis, biosynthesis biotransformation and biological activity. *Phytochemistry* **2002b**, *59*, 579-596.

Pezet, R.; Pont, V.; Hoang-Van, K. Evidence for oxidative detoxification of pterostilbene and resveratrol by a laccase-like stilbene oxidase produced by *Botrytis cinerea*. *Physiol. Mol. Plant. Pathol.* **1991**, *39*, 441-450.

Purdy, L. H. *Sclerotinia sclerotiorum*: history, diseases and symptomatology, host range, geographic distribution, and impact. *Phytopathol.* **1979**, *69*, 875-880.

Rai, J. N.; Dhawan, S. Studies on the purification and identification of toxic metabolite produced by *Sclerotinia sclerotiorum* causing white rot disease of crucifers. *Ind. Phytopathol.* **1976**, *29*, 407-411.

Regente, M.; Oliva, C. R.; Feldman, M. L.; Castagnaro, A. P.; Canal, L. A sunflower leaf antifungal peptide active against *Sclerotinia sclerotiorum*. *Physiologia Plantarum* **1997**, *100*, 178-182.

Repcak, M.; Imrich, J.; Franekova, M. Umbelliferone, a stress metabolite of *Chamomilla recutita* (L.) Rauschert. *J. Plant Physiol.* **2001**, *158*, 1085-1087.

Rouxel, T.; Kollman, A.; Ballesdent, M. H. Phytoalexins from the crucifers. In Handbook of Phytoalexin Metabolism and action; Daniel, M., Purkayastha, R. P., Eds.; Marcel Dekker, Inc.: New York, 1995; pp. 229-261.

Sassa, T., Aoki, H., Namiki, M., Munakata, K. Plant growth promoting metabolites of *Sclerotinia sclerotiorum*. Part I. Isolation and structures of sclerotinin A and B. *Agric. Biol. Chem.*, **1968**, *32*, 1471-1439.

Satomura, Y.; Sato, A. Isolation and physiological activity of sclerin, a metabolite of *Sclerotinia* fungus. *Agric. Biol. Chem.* **1963**, *29*, 337-344.

Sbaghi, M.; Jeandet, P.; Bessis, R.; Leroux, P. Degradation of stilbene-type phytoalexins in relation to the pathogenicity of *Botrytis cinerea* to grapevines. *Plant Pathol.* **1996**, *45*, 139-144.

Schäfer, W.; Straney, D.; Ciuffetti, L.; VanEtten, H. D. One enzyme makes a fungal pathogen, but not a saprophyte, virulent on a new host plant. *Science* **1989**, *246*, 247-249.

Schallenberg, J.; Meyer, E. Simple syntheses of 3-substituted indoles and their application for high yield ^{14}C-labelling. *Z. Naturforsch.* **1983**, *38b*, 108-112.

Schneider, J. A.; Nakanishi, K. A new class of sweet potato phytoalexins. *J. Chem Soc., Chem. Comm.* **1983**, *7*, 353-355.

Smith, C. J. Accumulation of phytoalexins: defence mechanism and stimulus response system. *New Phytologist* **1996**, *132*, 1-45.

Smith, D. A. Toxicity of phytoalexins. In: J. A. Bailey & J. W. Mansfield (Eds.), Phytoalexins, Blackie & Son, Glasgow, U.K., 1982, 218-252.

Smith, D. A.; Harrer, J. M.; Cleveland, T. E. Simultaneous detoxification of phytoalexins by *Fusarium solani* f. sp. *phaseoli*. *Phytopathol.* **1981**, *71*, 1212-1215.

Soby, S.; Cadera, S.; Bates, R.; VanEtten, H. D. Detoxification of the phytoalexins maackiain and medicarpin by fungal pathogens of alfalfa. *Phytochemistry* **1996**, *41*, 759-765.

Somei, M.; Kobayashi, K.; Shimizu, K.; Kawasaki, T. A simple synthesis of a phytoalexin, methoxybrassinin. *Heterocycles* **1992**, *33*, 77-80.

Starratt, A. N.; Ross, L. M.; Lazarovits, G. 1,8-Dihydroxynaphthalene monoglucoside, a new metabolite of *Sclerotinia sclerotiorum*, and the effect of tricyclazole on its production. *Can. J. Microbiol.* **2002**, *48*, 320-325.

Strobel, G. A. Phytotoxins. *Ann. Rev. Biochem.* **1982**, *51*, 309-333.

Suchy, M.; Kutschy, P.; Monde, K.; Goto, H.; Harada, N.; Takasugi, M.; Dzurilla, M.; Balentova, E. Synthesis, absolute configuration, and enantiomeric enrichment of a cruciferous oxindole phytoalexin, (*S*)-(-)-spirobrassinin, and its oxazoline analog. *J. Org. Chem.* **2001**, *66*, 3940-3947.

Sumner J. L.; Colotelo N. The fatty acid composition of sclerotia. *Can. J. Microbiol.* **1970**, *16*, 1171-1178.

Suzuki, K.; Sassa, T.; Tanaka, H.; Aoki, H.; Namiki, M. Sclerone, a new metabolite of *Sclerotinia sclerotiorum* (Lib.) de Bary. *Agric. Biol. Chem.* **1968**, *32*, 1471-1475.

Syu, W.; Don, M.; Lee, G.; Sun, C.; Cytotoxic and novel compounds from *Solanum indicum. J. Nat. Prod.* **2001**, *64*, 1232-1233.

Tahara, S.; Misumi, E.; Mizutani, J. Fungal metabolism of the prenylated isoflavone 2,3-dehydrokievitone. *Z. Naturforsch* **1987**, *42c*, 1055-1062.

Takasugi, M.; Katsui, N.; Shirata, A. Isolation of three novel sulfur-containing phytoalexins from the Chinese cabbage *Brassica campestris* L. ssp. *pekinensis* (Cruciferae). *J. Chem. Soc., Chem. Commun.* **1986**, 1077-1078.

Takasugi, M.; Monde K.; Katsui, N.; Shirata, A. Spirobrassinin, a novel sulfur-containing phytoalexin from the diakon *Rhaphanus sativus* L. var. *hortensis Chem. Lett.* **1987**, 1631-1632.

Takasugi, M.; Okinaka S.; Katsui, N.; Masamune, T.; Shirata, A.; Ohuchi, M. Isolation and structure of lettucenin A, a novel guaianolide phytoalexin from *Lactuca sativa* var. capitata (Compositae). *J. Chem. Soc., Chem. Commun.* **1985**, *10*, 621-622.

Tal, B.; Robeson, D. J. The induction, by fungal inoculation, of ayapin and scopoletin biosynthesis in *Helianthus annus. Phytochemistry* **1986**, *25*, 77-79.

Talalay, P.; Fahey, J. W. Phytochemicals from cruciferous plants protect against cancer by modulating carcinogen metabolism. *J. Nut.* **2001**, *131*, 3027S-3033S.

Thomzik, J. E.; Stenzel, K.; Stöcker, R.; Schreier, P. H.; Hain, R.; Stahl, D. J. Synthesis of a grapevine phytoalexin in transgenic tomatoes (*Lycopersicon esculentum* Mill.) conditions resistance against *Phytophthora infestans. Physiol. Mol. Plant Pathol.* **1997**, *51*, 265-278.

Tokoroyama, T., Kamikawa T., Kubota, T. The structure of sclerin, a metabolite of *Sclerotinia libertiana. Tetrahedron* **1968**, *24*, 2345-2355.

Tsuji, J.; Zook, M.; Somerville, S.; Last, R. L.; Hammerschmidt, R. Evidence that tryptophan is not a direct biosynthetic intermediate of camalexin in *Arabidopsis thaliana. Physiol. Mol. Plant Pathol.* **1993**, *43*, 221-229.

Tu, J. C. Tolerance of white bean (*Phaseolus vulgaris*) to white mold (*Sclerotinia sclerotiorum*) associated with tolerance to oxalic acid. *Physiol. Plant. Pathol.* **1985**, *26*, 111-117.

Turbek, C. S.; Li, D.; Choi, G. H.; Schardl, C. L.; Smith, D. A. Induction and purification of kievitone hydratase from *Fusarium solani* f. sp. *Phaseoli. Phytochemistry* **1990**, *29*, 2841-2846.

Turbek, C. S.; Smith, D. A.; Schardl, C. L. An extracellular enzyme from *Fusarium solani* f. sp. *Phaseoli,* which catalyzes hydration of the isoflavonoid phytoalexin phaseollidin. FEMS *Microbiol. Lett.* **1992**, *94*, 187-190.

Urdangarin, C.; Regente, M. C.; Jorrin, J.; Dela Canal, L. Sunflower coumarin phytoalexins inhibit the growth of the virulent pathogen *Sclerotinia sclerotiorum J. Phytopathol.* **1999**, *147*, 441-443.

Van den Heuvel, VanEtten, H. D.; Serum, J. W.; Coffen, D. L.; Williams, T. H. Identification of 1a-hydroxyphaseollone, a phaseollin metabolite produced by *Fusarium solani. Phytochemistry* **1974**, *13*, 1129-1131.

VanEtten, H. D.; Barz, W. Expression of pisatin demethylation ability in *Nectria haematococca. Arch. Microbiol.* **1981**, *129*, 56-60.

VanEtten, H. D.; Mansfield, J. W.; Bailey, J. A.; Farmer, E. E. Two classes of plant antibiotics: phytoalexins versus "phytoanticipins". *The Plant Cell* **1998**, *6*, 1191-1192.

VanEtten, H. D.; Matthews, D. E.; Matthews, P. S. Phytoalexin detoxification: importance for pathogenicity and practical implications. *Ann. Rev. Phytopathol.* **1989**, *27*, 143-164.

VanEtten, H. D.; Matthews, D. E.; Smith D. A. Metabolism of phytoalexins In: J. A. Bailey & J. W. Mansfield (Eds.), Phytoalexins, Blackie & Son, Glasgow, U.K., 1982, 181-217.

VanEtten, H. D.; Matthews, P. S.; Tegtmeier, K. J.; Dietert, M. F.; Stein, J. I. The association of pisatin tolerance and demethylation with virulence on pea in *Nectria haematococca. Physiol. Plant Pathol.* **1980**, *16*, 257-268.

VanEtten, H. D.; Pueppke, S. K.; Kelsey, T. C. 3, 6a-Dihydroxy-8,9-methylenedioxy pterocarpan as a metabolite of pisatin produced by *Fusarium solani* f. sp. *pisi. Phytochemistry* **1975**, *14*, 1103-1105.

VanEtten, H. D.; Sandrock, R. W.; Wasmann, C. C.; Soby, S. D.; McCluskey, K.; Wang, P. Detoxification of phytoanticipins and phytoalexins by phytopathogenic fungi. *Can. J. Bot.* **1995**, *73*(Suppl. 1), S518-S525.

VanEtten, H. D.; Temporini, E.; Wasmann, C. Phytoalexin (and phytoanticipin) tolerance as a virulence trait: why is it not required by all pathogens. *Physiol. Mol. Plant Pathol.* **2001**, *59*, 83-93.

Vurro, M.; Evidente, A.; Andolfi, A.; Zonno, M. C.; Giordano, F.; Motta, A. Brefeldin A and α,β-dehydrocurvularin, two phytotoxins from *Alternaria zinniae*, a control agent of *Xanthium occidentale*. *Plant Science* **1998**, *138*, 67-79.

Walker, R. R.; Wade, G. C.; Resistance of potato tubers (*Solanum tuberosum*) to *Phoma exiqua* var. exigua and *Phoma exigua* var. foveata. *Aust. J. Bot.* **1978**, *26*, 239-251.

Wang, J.; Ruan, D.; Cheng, Z.; Zhou, L. Phytoalexins from *Dracaena cochinchinensis* resin. *Yingyong Shengtai Xuebao* **1999**, *10*, 255-256.

Ward, E. W. B.; Stoessl, A. Postinfectional inhibitors from plants. III. Detoxification of capsidiol, an antifungal compound from peppers. *Phytopathol.* **1972**, *62*, 1186-1187.

Wasmann, C. C.; VanEtten, H. D. Transformation-mediated chromosome loss and disruption of a gene for pisatin demethylase decrease the virulence of *Nectria haematococca* on pea. *Mol. Plant – Microbe Int.* **1996**, *9*, 793-803.

Weete, J. D.; Weber D. J.; Tourneau, D. L. Hydrocarbons, free fatty acids and amino acids of sclerotia of *Sclerotinia sclerotiorum*. *Arch. Microbiol.* **1970**, *75*, 59-66.

Weigant, F.; Köster, J.; Weltzien, H. C.; Barz, W. Accumulation of phytoalexins and isoflavone glucosides in resistant and susceptible cultivars of *Cicer arietinum* during infection with *Ascochyta rabiei*. *J. Phytopathol.* **1986**, *115*, 214-221.

Weltring, K. M.; Altenburger, M. Metabolism of the phytoalexin rishitin by *Gibberella pulicaris* is highly reduced in liquid culture. *Z. Naturforsch* **1998**, *53c*, 806-810.

Weltring K M; Turgeon B G; Yoder O C; VanEtten H D. Isolation of a phytoalexin-detoxification gene from the plant pathogenic fungus *Nectria haematococca* by detecting its expression in *Aspergillus nidulans*. *Gene* **1988**, *68*, 335-344.

Weltring, K. M. Phytoalexins in the relation between plants and their fungal pathogens. In: U. Stahl, P. Tudzynski, Molecular biology of filamentous fungi, VCH, 1991, 111-124.

Weltring, K. M.; Mackenbrock, K.; Barz, W. Demethylation, methylation and 3'-hydroxylation of isoflavones by *Fusarium* fungi. *Z. Naturforsch* **1982**, *37c*, 570-574.

Wenkert, E.; Hanna, J. M.; Leftin, M. H.; Michelotti, E. L.; Potts, K. T.; Usifer, D. Replacement of methylthio functions on aromatic heterocycles by hydrogen, alkyl, and aryl groups via nickel-induced grignard reactions. *J. Org. Chem.* **1985**, *50*, 1125-1126.

Whitehead, I. M.; Atkinson, A. L.; Threlfall, D. R.; David, R. Studies on the biosynthesis and metabolism of the phytoalexin lubimin and related compounds in *Datura stramonium* L. *Planta* **1990**, *182*, 81-88.

Yamada, F.; Kobayashi, K.; Shimizu, A.; Aoki, N.; Somei, M. A synthesis method of indole-3-methanamine and/or gramine from indole-3-carboxyaldehyde, and its application for the synthesis of brassinin, its 4-substituted analogs, and 1,3,4,5-tetrahydropyrrolo[4,3,2-de] quinoline. *Heterocycles* **1993**, *36*, 2783-2804.

Yue, Q.; Bacon, C. W.; Richardson, M. D. Biotransformation of 2-benzoxazolinone and 6-methoxy-benzoxazolinone by *Fusarium moniliforrme*. *Phytochemistry* **1998**, *48*, 451-454.

Zenk, M. H.; Marcinek, H.; Weyler W.; Deus-Neumann B. Indoxyl-UDPG-glucosyl transferase from *Baphicacanthus cusia*. *Phytochemistry* **2000**, *53*, 201-207.

Zhou, T.; Boland, G. J. Mycelial growth and production of oxalic acid by virulent and hypovirulent isolates of *Sclerotinia sclerotiorum*. *Can. J. Plant Pathol.* **1999**, *21*, 93-99.

Zook, M. Biosynthesis of camalexin from tryptophan pathway intermediates in cell-suspension cultures of *Arabidopsis thaliana*. *Plant Physiol.* **1998**, *118*, 1389-1393.

APPENDIX: Calibration curves for standards determined at 220 nm

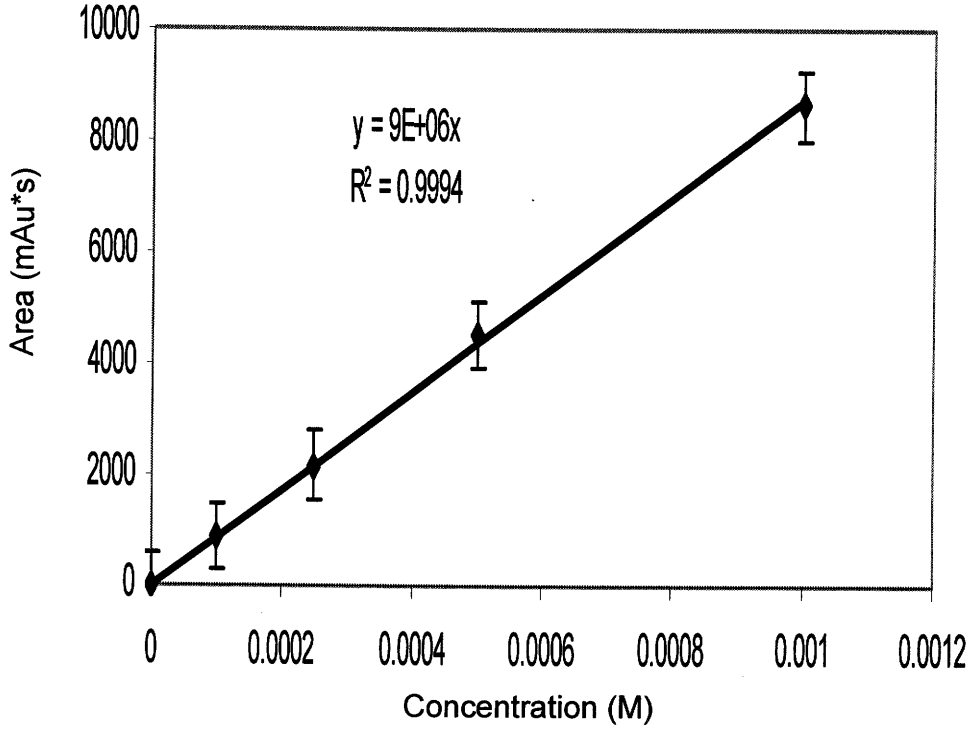

Figure 1. Calibration curve for 1-methoxyspirobrassinin (176)

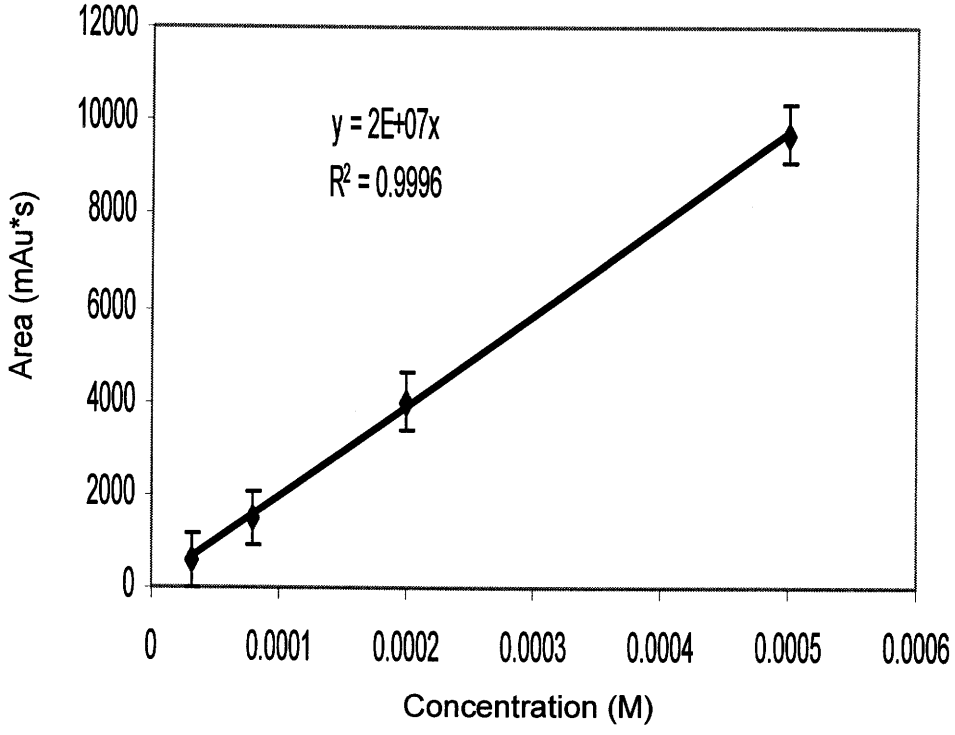

Figure 2. Calibration curve for indole-3-acetonitrile (178)

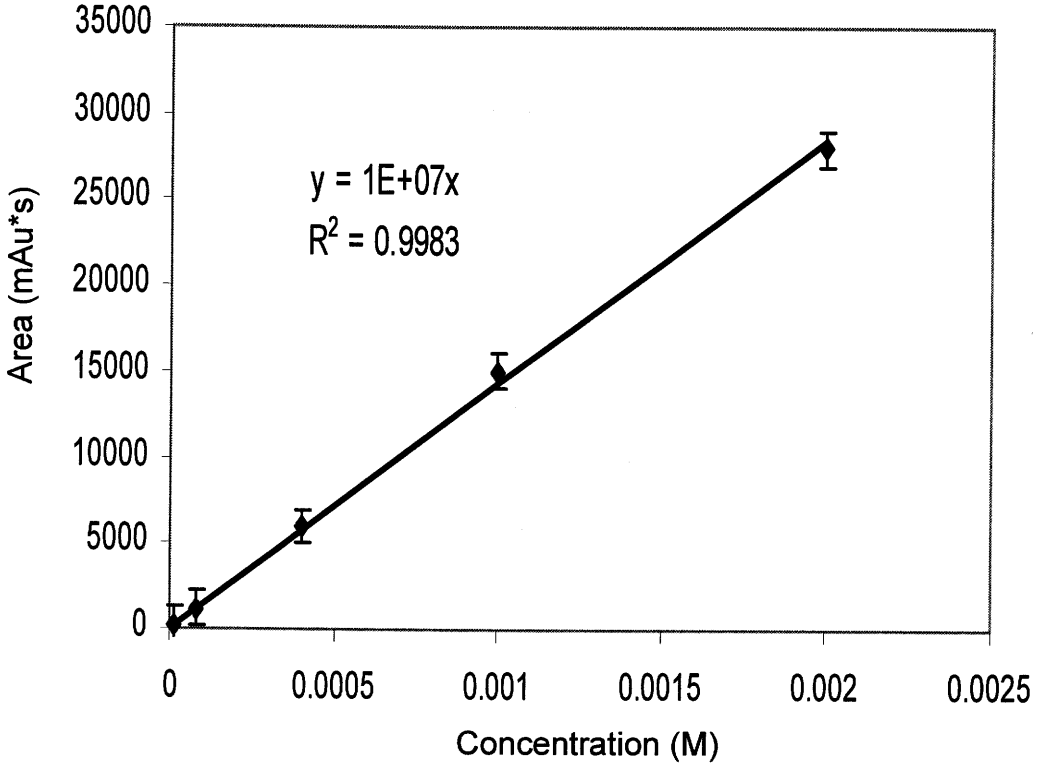

Figure 3. Calibration curve for arvelexin (179)

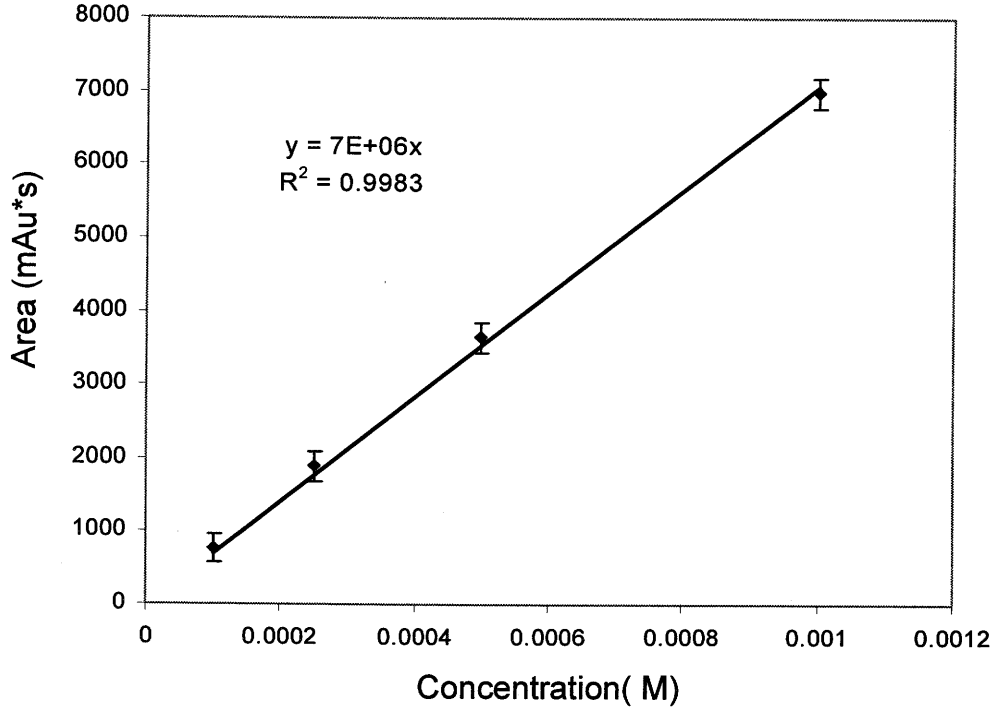

Figure 4. Calibration curve for erucalexin (204)

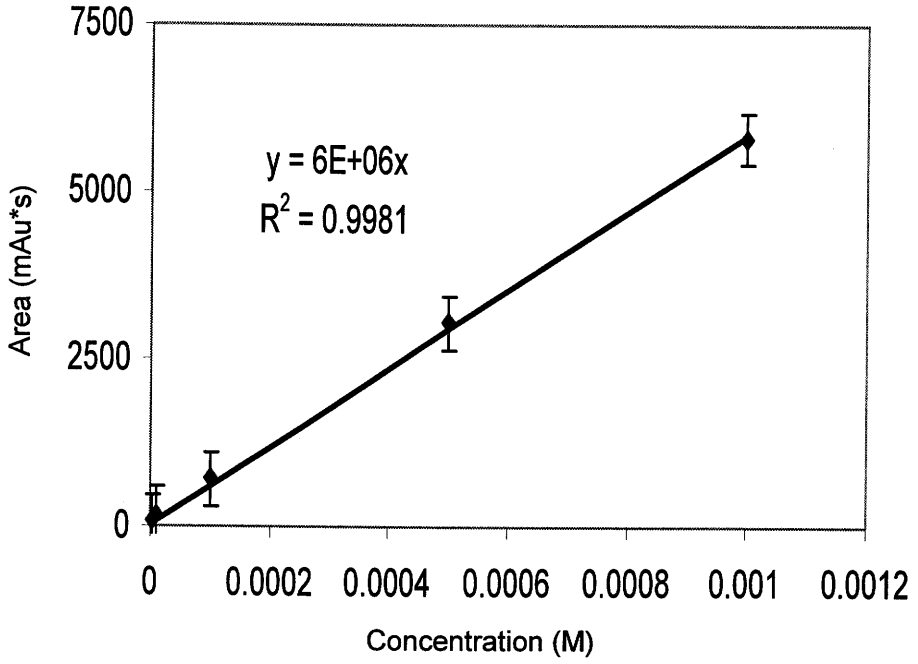

Figure 5. Calibration curve for 1-(β-D-glucopyranosyl)brassinin (234)

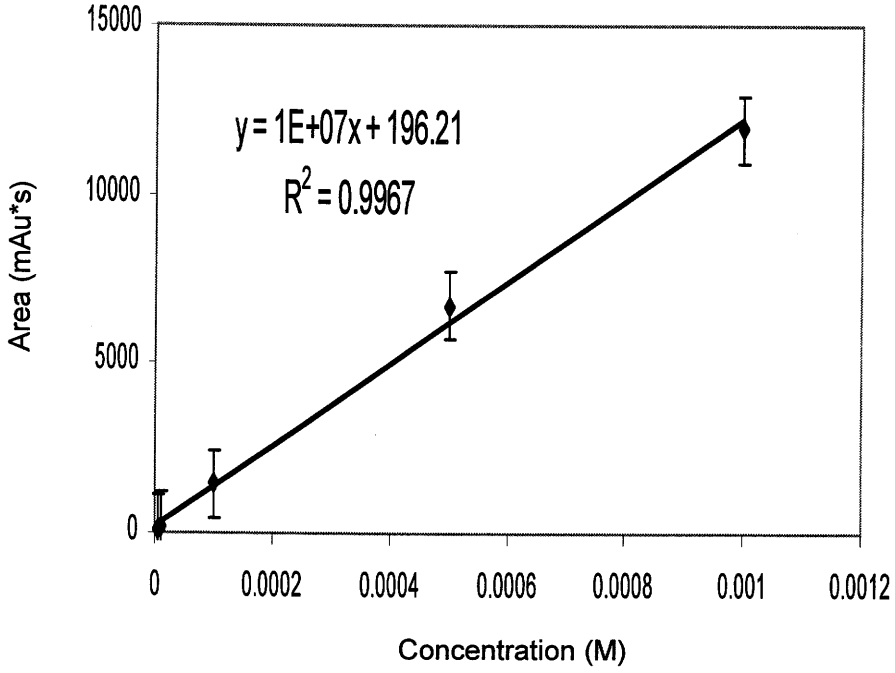

Figure 6. Calibration curve for methyl 1-(β-D-glucopyranosyl)tryptamine dithiocarbamate (235)

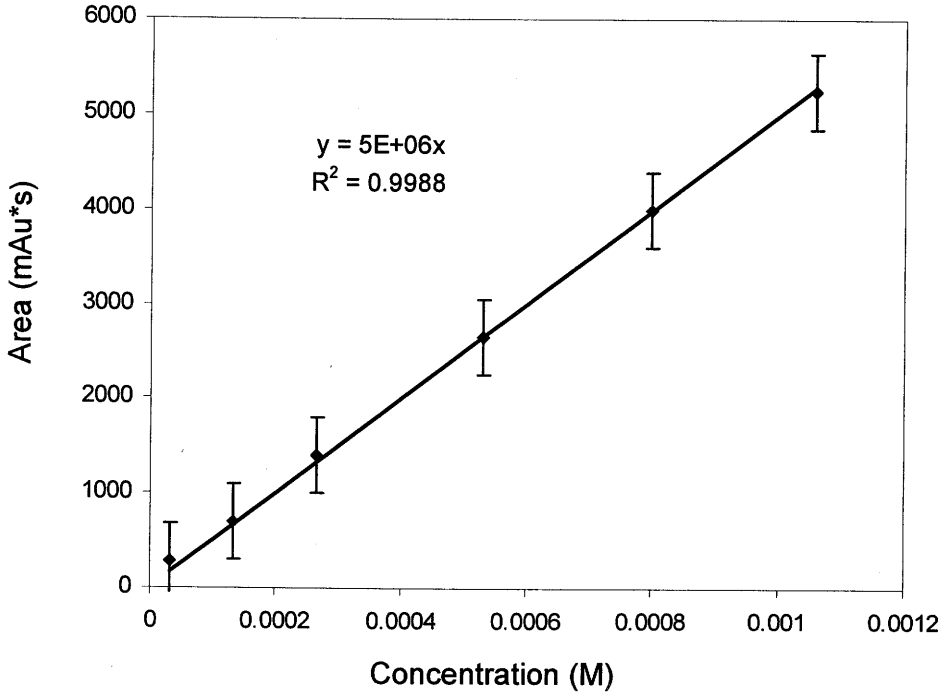

Figure 7.Calibration curve for 6-(*O*-β-D-glucopyranosyl)camalexin (237)

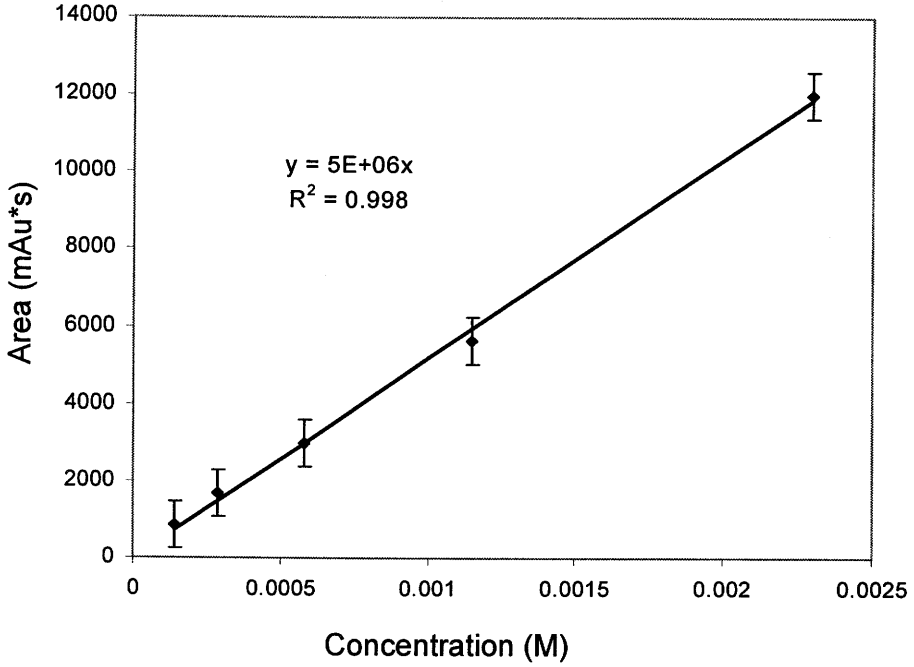

Figure 8. Calibration curve for 6-methoxy-1-(β-D-glucopyranosyl)camalexin (238)

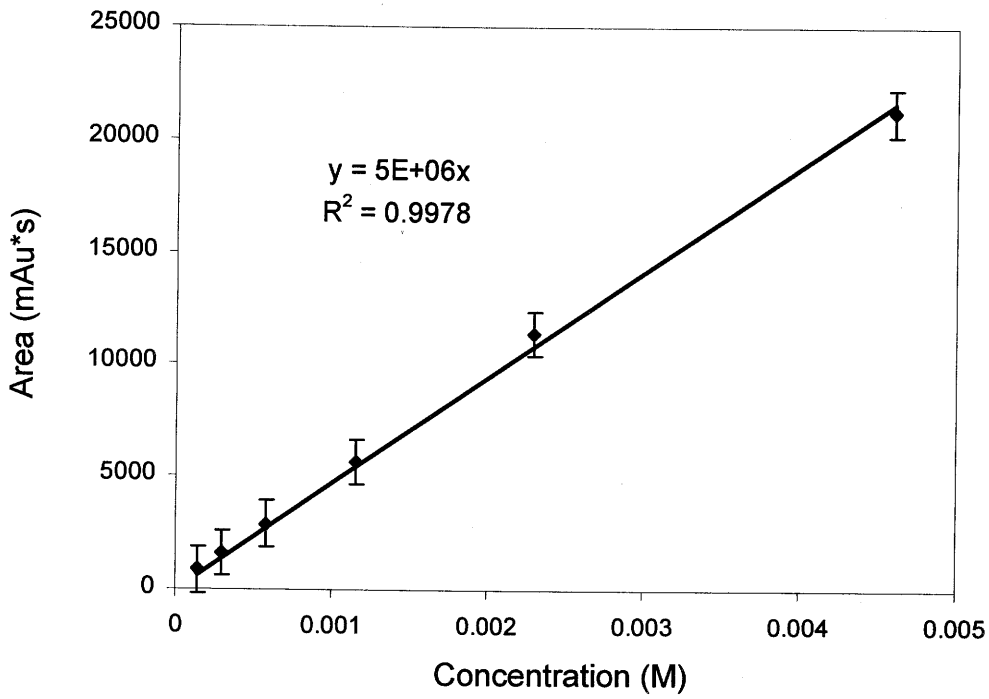

Figure 9. Calibration curve for 6-fluoro-1-(β-D-glucopyranosyl)camalexin (268)

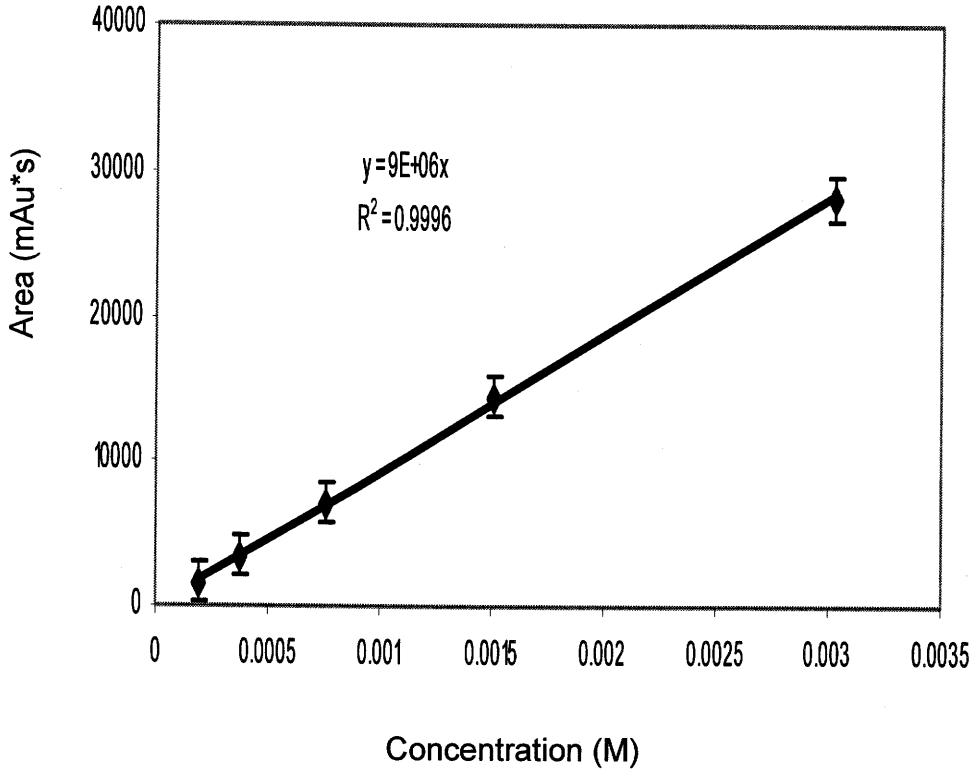

Figure 10. Calibration curve for 1-(β-D-glucopyranosyl)cyclobrassinin (271)

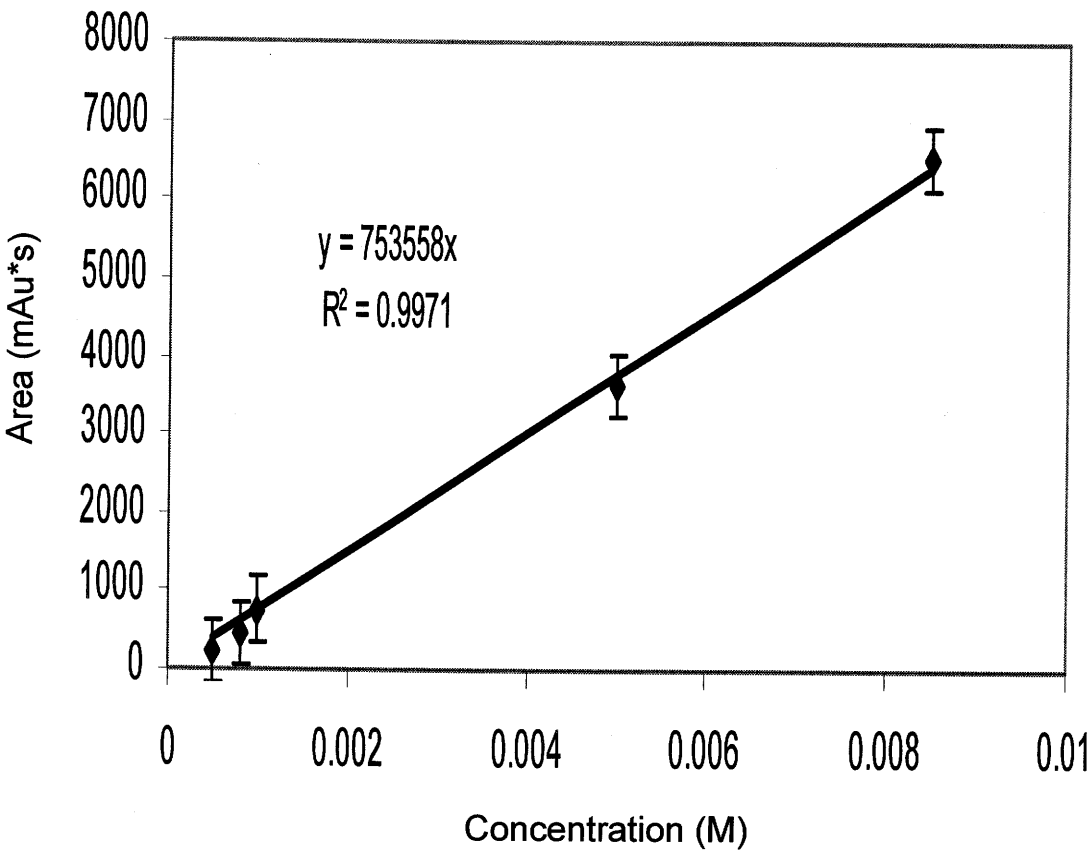

Figure 11. Calibration curve fo sclerin (17)